
Electronic Thesis and Dissertation Repository

1-31-2020 4:00 PM

Geometric State Observers for Autonomous Navigation Systems

Miaomiao Wang

Supervisor

Tayebi, Abdelhamid

The University of Western Ontario

Graduate Program in Electrical and Computer Engineering

A thesis submitted in partial fulfillment of the requirements for the degree in Doctor of Philosophy

© Miaomiao Wang 2020

Follow this and additional works at: <https://ir.lib.uwo.ca/etd>

 Part of the [Controls and Control Theory Commons](#), [Navigation, Guidance, Control, and Dynamics Commons](#), and the [Robotics Commons](#)

Abstract

The development of reliable state estimation algorithms for autonomous navigation systems is of great interest in the control and robotics communities. This thesis studies the state estimation problem for autonomous navigation systems. The first part of this thesis is devoted to the pose (orientation and position) estimation on the Special Euclidean group $\text{SE}(3)$. A generic globally exponentially stable hybrid estimation scheme for pose and velocity-bias estimation on $\text{SE}(3) \times \mathbb{R}^6$ is proposed. Moreover, an explicit hybrid observer, using inertial and landmark position measurements, is provided.

The second part of this thesis is devoted to the problem of simultaneous estimation of the attitude, position and linear velocity for inertial navigation systems (INSs). Three different types of nonlinear observers are developed to handle the following cases: continuous landmark position measurements, intermittent landmark position measurements and continuous stereo bearing measurements. First, a class of nonlinear geometric hybrid observers on the Lie group $\text{SE}_2(3)$, with global exponential stability guarantees, using continuous inertial measurement unit (IMU) and landmark position measurements is developed. Then, a class of nonlinear state observers, with strong stability guarantees, using intermittent landmark measurements is proposed. Finally, a class of state observers, with strong stability guarantees, directly incorporating body-frame stereo-bearing measurements, is proposed.

Summary for Lay Audience

The development of reliable state estimation algorithms for autonomous navigation systems is of great importance in the aerospace and robotics communities. This thesis studies the state estimation problem for autonomous navigation systems, such as unmanned aerial vehicles, autonomous underwater vehicles, unmanned surface vehicles and spacecraft. The first part is devoted to the pose (orientation and position) estimation. The second part of this thesis is devoted to the problem of simultaneous estimation of the attitude (orientation), position and linear velocity for inertial navigation systems. Different types of nonlinear observers are developed to handle the following cases: continuous landmark position measurements, intermittent landmark position measurements, and continuous stereo bearing measurements.

To all those whom I love...

Acknowledgements

I would first like to express my deepest gratitude to my advisor, Prof. Abdelhamid Tayebi, for his continuous support, guidance and encouragement throughout the four years I have spent at Western University. His patience, constructive feedback and suggestions helped me to smoothly conduct my research and write my thesis, and his optimism, excitement and passion for research and learning will continue to inspire me.

I would like to thank the members of my doctoral examination committee: Dr. Ilia Polushin, Dr. Mehrdad R. Kermani and Prof. Pei Yu for taking the time to serve as my PhD thesis examiners and for their constructive comments and feedback. I would especially like to thank Prof. Tarek Hamel from University of Nice Sophia Antipolis for agreeing to review and examine my thesis.

I would also like to thank my colleagues, Dr. Soulaimane Berkane and Dr. Abdelkader Abdessameud for the discussions we shared and from whom I continue to learn. I would also like to thank my friends at Western University for their help and valuable discussions.

Finally, I wish to thank my family for their endless support and encouragements. I am truly grateful to my wife, Caiping Zhang, and my lovely daughter, Shiying Wang, for their love, support and understanding, without which this thesis would not be possible.

Contents

Abstract	iii
Summary for Lay Audience	iv
Acknowledgements	vi
List of Figures	xi
List of Abbreviations	xiii
List of Symbols	xiv
1 Introduction	1
1.1 General introduction	1
1.2 Attitude estimation on $\text{SO}(3)$	2
1.3 Pose estimation on $\text{SE}(3)$	3
1.4 Full-state estimation for INSs	4
1.5 Thesis contributions	5
1.6 Thesis outline	8
2 Background and Preliminaries	10
2.1 General notations	10
2.2 Differential geometry	11
2.2.1 Differential manifold and Riemannian geometry	11
2.2.2 Matrix Lie groups and Lie algebras	13
2.3 State representations on matrix Lie groups	13
2.3.1 Attitude on Lie group $\text{SO}(3)$	13
2.3.2 Pose on Lie group $\text{SE}(3)$	17
2.3.3 Pose and linear velocity on Lie group $\text{SE}_2(3)$	20
2.4 Inertial navigation systems	21
2.4.1 Dynamic model for INSs	21
2.4.2 Inertial-vision systems	22
2.5 Hybrid systems framework	26
2.5.1 Hybrid systems concepts	26
2.5.2 Hybrid systems stability	28
2.6 Observability and Riccati differential equation	29

3 Hybrid Pose Estimation Using Inertial and Landmark Position Measurements	33
3.1 Introduction	33
3.2 Problem formulation	34
3.3 Gradient-based smooth observer design	37
3.4 Gradient-based hybrid observer design	38
3.4.1 Generic hybrid pose and velocity-bias estimation filter	38
3.4.2 Explicit hybrid observers design using the available measurements	41
3.5 Decoupling the rotational error dynamics from the translational error dynamics	43
3.6 Simulation results	47
3.7 Conclusion	48
4 Hybrid Nonlinear Observers for Inertial Navigation Using Landmark Measurements	52
4.1 Introduction	52
4.2 Problem formulation	53
4.3 Hybrid observers design using bias-free measurement	54
4.3.1 Continuous observer and undesired equilibria	54
4.3.2 Fixed-gain hybrid observer design	56
4.3.3 Variable-gain hybrid observer design	58
4.4 Hybrid observers design using biased angular velocity	60
4.4.1 Fixed-gain hybrid observer design	60
4.4.2 Variable-gain hybrid observer design	61
4.5 Hybrid observer design using biased angular velocity and linear acceleration	63
4.6 Simulation results	65
4.7 Experimental results	67
4.7.1 Experimental setting	67
4.7.2 Realtime implementation	68
4.7.3 Results	70
4.8 Conclusions	72
5 Hybrid State Estimation for Inertial Navigation Using Intermittent Measurements	73
5.1 Introduction	73
5.2 Problem formulation	74
5.3 Observers design with unknown gravity vector	76
5.3.1 Fixed-gain design	77
5.3.2 Variable-gain design	78
5.4 Observers design with known gravity vector	79
5.4.1 Fixed-gain design	81
5.4.2 Variable-gain design	82
5.5 Simulation results	83
5.6 Experimental results	83
5.7 Conclusion	85

6 Nonlinear Observers for Inertial Navigation Using Stereo Bearing Measurements	89
6.1 Introduction	89
6.2 Problem formulation	90
6.3 Nonlinear observers design with non-biased IMU measurements	91
6.3.1 AGAS for a class of nonlinear systems on $\text{SO}(3) \times \mathbb{R}^n$	91
6.3.2 Observer design using stereo bearing measurements	92
6.3.3 Simplified observer for $N > 3$ landmarks	95
6.4 Nonlinear observers design with biased IMU measurements	97
6.4.1 Biased accelerometer measurements only	97
6.4.2 Biased accelerometer and gyroscope measurements	100
6.5 Simulation results	104
6.5.1 Simulation with continuous and noise-free measurements	104
6.5.2 Simulation using real IMU data from the EuRoc dataset	104
6.6 Conclusion	106
7 Conclusions	108
Bibliography	110
A Proofs of Chapter 2	120
A.1 Proof of Lemma 2.4	120
A.2 Proof of Lemma 2.5	121
A.3 Proof of Lemma 2.6	123
A.4 Proof of Lemma 2.7	123
A.5 Proof of Lemma 2.11	124
Appendices	120
B Proofs of Chapter 3	126
B.1 Proof of Lemma 3.1	126
B.2 Proof of Lemma 3.2	127
B.3 Proof of Lemma 3.3	127
B.4 Proof of Proposition 3.1	129
B.5 Proof of Theorem 3.1	130
B.6 Proof of Theorem 3.2	131
B.7 Proof of Lemma 3.4	135
B.8 Proof of Lemma 3.5	136
B.9 Proof of Proposition 3.2	138
B.10 Proof of Theorem 3.3	139
C Proofs of Chapter 4	142
C.1 Proof of Proposition 4.2	142
C.2 Proof of Theorem 4.1	142
C.3 Proof of Lemma 4.1	144
C.4 Proof of Theorem 4.2	145

C.5 Proof of Theorem 4.3	146
C.6 Proof of Theorem 4.4	149
C.7 Proof of Lemma 4.3	150
D Proofs of Chapter 5	152
D.1 Solving the infinite-dimensional problem	152
D.2 Proof of Lemma 5.1	153
D.3 Proof of Theorem 5.1	154
D.4 Proof of Theorem 5.2	157
D.5 Proof of Lemma 5.2	158
D.6 Proof of Theorem 5.3	159
D.7 Proof of Theorem 5.4	160
E Proofs of Chapter 6	161
E.1 Proof of Theorem 6.1	161
E.2 Proof of Lemma 6.2	163
E.3 Proof of Lemma 6.3	164
E.4 Proof of Lemma 6.4	166
E.5 Proof of Lemma 6.5	167
E.6 Proof of Theorem 6.2	167
Curriculum Vitae	171

List of Figures

2.1	Coordinate systems: inertial frame \mathcal{I} and body-fixed frame \mathcal{B} .	14
2.2	Examples of inertial-vision system: Visual-Inertial Sensor [Nikolic et al., 2014] (left) and Intel RealSense Depth Camera D435i (right).	22
2.3	Geometric model of a pinhole camera	24
2.4	Geometric model of stereo camera	25
2.5	Example of stereo images with features detection and matching.	25
2.6	Examples of solutions to hybrid systems	27
3.1	Schematic of the proposed hybrid pose and velocity bias observer.	39
3.2	The landmarks coordinates in the inertial frame and body frame are represented with gray and blue lines, respectively.	41
3.3	The landmarks coordinates in the inertial frame and body frame are represented with gray and blue solid lines, respectively. The landmarks coordinates in the auxiliary frame are represented with dotted lines.	44
3.4	Three-dimensional trajectories in the case of noise-free output measurements and constant velocity-bias.	48
3.5	Estimation errors in the case of noise-free output measurements and constant velocity-bias.	49
3.6	Three-dimensional trajectories in the case of an additive white Gaussian noise of variance 0.1 in the output measurements and time-varying velocity-bias.	50
3.7	Estimation errors in the case of an additive white Gaussian noise of variance 0.1 in the output measurements and time-varying velocity-bias.	51
4.1	Simulation results with biased angular velocity $b_\omega = [-0.1 \ 0.02 \ 0.02]^\top$ and additive white Gaussian noise of 0.4 variance in the measurements of ω and a , and 0.1 variance in the landmark position measurements.	66
4.2	Simulation results with biased angular velocity $b_\omega = [-0.1 \ 0.02 \ 0.02]^\top$ and linear acceleration $b_a = [-0.01 \ 0.55 \ 0.07]^\top$, additive white Gaussian noise of 0.1 variance in the angular velocity, linear acceleration and landmark position measurements.	67
4.3	Example of features detection and tracking in the left and right images from a stereo camera using the MATLAB Computer Vision System Toolbox. Pictures come from the EuRoc dataset [Burri et al., 2016].	68

4.4	Experimental results using biased gyro and unbiased accelerometer measurements from the dataset V1_01_easy. The true and estimated trajectories are shown in the left plot. The estimation errors of rotation, position, velocity and IMU bias are shown in right plot.	70
4.5	Experimental results using biased gyro and accelerometer measurements from the dataset V1_01_easy. The true and estimated trajectories are shown in the left plot. The estimation errors of rotation, position, velocity and IMU bias are shown in right plot.	71
5.1	An example of the solution of the timer τ with $T_m = 1$ and $T_M = 2$	75
5.2	Nonlinear observer (5.9) with gravity vector estimation	76
5.3	Nonlinear observer (5.35) without gravity vector estimation	80
5.4	Simulation results using intermittent landmark measurements. The true and estimated trajectories are shown in the top. The estimation errors of rotation, position, linear velocity and gravity vector are shown in the bottom.	84
5.5	Experimental results using dataset V1_01_easy. The true (groundtruth) and estimated trajectories are shown in the top. The estimation errors of rotation, position, velocity and gravity vector are shown in the bottom.	86
5.6	Experimental results using dataset V1_02_medium. The true (groundtruth) and estimated trajectories are shown in the top. The estimation errors of rotation, position, velocity and gravity vector are shown in the bottom.	87
5.7	Experimental results using dataset V1_03_difficult. The true (groundtruth) and estimated trajectories are shown in the top. The estimation errors of rotation, position, velocity and gravity vector are shown in the bottom.	88
6.1	An illustration of the stereo vision system. The stereo bearing vectors are highlighted in blue arrows.	91
6.2	Nonlinear observer (6.9) using non-biased IMU and stereo bearing measurements	94
6.3	Simplified nonlinear observer (6.18) using non-biased IMU and stereo bearing measurements	97
6.4	Nonlinear observer (6.30) using biased IMU and stereo bearing measurements	100
6.5	Simulations results using ideal IMU measurements.	105
6.6	Simulations results using real IMU measurements from the EuRoc dataset V1_03_difficult.	107

List of Abbreviations

INS	– Inertial navigation system
VINS	– Vision-aided inertial navigation system
MEMS	– micro electro mechanical systems
UWB	– Ultra-wideband
UAV	– Unmanned aerial vehicle
AUV	– Autonomous underwater vehicle
USV	– Unmanned surface vehicle
IMU	– Inertial measurement unit
GNSS	– Global navigation satellite systems
GPS	– Global positioning system
LTV	– Linear time-varying
GAS	– Globally asymptotically stable
AGAS	– Almost globally asymptotically stable
GES	– Globally exponentially stable
CRE	– Continuous Riccati equation
CDRE	– Continuous-discrete Riccati equation
KF	– Kalman filter
EKF	– Extended Kalman filter
UKF	– Unscented Kalman filter
IEKF	– Invariant Extended Kalman filter
SLAM	– Simultaneous localization and mapping

List of Symbols

\mathbb{R}	– the set of real numbers
$\mathbb{R}_{\geq 0}$	– the set of nonnegative real numbers
\mathbb{N}	– the set of natural numbers
$\mathbb{N}_{>0}$	– the set of strictly positive natural numbers
\mathbb{R}^n	– the set of n -dimensional vectors or n -dimensional Euclidean space
$\mathbb{R}^{n \times m}$	– the set of real $n \times m$ matrices
\mathbb{S}^n	– the set of $(n + 1)$ -dimensional unit vectors
$\text{SO}(3)$	– the 3-dimensional Special Orthogonal group
$\mathfrak{so}(3)$	– the Lie algebra of $\text{SO}(3)$
$\text{SE}(3)$	– the 3-dimensional Special Euclidean group
$\mathfrak{se}(3)$	– the Lie algebra of $\text{SE}(3)$
Ad	– the adjoint map
$T_X G$	– the tangent space of Lie group G at $X \in G$
$f : M \rightarrow N$	– a mapping from M to N
$F : M \rightrightarrows N$	– a set-valued mapping from M to N
$x \mapsto f(x)$	– a mapping of an element x to a map $f(x)$
$\nabla_X f$	– the gradient of f at X
$\mathcal{D}_X f$	– the derivative of f at X
$f \circ g$	– the composition of maps f and g
$\text{tr}(A)$	– the trace of a matrix A
$\text{blkdiag}(\cdot)$	– the block diagonal matrix
$\mathcal{E}(A)$	– the set of eigenvectors of a matrix A
$\langle\langle A, B \rangle\rangle$	– the Euclidean inner product of matrices $A, B \in \mathbb{R}^{m \times n}$
$\ x\ $	– the Euclidean norm of a vector $x \in \mathbb{R}^n$
$\ X\ _F$	– the Frobenius norm of a matrix $X \in \mathbb{R}^{m \times n}$
$\arg \min$	– the argument of the minimum
$\arg \max$	– the argument of the maxima
$0_{n \times m}$	– an $n \times m$ matrix of zero elements
I_n	– an $n \times n$ identity matrix
λ_{\min}^A	– the minimum eigenvalue of matrix A
λ_{\max}^A	– the maximum eigenvalue of matrix A

Chapter 1

Introduction

1.1 General introduction

Over the last few decades, there have been increasing demands for developing reliable state estimation algorithms for autonomous navigation systems. Inertial navigation systems (INSs), which provide the orientation (attitude), position and linear velocity information of the vehicles, are widely used in many applications, such as unmanned aerial vehicles (UAVs), autonomous underwater vehicles (AUVs), unmanned surface vehicles (USVs) and space crafts [Britting, 1971; Bray, 2003; Grewal et al., 2007]. Recent advances in micro-electro-mechanical systems (MEMS) have made it possible to build small, inexpensive, and accurate Inertial Measurement Units (IMUs). Typically, INSs use an IMU, including an accelerometer and a gyroscope, to continuously calculate the orientation, position and linear velocity through integration. More precisely, the orientation can be obtained by integrating the angular velocity provided by the gyroscope, and the position and velocity can be obtained by integrating the linear acceleration provided by the accelerometer. However, this type of INSs suffers from integration drift since small errors in the measurements are integrated into progressively larger errors in attitude and linear velocity, and then compounded into greater errors in position [Britting, 1971].

Global navigation satellite systems (GNSSs), in particular the Global Positioning System (GPS), are widely used in INSs with low-cost inertial sensors to provide frequent position corrections and aiding (see for example [Grewal et al., 2007; Bryne et al., 2017], and references therein). This is due to the fact that INS and GPS have very complementary error characteristics: short-term position errors from the INS are relatively small, but they degrade without bound over time; GPS position errors are not good over the short term (generally speaking about 2 meters error), but they do not degrade with time. Therefore, stable position and velocity errors are guaranteed by properly combining the information from INS and GPS. However, the GPS signals are unreliable in indoor environments and urban canyons. An alternative solution is the Ultra-Wideband (UWB) range measurement system, which is a radio technology that uses a very low energy level for short-range, high-bandwidth (greater than 500Hz) communications [Adams et al., 2001; Zhou et al., 2010; Sachs, 2013; Zwirello et al., 2013; Gezici et al., 2005]. UWB range systems can provide position measurements similar to GPS, and are suitable for

short-range indoor applications. Another solution for indoor applications is the motion capture (also referred to as mo-cap or mocap) system, for example Vicon and OptiTrack, which consist of a set of cameras located in the environment recording the movement of the objects, for instance [Yuan and Chen, 2013]. However, motion capture and UWB systems are restricted to the domains where the motion space is expected to be small and fixed.

In the recent decades, vision-aided inertial navigation systems (VINSs) have made their appearance in the literature [Ohya et al., 1998; DeSouza and Kak, 2002; Mourikis and Roumeliotis, 2007; Panahandeh and Jansson, 2014; Santoso et al., 2016]. Unlike the GPS, UWB, and motion capture systems, vision sensors can be used in outdoor as well as indoor applications. Moreover, vision systems can provide rich information content about the environment, including moving targets and obstacles. Generally, an inertial-vision system consists of a low-cost IMU as an inertial sensor and onboard cameras as a vision system. In many practical applications, inertial-vision systems either use a single camera, known as monocular vision [George and Sukkarieh, 2007; Chowdhary, 2013; Qin et al., 2018], or two cameras, known as stereo-vision [Matthies and Shafer, 1987; Kriegman et al., 1989]. In the monocular vision systems, the information about metric distances (depth) is lost since all the 3-dimensional points are projected onto the 2-dimensional image plane [Hartley and Zisserman, 2003]. However, stereo vision systems can construct the 3-dimensional position of a landmark from the matched features in the two image-planes provided by the stereo images [Hartley and Zisserman, 2003; Corke, 2017].

This thesis focuses on the design of nonlinear geometric state observers of INSSs. In the following sections, we provide a general overview on the attitude estimation on $\text{SO}(3)$, pose estimation on $\text{SE}(3)$ and full-state (pose and linear velocity) estimation for autonomous navigation systems.

1.2 Attitude estimation on $\text{SO}(3)$

The attitude estimation problem has been of great interest to the research community since the early works that appeared in [Wahba, 1965; Shuster and Oh, 1981; Bar-Itzhack and Oshman, 1985; Markley, 1988]. It is well known that the attitude obtained from integrating the angular velocity may diverge beyond overtime because of the noise and bias in the low-cost sensor measurements. Nevertheless, there is no sensor that can directly provide the attitude of a rigid body system. In fact, only partial information about the rigid body's attitude can be obtained from, for instance, accelerometers, magnetometers, sun sensors and star trackers. Therefore, the attitude is usually determined from a set of body-frame vector measurements of known inertial directions, by solving an optimization problem, known as Wahba's problem [Wahba, 1965]. A great deal of research work has been devoted to solve Wahba's problem, such as the quaternion estimator (QUEST) [Shuster and Oh, 1981] and its extensions [Shuster, 1993; Crassidis et al., 2007]. However, this types of static determination algorithms are very sensitive to measurement noise, since significant errors may be generated from imperfect vector measurements. To overcome this problem, stochastic dynamic estimators based on Kalman

filtering techniques have been proposed in the literature, *e.g.*, multiplicative extended Kalman filter (MEKF) [Lefferts et al., 1982; Markley, 2003], additive extended Kalman filter [Bar-Itzhack and Oshman, 1985], intrinsic extended Kalman filter (IEKF) [Barrau and Bonnabel, 2014a]. Despite their popularity, these Kalman-type filters suffer from their large computational overhead and the lack of global stability guarantees.

Recently, nonlinear geometric observers on Lie groups have made their appearance in the literature [Mahony et al., 2008; Bonnabel et al., 2009a; Lageman et al., 2010; Khosravian et al., 2015b]. The invariant observers on $\text{SO}(3)$ proposed in [Mahony et al., 2008; Hua et al., 2014] are proven to guarantee almost global asymptotic stability, *i.e.*, the estimated attitude converges to the actual one from almost all initial conditions except from a set of Lebesgue measure zero. This is due to the fact that, for any smooth potential function on $\text{SO}(3)$, there exist at least four critical points where its gradient vanishes [Morse, 1934; Koditschek, 1989]. This is often referred to in the literature as the topological obstruction to global asymptotic stability. To overcome this topological obstruction and achieve global asymptotic (exponential) stability, some authors proposed attitude observers that are not confined to provide estimates that live in $\text{SO}(3)$ for all times [Batista et al., 2012a; Batista et al., 2012b]. On the other hand, motivated by the recent work in [Mayhew and Teel, 2011a; Mayhew and Teel, 2011b; Mayhew and Teel, 2013], a class of globally asymptotically (exponentially) stable hybrid attitude observers on $\text{SO}(3)$, relying on the concept of synergistic potential functions, has been proposed in [Wu et al., 2015; Berkane and Tayebi, 2017c; Berkane et al., 2017a]. There are also other interesting works on attitude estimation, such as the use of time-varying reference vectors [Grip et al., 2012; Trumpf et al., 2012], velocity-aided attitude estimation [Bonnabel et al., 2009b; Hua et al., 2016; Berkane and Tayebi, 2017a], and attitude estimation with intermittent vector measurements [Khosravian et al., 2015a; Berkane and Tayebi, 2019].

1.3 Pose estimation on $\text{SE}(3)$

In many applications, the estimation of the pose (attitude and position) is of great importance. A common solution to the pose estimation problem, for outdoor applications, is based on the use of an IMU (usually composed of a gyroscope, an accelerometer and a magnetometer), and a GPS. More precisely, the attitude can be estimated using body-frame observations of some known inertial vectors obtained from an IMU [Tayebi and McGilvray, 2006; Bonnabel et al., 2008; Mahony et al., 2008; Hua et al., 2014], and the position (and linear velocity) can be obtained from a GPS [Barczyk and Lynch, 2013; Barrau and Bonnabel, 2014b; Grip et al., 2013]. However, these IMU-based nonlinear attitude observers rely on the fact that the accelerometer provides a measurement of the gravity vector in the body-fixed frame, which is true only in the case of negligible linear accelerations. In applications involving accelerated rigid body systems, a typical solution consists in using linear velocity measurements together with IMU measurements with the so-called velocity-aided attitude observers [Bonnabel et al., 2009b; Roberts and Tayebi, 2011; Hua et al., 2016; Hua et al., 2017; Berkane and Tayebi, 2017a]. Moreover, recovering the position and linear velocity is a challenging task in GPS-denied environments (*e.g.*, indoor applications). Alternatively, the pose can be determined from points

obtained from vision systems, known as Perspective-n-Point (PnP) problem [Quan and Lan, 1999; Wu and Hu, 2006; Hesch and Roumeliotis, 2011]. To reduce the effect of measurement noise, dynamical pose estimators based on Kalman filtering techniques , with local stability guarantees, have been proposed [Wang and Wilson, 1992; Janabi-Sharifi and Marey, 2010; Chen, 2011; Hamel and Samson, 2018].

Recently, motivated by the work of [Mahony et al., 2008] on $\text{SO}(3)$, nonlinear complementary observers on $\text{SE}(3)$ have been proposed in [Baldwin et al., 2007; Hua et al., 2011]. However, in practical applications, measurements of group velocity (translational and rotational velocities) are often corrupted by unknown biases. Pose estimation using landmark position measurements and biased group velocity were considered in [Vasconcelos et al., 2010; Hua et al., 2015; Khosravian et al., 2015b]. A nice feature of [Hua et al., 2015] is that the observer incorporates (naturally) both inertial vector measurements (*e.g.*, from IMU) and landmark position measurements (*e.g.*, from a vision system). In [Khosravian et al., 2015b], more general invariant observers on Lie groups with biased input measurements and homogeneous outputs have been proposed. However, these observers are shown to guarantee almost global asymptotic stability due to the topological obstruction on $\text{SE}(3)$. Similar to the attitude estimation problem, this is the strongest result one can aim at when considering continuous time-invariant state observers on $\text{SE}(3)$. A solution with global asymptotic stability guarantees has been proposed in [Moeini and Namvar, 2016] which considers a non-geometric pose estimation problem using biased body-frame measurements of the system's linear and angular velocities as well as body-frame measurements of landmarks. The achieved global asymptotic stability results are due to the fact that the estimates are not confined to live in $\text{SE}(3)$ for all times. The design of pose observers with global asymptotic and exponential stability guarantees is an open problem that has been solved in this thesis using hybrid techniques.

1.4 Full-state estimation for INSs

In practice, it is difficult to obtain the linear velocity from low-cost sensors, in GPS-denied environments. This implies that pose observers based on group velocity are not implementable in practical applications where the measurements of linear velocity are not available. Therefore, developing reliable estimation algorithms that provide the attitude, position and linear velocity is of great importance (from theoretical and practical point of views) for inertial navigation systems. It is important to point out that the dynamics of the attitude, position and linear velocity are not (right or left) invariant, and hence, the extension of the existing invariant observers designed on $\text{SE}(3)$ to the estimation problem considered in this work is not trivial. Most of the existing results in the literature, for the state estimation problem for INSs, are filters of the Kalman-type (see for instance [Mourikis and Roumeliotis, 2007; Mourikis et al., 2009; Panahandeh and Jansson, 2014]). Recently, a stable IEKF, using a geometric error on matrix Lie groups, has been proposed in [Barrau and Bonnabel, 2017]. As pointed out in [Barrau and Bonnabel, 2017], the classical EKF may fail when the covariance matrices are not tuned properly. On the other hand, a Riccati-based geometric pose, linear velocity and gravity direction observer has been proposed in [Hua and Allibert, 2018]. However, both results are only shown to be

locally stable. This motivates us to design nonlinear observers for inertial navigation with global stability guarantees, which has been addressed in this thesis using hybrid techniques.

On the other hand, many practical applications involve different type of sensors with different bandwidths and communication delays, and as such, irregular sensors sampling may take place. For example, the landmark measurements from vision systems are obtained at much lower rates compared to IMU measurements due to hardware limitations of the vision sensors and the heavy image processing computations. In this case, IMU measurements can be easily considered as continuous compared to visual measurements. Therefore, the stability is not guaranteed if one tries to implement continuous-time observers [Hua and Allibert, 2018; Wang and Tayebi, 2020] in applications involving intermittent measurements combining sensors with different bandwidth characteristics (such as IMU and vision systems), and as such, the observers need to be carefully redesigned. In this context, the existing results in the literature, consider either continuous measurements or discrete measurement with a fixed sampling rate. There are very few references that have dealt with the state estimation problem for INS using continuous (high-rate) IMU and intermittent (low-rate) landmark position measurements [Barrau and Bonnabel, 2017]. Motivated by the work in [Ferrante et al., 2016; Li et al., 2017; Sferlazza et al., 2019; Berkane and Tayebi, 2017b; Berkane and Tayebi, 2019] addressing the estimation problem with intermittent measurements, hybrid nonlinear state estimation for INSs, using intermittent landmark position measurements, have been addressed in this thesis.

In fact, vision systems do not directly provide the 3-dimensional landmark position measurements, and as such, additional algorithms are needed for this purpose [Hartley and Zisserman, 2003; Corke, 2017]. From the model of a pinhole camera, the measurements obtained from images can be seen as a set of bearing vectors (unit vectors pointing to the landmarks from the optical center of the camera expressed in the camera frame). Therefore, it is of great interest to design observers for autonomous navigation systems using bearing-only measurements [Pachter and Porter, 2004; Baldwin et al., 2009; Le Bras et al., 2017; Hamel and Samson, 2018; Hamel and Samson, 2017]. Attitude and position observers with local stability guarantees have been proposed in [Baldwin et al., 2009; Hamel and Samson, 2018]. On the other hand, nonlinear observers with global exponential stability guarantees for position measurements, using biased velocity measurements, have been considered in [Le Bras et al., 2017; Hamel and Samson, 2017]. The problem of attitude, position and linear velocity estimation for INS using IMU and stereo bearing measurements has been addressed in this thesis.

1.5 Thesis contributions

In this thesis, several contributions to geometric state estimation for autonomous navigation systems are presented. Hybrid pose and velocity-bias observers on $\text{SE}(3)$ using inertial and landmark position measurements are proposed. Three types of estimation schemes for INSs are proposed depending on the type of measurements, such as continuous landmark position measurements, intermittent landmark position measurements, and continuous stereo bearing measurements. The contributions of the work presented

in this thesis can thus be summarized as follows:

- In Chapter 3, a new framework for global exponential pose and velocity-bias estimation on $\text{SE}(3) \times \mathbb{R}^6$ is proposed. Our framework can be seen as a non-trivial extension to the work of [Hua et al., 2015; Khosravian et al., 2015b] and [Berkane et al., 2017a]. On one hand, due to the topological obstruction on $\text{SE}(3)$, it is impossible to achieve global stability with smooth observers designed on $\text{SE}(3)$. On the other hand, since that $\text{SE}(3)$ is not compact as the Lie group $\text{SO}(3)$, hybrid techniques, relying on synergistic potential functions, cannot be easily applied on $\text{SE}(3)$. In this context, a new class of hybrid observers, relying on a new resetting mechanism, is proposed with global exponential stability guarantees. First, we propose a generic hybrid estimation scheme (depending on a generic potential function) evolving on $\text{SE}(3) \times \mathbb{R}^6$ for pose and velocity-bias estimation. Thereafter, the proposed estimation scheme is formulated explicitly in terms of inertial vectors and landmark measurements. Interestingly, the proposed estimation scheme leads to a decoupled rotational error dynamics from the translational dynamics, which is a nice feature in practical applications with noisy measurements and disturbances. The obtained results have been published in [Wang and Tayebi, 2017; Wang and Tayebi, 2019a].
- In Chapter 4, the problem of simultaneous attitude, position and linear velocity estimation using IMU and landmark measurements, is formulated using the matrix Lie group $\text{SE}_2(3)$ introduced in [Barrau and Bonnabel, 2017]. Then, two hybrid nonlinear observers, leading to global exponential stability, are proposed. The first observer relies on fixed gains, while the second one uses variable gains depending on the solution of a continuous Riccati equation (CRE). These observers are then extended to handle biased angular velocity and linear acceleration measurements. The proposed observers are endowed with global exponential stability guarantees. The resetting mechanism considered in the proposed observers is motivated from our work in [Wang and Tayebi, 2017; Wang and Tayebi, 2019a]. Contrary to the dynamics on the Lie groups $\text{SO}(3)$ and $\text{SE}(3)$, the dynamics of the attitude, position and linear velocity on $\text{SE}_2(3)$ are not invariant. As a consequence, the application of the hybrid observers proposed in [Berkane et al., 2017b; Wang and Tayebi, 2020] to our problem is not trivial. Unlike the observers on $\text{SE}(3)$ in [Vasconcelos et al., 2010; Hua et al., 2011; Hua et al., 2015; Khosravian et al., 2015b; Wang and Tayebi, 2017; Wang and Tayebi, 2020], the observers proposed in this chapter do not rely on the linear velocity measurements. Moreover, experimental results, using real IMU measurements and landmark position measurements obtained from stereo cameras, are presented to illustrate the performance of the proposed observers. This work has been reported in [Wang and Tayebi, 2018b; Wang and Tayebi, 2020]
- In Chapter 5, several solutions to the problem of simultaneous estimation of the attitude, position and linear velocity, for autonomous navigation using intermittent lankmark measurements, are presented. Two hybrid nonlinear observers for INS, with and without the knowledge of the gravity vector, have been proposed.

For each observer, we provide two different design approaches for the gain parameters; a fixed-gain approach relying on an infinite-dimensional optimization, and a variable-gain approach relying on a continuous-discrete Riccati equation (CDRE). The proposed observers are endowed with exponential stability guarantees with a large domain of attraction. The exponential stability results obtained in this work do not rely on linearizations compared to the recent work in [Barrau and Bonnabel, 2017; Hamel and Samson, 2018]. In fact, the proposed observers do not have any restrictions on the initial conditions of the position and linear velocity. In contrast to the present work, the hybrid observers proposed in [Wang and Tayebi, 2020] are not designed to handle intermittent landmark measurements. Moreover, the first hybrid observer proposed in this work does not require the knowledge of the gravity vector, which was not considered in [Barrau and Bonnabel, 2017; Wang and Tayebi, 2020]. Unlike the results of [Berkane and Tayebi, 2017b; Berkane and Tayebi, 2019], the estimated attitude from our hybrid observers is continuous, which is desirable in practice, especially when dealing with observer-controller implementations. These results have been published in [Wang and Tayebi, 2019c]

- In Chapter 6, full state estimation problem for INSs using (continuous) stereo bearing measurements has been addressed, which is motivated from the fact that vision systems do not provide direct 3-dimensional position measurements. Firstly, an AGAS result for a class of nonlinear systems on $\text{SO}(3) \times \mathbb{R}^n$ is proposed. Based on this result, an explicit nonlinear observer for INSs using non-biased IMU and stereo-bearing measurements is developed. To reduce the computational complexity, a simplified version has been proposed for the case of more than 3 non-coplanar landmarks. Instead of estimating the positions of all the landmarks, the estimates of only three axis vectors are considered assuming that there exist at least 4 non-coplanar landmarks available for measurements. Furthermore, these results are extended to handle the case of biased IMU measurements. The above results are reported in [Wang and Tayebi, 2019b]

List of publications

The materials presented in this dissertation are based on the following publications:

Journal Articles:

- M. Wang and A. Tayebi, ‘Nonlinear State Estimation for Inertial Navigation Systems With Intermittent Measurements’, *Automatica*, 2019, (Submission No. 19-0841).
- M. Wang and A. Tayebi, ‘Hybrid Nonlinear Observers for Inertial Navigation Using Landmark Measurements’, *IEEE Transactions on Automatic Control*, 2020, accepted.
- M. Wang and A. Tayebi, ‘Hybrid Pose and Velocity-bias Estimation on $\text{SE}(3)$ Using Inertial and Landmark Measurements’, *IEEE Transactions on Automatic Control*, 64(8), pp. 3399-3406, 2019.

Peer-Reviewed Conference Proceedings:

- M. Wang and A. Tayebi, ‘Nonlinear Observers for Stereo-Vision-Aided Inertial Navigation’, In *Proc. of 58th IEEE Conference on Decision and Control (CDC)*, Nice, France, pp. 2516-2521, 2019.
- M. Wang and A. Tayebi, ‘A Globally Exponentially Stable Nonlinear Hybrid Observer for 3D Inertial Navigation’, In *Proc. of the 57th IEEE Conference on Decision and Control (CDC)*, Miami Beach, FL, USA, pp. 1367- 1372, 2018.
- M. Wang and A. Tayebi,‘Globally Asymptotically Stable Hybrid Observers Design on $\text{SE}(3)$ ’, In *Proc. of the 56th IEEE Conference on Decision and Control (CDC)*, Melbourne, Australia, pp. 3033-3038, 2017.

1.6 Thesis outline

This thesis is organized as follows:

Chapter 2 presents the notations, background and preliminaries used throughout the thesis. Section 2.1 provides the general notations used in this thesis. Section 2.2 and Section 2.3 present the basic differential geometry tools and the state representations on matrix Lie groups. The dynamic model of the autonomous navigation systems considered in this work, and the measurement model of the inertial vision systems are given in Section 2.4. Section 2.5 presents the hybrid systems framework used in this work. Finally, Section 2.6 provides some useful identities and lemmas on the observability and Riccati differential equation.

Chapter 3 is devoted to the pose and group velocity-bias estimation problem on $\text{SE}(3) \times \mathbb{R}^6$ using inertial and landmark position measurements. Section 3.3 explains the topological obstruction for global asymptotic stability of gradient-based smooth observers on $\text{SE}(3)$. Section 3.4 presents a generic pose and velocity-bias estimation scheme with global asymptotic (exponential) stability guarantees. In Section 3.5, these results are extended to decouple the rotational error dynamics from the translational error dynamics using modified landmarks.

Chapter 4 is dedicated to the hybrid nonlinear observers design for INSs using IMU and landmark position measurements. Section 4.3 provides the design of the hybrid observers in the bias-free case. Both fixed gains and variable gains are considered. These results are extended to address the problem of biased angular velocity in Section 4.4. Section 4.5 deals with the case where both the angular velocity and linear acceleration measurements are biased.

Chapter 5 considers the problem of state estimation for INSs using continuous IMU and intermittent landmark position measurements. Section 5.3 provides the design of a hybrid observer with unknown gravity vector. Section 5.4 presents the design of the hybrid observer with known gravity vector. Both fixed gains and variable gains are considered for the proposed hybrid observers.

Chapter 6 addresses the problem of state estimation for INSs using IMU and stereo bearing measurements. Section 6.3 provides two observers for INSs using ideal IMU

measurements. Then, these observers are extended in Section 6.4 to handle biased IMU measurements.

Chapter 7 summarizes the findings of this thesis and presents some possible future directions.

Appendix A,B, C, D, E contain the detailed proofs of lemmas and theorems stated throughout this thesis.

Chapter 2

Background and Preliminaries

2.1 General notations

Given $A \in \mathbb{R}^{n \times m}$, a_{ij} refers to its (i, j) -th entry. For any matrix $A := [a_{ij}]_{i,j=1,\dots,n} \in \mathbb{R}^{n \times n}$, the trace of matrix A is denoted by $\text{tr}(A) = \sum_{i=1}^n a_{ii}$, and the determinant of A is denoted by $\det(A)$. Given any two matrices, $A, B \in \mathbb{R}^{m \times n}$, their ***Euclidean inner product*** is defined as $\langle\langle A, B \rangle\rangle := \text{tr}(A^\top B)$. The ***Euclidean norm*** of a vector $x \in \mathbb{R}^n$ is defined as $\|x\| := \sqrt{x^\top x}$, and the ***Frobenius norm*** of a matrix $A \in \mathbb{R}^{n \times m}$ is given by $\|A\|_F := \sqrt{\langle\langle A, A \rangle\rangle}$. Define A^\top as the transpose of matrix A . Given any $A \in \mathbb{R}^{n \times n}$ and $B \in \mathbb{R}^{m \times m}$, the Kronecker product is denoted by $A \otimes B \in \mathbb{R}^{mn \times mn}$. By $\text{blkdiag}(\cdot)$, we denote the block diagonal matrix. For a matrix $A \in \mathbb{R}^{n \times n}$, we denote by λ_i^A the i -th eigenvalue of A , and by λ_{\min}^A and λ_{\max}^A be the minimum and maximum eigenvalues of A , respectively. We also denote by $\mathcal{E}(A)$ the set of all eigenvectors of A , and by $\mathbb{E}(A) \subseteq \mathcal{E}(A)$ the eigenbasis set of A . Given a vector $a \in \mathbb{R}^n$, a_i refers to its i -th component. Let $\vec{e}_1, \dots, \vec{e}_n$ be the standard basis vectors of the linear space \mathbb{R}^n , that is, \vec{e}_i has all entries equal to zero except for the i -th entry which is equal to 1. Therefore, a vector $a = [a_1, \dots, a_n]^\top \in \mathbb{R}^n$ can be written as $a = \sum_{i=1}^n a_i \vec{e}_i$. For any two vectors $x, y \in \mathbb{R}^3$, their ***vector cross-product*** on \mathbb{R}^3 can be written as

$$a \times b = \sum_{i,j,k} \varepsilon_{ijk} a_i b_j \vec{e}_k \in \mathbb{R}^3 \quad (2.1)$$

where ε_{ijk} is the Levi-Cevita symbol defined by

$$\varepsilon_{ijk} = \begin{cases} +1 & \text{if } (m, n, l) \text{ is an even permutation of } (1, 2, 3) \\ -1 & \text{if } (m, n, l) \text{ is an odd permutation of } (1, 2, 3) \\ 0 & \text{otherwise} \end{cases}$$

Some of useful properties of the matrix trace $\text{tr}(\cdot)$ are summarized as follows:

$$\text{tr}(M) = \text{tr}(M^\top), \quad (2.2)$$

$$\text{tr}(M + N) = \text{tr}(M) + \text{tr}(N), \quad (2.3)$$

$$\text{tr}(NM) = \text{tr}(MN), \quad (2.4)$$

$$\text{tr}((M + M^\top)(N - N^\top)) = 0, \quad (2.5)$$

$$\text{tr}(xy^\top) = x^\top y, \quad (2.6)$$

for all $M, N \in \mathbb{R}^{3 \times 3}$, $x, y \in \mathbb{R}^3$. Let $A \in \mathbb{R}^{n \times n}$, $U, V \in \mathbb{R}^{n \times m}$ and $R \in \mathbb{R}^{m \times m}$. If A, R and $R^{-1} + V^\top A^{-1}U$ are invertible, then

$$(A + URV^\top)^{-1} = A^{-1} - A^{-1}U(R^{-1} + V^\top A^{-1}U)^{-1}V^\top A^{-1} \quad (2.7)$$

For any $A \in \mathbb{R}^{n \times n}$, $b \in \mathbb{R}^n$ and $d \in \mathbb{R}$, one has the following matrix decomposition:

$$\begin{bmatrix} A & b \\ b^\top & d \end{bmatrix} = \begin{bmatrix} I_n & bd^{-1} \\ 0_{1 \times n} & 1 \end{bmatrix} \begin{bmatrix} A - bb^\top d^{-1} & 0_{n \times 1} \\ 0_{1 \times n} & d \end{bmatrix} \begin{bmatrix} I_n & 0_{n \times 1} \\ b^\top d^{-1} & 1 \end{bmatrix}. \quad (2.8)$$

For a symmetric matrix $P \in \mathbb{R}^{n \times n}$, $P > 0$ ($P < 0$) denotes that P is positive (negative) definite. The time-derivative of a time-varying variable $x(t) \in \mathbb{R}^n$ is denoted by $\dot{x}(t) = \frac{d}{dt}x(t) := \lim_{h \rightarrow 0} \frac{1}{h}(x(t+h) - x(t))$. For the sake of simplicity, the argument of the time-dependent signals will be omitted throughout this thesis (*i.e.*, $x(t) \rightarrow x$).

2.2 Differential geometry

In this section, some useful concepts of a general differential manifold are presented and a brief discussion on matrix Lie groups and Lie algebras is provided.

2.2.1 Differential manifold and Riemannian geometry

Let \mathcal{M} be a smooth manifold embedded in \mathbb{R}^n . Consider a smooth map $\gamma : \mathbb{R} \rightarrow \mathcal{M}$ as a curve in \mathcal{M} . Defining a derivative of γ in the classical sense as $\dot{\gamma}(t) = \lim_{h \rightarrow 0} \frac{1}{h}(\gamma(t+h) - \gamma(t))$ fails for a general manifold, since the computation of the difference $\gamma(t+h) - \gamma(t)$ requires a vector space structure [Absil et al., 2009]. Hence, a new definition of the derivative of a map on a general manifold is necessary and important. Given an open interval $\mathbb{I} \subset \mathbb{R}$ containing 0 in its interior, define a smooth curve $\gamma : \mathbb{I} \rightarrow \mathcal{M}$ with $\gamma(0) = x$. The **tangent vector** at $x \in \mathcal{M}$ is defined as

$$\dot{\gamma}(0) = \left. \frac{d}{dt} \right|_{t=0} \gamma(t)$$

Definition 2.1 ([Holm et al., 2009]) *The set of all tangent vectors at a given point x , corresponding to all possible paths in \mathcal{M} through x , is called the **tangent space** to \mathcal{M} at point x , denoted by $T_x\mathcal{M}$.*

Definition 2.2 ([Holm et al., 2009]) *The disjoint union of all tangent space gives the **tangent bundle** of \mathcal{M} , denoted by $T\mathcal{M} = \bigcup_{x \in \mathcal{M}} T_x\mathcal{M}$.*

Given two smooth manifolds \mathcal{M} and \mathcal{N} , a map $f : \mathcal{M} \rightarrow \mathcal{N}$ is differentiable if it is differentiable at all points in its domain. The inverse image of a subset $\mathcal{N}_S \subset \mathcal{N}$ under the map f is the subset of \mathcal{M} denoted by $f^{-1}(\mathcal{N}_S) = \{x \in \mathcal{M} \mid f(x) \in \mathcal{N}_S\}$. The map f is a **diffeomorphism** if f is differentiable and has a differentiable inverse.

Definition 2.3 ([Holm et al., 2009]) Let $f : \mathcal{M} \rightarrow \mathcal{N}$ be a differentiable map between two smooth manifolds \mathcal{M} and \mathcal{N} . The **tangent map** of f at point $x \in \mathcal{M}$ denoted by $\mathcal{D}f_x : T_x\mathcal{M} \rightarrow T_{f(x)}\mathcal{N}$ is defined as

$$\mathcal{D}f_x(v) := \left. \frac{d}{dt} \right|_{t=0} f(\gamma(t))$$

where, $\gamma(t)$ is a smooth curve in \mathcal{M} with $\gamma(0) = x$ and $v = \dot{\gamma}(0) \in T_x\mathcal{M}$. All the maps of $\mathcal{D}f_x$ for all $x \in \mathcal{M}$, together define the tangent map of f .

Consider a smooth manifold \mathcal{M} and a point $x \in \mathcal{M}$. The **Riemannian metric** on manifold \mathcal{M} at point x is denoted as $\langle \cdot, \cdot \rangle_x : T_x\mathcal{M} \times T_x\mathcal{M} \rightarrow \mathbb{R}$.

Definition 2.4 ([Do Carmo, 1992]) Given a differentiable map $f : \mathcal{M} \rightarrow \mathbb{R}$, the **Riemannian gradient** of map f at point x , denoted by $\nabla_x f(x) \in T_x\mathcal{M}$, is the unique tangent vector satisfies

$$\mathcal{D}f_x(v) = \langle \nabla_x f(x), v \rangle_x, \quad \forall v \in T_x\mathcal{M}. \quad (2.9)$$

Throughout the thesis, the argument of x in $\nabla_x f(x)$ is omitted (*i.e.*, $\nabla_x f$) for the sake of simplicity. The mapping $\nabla f : \mathcal{M} \rightarrow T\mathcal{M}$ is called the gradient vector field [Bloch, 2003]. Considering a mapping $f : \mathcal{M} \times \mathcal{N} \rightarrow \mathbb{R}$, the notation $\nabla_x f(x, y)$ denotes the gradient of f with respect to x , and the notation $\nabla_y f(x, y)$ denotes the gradient of f with respect to y .

Definition 2.5 ([Palais and Terng, 2006]) Let \mathcal{M} be a Riemannian manifold. If $f : \mathcal{M} \rightarrow \mathbb{R}$ is a differentiable map, a point $x \in \mathcal{M}$ is a **critical point** of f on \mathcal{M} if its gradient at x satisfies $\nabla_x f(x) = 0$. The set of all critical points of f on \mathcal{M} , denoted by $C_f \mathcal{M} := \{x \in \mathcal{M} \mid \nabla_x f(x) = 0\} \subset \mathcal{M}$, is called the **critical set** of f on \mathcal{M} .

From the Definition 2.4 and Definition 2.5, at each critical point of f (*i.e.*, $x \in C_f \mathcal{M}$), it is easy to verify that $\mathcal{D}f_x(v) = 0$ for all $v \in T_x\mathcal{M}$.

Definition 2.6 Let \mathcal{M} be a smooth manifold. A continuously differentiable function $f : \mathcal{M} \rightarrow \mathbb{R}_{\geq 0}$ is called a **potential function** on \mathcal{M} with respect to the set $\mathcal{A} \subset \mathcal{M}$ if the following statements hold:

i) $f(x) > 0$ for all $x \in \mathcal{M}/\mathcal{A}$.

ii) $f(x) = 0$ for all $x \in \mathcal{A}$.

A metric (or distance) on a manifold \mathcal{M} shows how two points in \mathcal{M} are close to each other. More precisely, a metric on \mathcal{M} is a function $d_{\mathcal{M}} : \mathcal{M} \times \mathcal{M} \rightarrow \mathbb{R}_{\geq 0}$ that satisfies the following properties for all $x_1, x_2, x_3 \in \mathcal{M}$:

- 1) Non-negativity: $d_{\mathcal{M}}(x_1, x_2) \geq 0$.
- 2) Identity of indiscernibles: $d_{\mathcal{M}}(x_1, x_2) = 0$ if and only if $x_1 = x_2$.
- 3) Symmetry: $d_{\mathcal{M}}(x_1, x_2) = d_{\mathcal{M}}(x_2, x_1)$.
- 4) Triangle inequality: $d_{\mathcal{M}}(x_1, x_3) \leq d_{\mathcal{M}}(x_1, x_2) + d_{\mathcal{M}}(x_2, x_3)$

2.2.2 Matrix Lie groups and Lie algebras

Lie groups, special types of manifold, are the mathematical concept appropriate for describing continuously varying groups of transformations. A Lie group is a smooth manifold, denoted G , that is a group with the property that the operations of multiplication, $(g, h) \mapsto gh$ and inversion, $g \mapsto g^{-1}$, are smooth [Holm et al., 2009]. The Lie group considered in this thesis will often be a matrix Lie group. For example, a group describing the attitude (orientation) of a rigid body is called the matrix Lie group $\text{SO}(3)$, while a group describing the pose (orientation and position) of a rigid body is called the matrix Lie group $\text{SE}(3)$.

Definition 2.7 ([Bloch, 2003]) *A **matrix Lie group** is a subgroup of the general linear group, denoted $GL(n, \mathbb{R})$, which is the set of invertible $n \times n$ real matrices.*

Alternatively, a matrix Lie group is a matrix group that is also a submanifold of $\mathbb{R}^{n \times n}$ [Holm et al., 2009]. From Definition 2.1, the tangent space to G at $X \in G$, denoted $T_X G$, is defined as the set of all tangent vectors at X , corresponding to all possible paths in G through X .

The matrix commutator of any two matrices $A, B \in \mathbb{R}^{n \times n}$ is defined as $[A, B] := AB - BA$. For any $A, B, C \in \mathbb{R}^{n \times n}$, the matrix commutator operation has the properties $[A, B] = -[B, A]$ and $[[A, B], C] + [[B, C], A] + [[C, A], B] = 0$.

Definition 2.8 ([Bloch, 2003]) *The **Lie algebra** of a matrix Lie group G , is the tangent space at the identity $I \in G$, denoted \mathfrak{g} , with the corresponding Lie bracket.*

The Lie bracket on a matrix Lie algebra is the matrix commutator $[,]$, which means that the Lie algebra of a matrix Lie group is the space $T_I G$, together with the commutator operation [Holm et al., 2009].

2.3 State representations on matrix Lie groups

In this subsection, the kinematic equations of the robotic systems considered in this thesis, including the translational and rotational dynamics, will be derived. In robotics, multiple frames are commonly used in order to represent vectors and points in three-dimensional space. In this thesis, we define \mathcal{I} as an inertial reference frame attached to the origin on \mathbb{R}^3 and associated to the Cartesian coordinate system. Let \mathcal{B} be the body-fixed frame attached to the center of gravity of a rigid body, with respect to the inertial reference frame. An example of coordinate system is shown in the Figure 2.1.

2.3.1 Attitude on Lie group $\text{SO}(3)$

The attitude (or orientation) of a rigid body can be represented in different ways: Euler angles, Unit quaternion, and rotation matrix (see reference [Shuster, 1993] for more details). As pointed out in [Shuster, 1993], only the rotation matrix representation is unique and global. Therefore, throughout this thesis, we consider the rotation matrix as the attitude representation. The rotation matrix, also known as the Direction Cosine

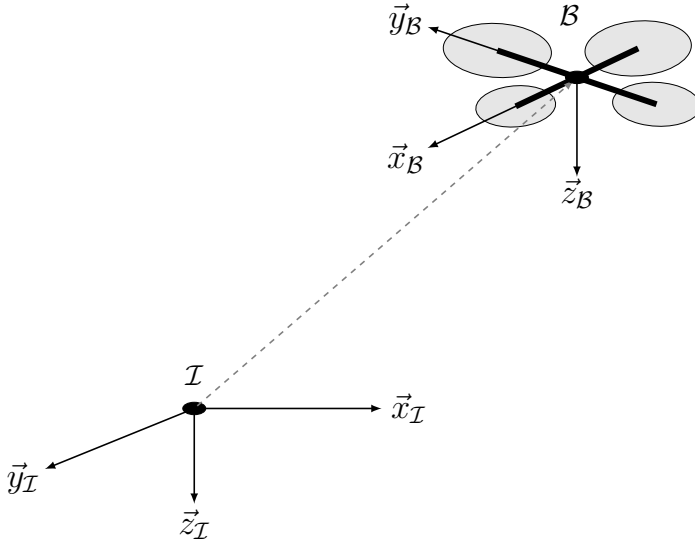


Figure 2.1: Coordinate systems: inertial frame \mathcal{I} and body-fixed frame \mathcal{B} .

Matrix (DCM), is denoted by $R \in \mathbb{R}^{3 \times 3}$. From Figure 2.1, the attitude of frame \mathcal{B} with respect to frame \mathcal{I} is defined as

$$R = \begin{bmatrix} \vec{x}_{\mathcal{B}} \cdot \vec{x}_{\mathcal{I}} & \vec{y}_{\mathcal{B}} \cdot \vec{x}_{\mathcal{I}} & \vec{z}_{\mathcal{B}} \cdot \vec{x}_{\mathcal{I}} \\ \vec{x}_{\mathcal{B}} \cdot \vec{y}_{\mathcal{I}} & \vec{y}_{\mathcal{B}} \cdot \vec{y}_{\mathcal{I}} & \vec{z}_{\mathcal{B}} \cdot \vec{y}_{\mathcal{I}} \\ \vec{x}_{\mathcal{B}} \cdot \vec{z}_{\mathcal{I}} & \vec{y}_{\mathcal{B}} \cdot \vec{z}_{\mathcal{I}} & \vec{z}_{\mathcal{B}} \cdot \vec{z}_{\mathcal{I}} \end{bmatrix} = \begin{bmatrix} \cos\langle \vec{x}_{\mathcal{B}}, \vec{x}_{\mathcal{I}} \rangle & \cos\langle \vec{y}_{\mathcal{B}}, \vec{x}_{\mathcal{I}} \rangle & \cos\langle \vec{z}_{\mathcal{B}}, \vec{x}_{\mathcal{I}} \rangle \\ \cos\langle \vec{x}_{\mathcal{B}}, \vec{y}_{\mathcal{I}} \rangle & \cos\langle \vec{y}_{\mathcal{B}}, \vec{y}_{\mathcal{I}} \rangle & \cos\langle \vec{z}_{\mathcal{B}}, \vec{y}_{\mathcal{I}} \rangle \\ \cos\langle \vec{x}_{\mathcal{B}}, \vec{z}_{\mathcal{I}} \rangle & \cos\langle \vec{y}_{\mathcal{B}}, \vec{z}_{\mathcal{I}} \rangle & \cos\langle \vec{z}_{\mathcal{B}}, \vec{z}_{\mathcal{I}} \rangle \end{bmatrix} \quad (2.10)$$

where we made use of the facts $x \cdot y = \|x\| \|y\| \cos(\angle(x, y))$ with $\angle(\cdot, \cdot)$ denoting the angle of two vectors, and the norms of the axis vectors are equal to one. It turns out that the rotation matrix R defined in (2.10) belongs to the **Special Orthogonal group** of dimension three, defined by

$$\text{SO}(3) := \{R \in \mathbb{R}^{3 \times 3} : R^T R = R R^T = I_3, \det(R) = 1\} \quad (2.11)$$

where I_3 is the 3-dimensional identity matrix. Note that $\text{SO}(3)$ is a matrix Lie group under the operation of matrix multiplication $R_1 R_2 \in \text{SO}(3)$ for any $R_1, R_2 \in \text{SO}(3)$. The Lie algebra of $\text{SO}(3)$ is denoted by

$$\mathfrak{so}(3) := \{\Omega \in \mathbb{R}^{3 \times 3} | \Omega^T = -\Omega\}. \quad (2.12)$$

Let \times be the vector cross-product on \mathbb{R}^3 and define the skew-symmetric map $(\cdot)^\times : \mathbb{R}^3 \rightarrow \mathfrak{so}(3)$ such that

$$x^\times = \begin{bmatrix} 0 & -x_3 & x_2 \\ x_3 & 0 & -x_1 \\ -x_2 & x_1 & 0 \end{bmatrix}, \quad \forall x = [x_1, x_2, x_3]^\top \in \mathbb{R}^3 \quad (2.13)$$

For each $x, y \in \mathbb{R}^3, A \in \mathbb{R}^{3 \times 3}, R \in \text{SO}(3)$, one has the following identities:

$$x^\times x = 0, \quad (2.14)$$

$$(x^\times)^3 = -\|x\|^2 x^\times, \quad (2.15)$$

$$x \times y = x^\times y, \quad (2.16)$$

$$x^\times y = -y^\times x, \quad (2.17)$$

$$x^\times y^\times = yx^\top - (x^\top y)I_3, \quad (2.18)$$

$$(x^\times y)^\times = x^\times y^\times - y^\times x^\times, \quad (2.19)$$

$$\langle \langle x^\times, y^\times \rangle \rangle = 2x^\top y, \quad (2.20)$$

$$((Ax) \times (Ay))^\times = A(x \times y)^\times A^\top, \quad (2.21)$$

$$Ax^\times + x^\times A^\top = ((\text{tr}(A)I - A^\top)x)^\times, \quad (2.22)$$

$$\text{tr}(Ax^\times) = 0, \quad \forall A = A^\top, \quad (2.23)$$

$$(Rx) \times (Ry) = R(x \times y), \quad (2.24)$$

$$(Rx)^\times = Rx^\times R^\top. \quad (2.25)$$

Define the inverse isomorphism of $(\cdot)^\times$ as $\text{vec} : \mathfrak{so}(3) \rightarrow \mathbb{R}^3$ such that

$$\text{vec}(\omega^\times) = \omega \text{ and } (\text{vec}(\Omega))^\times = \Omega, \quad \forall \omega \in \mathbb{R}^3, \Omega \in \mathfrak{so}(3).$$

Define $\mathbb{P}_{\mathfrak{so}(3)} : \mathbb{R}^{3 \times 3} \rightarrow \mathfrak{so}(3)$ as the anti-symmetric projection of a matrix $A \in \mathbb{R}^{3 \times 3}$ such that $\mathbb{P}_{\mathfrak{so}(3)}(A) = \frac{1}{2}(A - A^\top)$. For a matrix $A = [a_{ij}] \in \mathbb{R}^{3 \times 3}$, we define

$$\psi_{\mathfrak{so}(3)}(A) := \text{vec}(\mathbb{P}_{\mathfrak{so}(3)}(A)) = \frac{1}{2} \begin{bmatrix} a_{32} - a_{23} \\ a_{13} - a_{31} \\ a_{21} - a_{12} \end{bmatrix}. \quad (2.26)$$

Then, for any $A \in \mathbb{R}^{3 \times 3}, x, y \in \mathbb{R}^3, R \in \text{SO}(3)$, one has the following identities

$$\langle \langle A, x^\times \rangle \rangle = \langle \langle \mathbb{P}_{\mathfrak{so}(3)}(A), x^\times \rangle \rangle \quad (2.27)$$

$$\langle \langle A, x^\times \rangle \rangle = 2x^\top \psi_{\mathfrak{so}(3)}(A), \quad (2.28)$$

$$\psi_{\mathfrak{so}(3)}(AR) = R^\top \psi_{\mathfrak{so}(3)}(RA), \quad (2.29)$$

$$(x \times y)^\times = \mathbb{P}_{\mathfrak{so}(3)}(yx^\top), \quad (2.30)$$

$$x \times y = 2\psi_{\mathfrak{so}(3)}(yx^\top). \quad (2.31)$$

Let the map $\mathcal{R}_a : \mathbb{R} \times \mathbb{S}^2 \rightarrow \mathbb{R}^{3 \times 3}$ represent the well-known angle-axis parametrization of the attitude, which is given by

$$\mathcal{R}_a(\theta, u) := I_3 + \sin \theta u^\times + (1 - \cos \theta)(u^\times)^2 \quad (2.32)$$

with θ the rotation angle and u the rotation axis. Note that this angle-axis parametrization is not unique, for example $\mathcal{R}_a(\pi, u) = \mathcal{R}_a(-\pi, u)$ with some $u \in \mathbb{S}^2$. Let $M = M^\top$ be a positive semidefinite matrix, one can show that:

$$\text{tr}((I_3 - \mathcal{R}_a(\theta, u))M) = \text{tr}(-\sin \theta Mu^\times - (1 - \cos \theta)M(u^\times)^2)$$

$$\begin{aligned}
&= (1 - \cos \theta) \text{tr}(-M(uu^\top - u^\top u I_3)) \\
&= (1 - \cos \theta) u^\top (\text{tr}(M) - M) u
\end{aligned} \tag{2.33}$$

where we made use of the facts $\text{tr}(Mu^\times) = 0$ from (2.23), $u^\times u^\times = uu^\top - u^\top u I_3$ from (2.18). Let $d_{\text{SO}(3)} : \text{SO}(3) \times \text{SO}(3) \rightarrow \mathbb{R}_{\geq 0}$ be the Euclidean (Chordal) distance on $\text{SO}(3)$, which is denoted by the Frobenius norm on the embedding Euclidean space $\mathbb{R}^{3 \times 3}$ as follows:

$$d_{\text{SO}(3)}(R_1, R_2) := \|R_1 - R_2\|_F, \quad \forall R_1, R_2 \in \text{SO}(3). \tag{2.34}$$

One can verify that $d_{\text{SO}(3)}(R_1, R_2) = d_{\text{SO}(3)}(I_3, R_1^\top R_2) = d_{\text{SO}(3)}(I_3, R_2 R_1^\top)$. From the definition of Frobenius norm, for each $R \in \text{SO}(3)$ one can also show that $d_{\text{SO}(3)}(I, R) = \|I_3 - R\|_F = \sqrt{2\text{tr}(I_3 - R)} \leq \sqrt{8}$, where the fact $-1 \leq \text{tr}(R) \leq 3, \forall R \in \text{SO}(3)$ has been used. For the sake of simplicity, we consider the following normalized attitude norm $|R|_I \in [0, 1]$ on $\text{SO}(3)$ with respect to the identity I_3 :

$$|R|_I = \frac{d_{\text{SO}(3)}(I_3, R)}{\sqrt{8}} = \frac{\|I_3 - R\|_F}{\sqrt{8}} = \frac{1}{2} \sqrt{\text{tr}(I_3 - R)}. \tag{2.35}$$

The tangent space of the group $\text{SO}(3)$, is identified by $T_R \text{SO}(3) := \{R\Omega | R \in \text{SO}(3), \Omega \in \mathfrak{so}(3)\}$. Let $\langle \cdot, \cdot \rangle_R : T_R \text{SO}(3) \times T_R \text{SO}(3) \rightarrow \mathbb{R}$ be a Riemannian metric on $\text{SO}(3)$, such that

$$\langle R\Omega_1, R\Omega_2 \rangle_R := \langle \langle \Omega_1, \Omega_2 \rangle \rangle, \quad R \in \text{SO}(3), \Omega_1, \Omega_2 \in \mathfrak{so}(3).$$

Given a differentiable smooth function $f : \text{SO}(3) \rightarrow \mathbb{R}$, the gradient of f , denoted by $\nabla_R f \in T_R \text{SO}(3)$, relative to the Riemannian metric $\langle \cdot, \cdot \rangle_R$ is uniquely defined by

$$df \cdot R\Omega = \langle \nabla_R f, R\Omega \rangle_R = \langle \langle R^\top \nabla_R f, \Omega \rangle \rangle,$$

for all $R \in \text{SO}(3), \Omega \in \mathfrak{so}(3)$. A point $R \in \text{SO}(3)$ is called critical point of f if the gradient of f at point $R \in \text{SO}(3)$ is zero (*i.e.*, $\nabla_R f = 0$). The set of all critical points of f on $\text{SO}(3)$ is denoted by

$$C_{\text{SO}(3)} f := \{R \in \text{SO}(3) | \nabla_R f = 0\} \subset \text{SO}(3). \tag{2.36}$$

Throughout this thesis, we make use of the following useful lemmas on $\text{SO}(3)$:

Lemma 2.1 ([Berkane et al., 2017b; Berkane, 2017]) *Let $M = M^\top$ be a positive semi-definite matrix such that $\bar{M} := \frac{1}{2}(\text{tr}(M)I - M)$ is positive definite. Then, for any $x, y \in \mathbb{R}^3$, the following properties hold for all $R \in \text{SO}(3)$:*

$$4\lambda_{\min}^{\bar{M}} |R|_I^2 \leq \text{tr}((I_3 - R)M) \leq 4\lambda_{\max}^{\bar{M}} |R|_I^2, \tag{2.37}$$

$$\|\psi_{\mathfrak{so}(3)}(MR)\|^2 = \alpha(M, R) \text{tr}((I_3 - R)\underline{M}), \tag{2.38}$$

$$\psi_{\mathfrak{so}(3)}(R)^\top \psi_{\mathfrak{so}(3)}(MR) = \psi_{\mathfrak{so}(3)}(R)^\top \bar{M} \psi_{\mathfrak{so}(3)}(R), \tag{2.39}$$

$$x^\top (\lambda_{\min}^{\bar{M}} I_3 - E(MR))x \leq 2\lambda_{\max}^{\bar{M}} |R|_I^2 \|x\|^2, \tag{2.40}$$

$$2x^\top (E(M) - E(M\tilde{R}))y \leq \text{tr}((I_3 - R)M)x^\top y + \|(I_3 - R)M\|_F \|x\| \|y\|, \tag{2.41}$$

$$\|E(MR)\|_F \leq \|\bar{M}\|_F, \quad (2.42)$$

where $\underline{M} := \text{tr}(\bar{M}^2)I_3 - 2\bar{M}^2$, $E(MR) := \frac{1}{2}(\text{tr}(MR)I_3 - R^\top M)$, and $\alpha(M, R) := 1 - |R|_I^2 \cos(\angle(u, \bar{M}u))$ with $u \in \mathbb{S}^2$ denoting the axis of the rotation R and $\angle(\cdot, \cdot)$ denoting the angle between two vectors. Moreover, Consider the trajectory of $\dot{R} = R\omega^\times$ with $R(0) \in \text{SO}(3)$ and $\omega(t) \in \mathbb{R}^3$. Then the following identities hold:

$$\frac{d}{dt} \text{tr}((I - R)M) = 2\omega^\top \psi_{\mathfrak{so}(3)}(MR), \quad (2.43)$$

$$\frac{d}{dt} \psi_{\mathfrak{so}(3)}(MR) = E(MR)\omega. \quad (2.44)$$

Lemma 2.2 ([Berkane, 2017]) Let $M = \sum_{i=1}^N k_i r_i r_i^\top$ with $N \in \mathbb{N}_{>0}$, $k_i > 0$ and $r_i \in \mathbb{R}^3$, $i = 1, \dots, n$. Then, the following identities hold for any $R, \bar{R} \in \text{SO}(3)$

$$\text{tr}((I_3 - R\bar{R}^\top)M) = \frac{1}{2} \sum_{i=1}^N k_i \|R^\top r_i - \bar{R}^\top r_i\|^2, \quad (2.45)$$

$$\psi_{\mathfrak{so}(3)}(MRR^\top) = \frac{1}{2} \bar{R} \sum_{i=1}^N k_i (R^\top r_i \times \bar{R}^\top r_i) = \frac{1}{2} \sum_{i=1}^N k_i (\bar{R} R^\top r_i \times r_i). \quad (2.46)$$

From (2.38) and (2.35), one can show that

$$\|\psi_{\mathfrak{so}(3)}(R)\|^2 = (1 - |R|_I^2) \text{tr}(I_3 - R) = 4(1 - |R|_I^2)|R|_I^2 \leq 1 \quad (2.47)$$

where we made use of the facts $|R|_I^2 \in [0, 1]$ and $f(x) = 4(1 - x)x \leq 1, \forall x \in [0, 1]$.

Lemma 2.3 Let $M \in \mathbb{R}^{3 \times 3}$ be symmetric and positive semi-definite with three distinct eigenvalues. Then, the solutions of $MR = R^\top M$ with $R \in \text{SO}(3)$ satisfy

$$R \in \{I_3\} \cup \{R = \mathcal{R}_a(\pi, v), v \in \mathcal{E}(M)\}, \quad (2.48)$$

where $\mathcal{E}(M)$ is the set of eigenvectors of M .

The proof of Lemma 2.3 is obtained by following the similar steps as in the proof of [Mahony et al., 2008, Theorem 5.1] and [Mayhew and Teel, 2011b, Lemma 2].

2.3.2 Pose on Lie group $\text{SE}(3)$

The pose of a rigid body is represented by the pair (R, p) with $R \in \text{SO}(3)$ being the orientation of the body-fixed frame attached to the center of the rigid body with respect to the inertial frame, and $p \in \mathbb{R}^3$ being the position of the rigid body expressed in the inertial frame. The three-dimensional **Special Euclidean group**, denoted by $\text{SE}(3)$, is defined as

$$\text{SE}(3) := \{g = \mathcal{T}_{\text{SE}(3)}(R, p) \in \mathbb{R}^{4 \times 4} \mid R \in \text{SO}(3), p \in \mathbb{R}^3\},$$

with the map $\mathcal{T}_{\text{SE}(3)} : \text{SO}(3) \times \mathbb{R}^3 \rightarrow \text{SE}(3)$ given by

$$\mathcal{T}_{\text{SE}(3)}(R, p) := \begin{bmatrix} R & p \\ 0_{1 \times 3} & 1 \end{bmatrix}. \quad (2.49)$$

The inverse of g can be expressed in matrix form as

$$g^{-1} = \mathcal{T}_{\text{SE}(3)}(R^\top, -R^\top p) = \begin{bmatrix} R^\top & -R^\top p \\ 0_{1 \times 3} & 1 \end{bmatrix} \quad (2.50)$$

It is easy to verify that $gg^{-1} = g^{-1}g = I_4$. The Lie algebra of $\text{SE}(3)$, denoted by $\mathfrak{se}(3)$, is given by

$$\mathfrak{se}(3) := \left\{ U \in \mathbb{R}^{4 \times 4} \mid U = \begin{bmatrix} \Omega & v \\ 0_{1 \times 3} & 0 \end{bmatrix}, \Omega \in \mathfrak{so}(3), v \in \mathbb{R}^3 \right\}. \quad (2.51)$$

with $\mathfrak{so}(3)$ defined in (2.12). Similar to the map $(\cdot)^\times$ defined on \mathbb{R}^3 , we introduce a wedge map $(\cdot)^\wedge : \mathbb{R}^6 \rightarrow \mathfrak{se}(3)$, which is defined as

$$\xi^\wedge := \begin{bmatrix} \omega^\times & v \\ 0_{1 \times 3} & 0 \end{bmatrix}, \quad \xi := \begin{bmatrix} \omega \\ v \end{bmatrix}. \quad (2.52)$$

The tangent space of the group $\text{SE}(3)$, is identified by $T_g \text{SE}(3) := \{gU \mid g \in \text{SE}(3), U \in \mathfrak{se}(3)\}$. Let $\langle \cdot, \cdot \rangle_g : T_g \text{SE}(3) \times T_g \text{SE}(3) \rightarrow \mathbb{R}$ be a Riemannian metric on $\text{SE}(3)$, such that

$$\langle gU, gU_2 \rangle_g := \langle \langle U_1, U_2 \rangle \rangle, \quad \forall g \in \text{SE}(3), U_1, U_2 \in \mathfrak{se}(3).$$

Given a differentiable smooth function $f : \text{SE}(3) \rightarrow \mathbb{R}$, the gradient of f , denoted by $\nabla_g f \in T_g \text{SE}(3)$, relative to the Riemannian metric $\langle \cdot, \cdot \rangle_g$ is uniquely defined by

$$df \cdot gU = \langle \nabla_g f, gU \rangle_g = \langle \langle g^{-1} \nabla_g f, U \rangle \rangle, \quad (2.53)$$

for all $g \in \text{SE}(3), U \in \mathfrak{se}(3)$. A point $g \in \text{SE}(3)$ is called critical point of f if the gradient of f at g is zero (*i.e.*, $\nabla_g f = 0$). The set of all critical points of f on $\text{SE}(3)$ is denoted by

$$C_{\text{SE}(3)} f := \{g \in \text{SE}(3) \mid \nabla_g f = 0\} \subset \text{SE}(3). \quad (2.54)$$

For any $g \in \text{SE}(3)$, we define $|g|_I$ as the distance with respect to I_4 , which is given by

$$|g|_I := \|I_4 - g\|_F = \sqrt{\|I_3 - R\|_F^2 + \|p\|^2} = \sqrt{8|R|_I^2 + \|p\|^2} \quad (2.55)$$

Let $\mathbb{P}_{\mathfrak{se}(3)} : \mathbb{R}^{4 \times 4} \rightarrow \mathfrak{se}(3)$ denote the projection of \mathbb{A} on the Lie algebra $\mathfrak{se}(3)$, such that for all $A_1 \in \mathbb{R}^{3 \times 3}, a_2, a_3^\top \in \mathbb{R}^3$ and $a_4 \in \mathbb{R}$

$$\mathbb{P}_{\mathfrak{se}(3)} \left(\begin{bmatrix} A_1 & a_2 \\ a_3 & a_4 \end{bmatrix} \right) := \begin{bmatrix} \mathbb{P}_{\mathfrak{so}(3)}(A_1) & a_2 \\ 0_{1 \times 3} & 0 \end{bmatrix}. \quad (2.56)$$

For all $U \in \mathfrak{se}(3), A \in \mathbb{R}^{4 \times 4}$ one has $\langle \langle A, U \rangle \rangle = \langle \langle U, \mathbb{P}_{\mathfrak{se}(3)}(A) \rangle \rangle = \langle \langle \mathbb{P}_{\mathfrak{se}(3)}(A), U \rangle \rangle$. Let $\text{vex} : \mathfrak{se}(3) \rightarrow \mathbb{R}^6$ denote the inverse isomorphism of the map $(\cdot)^\wedge$, such that $\text{vex}(\xi^\wedge) = \xi$

and $(\text{vex}(U))^\wedge = U$, for all $\xi \in \mathbb{R}^6$ and $U \in \mathfrak{se}(3)$. For a matrix $A = \begin{bmatrix} A_1 & a_2 \\ a_3 & a_4 \end{bmatrix}$ with $A_1 \in \mathbb{R}^{3 \times 3}, a_2, a_3^\top \in \mathbb{R}^3$ and $a_4 \in \mathbb{R}$, we also define the following map:

$$\begin{aligned} \psi_{\mathfrak{se}(3)}(A) &:= \Theta \text{vex}(\mathbb{P}_{\mathfrak{se}(3)}(A)) \\ &= \begin{bmatrix} \psi_{\mathfrak{so}(3)}(A_1) \\ \frac{1}{2}b \end{bmatrix} = \frac{1}{2} \begin{bmatrix} a_{32} - a_{23} \\ a_{13} - a_{31} \\ a_{21} - a_{12} \\ b \end{bmatrix}, \end{aligned} \quad (2.57)$$

with $A_1 = [a_{ij}]$ and $\Theta := \text{blkdiag}(I_3, \frac{1}{2}I_3)$. Then, it is verified that for all $\mathbb{A} \in \mathbb{R}^{4 \times 4}, y \in \mathbb{R}^6$

$$\langle \langle A, y^\wedge \rangle \rangle = 2y^\top \psi_{\mathfrak{se}(3)}(A) \quad (2.58)$$

Given a rigid body with configuration $g \in \text{SE}(3)$, the adjoint map $\text{Ad}_g(\cdot) : \text{SE}(3) \times \mathfrak{se}(3) \rightarrow \mathfrak{se}(3)$ is given by

$$\text{Ad}_g(U) := gUg^{-1}, \quad \forall g \in \text{SE}(3), U \in \mathfrak{se}(3). \quad (2.59)$$

The matrix representation of the adjoint map on $\mathfrak{se}(3)$ is defined as

$$\text{Ad}_g := \begin{bmatrix} R & 0_{3 \times 3} \\ p^\times R & R \end{bmatrix} \in \mathbb{R}^{6 \times 6}, \quad \forall g = \mathcal{T}_{\text{SE}(3)}(R, p) \quad (2.60)$$

such that

$$gx^\wedge g^{-1} = (\text{Ad}_g x)^\wedge, \quad \forall g \in \text{SE}(3), x \in \mathbb{R}^6. \quad (2.61)$$

One verifies that $\text{Ad}_{g_1}\text{Ad}_{g_2} = \text{Ad}_{g_1g_2}$, for all $g_1, g_2 \in \text{SE}(3)$. Define $\text{Ad}_g^*(\cdot)$ as the Hermitian adjoint of $\text{Ad}_g(\cdot)$ with respect to the matrix inner product $\langle \langle \cdot, \cdot \rangle \rangle$ on $\mathfrak{se}(3)$ associated with the right-invariant Riemannian metric, such that for all $U_1, U_2 \in \mathfrak{se}(3), g \in \text{SE}(3)$

$$\langle \langle U_2, \text{Ad}_g(U_1) \rangle \rangle = \langle \langle \text{Ad}_g^*(U_2), U_1 \rangle \rangle, \quad (2.62)$$

For each $g = \mathcal{T}_{\text{SE}(3)}(R, p)$, the matrix representation of the Hermitian adjoint map $\text{Ad}_g^*(\cdot)$ is given by

$$\text{Ad}_g^* := \begin{bmatrix} R^\top & -R^\top p^\times \\ 0_{3 \times 3} & R^\top \end{bmatrix}. \quad (2.63)$$

For the sake of simplicity, we denote $(g^{-1})^\top$ as $g^{-\top}$. Then for any $U \in \mathfrak{se}(3)$ and $g \in \text{SE}(3)$, one has

$$\psi_{\mathfrak{se}(3)}(g^\top U g^{-\top}) = \text{Ad}_g^* \psi_{\mathfrak{se}(3)}(U) \quad (2.64)$$

Given any two vectors $r, b \in \mathbb{R}^4$, we define the following wedge product (exterior product) \wedge as

$$b \wedge r := \begin{bmatrix} b_v \times r_v \\ b_s r_v - r_s b_v \end{bmatrix} \in \mathbb{R}^6, \quad (2.65)$$

where $r = (r_v^\top, r_s)^\top, b = (b_v^\top, b_s)^\top$ with $r_v, b_v \in \mathbb{R}^3$ and $r_s, b_s \in \mathbb{R}$.

Lemma 2.4 Consider the wedge product defined in (2.65). For all $r, b \in \mathbb{R}^4, g \in \text{SE}(3)$, one can verify that

$$r \wedge r = 0, \quad (2.66)$$

$$b \wedge r = -r \wedge b, \quad (2.67)$$

$$\psi_{\mathfrak{se}(3)}((I - g)rr^\top) = \frac{1}{2}(gr) \wedge r, \quad (2.68)$$

$$(gb) \wedge (gr) = \text{Ad}_{g^{-1}}^*(b \wedge r). \quad (2.69)$$

Proof See Appendix A.1.

Lemma 2.5 Let \mathcal{M}_0^4 denote the sub-manifold of $\mathbb{R}^{4 \times 4}$, defined as

$$\mathcal{M}_0^4 := \left\{ M \mid M = \begin{bmatrix} M_1 & m_2 \\ 0_{1 \times 3} & 0 \end{bmatrix}, M_1 \in \mathbb{R}^{3 \times 3}, m_2 \in \mathbb{R}^3 \right\}.$$

Then, for all $g \in \text{SE}(3), M, \bar{M} \in \mathcal{M}_0^4$ and $A \in \mathbb{R}^{4 \times 4}$, the following properties hold

$$MA \in \mathcal{M}_0 \quad (2.70)$$

$$gM \in \mathcal{M}_0 \quad (2.71)$$

$$\mathbb{P}_{\mathfrak{se}(3)}(gM) = \mathbb{P}_{\mathfrak{se}(3)}(g^{-\top}M), \quad (2.72)$$

$$\text{tr}(g^\top g M \bar{M}^\top) = \text{tr}(M \bar{M}^\top), \quad (2.73)$$

$$\psi_{\mathfrak{se}(3)}(g^\top g M) = \psi_{\mathfrak{se}(3)}(M), \quad (2.74)$$

$$\text{Ad}_g^* \psi_{\mathfrak{se}(3)}(M) = \psi_{\mathfrak{se}(3)}(g^\top M g^{-\top}). \quad (2.75)$$

Proof See Appendix A.2.

Note that from the definition of $\mathfrak{se}(3)$ in (2.51), one has $\mathfrak{se}(3) \subset \mathcal{M}_0^4$. Moreover, one can show that (2.64) is a special case of (2.75).

2.3.3 Pose and linear velocity on Lie group $\text{SE}_2(3)$

We consider the extended Special Euclidean group of order 3 introduced in [Barrau and Bonnabel, 2017] as $\text{SE}_2(3) := \text{SO}(3) \times \mathbb{R}^3 \times \mathbb{R}^3 \subset \mathbb{R}^{5 \times 5}$, which is defined as

$$\text{SE}_2(3) := \{X = \mathcal{T}_{\text{SE}_2(3)}(R, v, p) \mid R \in \text{SO}(3), p, v \in \mathbb{R}^3\} \quad (2.76)$$

The map $\mathcal{T}_{\text{SE}_2(3)} : \text{SO}(3) \times \mathbb{R}^3 \times \mathbb{R}^3 \rightarrow \text{SE}_2(3)$ is defined by

$$\mathcal{T}_{\text{SE}_2(3)}(R, v, p) = \begin{bmatrix} R & v & p \\ 0_{1 \times 3} & 1 & 0 \\ 0_{1 \times 3} & 0 & 1 \end{bmatrix}. \quad (2.77)$$

For every $X = \mathcal{T}_{\text{SE}_2(3)}(R, v, p)$, one has the inverse of X as $X^{-1} = \mathcal{T}_{\text{SE}_2(3)}(R^\top, -R^\top v, -R^\top p)$. Denote $T_X \text{SE}_2(3) \in \mathbb{R}^{5 \times 5}$ as the tangent space of $\text{SE}_2(3)$ at point X . The Lie algebra of $\text{SE}_2(3)$, denoted by $\mathfrak{se}_2(3)$, is given by

$$\mathfrak{se}_2(3) := \left\{ U = \begin{bmatrix} \Omega & \alpha & v \\ 0_{2 \times 3} & 0_{2 \times 3} & 0_{2 \times 3} \end{bmatrix} \in \mathbb{R}^{5 \times 5} \mid \Omega \in \mathfrak{so}(3), v, \alpha \in \mathbb{R}^3 \right\},$$

with $\mathfrak{so}(3)$ defined in (2.12). Let $\mathbb{P}_{\mathfrak{se}_2(3)} : \mathbb{R}^{5 \times 5} \rightarrow \mathfrak{se}_2(3)$ denote the projection of A on the Lie algebra $\mathfrak{se}_2(3)$, such that, for all $A_1 \in \mathbb{R}^{3 \times 3}, a_2, \dots, a_5 \in \mathbb{R}^3$ and $a_6, \dots, a_9 \in \mathbb{R}$, one has

$$\mathbb{P}_{\mathfrak{se}_2(3)} \left(\begin{bmatrix} A_1 & a_2 & a_3 \\ a_4^\top & a_6 & a_7 \\ a_5^\top & a_8 & a_9 \end{bmatrix} \right) = \begin{bmatrix} \mathbb{P}_{\mathfrak{so}(3)}(A_1) & a_2 & a_3 \\ 0_{1 \times 3} & 0 & 0 \\ 0_{1 \times 3} & 0 & 0 \end{bmatrix}. \quad (2.78)$$

For all $U \in \mathfrak{se}_2(3)$, $A \in \mathbb{R}^{5 \times 5}$ one has $\langle\langle A, U \rangle\rangle = \langle\langle U, \mathbb{P}_{\mathfrak{se}_2(3)}(A) \rangle\rangle = \langle\langle \mathbb{P}_{\mathfrak{se}_2(3)}(A), U \rangle\rangle$. Given a rigid body with configuration $X \in \text{SE}_2(3)$, the adjoint map $\text{Ad} : \text{SE}_2(3) \times \mathfrak{se}_2(3) \rightarrow \mathfrak{se}_2(3)$ is given by

$$\text{Ad}_X U := XUX^{-1}, \quad X \in \text{SE}_2(3), U \in \mathfrak{se}_2(3). \quad (2.79)$$

For all $X_1, X_2 \in \text{SE}_2(3), U \in \mathfrak{se}_2(3)$, one can verify that $\text{Ad}_{X_1} \text{Ad}_{X_2} U = \text{Ad}_{X_1 X_2} U$.

2.4 Inertial navigation systems

2.4.1 Dynamic model for INNs

Let $R \in \text{SO}(3)$ be the rotation that describes the orientation of the body-fixed frame \mathcal{B} with respect to the inertial frame \mathcal{I} . Also, let $\omega \in \mathbb{R}^3$ be the angular velocity of the body-fixed frame with respect to the inertial frame \mathcal{I} , expressed in the body-fixed frame \mathcal{B} . The dynamics of the attitude R are governed by

$$\dot{R} = R\omega^\times \quad (2.80)$$

where $(\cdot)^\times$ denotes the skew-symmetric map defined in (2.13). Let $p \in \mathbb{R}^3$ denote the position of the center of gravity of the rigid body expressed in the inertial frame \mathcal{I} , and let $\bar{v} \in \mathbb{R}^3$ denote the liner velocity of the center of gravity of the rigid body expressed in the body-fixed frame \mathcal{B} . The dynamics of p are given by

$$\dot{p} = R\bar{v}. \quad (2.81)$$

Let $g = \mathcal{T}_{\text{SE}(3)}(R, p) \in \text{SE}(3)$ be the pose of the rigid body with the map $\mathcal{T}_{\text{SE}(3)}$ defined in (2.49). Then, in view of (2.80) and (2.81), the dynamics of the pose g are given by

$$\dot{g} = g\xi^\wedge. \quad (2.82)$$

where $\xi = [\omega^\top, \bar{v}^\top]^\top \in \mathbb{R}^6$ denotes the group velocity on $\text{SE}(3)$ and the map $(\cdot)^\wedge$ is defined in (2.52). Let $v \in \mathbb{R}^3$ be the linear velocity expressed in the inertial frame \mathcal{I} . Then, the relation between v and \bar{v} is given by $v = R\bar{v}$. Therefore, the dynamics of the inertial navigation system are given by

$$\dot{R} = R\omega^\times \quad (2.83)$$

$$\dot{p} = v \quad (2.84)$$

$$\dot{v} = g + Ra \quad (2.85)$$

where \mathbf{g} denotes the gravity vector expressed in the inertial frame, and $a \in \mathbb{R}^3$ denotes the body-frame “apparent acceleration” capturing all non-gravitational forces applied to the rigid body expressed in the body-fixed frame. Let $X = \mathcal{T}_{\text{SE}_2(3)}(R, v, p)$ with the map $\mathcal{T}_{\text{SE}_2(3)}$ defined in (2.77). We consider the configuration of the rigid body represented by an element of the matrix Lie group $X \in \text{SE}_2(3)$. Let us introduce the nonlinear map $f : \text{SE}_2(3) \times \mathbb{R}^3 \times \mathbb{R}^3 \rightarrow T_X \text{SE}_2(3)$, such that the kinematics (2.83)-(2.85) can be rewritten in the following compact form [Barrau and Bonnabel, 2017]:

$$\dot{X} = f(X, \omega, a) := \begin{bmatrix} R\omega^\times & \mathbf{g} + Ra & v \\ 0_{1 \times 3} & 0 & 0 \\ 0_{1 \times 3} & 0 & 0 \end{bmatrix}. \quad (2.86)$$

Let $X_1, X_2 \in \text{SE}_2(3)$ be two distinct trajectories. The dynamics of the right-invariant error $\eta := X_1 X_2^{-1}$ are given by

$$\dot{\eta} = f(\eta, \omega, a) - \eta f(I, \omega, a), \quad (2.87)$$

which implies that the right-invariant error η has a state-trajectory independent propagation [Barrau and Bonnabel, 2017].

2.4.2 Inertial-vision systems

Throughout this thesis, some experimental results are presented using inertial-vision systems. Hence, the inertial-vision systems considered in this work will be discussed in this subsection. In GPS-denied environments, such as indoor applications, recovering the position and linear velocity is a challenging task. Recently, inertial-vision systems combining a low-cost IMU and on-board cameras have made their appearance in the literature.



Figure 2.2: Examples of inertial-vision system: Visual-Inertial Sensor [Nikolic et al., 2014] (left) and Intel RealSense Depth Camera D435i (right).

In robotic systems, IMU is instrumental to measure the motion changes with respect to an inertial frame. An IMU usually consists of a three-axis gyroscope, a three-axis accelerometer and a three-axis magnetometer. The measurement models of the IMU are described as follows:

- The gyroscope measures the angular velocity of a rigid body relative to the inertial frame expressed in the body-fixed frame \mathcal{B} :

$$\omega_y = \omega + b_\omega + n_g \quad (2.88)$$

where ω is the actual angular velocity expressed in the body-fixed frame, b_ω and n_g denote the constant (or slowly time-varying) gyro bias and the additive measurement noise, respectively.

- The accelerometer measures the instantaneous linear acceleration of a rigid body expressed in the body-fixed frame \mathcal{B} :

$$a_y = R^\top(\dot{v} - \mathbf{g}) + b_a + n_a \quad (2.89)$$

where R is the rotation matrix, \dot{v} is the derivative of the linear velocity expressed in the inertial frame, and b_a and n_a denote the bias term and the additive measurement noise, respectively. When the linear velocity is constant or slowly time-varying (*i.e.*, $\dot{v} \approx 0$), the measurements of the accelerometer can be simplified as follows:

$$a_y = R^\top \mathbf{g} + b_a + n_a \quad (2.90)$$

- The magnetometer provides measurements of the ambient magnetic field, which is defined by

$$m_y = D_m R^\top m_{\mathcal{I}} + b_m + n_m \quad (2.91)$$

where D_m is the distortion matrix, $m_{\mathcal{I}}$ is the Earth's magnetic field vector (expressed in the inertial frame), b_m is the body-fixed frame expression of the local magnetic disturbance, and n_m is the measurement noise. The distortion matrix D_m and magnetic disturbance b_m are very sensitive to the local magnetic field. With the well-calibrated distortion matrix D_m and local magnetic disturbance b_m , the magnetometer measurements can be corrected as follows:

$$m_y = R^\top m_{\mathcal{I}} + D_m^{-1} n_m \quad (2.92)$$

The calibration of the gyroscope, accelerometer and magnetometer are instrumental in practical applications. The reader can find more information in [Batista et al., 2010; Foster and Elkaim, 2008; Barczyk, 2012; Olivares et al., 2009] and references therein.

In the rest of this subsection, a geometric model of the stereo vision system is discussed and the three-dimensional position reconstruction from stereo images are provided. We define an image I_m by a map of a two-dimensional surface of pixels brightness [0, 255]. Define $z = [u, v, 1]^\top \in \mathbb{R}^3$ as the coordinates of a pixel. The origin $z_0 = [0, 0, 1]^\top$ is conveniently associated to the top-left pixel of the image. Consider a frame \mathcal{C} attached to the camera's optical center, and the three-dimensional camera-frame coordinate of a point p_i (coordinate in the inertial frame) defined by $p_i^{\mathcal{C}} = [p_{i,x}^{\mathcal{C}}, p_{i,y}^{\mathcal{C}}, p_{i,z}^{\mathcal{C}}]^\top$. Then the geometric measurement model of a pinhole camera is given by

$$z_i = \begin{bmatrix} u_i \\ v_i \\ 1 \end{bmatrix} = \frac{1}{p_{i,z}^{\mathcal{C}}} \begin{bmatrix} 1/\rho_x & 0 & u_c \\ 0 & 1/\rho_y & v_c \\ 0 & 0 & 1 \end{bmatrix} \begin{bmatrix} f & 0 & 0 \\ 0 & f & 0 \\ 0 & 0 & 1 \end{bmatrix} p_i^{\mathcal{C}} \quad (2.93)$$

where ρ_x, ρ_y are the width and height of each pixel respectively, f is the focal length expressed in pixels, and (u_c, v_c) are the coordinates of the camera's principal point, w.r.t.

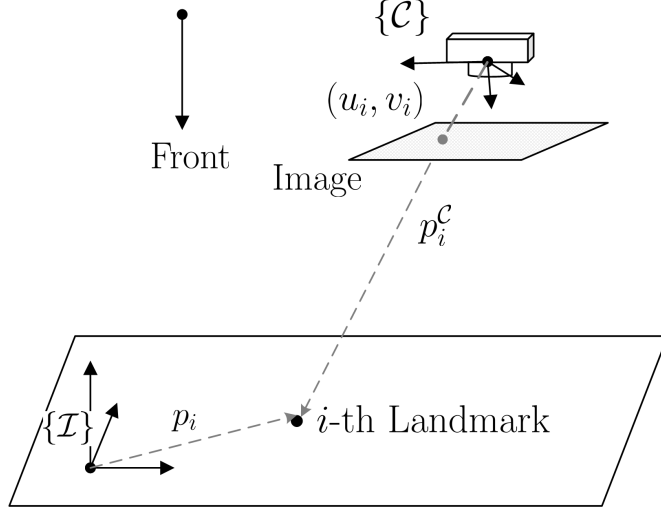


Figure 2.3: Geometric model of a pinhole camera

the center of the image in pixels. We define the following intrinsic matrix parameter of the camera:

$$\mathcal{K} := \begin{bmatrix} \frac{1}{\rho_x} & 0 & u_c \\ 0 & \frac{1}{\rho_y} & v_c \\ 0 & 0 & 1 \end{bmatrix} \begin{bmatrix} f & 0 & 0 \\ 0 & f & 0 \\ 0 & 0 & 1 \end{bmatrix} = \begin{bmatrix} \frac{f}{\rho_x} & 0 & u_c \\ 0 & \frac{f}{\rho_y} & v_c \\ 0 & 0 & 1 \end{bmatrix} \quad (2.94)$$

We consider the model of a stereo camera given in Figure 2.4. Let p_i be the coordinate of the i -th landmark expressed in the inertial frame \mathcal{I} . Then, the coordinate of the i -th landmark expressed in the body-fixed frame \mathcal{B} is given by $p_i^{\mathcal{B}} := R^{\top}(p_i - p)$. Let \mathcal{C}_L and \mathcal{C}_R be the frames attached to the left camera and the right camera, respectively. The position of the i -th landmark expressed in the left (or right) camera frames is defined as $p_i^{\mathcal{C}_L} := R_{cL}^{\top}(p_i^{\mathcal{B}} - p_L)$ (or $p_i^{\mathcal{C}_R} := R_{cR}^{\top}(p_i^{\mathcal{B}} - p_R)$) with (R_{cL}, p_L) (or (R_{cR}, p_R)) being the homogeneous transformation from the body-fixed frame to the left (or right) camera frame, respectively. Define the pixels measurement of the i -th landmark in the left and right images as (u_i^L, v_i^L) and (u_i^R, v_i^R) , respectively. The measurement of the stereo camera is given as follows:

$$z_i^L := \begin{bmatrix} u_i^L \\ v_i^L \\ 1 \end{bmatrix} = \lambda_L \mathcal{K}_L p_i^{\mathcal{C}_L}, \quad z_i^R := \begin{bmatrix} u_i^R \\ v_i^R \\ 1 \end{bmatrix} = \lambda_R \mathcal{K}_R p_i^{\mathcal{C}_R}, \quad (2.95)$$

with some scalars $\lambda_L, \lambda_R > 0$ and $\mathcal{K}_L, \mathcal{K}_R \in \mathbb{R}^{3 \times 3}$ denoting the intrinsic matrices of the left and right cameras, respectively. Let us introduce the following bearing vector:

$$x_i^L := \frac{p_i^{\mathcal{C}_L}}{\|p_i^{\mathcal{C}_L}\|} = \frac{R_{cL}^{\top}(p_i^{\mathcal{B}} - p_L)}{\|p_i^{\mathcal{B}} - p_L\|}, \quad x_i^R := \frac{p_i^{\mathcal{C}_R}}{\|p_i^{\mathcal{C}_R}\|} = \frac{R_{cR}^{\top}(p_i^{\mathcal{B}} - p_R)}{\|p_i^{\mathcal{B}} - p_R\|} \quad (2.96)$$

where $i = 1, 2, \dots, N$. From (2.95), the bearing vectors $x_i^s \in \mathbb{S}^2$ for all $s \in \{L, R\}$ and $i = 1, 2, \dots, N$ can be rewritten in terms of pixel measurements

$$x_i^L = \frac{1}{\|\mathcal{K}_L^{-1} z_i^L\|} \mathcal{K}_L^{-1} z_i^L, \quad x_i^R = \frac{1}{\|\mathcal{K}_R^{-1} z_i^R\|} \mathcal{K}_R^{-1} z_i^R. \quad (2.97)$$

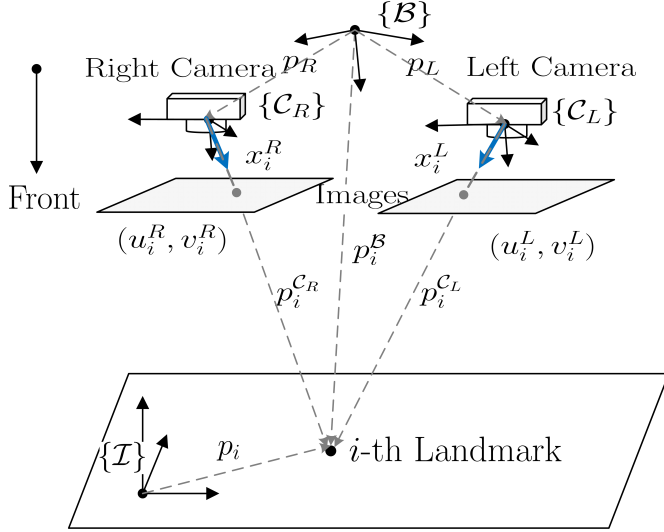


Figure 2.4: Geometric model of stereo camera

Figure 2.5 gives an example of stereo images and the results of feature detection and matching.

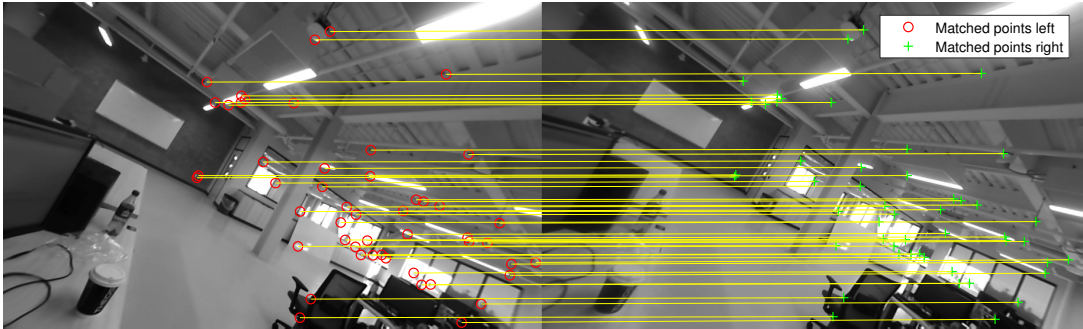


Figure 2.5: Example of stereo images with features detection and matching.

The stereo camera provides the three-dimensional position measurements of the landmarks. For the sake of simplicity, let the left camera be the dominant camera and assume that $R_{cL} = R_{cR}$ with a proper design. Let $b_{LR} = R_{cL}^\top(p_L - p_R)$ be the vector from the left camera to the right camera expressed in the left camera frame, and thus $p_i^{C_R} = p_i^{C_L} + b_{LR}$. Note that (R_{cL}, p_L) and b_{LR} are available from a set of stereo vision calibrations.

Lemma 2.6 *The three-dimensional coordinates p_i^B of the landmark p_i expressed in body-fixed frame \mathcal{B} , can be written in terms of the stereo bearing measurements as*

$$p_i^B = R_{cL} \left(\frac{x_i^L \|b_{LR} \times x_i^R\| + x_i^R \|b_{LR} \times x_i^L\|}{2\|x_i^L \times x_i^R\|} - \frac{1}{2}b_{LR} \right) + p_L \quad (2.98)$$

Proof See Appendix A.3.

The procedure for three-dimensional landmark position measurements are summarized as follows:

- Calibrate the parameters of stereo camera: $\mathcal{K}_L, \mathcal{K}_R, R_{cL}, p_L, b_{LR}$;
- Detect and match the landmarks in left and right images, and then read the pixel measurements (u_i^L, v_i^L) and (u_i^R, v_i^R) ;
- Calculate the stereo bearings x_i^L, x_i^R from (2.97) using pixel measurements in left and right images;
- Calculate the three-dimensional landmark position measurements p_i^B from (2.98).

2.5 Hybrid systems framework

2.5.1 Hybrid systems concepts

In this thesis, we consider the framework of hybrid dynamical systems developed in [Goebel et al., 2009; Goebel et al., 2012]. Let \mathcal{M} be a given manifold embedded in \mathbb{R}^n and $T\mathcal{M}$ be the tangent space of \mathcal{M} . A hybrid system is a dynamical system that contains both continuous flows and discrete jumps of the state. A general model of a hybrid system take the following form:

$$\mathcal{H} : \begin{cases} \dot{x} \in F(x), & x \in \mathcal{F} \\ x^+ \in G(x), & x \in \mathcal{J} \end{cases} \quad (2.99)$$

where

- $\mathcal{F} \subset \mathcal{M}$ is the *flow set*;
- $\mathcal{J} \subset \mathcal{M}$ is the *jump set*;
- The *flow map* $F : \mathcal{M} \rightrightarrows T\mathcal{M}$ describes the continuous flow on \mathcal{F} ;
- The *jump map* $G : \mathcal{M} \rightrightarrows \mathcal{M}$ describes the discrete flow on \mathcal{J} .

Note that \rightrightarrows denotes a set-valued mapping, and x^+ denotes the value x after an instantaneous jump, namely, $x^+ := x(t, j + 1)$ with $x(t, j)$ denoting the value of x before the jump.

The solutions to a hybrid system are obtained on a **hybrid time domain** parametrized by the amount of time spent in the flow set $t \in \mathbb{R}_{\geq 0}$ and by the number of jumps of the state $j \in \mathbb{N}$. Define a hybrid time domain as a subset $E \subset \mathbb{R}_{\geq 0} \times \mathbb{N}$ in the form

$$E = \bigcup_{j=0}^{J-1} ([t_j, t_{j+1}] \times \{j\}),$$

for some finite sequence $0 = t_0 \leq t_1 \leq \dots \leq t_J$, with the “last” interval possibly in the form $([t_{J-1}, t_J] \times \{J\})$ or $([t_{J-1}, +\infty) \times \{J\})$. On each hybrid time domain there is a natural ordering of points : $(t, j) \preceq (t', j')$ if $t \leq t'$ and $j \leq j'$. A hybrid arc is a function $x : \text{dom}x \rightarrow \mathcal{M}$, where $\text{dom}x$ is a hybrid time domain and, for each fixed j , $t \mapsto x(t, j)$

is a locally absolutely continuous function¹ on the interval $I_j = \{t : (t, j) \in \text{dom}x\}$. A hybrid arc x is a solution to the hybrid system \mathcal{H} (see examples in Figure 2.6) if

- $x(0, 0) \in \bar{\mathcal{F}} \cup \mathcal{J}$ with $\bar{\mathcal{F}}$ denoting the closure of \mathcal{F} .
- For all $j \in \mathbb{N}$ such that I^j has a nonempty interior

$$\begin{cases} x(t, j) \in \mathcal{F} & \text{for all } t \in [\min I_j, \sup I_j] \\ \dot{x}(t, j) \in F(x(t, j)) & \text{for almost all } t \in I_j \end{cases} \quad (2.100)$$

- For all $(t, j) \in \text{dom}x$ such that $(t, j+1) \in \text{dom}x$,

$$\begin{cases} x(t, j) \in \mathcal{J} \\ x(t, j+1) \in G(x(t, j)) \end{cases} \quad (2.101)$$

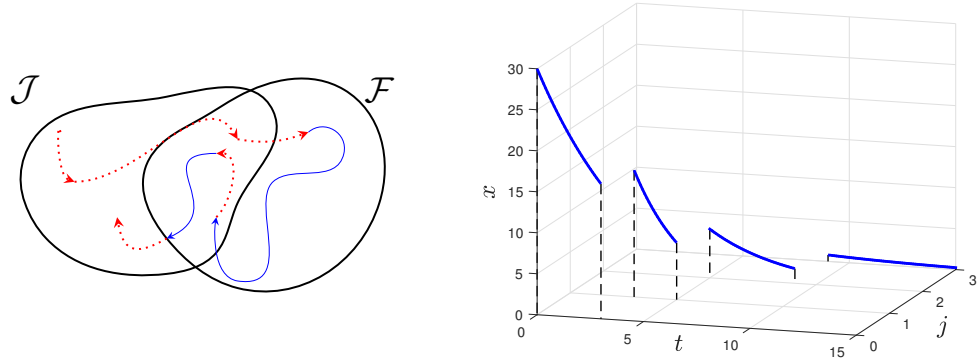


Figure 2.6: Examples of solutions to hybrid systems

A solution x to \mathcal{H} is **maximal** if it cannot be extended by flowing nor jumping, and it is **complete** if its domain $\text{dom}x$ is unbounded, and **precompact** if it is complete and bounded. We denote $\mathcal{S}_{\mathcal{H}}$ as the set of all maximal solutions x to \mathcal{H} , and $x \in \mathcal{S}_{\mathcal{H}}$ means that x is a maximal solution to \mathcal{H} . Three basic conditions/assumptions are introduced to guarantee the existence of solutions, the robustness of stability to small perturbations and other useful properties. The hybrid system \mathcal{H} satisfies the hybrid basic conditions if:

- \mathcal{F} and \mathcal{J} are closed sets in \mathcal{M} (embedded in \mathbb{R}^n).
- $F : \mathcal{M} \rightrightarrows T\mathcal{M}$ is outer semicontinuous² and locally bounded³ relative to \mathcal{F} , and F is nonempty and convex⁴ for every $x \in \mathcal{F}$.

¹A function is locally absolutely continuous if its derivative is continuous for almost all time, and the function can be recovered by integrating the derivative.

²A set-valued mapping $F : X \rightrightarrows Y$ is outer semicontinuous (inner semicontinuous) at x_0 if $\limsup_{x \rightarrow x_0} \subseteq F(x_0)$ ($\liminf_{x \rightarrow x_0} \supseteq F(x_0)$).

³A function $f : X \rightarrow Y$ is said to be locally bounded if for every $x_0 \in X$, there exists an open interval I containing x_0 such that f is uniformly bounded on I .

⁴ $F(x)$ is a convex set if each point on a line connecting two points in $F(x)$ is also in $F(x)$.

- $G : \mathcal{M} \rightrightarrows \mathcal{M}$ is outer semicontinuous and locally bounded relative to \mathcal{J} , and G is nonempty for every $x \in \mathcal{J}$.

2.5.2 Hybrid systems stability

Given a closed set $\mathcal{A} \subset \mathcal{M}$ and a point $x \in \mathcal{M}$, define $|x|_{\mathcal{A}}$ as the distance of $x \in \mathcal{M}$ to \mathcal{A} , that is $|x|_{\mathcal{A}} := \inf_{\bar{x} \in \mathcal{A}} d_{\mathcal{M}}(x, \bar{x})$ with $d_{\mathcal{M}}(\cdot, \cdot) : \mathcal{M} \times \mathcal{M} \rightarrow \mathbb{R}_{\geq 0}$ being a distance between two points on \mathcal{M} .

Definition 2.9 (Uniform global stability concepts [Goebel et al., 2009]) Consider a hybrid system \mathcal{H} in \mathcal{M} . A compact set $\mathcal{A} \subset \mathcal{M}$ is said to be

- uniformly globally stable for \mathcal{H} if there exists a class- \mathcal{K}_{∞} ⁵ α such that any solution x to \mathcal{H} satisfies $|x(t, j)|_{\mathcal{A}} \leq \alpha(|x(0, 0)|_{\mathcal{A}})$ for all $(t, j) \in \text{dom}x$.
- uniformly globally pre-attractive for \mathcal{H} if for each $\epsilon > 0$ and $\delta > 0$ there exists $T > 0$ such that for any solution x to \mathcal{H} with $|x(0, 0)|_{\mathcal{A}} \leq \delta$, $(t, j) \in \text{dom}x$ and $t + j \geq T$ imply $|x(t, j)|_{\mathcal{A}} \leq \epsilon$.
- uniformly globally pre-asymptotically stable for \mathcal{H} if it is both uniformly globally stable and uniformly globally pre-attractive.

Note that the term “*pre*” indicates that maximal solutions are not required to be complete. Assuming that each maximal solution to \mathcal{H} is complete, a compact set $\mathcal{A} \subset \mathcal{M}$ is said to be: globally attractive for \mathcal{H} if $\lim_{t+j \rightarrow \infty} |x(t, j)|_{\mathcal{A}} = 0$; asymptotically stable if it is both stable and attractive [Sanfelice et al., 2007]. Asymptotic stability of a closed set, rather than of an equilibrium point, is considered here since the solutions of a hybrid system often do not settle down to an equilibrium point. Hence, asymptotic stability of an equilibrium point is a special case of asymptotic stability of a closed set.

Consider a continuous function $V : \mathcal{M} \rightarrow \mathbb{R}$, continuously differentiable on a neighborhood of \mathcal{F} . We introduce the following functions:

$$\mu_{\mathcal{J}}(x) = \begin{cases} \max_{x^+ \in G(x)} \{V(x^+) - V(x)\} & \text{if } x \in \mathcal{J} \\ -\infty & \text{otherwise,} \end{cases} \quad (2.102)$$

$$\mu_{\mathcal{F}}(x) = \begin{cases} \max_{v \in F(x)} \langle \nabla V(x), v \rangle & \text{if } x \in \mathcal{F} \\ -\infty & \text{otherwise,} \end{cases} \quad (2.103)$$

The following theorem provides the invariance principle with $\mu_{\mathcal{F}}(x)$ and $\mu_{\mathcal{J}}(x)$ functions.

Theorem 2.1 (Hybrid invariance principle [Goebel et al., 2009]) Consider a function $V : \mathcal{M} \rightarrow \mathbb{R}$, continuously differentiable on a neighborhood of \mathcal{F} . Suppose that for a given set $U \subset \mathcal{M}$,

$$\mu_{\mathcal{F}}(z) \leq 0, \mu_{\mathcal{J}}(z) \leq 0, \forall z \in U \quad (2.104)$$

⁵A class of function from $\mathbb{R}_{\geq 0}$ to $\mathbb{R}_{\geq 0}$ that are continuous, zero at zero, strictly increasing and unbounded.

Let a precompact $x^* \in \mathcal{S}_{\mathcal{H}}$ be such that $\overline{\text{rg}x^*} \subset U$, with $\text{rg}x := x(\text{dom}x)$ being the range of x . Then, for some $r \in V(U)$, x^* approaches the nonempty set which is the largest weakly invariant subset of

$$V^{-1}(r) \cap U \cap \left[\overline{\mu_{\mathcal{F}}^{-1}(0)} \cup (\mu_{\mathcal{J}}^{-1}(0) \cap G(\mu_{\mathcal{J}}^{-1}(0))) \right] \quad (2.105)$$

The following definition of exponential stability is considered, since most of the stability results of the observers designed in this thesis are exponential.

Definition 2.10 (Exponential stability [Teel et al., 2013]) A closed set $\mathcal{A} \subset \mathcal{M}$ is said to be (locally) exponentially stable for the hybrid system \mathcal{H} if there exist strictly positive scalars κ, λ and μ such that, each solution x satisfying $|x(0, 0)|_{\mathcal{A}} < \mu$ also satisfies, for all $(t, j) \in \text{dom}x$,

$$|x(t, j)|_{\mathcal{A}} \leq \kappa \exp(-\lambda(t + j)) |x(0, 0)|_{\mathcal{A}}. \quad (2.106)$$

It is said to be globally exponentially stable if one allows $\mu \rightarrow +\infty$.

Note that the above definition of exponential stability is uniform exponential stability when the scalars κ and λ are independent from the initial conditions. Given $\mu > 0$, define $\mathcal{A} + \mu\mathbb{B} = \{x \in \mathcal{M} : |x|_{\mathcal{A}} < \mu\}$. A sufficient condition for exponential stability is given in the following theorem.

Theorem 2.2 ([Teel et al., 2013]) For the system (2.99), the closed set \mathcal{A} is locally exponentially stable if there exist positive real numbers $\underline{\alpha}, \bar{\alpha}, \lambda_F, \lambda_J, \mu, p$ and a function $V : \text{dom}V \rightarrow \mathbb{R}$, where $\mathcal{F} \cup \mathcal{J} \cup G(\mathcal{J}) \subset \text{dom}V \subseteq \mathcal{M}$, that is continuously differentiable on an open set containing $\overline{\mathcal{F}}$ and satisfies

$$\underline{\alpha}|x|_{\mathcal{A}}^p \leq V(x) \leq \bar{\alpha}|x|_{\mathcal{A}}^p, \quad \forall x \in (\mathcal{F} \cup \mathcal{J} \cup G(\mathcal{J})) \cap (\mathcal{A} + \mu\mathbb{B}), \quad (2.107)$$

$$\langle \nabla V(x), f \rangle \leq -\lambda_F V(x), \quad \mathcal{F} \cap (\mathcal{A} + \mu\mathbb{B}), f \in F(x), \quad (2.108)$$

$$V(g) \leq \exp(-\lambda_J)V(x), \quad \mathcal{J} \cap (\mathcal{A} + \mu\mathbb{B}), g \in G(x), \quad (2.109)$$

If these bounds hold with $\mu = +\infty$ then the set \mathcal{A} is globally exponentially stable.

2.6 Observability and Riccati differential equation

This section reviews some useful observability tools for linear time-varying systems. Consider a generic linear time-varying (LTV) system

$$\begin{aligned} \dot{x} &= A(t)x + B(t)u \\ y &= C(t)x \end{aligned} \quad (2.110)$$

with $x \in \mathbb{R}^n, u \in \mathbb{R}^m, y \in \mathbb{R}^p$, and $A(t) \in \mathbb{R}^{n \times n}, B(t) \in \mathbb{R}^{p \times m}$ and $C(t) \in \mathbb{R}^{m \times n}$ being matrix-valued functions of time t .

In linear systems theory, the system is said to be observable if for any unknown initial state $x(0)$, there exists a finite $t_1 > 0$ such that the knowledge of the input u and

the output y over $[0, t_1]$ suffices to determine uniquely the initial state $x(0)$; Otherwise, the system is said to be unobservable [Chen, 1999]. For linear time-invariant systems, observability is guaranteed if the Kalman rank condition is satisfied. However, for LTV systems, there exist different types of observability properties, for instance, differential, instantaneous, or uniform observability. We are more interested in uniform observability to ensure exponential stability of the estimators derived in this thesis. Suppose that the matrix-valued functions $A(t)$, $B(t)$ and $C(t)$ are continuous and bounded for all $t \geq 0$. Let $\Phi(t, \tau)$ be the **state transition matrix** of $\dot{x} = A(t)x$ such that $\frac{d}{dt}\Phi(t, \tau) = A(t)\Phi(t, \tau)$, $\Phi(t, t) = I_n$ and $\Phi^{-1}(t, \tau) = \Phi(\tau, t)$. The following definition formulates the well-known uniform observability in terms of an associated Gramian matrix:

Definition 2.11 ([Bucy, 1967]) *The pair $(A(t), C(t))$ in (2.110) is uniformly observable if there exist constants $\delta, \mu > 0$ such that*

$$W_O(t, t + \delta) := \frac{1}{\delta} \int_t^{t+\delta} \Phi(\tau, t)^\top C(\tau)^\top C(\tau) \Phi(\tau, t) d\tau \geq \mu I_n, \quad \forall t \geq 0 \quad (2.111)$$

where $W_O(t, t + \delta)$ is called the **Observability Gramian** of system (2.110).

Note that the Observability Gramian $W_O(t, t + \delta)$ is naturally upper bounded by some constant since the matrices $A(t)$ and $C(t)$ are bounded for all $t \geq 0$ by assumption. Some special cases for calculating the state transition matrix $\Phi(t, \tau)$ are given as follows [Aplevich, 2000]:

- If $A(t)$ is a constant matrix, then $\Phi(t, \tau) = \exp(A(t - \tau))$.
- If $A(t)A(\tau) = A(\tau)A(t)$ for every t, τ , then the state transition matrix can be expressed as $\Phi(t, \tau) = \exp(\int_\tau^t A(s)ds)$.
- If $A(t) = \begin{bmatrix} \mathbf{0} & F(t) \\ \mathbf{0} & \mathbf{0} \end{bmatrix}$, then the state transition matrix can be expressed as

$$\Phi(t, \tau) = \begin{bmatrix} I & \int_\tau^t F(s)ds \\ \mathbf{0} & I \end{bmatrix}.$$

The following lemma provides a special case of state transition matrix, which is used throughout this thesis:

Lemma 2.7 *Let $A(t) = S(t) + \bar{A}$ with \bar{A} being a constant matrix. If there exist an invertible matrix-valued function $T(t)$ such that $\dot{T}(t) = S(t)T(t)$ and $T(t)\bar{A} = \bar{A}T(t)$, then the state transition matrix $\Phi(t, \tau)$ associated to $A(t)$ can be expressed as*

$$\Phi(t, \tau) = T(t)\bar{\Phi}(t, \tau)T^{-1}(\tau) \quad (2.112)$$

where $\bar{\Phi}(t, \tau) = \exp(\bar{A}(t - \tau))$ is the state transition matrix associated to \bar{A} .

Proof See Appendix A.4.

Note that finding the matrix-valued function $T(t)$ such that $\dot{T}(t) = S(t)T(t)$ is the key of Lemma (2.7). Two special cases are discussed as follows: If $S(t_1)S(t_2) = S(t_2)S(t_1)$ holds for every $t_1, t_2 \geq 0$, the matrix $T(t)$ can be chosen as $T(t) = \exp(\int_0^t S(\tau)d\tau)$; If $S(t) = \text{blkdiag}((w(t))^\times, (w(t))^\times, \dots, (w(t))^\times)$ with $w \in \mathbb{R}^3$ and $(\cdot)^\times$ defined in (2.13), one can choose $T(t) = \text{blkdiag}(\bar{R}(t), \bar{R}(t), \dots, \bar{R}(t))$ with the rotation matrix \bar{R} generated by $\dot{\bar{R}} = (w(t))^\times \bar{R}(t)$ and $\bar{R}(0) \in \text{SO}(3)$.

In some situations, it is difficult to check condition (2.111) since it requires explicit knowledge of the transition matrix. Suppose that there exists a constant $q \in \mathbb{N}$ such that $A(t)$ and $C(t)$ in (2.110) are q and $q+1$ times continuously differentiable, respectively. The following lemmas provide sufficient conditions for uniform observability in terms of the matrices $A(t)$ and $C(t)$, and their time-derivatives:

Lemma 2.8 ([Bristeau et al., 2010]) *The observability Gramian of system (2.110) satisfies the condition (2.111) if there exists a (strictly) positive constant $\mu > 0$ such that for all $t \geq 0$*

$$\mathcal{O}^\top(t)\mathcal{O}(t) \geq \mu I_n \quad (2.113)$$

where the matrix-valued function \mathcal{O} is defined as

$$\mathcal{O}(t) = \begin{bmatrix} N_0(t) \\ N_1(t) \\ \vdots \\ N_q(t) \end{bmatrix} \quad (2.114)$$

with $N_0(t) = C(t)$ and $N_{k+1}(t) = N_k(t)A(t) + \dot{N}_k(t)$ for all $k = 1, 2, \dots, q$.

Lemma 2.9 ([Scandaroli, 2013]) *The observability Gramian of system (2.110) satisfies the condition (2.111) if the matrix-valued function $\bar{\mathcal{O}}(t)$ composed of row vectors of $\mathcal{O}(t)$ defined in (2.114) is well-defined and bounded for all $t \geq 0$, and there exist some (strictly) positive constants δ, μ such that*

$$\frac{1}{\delta} \int_t^{t+\delta} \det(\bar{\mathcal{O}}^\top(\tau)\bar{\mathcal{O}}(\tau)) d\tau \geq \mu I_n, \quad \forall t \geq 0 \quad (2.115)$$

Note that the condition in Lemma 2.8 is stronger than that in the Lemma 2.9, and can be seen as a special case of Lemma 2.9. Moreover, condition (2.113) is satisfied by checking that matrix $\mathcal{O}(t)$ has full rank for all $t \geq 0$.

We consider the following continuous Riccati equation (CRE):

$$\dot{P} = A(t)P + PA^\top(t) - PC^\top(t)Q(t)C(t)P + V(t), \quad (2.116)$$

where $P(0) \in \mathbb{R}^{n \times n}$ is a symmetric positive definite matrix and $V(t) \in \mathbb{R}^{n \times n}$ and $Q(t) \in \mathbb{R}^{m \times m}$ are uniformly positive definite matrices. To establish global existence, uniqueness and boundedness of the solution to the CRE (2.116), sufficient conditions are presented in the following lemma:

Lemma 2.10 ([Bucy, 1967; Bucy, 1972]) *If there exist constants $\delta, \mu_q, \mu_v > 0$ such that $\forall t \geq 0$*

$$W_V(t, t + \delta) := \frac{1}{\delta} \int_t^{t+\delta} \Phi(t + \delta, \tau) V(\tau) \Phi^\top(t + \delta, \tau) d\tau \geq \mu_v I_n, \quad (2.117)$$

$$W_Q(t, t + \delta) := \frac{1}{\delta} \int_t^{t+\delta} \Phi^\top(\tau, t) C(\tau)^\top Q(\tau) C(\tau) \Phi(\tau, t) d\tau \geq \mu_q I_n, \quad (2.118)$$

there exist positive constants $0 < p_m \leq p_M < \infty$ such that the solution of the CRE (2.116) satisfies $p_m I_n \leq P(t) \leq p_M I_n$ for all $t > \delta$.

Matrix $W_Q(t, t + \delta)$ is called the **Riccati observability Gramian** associated to the triplet (A, C, Q) . Note that if $Q(t) \geq \epsilon I_m > 0$, Riccati observability Gramian condition (2.118) is consequently satisfied from the condition (2.111) since $W_Q(t, t + \delta) \geq \epsilon W_o(t, t + \delta) \geq \epsilon \mu_o I_n$ for all $t \geq 0$. Note that in the traditional Kalman filter, $Q^{-1}(t)$ and $V(t)$ are interpreted as the covariance matrices for the output y and the process.

Assume that there exists a strictly increasing sequence $\{t_j\}_{j \in \mathbb{N}}$ with $t_0 = 0$ and $T_m \leq t_{j+1} - t_j \leq T_M$ with $j \in \mathbb{N}$ and constants $0 < T_m \leq T_M$. In this thesis, we also make use of the following continuous-discrete Riccati equation (CDRE)

$$\dot{P} = A(t)P + PA^\top(t) + V(t), \quad t \in [t_j, t_{j+1}], j \in \mathbb{N}, \quad (2.119)$$

$$P^+ = P - PC^\top(t)(C(t)PC^\top(t) + Q^{-1}(t))^{-1}C(t)P, \quad t \in \{t_j\}, j \in \mathbb{N}_{>0}, \quad (2.120)$$

where $P(0) \in \mathbb{R}^{n \times n}$ is a symmetric positive definite matrix and $V(t) \in \mathbb{R}^{n \times n}$ and $Q(t) \in \mathbb{R}^{m \times m}$ are uniformly positive definite matrices. Note that if $P(t, j)$ denotes the solution of P before a jump, then the solution of P after the jump is denoted as $P^+ = P(t, j+1)$.

Lemma 2.11 *Consider the CDRE (2.119)-(2.120) with $P(0)$ being symmetric positive definite. If $Q(t)$ is positive definite, and $V(t)$ is positive semidefinite, then the solution P to the CDRE is positive definite and well defined on $\mathbb{R}_{\geq 0}$.*

Proof See Appendix A.5.

The following lemma, modified from [Deyst and Price, 1968; Barrau and Bonnabel, 2017], provides sufficient conditions guaranteeing the boundedness and well-conditioning of the solution P to the CDRE (2.119)-(2.120).

Lemma 2.12 ([Deyst and Price, 1968; Barrau and Bonnabel, 2017]) *If there exist constants $\Gamma, \mu_v, \mu_V, \mu_q, \mu_Q > 0$ such that $\forall j \geq 0$*

$$\begin{aligned} \mu_v I &\leq \int_{t_j}^{t_{j+\Gamma}} \Phi(t_{j+\Gamma}, \tau) V(\tau) \Phi^\top(t_{j+\Gamma}, \tau) d\tau \leq \mu_V I \\ \mu_q I &\leq \sum_{i=j}^{j+\Gamma} \Phi^\top(t_i, t_j) C(t_i)^\top Q(t_i) C(t_i) \Phi(t_i, t_j) \leq \mu_Q I \end{aligned}$$

there exist constants $0 < p_m \leq p_M < \infty$ such that the solution of the CDRE (2.119)-(2.120) satisfies $p_m I \leq P \leq p_M I$ for all $t > t_\Gamma$.

Chapter 3

Hybrid Pose Estimation Using Inertial and Landmark Position Measurements

3.1 Introduction

In this chapter, the problem of pose and velocity-bias estimation on $\text{SE}(3) \times \mathbb{R}^6$, using inertial and landmark position measurements, is considered. Recently, nonlinear invariant observers on the Lie group $\text{SE}(3)$ have made their appearance in the literature [Baldwin et al., 2007; Hua et al., 2011; Vasconcelos et al., 2010; Khosravian et al., 2015b; Hua et al., 2015]. These smooth invariant observers are shown to be almost globally asymptotically stable. To overcome the above mentioned topological obstruction to global asymptotic stability of $\text{SE}(3)$ ¹, we propose a generic hybrid estimation scheme (depending on a generic potential function on $\text{SE}(3)$) evolving on $\text{SE}(3) \times \mathbb{R}^6$ for pose and velocity-bias estimation. Unlike the exiting results in the literature, the proposed hybrid observer is shown to be globally exponentially stable. To the best of our knowledge, there is no work in the literature achieving such results on the matrix Lie group $\text{SE}(3)$. The proposed hybrid estimation scheme, uses a new observer-state jump mechanism, inspired from [Berkane and Tayebi, 2017a], which changes directly the observer state through appropriate jumps in the direction of a decreasing potential function on $\text{SE}(3)$. The jump transitions occur when the pose estimation error is close to an undesired critical point of the potential function on $\text{SE}(3)$. It is important to point out that the proposed observer-state jump mechanism is different from the approaches used in [Mayhew and Teel, 2011a; Wu et al., 2015; Berkane et al., 2017a] which consist in incorporating the jumps in the observer's correcting term derived from a family of synergistic potential functions.

Next, an explicit hybrid observer for pose and velocity-bias estimation relying on inertial and landmark position measurements is proposed, which is shown to have global exponential stability guarantees. However, the error dynamics of the rotation and po-

¹This topological obstruction to global asymptotic stability is mainly due to the Lie group $\text{SO}(3)$ which is embedded in $\text{SE}(3)$. More details about the topological obstructions on $\text{SO}(3)$ can be found in [Morse, 1934; Ljusternik and Schnirelmann, 1934; Koditschek, 1989].

sition, from the proposed explicit hybrid observer, are coupled when the inertial and landmark position measurements are used directly. This means that a large position estimation error may drive the estimated rotation error far away from the identity on $\text{SO}(3)$. To solve this problem, the explicit hybrid observer is re-designed using modified landmarks, leading to a decoupled rotational error dynamics from the translation error dynamics in the bias-free case. Finally, to fully solve the coupling issue in the presence of biased linear and angular velocities, we propose a practically implementable version of the proposed explicit hybrid observer. These results appeared in our work [Wang and Tayebi, 2017; Wang and Tayebi, 2018c; Wang and Tayebi, 2019a].

3.2 Problem formulation

Let $p \in \mathbb{R}^3$ denote the rigid body position expressed in the inertial frame \mathcal{I} , and $R \in \text{SO}(3)$ the rigid body attitude describing the rotation of frame \mathcal{B} with respect to frame \mathcal{I} . The dynamics of the position p and the attitude R of a rigid body are given by

$$\dot{R} = R\omega^\times \quad (3.1)$$

$$\dot{p} = R\bar{v}, \quad (3.2)$$

where $\omega \in \mathbb{R}^3$ denotes the angular velocity of the body-fixed frame \mathcal{B} with respect to the inertial frame \mathcal{I} , expressed in frame \mathcal{B} , and $\bar{v} \in \mathbb{R}^3$ is the translational linear velocity, expressed in frame \mathcal{B} . Recall that the pose of the rigid body can be represented by $g = \mathcal{T}_{\text{SE}(3)}(R, p) \in \text{SE}(3)$, with the map $\mathcal{T}_{\text{SE}(3)}$ defined in (2.49). Then, the dynamics of the pose g are governed by

$$\dot{g} = g\xi^\wedge, \quad (3.3)$$

where $\xi := (\omega^\top, \bar{v}^\top)^\top \in \mathbb{R}^6$. Note that system (3.3) is left invariant in the sense that it preserves the Lie group invariance properties with respect to constant translation and constant rotation of the body-fixed frame \mathcal{B} . Let the group velocity be piecewise-continuous, and consider the following biased group velocity measurement:

$$\xi_y := \xi + b_\xi, \quad (3.4)$$

where $b_\xi := (b_\omega^\top, b_v^\top)^\top \in \mathbb{R}^6$ denotes the unknown constant group velocity bias, with $b_\omega, b_v \in \mathbb{R}^3$ being the unknown (constant) angular velocity bias and linear velocity bias, respectively. Moreover, a family of n constant homogeneous vectors $r_i \in \mathbb{R}^4, i = 1, 2, \dots, N$, known in the inertial frame \mathcal{I} , are assumed to be measured in frame \mathcal{B} as

$$b_i = h(g, r_i) := g^{-1}r_i, \quad i = 1, 2, \dots, N. \quad (3.5)$$

Note that the *right group action* $h : \text{SE}(3) \times \mathbb{R}^4 \rightarrow \mathbb{R}^4$ satisfies: for all $g_1, g_2 \in \text{SE}(3)$ and $r \in \mathbb{R}^4$, one has $h(g_2, h(g_1, r)) = h(g_1g_2, r)$. Assume that, among the N reference vectors, there are $N_1 \in \mathbb{N}_{>0}$ feature points (or landmarks) and $N_2 \in \mathbb{N}$ inertial vectors with the form

$$r_i = \begin{bmatrix} p_i^\mathcal{I} \\ 1 \end{bmatrix}, i = 1, 2, \dots, N_1 \quad r_{j+N_1} = \begin{bmatrix} v_j^\mathcal{I} \\ 0 \end{bmatrix}, j = 1, 2, \dots, N_2 \quad (3.6)$$

Then, the measurements of the landmarks and inertial vectors defined in (3.5) can be explicitly expressed in terms of inertial and landmark measurements as

$$b_i = \begin{bmatrix} p_i^{\mathcal{B}} \\ 1 \end{bmatrix}, \forall i = 1, 2, \dots, N_1, \quad b_{j+N_1} = \begin{bmatrix} v_j^{\mathcal{B}} \\ 0 \end{bmatrix}, \forall j = 1, 2, \dots, N_2. \quad (3.7)$$

with $p_i^{\mathcal{B}} := R^T(p_i^{\mathcal{I}} - p)$ being the i -th landmark measurement and $v_j^{\mathcal{B}} := R^T v_j^{\mathcal{I}}$ being the j -th inertial vector measurement. Let us introduce a set of scalar weights $\{\alpha_i\}$ with $\alpha_i > 0$ for all $i = 1, 2, \dots, N_1$ and $\sum_{i=1}^{N_1} \alpha_i = 1$. For the sake of simplicity, we introduce the following weighted geometric center of landmarks:

$$p_c^{\mathcal{I}} := \sum_{i=1}^{N_1} \alpha_i p_i^{\mathcal{I}}. \quad (3.8)$$

Assumption 3.1 *Among the n measurements, at least one landmark point is measured, and at least two vectors from the set*

$$V^{\mathcal{I}} := \{\bar{v}_1^{\mathcal{I}}, \dots, \bar{v}_{N_1}^{\mathcal{I}}, v_1^{\mathcal{I}}, \dots, v_{N-N_1}^{\mathcal{I}}\}, \quad \bar{v}_i^{\mathcal{I}} := p_i^{\mathcal{I}} - p_c^{\mathcal{I}}, \forall i = 1, 2, \dots, N_1$$

are non-collinear.

Remark 3.1 *From Assumption 3.1 one verifies that $N_1 \geq 1$ and $N \geq 3$. This assumption is standard in estimation problems in $\text{SE}(3)$, e.g., [Vasconcelos et al., 2010; Hua et al., 2011; Hua et al., 2015], which is satisfied in the following particular cases:*

- Three different landmark points are measured such that the corresponding $\bar{v}_i^{\mathcal{I}}$, $i = 1, 2, 3$, are non-collinear.
- One landmark point and two non-collinear inertial vectors are measured.
- Two different landmark points and one inertial vector are measured such that the corresponding $v_1^{\mathcal{I}}$ and $\bar{v}_i^{\mathcal{I}}$, $i = 1, 2$ are non-collinear.

Some useful properties are presented in the following lemmas whose proofs are given in Appendix B.

Lemma 3.1 *Consider a family of n elements of homogeneous space $r_i \in \mathbb{R}^4$, $i = 1, 2, \dots, N$ defined in (3.6). Given $k_i \geq 0$ for all $i = 1, 2, \dots, N$, define the following matrix*

$$\mathbb{A} := \sum_{i=1}^N k_i r_i r_i^T = \begin{bmatrix} A & b \\ b^T & d \end{bmatrix} \in \mathbb{R}^{4 \times 4}, \quad (3.9)$$

where $A := \sum_{i=1}^{N_1} k_i p_i^{\mathcal{I}} (p_i^{\mathcal{I}})^T + \sum_{j=1}^{N_2} k_{j+N_1} v_j^{\mathcal{I}} (v_j^{\mathcal{I}})^T$, $b := \sum_{i=1}^{N_1} k_i p_i^{\mathcal{I}}$ and $d := \sum_{i=1}^{N_1} k_i$. Then, under Assumption 3.1 the following statements hold:

- 1) $d > 0$.
- 2) Matrix $M := A - bb^T d^{-1}$ is positive semi-definite.

3) Matrix $\bar{M} := \frac{1}{2}(\text{tr}(M)I_3 - M)$ is positive definite.

Lemma 3.2 Let $\mathbb{A} = \sum_{i=1}^N k_i r_i r_i^\top$ with $k_i > 0$ and $r_i \in \mathbb{R}^4, i = 1, 2, \dots, N$. Then, for all $g, \bar{g} \in \text{SE}(3)$, the following identities hold:

$$\text{tr}((I_4 - g)\mathbb{A}(I_4 - g)^\top) = \sum_{i=1}^N k_i \|r_i - g^{-1}r_i\|^2, \quad (3.10)$$

$$\psi_{\text{se}(3)}(\mathbb{P}_{\text{se}(3)}((I_4 - g^{-1})\mathbb{A})) = \frac{1}{2} \sum_{i=1}^N k_i (g^{-1}r_i) \wedge r_i, \quad (3.11)$$

$$\text{Ad}_{\bar{g}}^* \sum_{i=1}^N k_i (\bar{g}g^{-1}r_i) \wedge r_i = \sum_{i=1}^N k_i (g^{-1}r_i) \wedge (\bar{g}^{-1}r_i). \quad (3.12)$$

Lemma 3.3 Let $M = M^\top$ be a positive semi-definite matrix under Assumption 3.1 and \mathbb{U} be a nonempty finite set of unit vectors. Consider the map $\Delta_M : \mathbb{S}^2 \times \mathbb{U} \rightarrow \mathbb{R}$ defined as

$$\Delta_M(u, v) := u^\top (\text{tr}(M_v)I_3 - M_v)u, \quad (3.13)$$

where $M_v := M(I_3 - 2vv^\top)$ and $v \in \mathcal{E}(M)$. Define the constant scalar

$$\Delta_M^* := \min_{v \in \mathcal{E}(M)} \max_{u \in \mathbb{U}} \Delta_M(u, v). \quad (3.14)$$

Then, the following results hold:

1) Let \mathbb{U} be a superset of $\mathbb{E}(M)$ (i.e., $\mathbb{U} \supseteq \mathbb{E}(M)$), then the following inequality holds:

$$\Delta_M^* \geq \begin{cases} \frac{2}{3}\lambda_1^M & \text{if } \lambda_1^M = \lambda_2^M = \lambda_3^M > 0 \\ \min\{2\lambda_1^M, \lambda_3^M\} & \text{if } \lambda_1^M = \lambda_2^M \neq \lambda_3^M > 0 \\ \text{tr}(M) - \lambda_{\max}^M & \text{if } \lambda_i^M \neq \lambda_j^M \geq 0, i \neq j \end{cases} \quad (3.15)$$

2) Let M be a matrix such that $\text{tr}(M) - 2\lambda_{\max}^M > 0$, and let \mathbb{U} be a set that contains any three orthogonal unit vectors in \mathbb{R}^3 , then the following inequality holds:

$$\Delta_M^* \geq \frac{2}{3}(\text{tr}(M) - 2\lambda_{\max}^M). \quad (3.16)$$

Lemma 3.3 provides two approaches for the design of the nonempty finite set \mathbb{U} such that $\Delta_M^* = \min_{v \in \mathcal{E}(M)} \max_{u \in \mathbb{U}} \Delta_M(u, v) > 0$, and the lower bound of Δ_M^* exists. Note that approach 1) can cover most of the cases of matrix M , however it requires the information about the eigenvectors of M . Approach 2) does not need any information about the eigenvectors of M , but it requires a stronger condition $\text{tr}(M) - 2\lambda_{\max}^M > 0$. In practice, one can choose either approach for the design of the set \mathbb{U} as long as the conditions are satisfied.

Assumption 3.2 The pose g and group velocity ξ of the rigid body are uniformly bounded.

Our objective is to design a globally exponentially stable hybrid pose and velocity-bias estimation scheme that provides estimates \hat{g} and \hat{b}_ξ of the pose g and the group velocity-bias b_ξ , respectively, using the available measurements satisfying Assumption 3.1 and Assumption 3.2.

3.3 Gradient-based smooth observer design

In this section, a gradient-based smooth observer, inspired from [Baldwin et al., 2007; Hua et al., 2011; Vasconcelos et al., 2010; Khosravian et al., 2015b; Hua et al., 2015], is considered relying on a generic potential function on $\text{SE}(3)$. Consider a positive-valued continuously differentiable potential function $\mathcal{U} : \text{SE}(3) \rightarrow \mathbb{R}_{\geq 0}$. From the properties of potential function on manifolds, one has $\mathcal{U}(g) \geq 0$ for all $g \in \text{SE}(3)$ and $\mathcal{U}(g) = 0$ if and only if $g = I_4$. We define $\nabla_g \mathcal{U}$ as the gradient of \mathcal{U} at point $g \in \text{SE}(3)$.

Let \hat{g} be the estimate of the pose g , and $\tilde{g} = g\hat{g}^{-1}$ be the geometric pose estimation error on $\text{SE}(3)$. The geometric error \tilde{g} ensures that $\tilde{g} \in \text{SE}(3)$ for all $\hat{g} \in \text{SE}(3)$, and $\tilde{g} = I_4$ if and only if $\hat{g} = g$. Let $\hat{g} := \mathcal{T}_{\text{SE}(3)}(\hat{R}, \hat{p})$ with \hat{R} being the estimate of the attitude R , and \hat{p} being the estimate of the linear position p . Then, $\tilde{g} = \mathcal{T}_{\text{SE}(3)}(\tilde{R}, \tilde{p})$ implies that $\tilde{R} = R\hat{R}^{-1} = R\hat{R}^\top$ and $\tilde{p} = p - R\hat{R}^\top\hat{p}$. The first term \tilde{R} denotes the geometric attitude estimation error on $\text{SO}(3)$ and the second term \tilde{p} denotes the geometric position estimation error. Unlike the classical linear error $p - \hat{p}$, the geometric error $\tilde{p} = R(R^\top p - \hat{R}^\top\hat{p})$ considers the body-fixed frame estimation error expressed in the inertial frame. Let b_ξ denote the estimate of the group velocity bias. Define $\tilde{b}_\xi := \hat{b}_\xi - b_\xi$ as the bias estimation error. A gradient-based continuous observer, motivated from [Hua et al., 2015], is generalized as follows

$$\dot{\hat{g}} = \hat{g}(\xi_y - \hat{b}_\xi + k_\beta \beta)^\wedge \quad (3.17)$$

$$\dot{\hat{b}}_\xi = -\Gamma \sigma_b \quad (3.18)$$

$$\beta := \text{Ad}_{\hat{g}^{-1}} \psi_{\mathfrak{se}(3)}(\tilde{g}^{-1} \nabla_{\tilde{g}} \mathcal{U}), \quad (3.19)$$

$$\sigma_b := \text{Ad}_{\hat{g}}^* \psi_{\mathfrak{se}(3)}(\tilde{g}^{-1} \nabla_{\tilde{g}} \mathcal{U}), \quad (3.20)$$

where $\hat{g}(0) \in \text{SE}(3)$, $\hat{b}_\xi(0) \in \mathbb{R}^6$, $\Gamma \in \mathbb{R}^{6 \times 6}$ and $k_\beta > 0$. The map $\psi_{\mathfrak{se}(3)}$ is given in (2.57), Ad and Ad^* are the adjoint and co-adjoint maps on $\mathfrak{se}(3)$. The dynamics of \hat{g} is essentially a copy of the pose dynamics (3.3), with a bias compensation term \hat{b}_ξ , and an innovation term β . The design of the dynamics of the bias estimate \hat{b}_ξ and the innovation term β , relies on the gradient of the potential function \mathcal{U} .

In view of (3.3), (3.4), (3.17)-(3.20), one has the following closed-loop system:

$$\dot{\tilde{g}} = \tilde{g}(\text{Ad}_{\tilde{g}} \tilde{b}_\xi - k_\beta \psi_{\mathfrak{se}(3)}(\tilde{g}^{-1} \nabla_{\tilde{g}} \mathcal{U}))^\wedge \quad (3.21)$$

$$\dot{\tilde{b}}_\xi = -\Gamma \text{Ad}_{\tilde{g}}^* \psi_{\mathfrak{se}(3)}(\tilde{g}^{-1} \nabla_{\tilde{g}} \mathcal{U}) \quad (3.22)$$

The equilibrium set for (3.21)-(3.22) is given by

$$\Psi_{\mathcal{U}} := \left\{ (\tilde{g}, \tilde{b}_\xi) \in \text{SE}(3) \times \mathbb{R}^6 \mid \psi_{\mathfrak{se}(3)}(\tilde{g}^{-1} \nabla_{\tilde{g}} \mathcal{U}) = 0_{6 \times 1}, \tilde{b}_\xi = 0_{6 \times 1} \right\}. \quad (3.23)$$

Since $\tilde{g}^{-1} \nabla_{\tilde{g}} \mathcal{U} \in \mathfrak{se}(3)$, one concludes that $\nabla_{\tilde{g}} \mathcal{U} = 0$ if and only if $\psi_{\mathfrak{se}(3)}(\tilde{g}^{-1} \nabla_{\tilde{g}} \mathcal{U}) = 0$. Let $C_{\text{SE}(3)} \mathcal{U}$ be the set of all critical points of \mathcal{U} on $\text{SE}(3)$. Then, the equilibrium set $\Psi_{\mathcal{U}}$ defined in (3.23) can be rewritten as

$$\Psi_{\mathcal{U}} = \left\{ (\tilde{g}, \tilde{b}_\xi) \in \text{SE}(3) \times \mathbb{R}^6 \mid \tilde{g} \in C_{\text{SE}(3)} \mathcal{U}, \tilde{b}_\xi = 0_{6 \times 1} \right\}. \quad (3.24)$$

Due to the continuity of the Lie group $\text{SE}(3)$ and the fact that the potential function \mathcal{U} has a unique global minimum at I_4 (*i.e.*, $\mathcal{U}(I_4) = 0$), one has $I_4 \in C_{\text{SE}(3)}\mathcal{U}$, (*i.e.*, $\nabla_{I_4}\mathcal{U} = 0$). Hence, one can conclude that $(I_4, 0) \in \Psi_{\mathcal{U}}$. The following result shows that the equilibrium point $(I_4, 0)$ of system (3.21)-(3.22) is locally asymptotically stable.

Proposition 3.1 *Consider the closed-loop system (3.21)-(3.22) with the gains $\Gamma, k_\beta > 0$. Then, the equilibrium point $(I_4, 0)$ is locally asymptotically stable.*

Proof See Appendix B.4.

Remark 3.2 *Proposition 3.1 provides a local asymptotic stability result using a general potential function \mathcal{U} on $\text{SE}(3)$. As shown in [Koditschek, 1989], no smooth vector field on Lie groups, which are not homeomorphic to \mathbb{R}^n , can have a global attractor. From the Lusternik-Schnirelmann theorem [Ljusternik and Schnirelmann, 1934] and Morse theory [Morse, 1934], there exist at least four critical points for any smooth function on $\text{SO}(3)$. This implies that any smooth potential function on $\text{SE}(3)$, has at least four critical points.*

Remark 3.3 *The best result one can achieve for smooth (time-invariant) observers on $\text{SE}(3)$, is almost globally asymptotically stable. If the potential function \mathcal{U} on $\text{SE}(3)$ and the set of critical points of \mathcal{U} have been specified, almost global asymptotic stability can be shown using similar steps as in the proof of [Hua et al., 2015, Theorem 1].*

3.4 Gradient-based hybrid observer design

In this section, we redesign the estimation scheme for pose and velocity-bias on $\text{SE}(3) \times \mathbb{R}^6$ to guarantee global asymptotic (exponential) stability using the hybrid dynamic framework discussed in Section 2.5.

3.4.1 Generic hybrid pose and velocity-bias estimation filter

Given a nonempty finite set $\mathbb{Q} \subset \text{SE}(3)$, we propose the following generic hybrid pose and velocity-bias estimation scheme relying on a generic potential function on $\text{SE}(3) \times \mathbb{R}^6$:

$$\underbrace{\begin{aligned} \dot{\hat{g}} &= \hat{g}(\xi_y - \hat{b}_\xi + k_\beta \beta)^\wedge \\ \dot{\hat{b}}_\xi &= -\Gamma \sigma_b \end{aligned}}_{(\hat{g}, \hat{b}_\xi) \in \mathcal{F}_o} \quad \underbrace{\begin{aligned} \hat{g}^+ &= g_q^{-1} \hat{g}, g_q \in \gamma(\hat{g}) \\ \hat{b}_\xi^+ &= \hat{b}_\xi \end{aligned}}_{(\hat{g}, \hat{b}_\xi) \in \mathcal{J}_o}, \quad (3.25)$$

$$\beta := \text{Ad}_{\tilde{g}^{-1}} \psi_{\text{se}(3)}(\tilde{g}^{-1} \nabla_{\tilde{g}} \mathcal{U}), \quad (3.26)$$

$$\sigma_b := \text{Ad}_{\tilde{g}}^* \psi_{\text{se}(3)}(\tilde{g}^{-1} \nabla_{\tilde{g}} \mathcal{U}), \quad (3.27)$$

where $\hat{g}(0) \in \text{SE}(3)$, $\hat{b}_\xi(0) \in \mathbb{R}^6$, $\Gamma := \text{diag}(k_\omega I_3, k_v I_3) \in \mathbb{R}^{6 \times 6}$ and $k_\omega, k_v, k_\beta > 0$. The set-valued map $\gamma : \text{SE}(3) \rightrightarrows \mathbb{Q}$ is defined as $\gamma(\hat{g}) := \{g_q \in \mathbb{Q} : g_q = \arg \min_{g_q \in \mathbb{Q}} \mathcal{U}(\tilde{g}g_q)\}$. The flow set \mathcal{F}_o and jump set \mathcal{J}_o are defined by

$$\mathcal{F}_o := \{(\hat{g}, \hat{b}_\xi) \in \text{SE}(3) \times \mathbb{R}^6 : \mathcal{U}(\tilde{g}) - \min_{g_q \in \mathbb{Q}} \mathcal{U}(\tilde{g}g_q) \leq \delta\}, \quad (3.28)$$

$$\mathcal{J}_o := \{(\hat{g}, \hat{b}_\xi) \in \text{SE}(3) \times \mathbb{R}^6 : \mathcal{U}(\tilde{g}) - \min_{g_q \in \mathbb{Q}} \mathcal{U}(\tilde{g}g_q) \geq \delta\}, \quad (3.29)$$

for some $\delta > 0$. The potential function \mathcal{U} , and the parameters δ and the set $\mathbb{Q} \subset \text{SE}(3)$ will be designed later. Note that the vector ξ_y involved in (3.25) is a known bounded function of time. Note also that $\mathcal{U}(\tilde{g})$ and $\mathcal{U}(\tilde{g}g_q)$ involved in (3.28) and (3.29), and $\psi_{\text{se}(3)}(\tilde{g}^{-1}\nabla_{\tilde{g}}\mathcal{U})$ involved in (3.26) and (3.27) can be rewritten in terms of \hat{g} and the available measurements as it is going to be shown later.

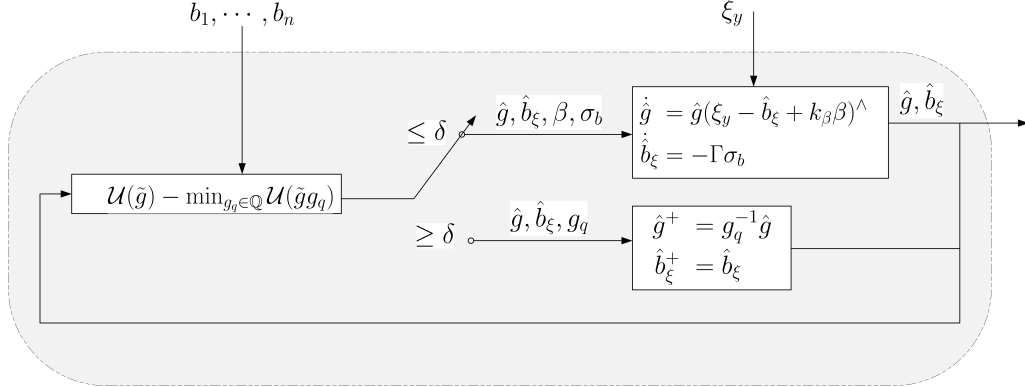


Figure 3.1: Schematic of the proposed hybrid pose and velocity bias observer.

Let us introduce the extended space and state as $\mathcal{S} := \text{SE}(3) \times \mathbb{R}^6 \times \text{SE}(3) \times \mathbb{R}^6 \times \mathbb{R}_{\geq 0}$ and $x := (\tilde{g}, \tilde{b}_\xi, \hat{g}, \hat{b}_\xi, t) \in \mathcal{S}$. In view of (3.3), (3.4), (3.25)-(3.27), one has the following hybrid closed-loop system:

$$\mathcal{H} : \begin{cases} \dot{x} \in F(x) & x \in \mathcal{F}_c := \{x \in \mathcal{S} : (\hat{g}, \hat{b}_\xi) \in \mathcal{F}_o\} \\ x^+ \in G(x) & x \in \mathcal{J}_c := \{x \in \mathcal{S} : (\hat{g}, \hat{b}_\xi) \in \mathcal{J}_o\} \end{cases} \quad (3.30)$$

with

$$F(x) = \begin{pmatrix} \tilde{g}(\text{Ad}_{\tilde{g}}\tilde{b}_\xi - k_\beta\psi_{\text{se}(3)}(\tilde{g}^{-1}\nabla_{\tilde{g}}\mathcal{U}))^\wedge \\ -\Gamma\text{Ad}_{\tilde{g}}^*\psi_{\text{se}(3)}(\tilde{g}^{-1}\nabla_{\tilde{g}}\mathcal{U}) \\ \hat{g}(\xi_y - \hat{b}_\xi + k_\beta\text{Ad}_{\hat{g}^{-1}}\psi_{\text{se}(3)}(\tilde{g}^{-1}\nabla_{\tilde{g}}\mathcal{U}))^\wedge \\ -\Gamma\text{Ad}_{\hat{g}}^*\psi_{\text{se}(3)}(\tilde{g}^{-1}\nabla_{\tilde{g}}\mathcal{U}) \\ 1 \end{pmatrix}, \quad G(x) = \begin{pmatrix} \tilde{g}g_q \\ \tilde{b}_\xi \\ g_q^{-1}\hat{g} \\ \hat{b}_\xi \\ t \end{pmatrix}.$$

Note that the closed-loop system (3.30) satisfies the hybrid basic conditions of [Goebel et al., 2009] and is autonomous. Let $\mathcal{X}_{\mathcal{U}}$ be the set of undesired critical points such that $\mathcal{X}_{\mathcal{U}} = C_{\text{SE}(3)}\mathcal{U}/\{I_4\}$. Define the closed set $\bar{\mathcal{A}} := \{x \in \mathcal{S} : \tilde{g} = I_4, \tilde{b}_\xi = 0_{6 \times 1}\}$ and let $|x|_{\bar{\mathcal{A}}}$ denote the distance to the set $\bar{\mathcal{A}}$ such that $|x|_{\bar{\mathcal{A}}}^2 := \inf_{y=(I_4, 0, \tilde{g}, \tilde{b}_\xi, \tilde{t}) \in \bar{\mathcal{A}}} (\|I_4 - \tilde{g}\|_F^2 + \|\tilde{b}_\xi\|^2 + \|\tilde{g} - \hat{g}\|_F^2 + \|\tilde{b}_a - \hat{b}_\xi\|^2 + \|\tilde{t} - t\|^2) = \|\tilde{g}\|_I^2 + \|\tilde{b}_\xi\|^2$.

Now, one can state one of our main results modified from [Wang and Tayebi, 2017] that provides a hybrid pose and velocity-bias estimation relying on a general potential function on $\text{SE}(3)$.

Theorem 3.1 Consider system (3.30) with a continuously differentiable potential function \mathcal{U} on $\text{SE}(3)$, and choose the nonempty finite \mathbb{Q} and the gap $\delta > 0$ such that

$$\mathcal{U}(\tilde{g}) - \min_{g_q \in \mathbb{Q}} \mathcal{U}(\tilde{g}g_q) > \delta, \quad \forall \tilde{g} \in \mathcal{X}_{\mathcal{U}} \quad (3.31)$$

Then, the number of discrete jumps is finite and the equilibrium set $\bar{\mathcal{A}}$ is globally asymptotically stable.

Proof See Appendix B.5.

Remark 3.4 The observers proposed in [Baldwin et al., 2007; Baldwin et al., 2009; Hua et al., 2011; Vasconcelos et al., 2010; Hua et al., 2015] are shown to guarantee almost global asymptotic stability due to the topological obstruction when considering continuous time-invariant state observers on $\text{SE}(3)$. The proposed hybrid observer in Theorem 1, uses a new switching mechanism, inspired from [Berkane and Tayebi, 2017a], which changes directly the observer state through appropriate jumps in the direction of a decreasing potential function on $\text{SE}(3)$. The jump transitions occur when the estimation error is close to the critical points. This resetting mechanism is different from the approach used in [Wu et al., 2015; Berkane et al., 2016] which consists in incorporating the jumps in the observer's correcting term.

The following theorem provides sufficient conditions on a general potential function on $\text{SE}(3)$ for global exponential stability of the hybrid system (3.30).

Theorem 3.2 Consider system (3.30) with a continuously differentiable potential function \mathcal{U} on $\text{SE}(3)$, and choose the nonempty finite \mathbb{Q} and the gap $\delta > 0$ such that:

$$\alpha_1 |\tilde{g}|_I^2 \leq \mathcal{U}(\tilde{g}) \leq \alpha_2 |\tilde{g}|_I^2, \quad x \in \mathcal{S}, \quad (3.32)$$

$$\alpha_3 |\tilde{g}|_I^2 \leq \|\psi_{\text{se}(3)}(\tilde{g}^{-1} \nabla_{\tilde{g}} \mathcal{U})\|^2 \leq \alpha_4 |\tilde{g}|_I^2, \quad x \in \mathcal{F}_c, \quad (3.33)$$

$$\|\text{Ad}_{\tilde{g}}^* \psi_{\text{se}(3)}(\tilde{g}^{-1} \nabla_{\tilde{g}} \mathcal{U})\|^2 \leq \alpha_5 |\tilde{g}|_I^2, \quad x \in \mathcal{F}_c, \quad (3.34)$$

where $\alpha_1, \dots, \alpha_5$ are strictly positive scalars. Let Assumption 3.1 and Assumption 3.2 hold. Then, the number of jumps is finite and for any initial condition $x(0, 0) \in \mathcal{S}$, the solution $x(t, j)$ is complete and there exist $k > 0$ and $\lambda > 0$ (depending on the initial conditions) such that

$$|x(t, j)|_{\bar{\mathcal{A}}} \leq k \exp(-\lambda(t + j)) |x(0, 0)|_{\bar{\mathcal{A}}}, \quad (3.35)$$

for all $(t, j) \in \text{dom}x$.

Proof See Appendix B.6.

Remark 3.5 Theorem 3.2 provides global exponential stability results for the generic estimation scheme (3.25)-(3.29) relying on a generic potential function \mathcal{U} . The flow and jump sets \mathcal{F}_o and \mathcal{J}_o , given in (3.28)-(3.29), depend on some parameters δ and \mathbb{Q} that have to be designed together with the potential function \mathcal{U} such that conditions (3.32)-(3.34) are fulfilled. It is worth pointing out that condition (3.33) implies that the undesired critical points belong to the jump set \mathcal{J}_o . In the next section, we will design \mathcal{U} , δ and \mathbb{Q} such that (3.32)-(3.34) are fulfilled.

3.4.2 Explicit hybrid observers design using the available measurements

In this subsection, we provide an explicit expression for the proposed hybrid observers in terms of inertial and landmark position measurements (see an example of landmark measurements in Figure 3.2). Before proceeding with the design, some useful properties

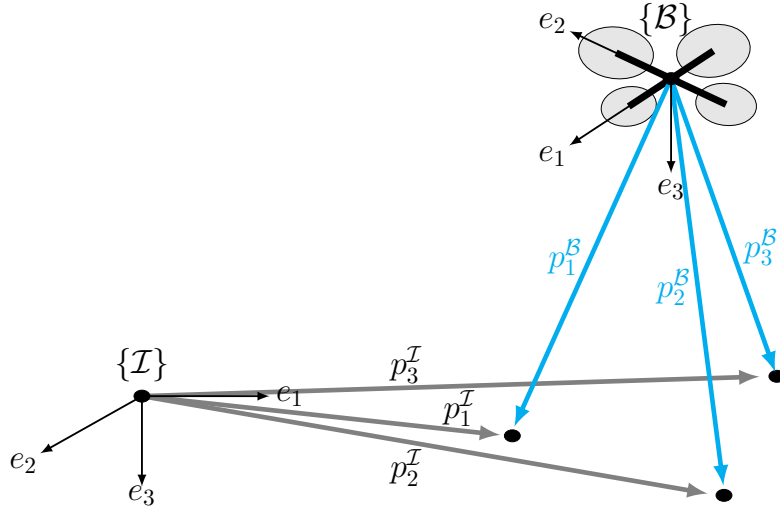


Figure 3.2: The landmarks coordinates in the inertial frame and body frame are represented with gray and blue lines, respectively.

are presented in the following lemmas whose proofs are given in Appendix B.

Lemma 3.4 *Let Assumption 3.1 hold and consider the following smooth potential function on $\text{SE}(3)$:*

$$\mathcal{U}(g) = \frac{1}{2} \text{tr}((I_4 - g)\mathbb{A}(I_4 - g)^\top), \quad (3.36)$$

where the matrix \mathbb{A} is defined in (3.9). For any $g = \mathcal{T}_{\text{SE}(3)}(R, p) \in \text{SE}(3)$, one has

$$\nabla_g \mathcal{U}(g) := g \mathbb{P}_{\text{se}(3)}((I_4 - g^{-1})\mathbb{A}), \quad (3.37)$$

$$\begin{aligned} \Psi_{\mathcal{U}}(g) &:= \{I_4\} \bigcup \left\{ g = \mathcal{T}_{\text{SE}(3)}(R, p) : R = \mathcal{R}_a(\pi, v), \right. \\ &\quad \left. p = (I_3 - \mathcal{R}_a(\pi, v))bd^{-1}, v \in \mathcal{E}(M) \right\}. \end{aligned} \quad (3.38)$$

Lemma 3.5 *Consider the potential function (3.36) under Assumption 3.1. Define the following set:*

$$\mathbb{Q} := \{\mathcal{T}_{\text{SE}(3)}(R, p) \in \text{SE}(3) | R = \mathcal{R}_a(\theta^*, u), p = (I_3 - \mathcal{R}_a(\theta^*, u))bd^{-1}, u \in \mathbb{U}\}. \quad (3.39)$$

where a constant $\theta^* \in (0, \pi]$ and a finite nonempty set $\mathbb{U} = \{u_q | u_q \in \mathbb{S}^2, q = 1, \dots, m\}$. There exist strictly positive scalars $\alpha_1, \alpha_2, \alpha_3$ and α_4 , such that the following inequalities hold:

$$\alpha_1|g|_I^2 \leq \mathcal{U}(g) \leq \alpha_2|g|_I^2, \quad g \in \text{SE}(3) \quad (3.40)$$

$$\alpha_3|g|_I^2 \leq \|\psi_{\text{se}(3)}(g^{-1}\nabla_g \mathcal{U})\|^2 \leq \alpha_4|g|_I^2, \quad g \in \Upsilon \quad (3.41)$$

$$\|\text{Ad}_{g^{-1}}^*\psi_{\text{se}(3)}(g^{-1}\nabla_g \mathcal{U})\|^2 \leq \alpha_4|g|_I^2, \quad g \in \Upsilon. \quad (3.42)$$

where $\Upsilon := \{g \in \text{SE}(3) : \mathcal{U}(g) - \min_{g_q \in \mathbb{Q}} \mathcal{U}(gg_q) \leq \delta\}$ with $\delta < (1 - \cos \theta^*)\Delta_M^*$, \mathbb{U} and Δ_M^* designed as per Lemma 3.3.

In view of (3.5), (3.10) and (3.36), let us introduce the following potential function which can be written in terms of the homogeneous output measurements:

$$\mathcal{U}_1(\tilde{g}) := \frac{1}{2}\text{tr}((I_4 - \tilde{g})\mathbb{A}(I_4 - \tilde{g})^\top) = \frac{1}{2}\sum_{i=1}^N k_i\|r_i - \hat{g}b_i\|^2, \quad (3.43)$$

where the matrix \mathbb{A} is given in (3.9). Making use of (3.11), (3.12) in Lemma 3.2 and (3.37) in Lemma 3.4, one has the following identities:

$$\psi_{\text{se}(3)}(\tilde{g}^{-1}\nabla_{\tilde{g}} \mathcal{U}_1) = \frac{1}{2}\sum_{i=1}^N k_i(\hat{g}b_i) \wedge r_i, \quad (3.44)$$

$$\text{Ad}_{\tilde{g}}^*\psi_{\text{se}(3)}(\tilde{g}^{-1}\nabla_{\tilde{g}} \mathcal{U}_1) = \frac{1}{2}\sum_{i=1}^N k_i b_i \wedge (\hat{g}^{-1}r_i). \quad (3.45)$$

Proposition 3.2 Consider the following hybrid state observer:

$$\underbrace{\begin{array}{lcl} \dot{\hat{g}} &= \hat{g}(\xi_y - \hat{b}_\xi + k_\beta \beta)^\wedge & \hat{g}^+ = g_q^{-1}\hat{g}, g_q \in \gamma(\hat{g}) \\ \dot{\hat{b}}_\xi &= -\Gamma\sigma_b & \hat{b}_\xi^+ = \hat{b}_\xi \end{array}}_{(\hat{g}, \hat{b}_\xi) \in \mathcal{F}_o} \quad , \quad (3.46)$$

$$\beta = \frac{1}{2}\text{Ad}_{\hat{g}^{-1}}\sum_{i=1}^N k_i(\hat{g}b_i) \wedge (r_i), \quad (3.47)$$

$$\sigma_b = \frac{1}{2}\sum_{i=1}^N k_i b_i \wedge (\hat{g}^{-1}r_i). \quad (3.48)$$

Choose the set \mathbb{Q} as per Lemma 3.5. Let Assumption 3.1 and Assumption 3.2 hold. Then, the results of Theorem 3.2 hold.

Proof See Appendix B.9.

Remark 3.6 In view of (3.3), (3.25), (3.47) and (3.48), the rotational and translational error dynamics in the flow \mathcal{F}_c are given by

$$\dot{\tilde{R}} = \tilde{R}(-k_\beta(\psi_{\mathfrak{so}(3)}(M\tilde{R}) + \frac{1}{2}b^\times\tilde{R}^\top\tilde{p}_e) + (\hat{R}\tilde{b}_\omega))^\times, \quad (3.49)$$

$$\dot{\tilde{p}} = -\frac{1}{2}k_\beta d\tilde{p}_e + \tilde{R}(\hat{p}^\times\hat{R}\tilde{b}_\omega + \hat{R}\tilde{b}_v), \quad (3.50)$$

$$\dot{\tilde{b}}_\omega = -k_\omega(\hat{R}^\top((\psi_{\mathfrak{so}(3)}(M\tilde{R}) + \frac{1}{2}b^\times\tilde{R}^\top\tilde{p}_e)) - \frac{1}{2}d\hat{R}^\top\hat{p}^\times\tilde{p}_e) \quad (3.51)$$

$$\dot{\tilde{b}}_v = -\frac{1}{2}k_v d\hat{R}^\top\tilde{p}_e \quad (3.52)$$

where $\tilde{p}_e := \tilde{p} - (I_3 - \tilde{R})bd^{-1}$ and $\tilde{b}_\xi = [\tilde{b}_\omega^\top, \tilde{b}_v^\top]^\top$. The error dynamics (3.49)-(3.50) have the same form as Eq. (23) in [Hua et al., 2011], in the velocity-bias-free case. Note that the dynamics of \tilde{R} and \tilde{p} are coupled as long as $b = dp_c^\mathcal{T} \neq 0$. Therefore, it is expected that noisy or erroneous position measurements would affect the attitude estimation. This motivated us to re-design the estimation scheme in a way that leads to a decoupled rotational error dynamics from the translational error dynamics.

3.5 Decoupling the rotational error dynamics from the translational error dynamics

Define an auxiliary configuration $g_c := \mathcal{T}_{\text{SE}(3)}(I_3, p_c^\mathcal{T})$ with $p_c^\mathcal{T} = \alpha_i p_i^\mathcal{T}$ and $\alpha_i := k_i / \sum_{i=1}^{N_1} k_i$. Consider the modified inertial elements of the homogeneous space \bar{r}_i , defined as $\bar{r}_i := h(g_c, r_i) = g_c^{-1}r_i$, $i = 1, 2, \dots, N$. Define the modified inertial landmarks as $\bar{p}_i^\mathcal{T} := p_i^\mathcal{T} - p_c$. It is clear that $\sum_{i=1}^{N_1} \alpha_i \bar{p}_i^\mathcal{T} = 0$, which implies that the centroid of the weighted modified landmarks coincides with the origin (see, for instance, Figure 3.3). This property is instrumental in achieving a decoupled rotational error dynamics from the translational error dynamics. Note that in [Vasconcelos et al., 2010] this property has been achieved through the choice of the parameters α_i assuming that the landmark points are linearly dependent. Our approach does not put such restrictions on the landmarks and the parameters α_i .

Define the modified pose and pose estimate as $\underline{g} := g_c^{-1}g = \mathcal{T}_{\text{SE}(3)}(R, p - p_c)$ and $\hat{g} := g_c^{-1}\hat{g} = \mathcal{T}_{\text{SE}(3)}(\hat{R}, \hat{p} - p_c)$. Define the new pose estimation error $\tilde{g} := \underline{g}\hat{g}^{-1} = g_c^{-1}g\hat{g}^{-1}g_c$. It is clear that $\tilde{g} = I_4$ if $\underline{g} = I_4$. On the other hand, the new pose estimation error can be rewritten as $\tilde{g} = \mathcal{T}_{\text{SE}(3)}(\underline{R}, \underline{p})$ with $\underline{R} = R\hat{R}^\top = \tilde{R}$ and $\underline{p} = (p - p_c) - R\hat{R}^\top(\hat{p} - p_c) = \tilde{p} - (I_3 - \tilde{R})p_c$. This shows that the new pose estimation error shares the same attitude estimation error \tilde{R} as \tilde{g} , while it involves a new transformed position estimation error \tilde{p} . From the definition of p_c , one can show that $p_c = bd^{-1}$ with vector b and scalar d defined in (3.9). One can also verify that $b_i = h(g_c^{-1}g, \bar{r}_i) = \underline{g}^{-1}\bar{r}_i$ for all $i = 1, 2, \dots, N$. Let us introduce the following potential function:

$$\mathcal{U}_2(\tilde{g}) := \frac{1}{2}\text{tr}((I_4 - \tilde{g})\bar{\mathbb{A}}(I_4 - \tilde{g})^\top) = \frac{1}{2}\sum_{i=1}^N k_i \|\bar{r}_i - \underline{g}b_i\|^2, \quad (3.53)$$

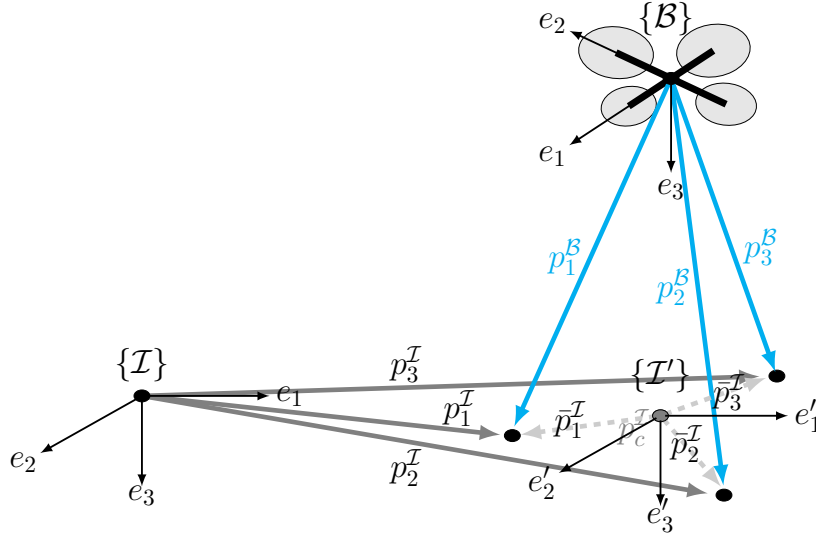


Figure 3.3: The landmarks coordinates in the inertial frame and body frame are represented with gray and blue solid lines, respectively. The landmarks coordinates in the auxiliary frame are represented with dotted lines.

where $\bar{\mathbb{A}} := \sum_{i=1}^N k_i \bar{r}_i \bar{r}_i^\top = \text{diag}(M, d)$. In view of (2.73), (3.43) and (3.53), one can show that, for any $\tilde{g} \in \text{SE}(3)$, $\mathcal{U}_2(\underline{\tilde{g}}) = \mathcal{U}_2(g_c^{-1} \tilde{g} g_c) = \mathcal{U}_1(\tilde{g})$. In the sequel, we will make use of $\mathcal{U}_2(\underline{\tilde{g}})$ and $\mathcal{U}_1(\tilde{g})$ equivalently. Making use of (3.11) in Lemma 3.2 and (3.37) in Lemma 3.4, one can also show that

$$\psi_{\mathfrak{se}(3)}(\underline{\tilde{g}}^{-1} \nabla_{\underline{\tilde{g}}} \mathcal{U}_2) = \frac{1}{2} \sum_{i=1}^N k_i (g_c^{-1} \hat{g} b_i) \wedge (g_c^{-1} r_i), \quad (3.54)$$

Define the extended state $x' := (\underline{\tilde{g}}, \hat{b}, \hat{g}, \hat{b}_\xi, t) \in \mathcal{S}$ and the closed set $\bar{\mathcal{A}}' := \{x' \in \mathcal{S} : \underline{\tilde{g}} = I_4, \hat{b}_\xi = 0_{6 \times 1}\}$. Let $|x'|_{\bar{\mathcal{A}}'}$ denote the distance to the set $\bar{\mathcal{A}}'$ such that $|x'|_{\bar{\mathcal{A}}'}^2 := \inf_{y=(I_4, 0, \hat{g}, \hat{b}_a, \bar{t}) \in \bar{\mathcal{A}'}} (\|I_4 - \underline{\tilde{g}}\|_F^2 + \|\hat{b}_\xi\|^2 + \|\hat{g} - \hat{g}\|_F^2 + \|\hat{b}_a - \hat{b}_\xi\|^2 + \|\bar{t} - t\|^2) = |\underline{\tilde{g}}|_I^2 + \|\hat{b}_\xi\|^2$.

Proposition 3.3 Consider the following hybrid state observer:

$$\underbrace{\begin{aligned} \dot{\hat{g}} &= \hat{g}(\xi_y - \hat{b}_a + k_\beta \beta)^\wedge \\ \dot{\hat{b}}_\xi &= -\Gamma \sigma_b \end{aligned}}_{(\hat{g}, \hat{b}_a) \in \mathcal{F}_o} \quad \underbrace{\begin{aligned} \hat{g}^+ &= g_q^{-1} \hat{g}, g_q \in \gamma(\hat{g}) \\ \hat{b}_\xi^+ &= \hat{b}_a \end{aligned}}_{(\hat{g}, \hat{b}_a) \in \mathcal{J}_o}, \quad (3.55)$$

$$\beta = \frac{1}{2} \text{Ad}_{\hat{g}^{-1} g_c} \sum_{i=1}^N k_i (g_c^{-1} \hat{g} b_i) \wedge (g_c^{-1} r_i) \quad (3.56)$$

$$\sigma_b = \frac{1}{2} \sum_{i=1}^N k_i b_i \wedge (\hat{g}^{-1} r_i). \quad (3.57)$$

Choose the set \mathbb{Q} designed as per Lemma 3.5. Let Assumption 3.1 and Assumption 3.2 hold. Then, the number of jumps is finite and for any initial condition $x'(0, 0) \in \mathcal{S}$, the solution $x'(t, j)$ is complete and there exist $\bar{k} > 0$ and $\bar{\lambda} > 0$ (depending on the initial conditions) such that

$$|x'(t, j)|_{\bar{\mathcal{A}'}} \leq \bar{k} \exp(-\bar{\lambda}(t + j)) |x'(0, 0)|_{\bar{\mathcal{A}'}}, \quad (3.58)$$

for all $(t, j) \in \text{dom}x'$.

Proof The proof is similar to the proof of Proposition 3.2, which is omitted here.

Remark 3.7 Interestingly, in view of (3.11)-(3.12), one obtains the following expression of β :

$$\begin{aligned} \beta &= \frac{1}{2} \text{Ad}_{\hat{g}^{-1}g_c} \sum_{i=1}^N k_i(g_c^{-1}\hat{g}b_i) \wedge (g_c^{-1}r_i) \\ &= \frac{1}{2} \text{Ad}_{\hat{g}^{-1}} \text{Ad}_{g_c} \text{Ad}_{g_c}^* \sum_{i=1}^N k_i(\hat{g}b_i) \wedge (r_i) \end{aligned} \quad (3.59)$$

It is worth pointing that the sole difference between this new observer and the observer in Proposition 1 lies in the definition of β (see (3.47) and (3.59)). In view of (3.3), (3.55)-(3.57), the error dynamics can be written as

$$\dot{\underline{\tilde{R}}} = \tilde{R}(-k_\beta \psi_{\mathfrak{so}(3)}(M\tilde{R}) + (\underline{\tilde{R}}\tilde{b}_\omega))^\times, \quad (3.60)$$

$$\dot{\underline{\tilde{p}}} = -\frac{1}{2}k_\beta d\underline{\tilde{p}} + \tilde{R}(\underline{\tilde{p}}^\times \hat{R}\tilde{b}_\omega + \underline{\tilde{R}}\tilde{b}_v), \quad (3.61)$$

$$\dot{\tilde{b}}_\omega = -k_\omega \left(\hat{R}^\top \psi_{\mathfrak{so}(3)}(M\tilde{R}) - \frac{1}{2}d\hat{R}^\top \underline{\tilde{p}}^\times \hat{R}^\top \underline{\tilde{p}} \right) \quad (3.62)$$

$$\dot{\tilde{b}}_v = -\frac{1}{2}k_v d\hat{R}^\top \hat{R}^\top \underline{\tilde{p}}. \quad (3.63)$$

It is clear that, in the velocity bias-free case, in contrast to (3.49), the dynamics of $\underline{\tilde{R}}$ do not depend on $\underline{\tilde{p}}$ as shown in (3.60), and $\underline{\tilde{p}}$ enjoys exponential stability when $\tilde{b}_\xi = 0_{6 \times 1}$ as it can be seen from (3.61). However, when the velocity bias is considered, the rotational error dynamics is affected by the estimated position \hat{p} involved in the dynamics of \tilde{b}_ω in (3.62). In order to achieve the decoupling property, in the case where the velocity bias is not neglected, the following modified estimation scheme is proposed.

Let us consider the following modified estimation scheme:

$$\underbrace{\begin{aligned} \dot{\hat{g}} &= \hat{g}(\xi_y - \hat{b}_\xi + k_\beta \beta)^\wedge & \hat{g}^+ &= g_q^{-1}\hat{g}, \quad g_q \in \gamma(\hat{g}) \\ \dot{\hat{b}}_\xi &= -\Gamma \sigma_b \end{aligned}}_{(\hat{g}, \hat{b}_\xi) \in \mathcal{F}_o} \quad \underbrace{\begin{aligned} \hat{b}_\xi^+ &= \hat{b}_\xi \end{aligned}}_{(\hat{g}, \hat{b}_\xi) \in \mathcal{J}_o}, \quad (3.64)$$

$$\beta = \frac{1}{2} \text{Ad}_{\hat{g}^{-1}g_c} \sum_{i=1}^N k_i(g_c^{-1}\hat{g}b_i) \wedge (g_c^{-1}r_i), \quad (3.65)$$

$$\sigma_b = \frac{1}{2} \Lambda^\top \sum_{i=1}^N k_i (g_c^{-1} \hat{g} b_i) \wedge (g_c^{-1} r_i). \quad (3.66)$$

where $\Lambda := \text{blkdiag}(\hat{R}, \hat{R})$. In view of (3.3), (3.64)-(3.66) one can write the closed-loop system as an autonomous hybrid system.

$$\mathcal{H}' : \begin{cases} \dot{x}' \in F(x') & x' \in \mathcal{F}'_c := \{x' \in \mathcal{S} : (\hat{g}, \hat{b}_\xi) \in \mathcal{F}_o\} \\ x'^+ \in G(x') & x' \in \mathcal{J}'_c := \{x' \in \mathcal{S} : (\hat{g}, \hat{b}_\xi) \in \mathcal{J}_o\} \end{cases} \quad (3.67)$$

with

$$F(x') = \begin{pmatrix} \underline{\tilde{g}}(\text{Ad}_{\underline{\tilde{g}}} \tilde{b}_\xi - k_\beta \psi_{\mathfrak{se}(3)}(\underline{\tilde{g}}^{-1} \nabla_{\underline{\tilde{g}}} \mathcal{U}_2))^\wedge \\ -\Gamma \Lambda^\top \psi_{\mathfrak{se}(3)}(\underline{\tilde{g}}^{-1} \nabla_{\underline{\tilde{g}}} \mathcal{U}_2) \\ \hat{g}(\xi_y - \hat{b}_\xi + k_\beta \text{Ad}_{\underline{\tilde{g}}^{-1}} \psi_{\mathfrak{se}(3)}(\underline{\tilde{g}}^{-1} \nabla_{\underline{\tilde{g}}} \mathcal{U}_2))^\wedge \\ -\Gamma \Lambda^\top \psi_{\mathfrak{se}(3)}(\underline{\tilde{g}}^{-1} \nabla_{\underline{\tilde{g}}} \mathcal{U}_2) \\ 1 \end{pmatrix}, G(x') = \begin{pmatrix} \underline{\tilde{g}} \bar{g}_q \\ \tilde{b}_\xi \\ g_q^{-1} \hat{g} \\ \hat{b}_\xi \\ t \end{pmatrix}.$$

Now, one can state the following theorem:

Theorem 3.3 Consider the closed-loop system (3.67) with potential function \mathcal{U}_2 in (3.53). Choose the set \mathbb{Q} as per Lemma 3.5. Let Assumption 3.1 and Assumption 3.2 hold. Then, the number of jumps is finite and for any initial condition $x'(0, 0) \in \mathcal{S}$, the solution $x'(t, j)$ is complete and there exist $k' > 0$ and $\lambda' > 0$ (depending on the initial conditions) such that

$$|x'(t, j)|_{\bar{\mathcal{A}'}} \leq k' \exp(-\lambda'(t + j)) |x'(0, 0)|_{\bar{\mathcal{A}'}}, \quad (3.68)$$

for all $(t, j) \in \text{dom}x'$.

Proof See Appendix B.10.

Remark 3.8 From (3.12), (3.65) and (3.66), one can show that

$$\beta = \frac{1}{2} \text{Ad}_{\hat{g}^{-1}} \text{Ad}_{g_c} \text{Ad}_{g_c}^* \sum_{i=1}^N k_i (\hat{g} b_i) \wedge (r_i) \quad (3.69)$$

$$\sigma_b = \frac{1}{2} \Lambda^\top \text{Ad}_{g_c}^* \sum_{i=1}^N k_i (\hat{g} b_i) \wedge (r_i). \quad (3.70)$$

In view of (3.46)-(3.48) and (3.64), (3.69)-(3.70), one can notice that the difference between the observer in Theorem 3.3 and the observer in Proposition 3.2 is related to the terms β and σ_b . It is worth pointing out that the observer in Theorem 3.3, without “hybridation” (i.e., in the flow set), is not gradient-based as observers proposed in Section 3.3 and [Lageman et al., 2010; Hua et al., 2011; Hua et al., 2015; Khosravian et al., 2015b].

Remark 3.9 In view of (3.12), (3.37) and (3.67), one has the following error dynamics in the flows:

$$\dot{\underline{R}} = \tilde{R}(-k_\beta \psi_{\mathfrak{so}(3)}(M\tilde{R}) + \hat{R}\tilde{b}_\omega)^\times, \quad (3.71)$$

$$\dot{\underline{p}} = -\frac{1}{2}k_\beta d\tilde{p} + \tilde{R}(\hat{p}^\times \underline{R}\tilde{b}_\omega + \underline{R}\tilde{b}_v), \quad (3.72)$$

$$\dot{\tilde{b}}_\omega = -k_\omega \underline{R}^\top \psi_{\mathfrak{so}(3)}(M\tilde{R}), \quad (3.73)$$

$$\dot{\tilde{b}}_v = -\frac{1}{2}k_v d\underline{R}^\top \tilde{R}^\top \underline{p}. \quad (3.74)$$

Note that the rotational error dynamics (3.71) together with (3.73) do not depend on the translational estimation, which guarantees the aimed at decoupling property.

3.6 Simulation results

In this section, numerical simulation results are presented to illustrate the performance of the hybrid gradient-based pose observer proposed in Proposition 3.2 and the hybrid decoupled pose observer proposed in Theorem 3.3, referred to, respectively, as HGPO and HDPO. For comparison purposes, we refer to the smooth gradient-based pose observer (*i.e.*, the HGPO in Proposition 3.2 without the jumps) as SGPO.

As commonly used in practical applications, to avoid the bias estimation drift, in the presence of measurement noise, we introduce the following projection mechanism [Ioannou and Sun, 1995]:

$$\mathbf{P}_\delta^\epsilon(\hat{b}, \Gamma\sigma) := \begin{cases} \Gamma\sigma, & \text{if } \hat{b} \in \Pi_\delta \text{ or } \nabla_{\hat{b}}\mathcal{P}^\top \Gamma\sigma \leq 0 \\ \left(I - \varrho_\epsilon(\hat{b})\Gamma \frac{\nabla_{\hat{b}}\mathcal{P}\nabla_{\hat{b}}\mathcal{P}^\top}{\nabla_{\hat{b}}\mathcal{P}^\top \Gamma \nabla_{\hat{b}}\mathcal{P}}\right)\Gamma\sigma, & \text{otherwise} \end{cases}, \quad (3.75)$$

where $\hat{b}, \sigma \in \mathbb{R}^n, \Gamma \in \mathbb{R}^{n \times n}, \mathcal{P}(\hat{b}) := \|\hat{b}\| - \delta, \Pi_\delta := \{\hat{b} | \mathcal{P}(\hat{b}) \leq 0\}$, and $\varrho_\epsilon(\hat{b}) := \min\{1, \mathcal{P}(\hat{b})/\epsilon\}$ for some positive parameters δ and ϵ . Given $\|\hat{b}(0)\| < \Delta$, one can verify that the projection map $\mathbf{P}_\delta^\epsilon$ is locally Lipschitz in its arguments and satisfies the following properties:

- 1) $\|\hat{b}(t)\| \leq \delta + \epsilon$, for all $t \geq 0$;
- 2) $\tilde{b}^\top \Gamma^{-1} \mathbf{P}_\delta^\epsilon(\hat{b}, \Gamma\sigma) \leq \tilde{b}^\top \sigma$ and $\|\mathbf{P}_\delta^\epsilon(\hat{b}, \Gamma\sigma)\| \leq \|\Gamma\sigma\|$.

We consider the case where three inertial vectors $v_1^\mathcal{I} = [0 \ 0 \ 1]^\top, v_2^\mathcal{I} = [\frac{\sqrt{3}}{2} \ \frac{1}{2} \ 0]^\top, v_3^\mathcal{I} = [-\frac{1}{2} \ \frac{\sqrt{3}}{2} \ 0]^\top$ and one landmark $p^\mathcal{I} = [\frac{\sqrt{2}}{2} \ \frac{\sqrt{2}}{2} \ 2]^\top$ are available. The initial pose for all the observers is taken as the identity *i.e.*, $\hat{g}(0) = I_4$. The system's initial conditions are taken as follows: $R(0) = \mathcal{R}_a(\pi, v)$ with $v = [1 \ 0 \ 0]^\top$ and $p(0) = [0 \ 1 \ 4]^\top$. The system is driven by the following linear and angular velocities:

$$v(t) = 2[\cos(t) \ \sin(t) \ 0]^\top \quad \omega(t) = [-\sin(t) \ \cos(t) \ 0]^\top.$$

For the hybrid design, we choose $\theta^* = 2\pi/3$, $\delta = 1$ and $\mathbb{U} = \mathbb{E}(M)$. The gain parameters involved in all the observers are taken as follows: $k_i = 1, i = 1, \dots, 4$, $k_\beta = 1$, $k_\omega = 1$, $k_v = 1$.

Two simulations have been presented using non-noisy output measurements and constant velocity-bias $b_a = [-0.02 \ 0.02 \ 0.1 \ 0.2 \ -0.1 \ 0.01]^\top$, and noisy output measurements output measurements and time-varying velocity-bias $b_a(t) = \cos(0.02t)[-0.02 \ 0.02 \ 0.1 \ 0.2 \ -0.1 \ 0.01]^\top$, respectively. The simulation results with non-noisy output measurements and constant velocity-bias are given in Figure 3.4 - Figure 3.5, and the simulation results with an additive white Gaussian noise of variance 0.1 in the output measurements and time-varying velocity-bias are given in Figure 3.6 - Figure 3.7. From Figure 3.4- Figure 3.7, one can clearly see the improved performance of the decoupled hybrid observer, which is faster as compared to the non-decoupled hybrid observer and non-hybrid observer.

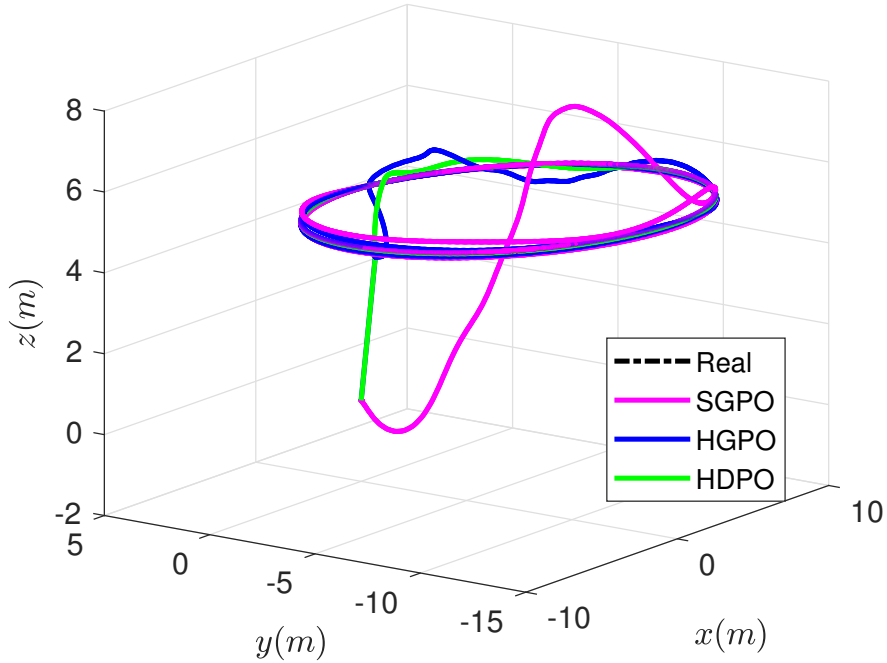


Figure 3.4: Three-dimensional trajectories in the case of noise-free output measurements and constant velocity-bias.

3.7 Conclusion

In this chapter, we addressed the problem of pose and velocity-bias estimation for a rigid body using inertial and landmark position measurements. First, a gradient-based smooth pose and velocity-bias estimation scheme on $\text{SE}(3) \times \mathbb{R}^6$, relying on a general potential function on Lie group $\text{SE}(3)$, was presented. Proposition 3.1 shows that, for any potential function on $\text{SE}(3)$, the gradient-based smooth observer is locally asymptotically stable.

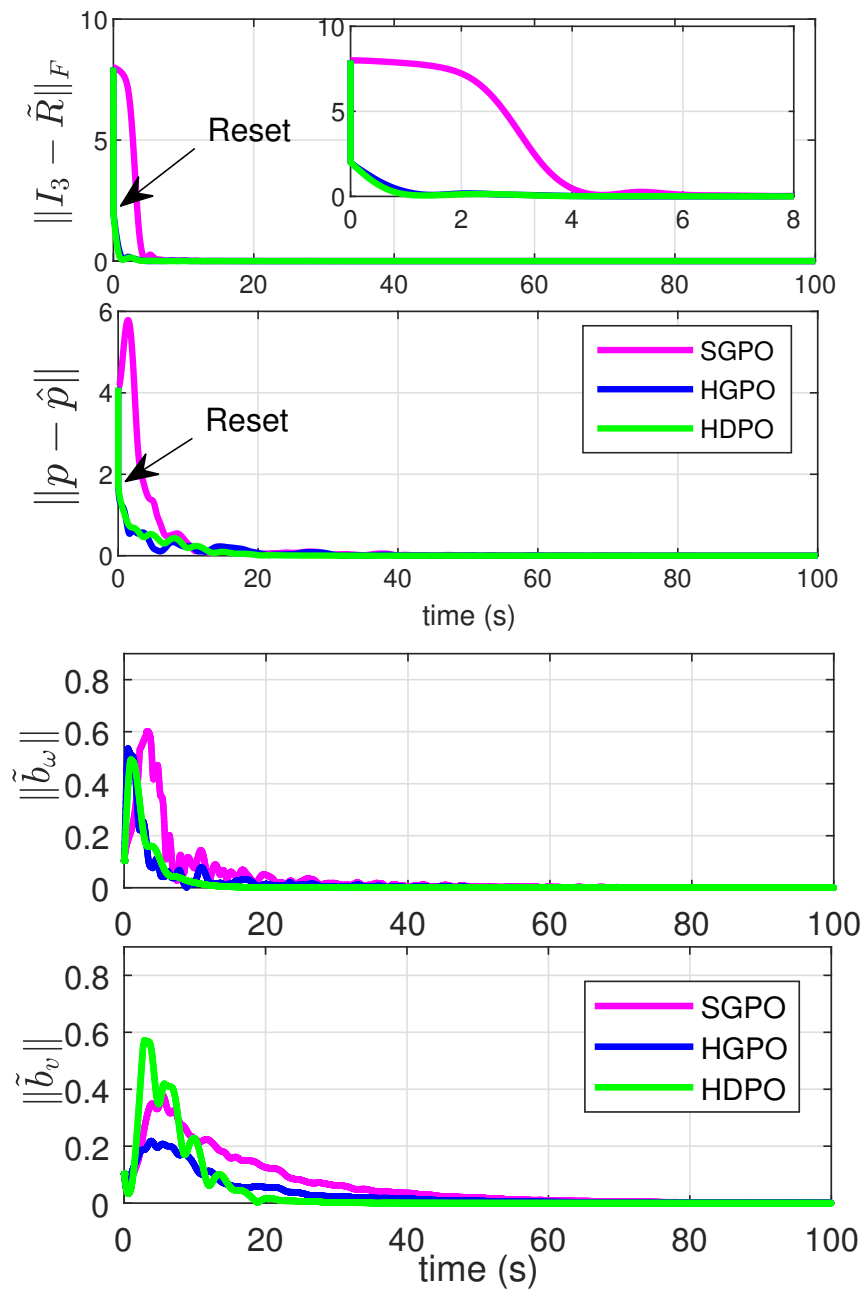


Figure 3.5: Estimation errors in the case of noise-free output measurements and constant velocity-bias.

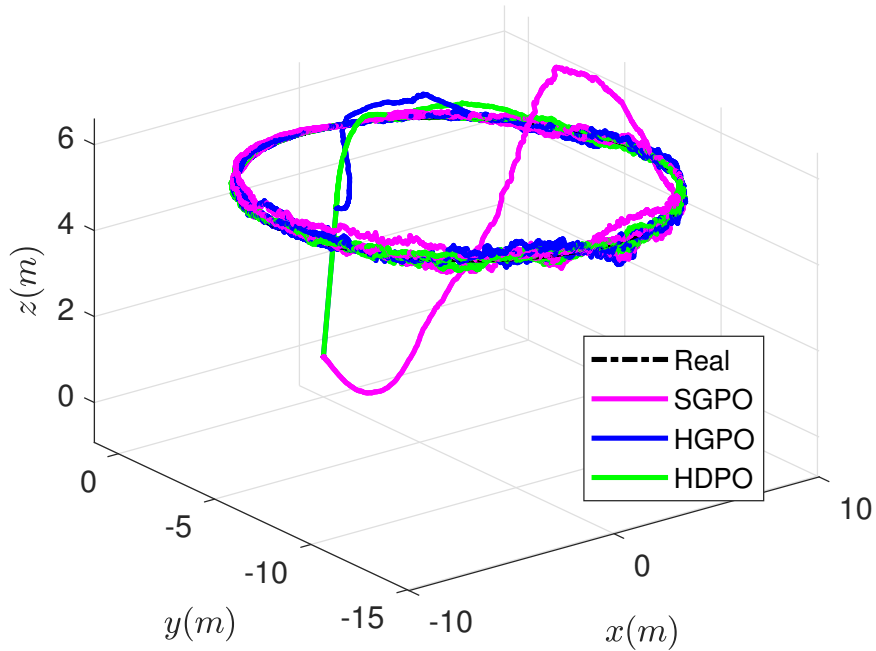


Figure 3.6: Three-dimensional trajectories in the case of an additive white Gaussian noise of variance 0.1 in the output measurements and time-varying velocity-bias.

To overcome the topological obstruction to global asymptotic stability on $\text{SE}(3)$, the gradient-based smooth observer has been extended using the hybrid systems framework. The proposed hybrid gradient-based observer relies on an observer-state jump mechanism designed to avoid the undesired critical points while ensuring a decrease of the potential function in the flow and jump sets. The proposed hybrid observer has been shown to be globally asymptotically stable in Theorem 3.1, relying on a generalized potential function on $\text{SE}(3)$. Moreover, this result was further extended to achieve global exponential stability in Theorem 3.2. Then, the proposed hybrid observer is formulated in terms of homogeneous output measurements of known inertial vectors and landmark points. Proposition 3.2 shows that this explicit hybrid observer guarantees global exponential stability.

The attitude and position error dynamics of the explicit gradient-based hybrid observer are coupled, when applying the landmark position measurements directly. This may deteriorate the performance of the attitude estimation when the position estimation error is large. To overcome this coupling issue, a coordinate transformation on the landmarks is introduced. A new hybrid observer using the modified landmarks has been proposed in Theorem 3.3 with global exponential stability guarantees. Finally, a modified observer, leading to a decoupled rotational error dynamics from the translational error dynamics, is proposed. This modified hybrid observer is also shown to be globally exponentially stable in Theorem 3.3. Simulation results with noise-free and noisy output measurements, illustrating the performance of the proposed hybrid observers, have been provided.

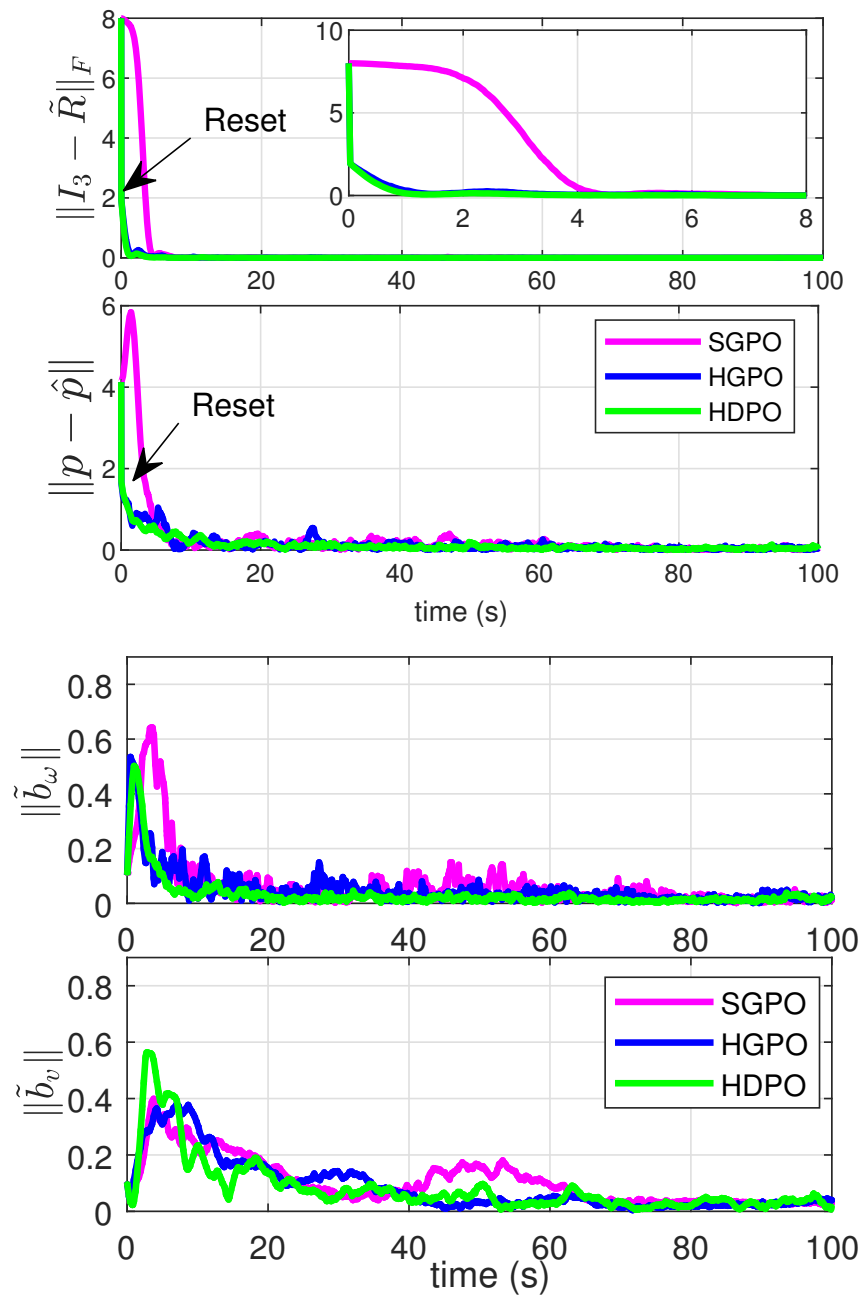


Figure 3.7: Estimation errors in the case of an additive white Gaussian noise of variance 0.1 in the output measurements and time-varying velocity-bias.

Chapter 4

Hybrid Nonlinear Observers for Inertial Navigation Using Landmark Measurements

4.1 Introduction

This chapter considers the problem of state estimation for inertial navigation systems relying on landmark position measurements. In the previous chapter, we addressed the problem of attitude and position estimation using group velocity measurements. However, obtaining the linear velocity in the body-fixed frame is challenging in low-cost applications, and obtaining the linear velocity in the inertial frame is difficult in GPS-denied environments. Hence, it is of great importance, from theoretical and practical point of views, to develop an estimation algorithm that provides, simultaneously, the estimates of attitude, position and linear velocity for inertial navigation systems. Due to the fact that the dynamics of the attitude, position and linear velocity are not (right or left) invariant, the extension of the existing invariant observers designed on $\text{SE}(3)$ [Hua et al., 2011; Vasconcelos et al., 2010; Hua et al., 2015; Khosravian et al., 2015b; Wang and Tayebi, 2017; Wang and Tayebi, 2020] to the estimation problem considered in this chapter is not trivial. Most of the existing results in the literature, for the state estimation problem for inertial navigation systems, are based-on the Kalman filter [Mourikis and Roumeliotis, 2007; Mourikis et al., 2009; Panahandeh and Jansson, 2014], the invariant extended Kalman Filter (IEKF) on matrix Lie groups [Barrau and Bonnabel, 2017], and the Riccati-based geometric observer [Hua and Allibert, 2018]. However, these results are only shown to be locally stable relying on linearizations.

In this chapter, we formulate the estimation problem for inertial navigation systems using the matrix Lie group $\text{SE}_2(3)$ introduced in [Barrau and Bonnabel, 2017]. First, we propose two nonlinear geometric hybrid observers, using ideal IMU and landmark measurements, for the estimation of the attitude, position and linear velocity. The first observer relies on fixed gains, while the second one uses variable gains. Both hybrid observers, relying on the resetting mechanism extended from the previous chapter, leads to global exponential stability. These results are also extended to deal with the gyro-bias

and accelerometer-bias situations, which were not considered in the geometric observers of [Barrau and Bonnabel, 2017; Hua and Allibert, 2018]. To the best of our knowledge, there are no results in the literature achieving such strong stability properties for the estimation problem at hand. Moreover, experimental results using IMU and stereo camera measurements are presented to illustrate the performance of the proposed observers. These results appeared in our work [Wang and Tayebi, 2018b; Wang and Tayebi, 2020].

4.2 Problem formulation

Consider a rigid body system, navigating in a three-dimensional space, modeled as (2.83)-(2.85), *i.e.*,

$$\dot{R} = R\omega^\times, \quad (4.1)$$

$$\dot{p} = v, \quad (4.2)$$

$$\dot{v} = g + Ra, \quad (4.3)$$

where $g \in \mathbb{R}^3$ denotes the gravity vector, $\omega \in \mathbb{R}^3$ denotes the angular velocity expressed in the body-frame, and $a \in \mathbb{R}^3$ is the body-frame “apparent acceleration” capturing all non-gravitational forces applied to the rigid body expressed in the body-frame. Let $X = \mathcal{T}_{\text{SE}_2(3)}(R, v, p) \in \text{SE}_2(3)$ with the map $\mathcal{T}_{\text{SE}_2(3)}$ defined in (2.77). Then, the kinematics (4.1)-(4.3) can be rewritten in the following compact form:

$$\dot{X} = f(X, \omega, a), \quad (4.4)$$

with the nonlinear map $f : \text{SE}_2(3) \times \mathbb{R}^3 \times \mathbb{R}^3 \rightarrow T_X \text{SE}_2(3)$ defined in (2.86).

We assume that ω and a are continuous and available for measurement. Consider a family of $N \in \mathbb{N}_{>0}$ landmarks available for measurement, and let $p_i \in \mathbb{R}^3$ be the position of the i -th landmark expressed in the inertial frame \mathcal{I} . The landmark measurements expressed in the body-frame \mathcal{B} are denoted as

$$y_i := R^\top(p_i - p), \quad i = 1, 2, \dots, N. \quad (4.5)$$

The three-dimensional landmark position measurements can be obtained, for instance, using bearing measurements generated from a stereo vision system as (2.98). Let $r_i := [p_i^\top \ 0 \ 1]^\top \in \mathbb{R}^5$ for all $i = 1, 2, \dots, N$ be the new inertial reference vectors with respect to the inertial frame $\{\mathcal{I}\}$, and $b_i := [y_i^\top \ 0 \ 1]^\top \in \mathbb{R}^5$ be their measurements expressed in the body-frame $\{\mathcal{B}\}$. From (4.5), one has

$$b_i = h(X, r_i) := X^{-1}r_i, \quad i = 1, 2, \dots, N. \quad (4.6)$$

Note that, the Lie group action $h : \text{SE}_2(3) \times \mathbb{R}^5 \rightarrow \mathbb{R}^5$ is a *right group action* in the sense that for all $X_1, X_2 \in \text{SE}_2(3)$ and $r \in \mathbb{R}^5$, one has $h(X_2, h(X_1, r)) = h(X_1 X_2, r)$. For later use, we define $r := [r_1 \ r_2 \ \dots \ r_N] \in \mathbb{R}^{5 \times N}$ and $b := [b_1 \ b_2 \ \dots \ b_N] \in \mathbb{R}^{5 \times N}$.

Assumption 4.1 *Assume that there exist at least three non-collinear landmarks among the $N \geq 3$ measurable landmarks.*

Assumption 4.1 is common in pose estimation on $\text{SE}(3)$ using landmark measurements [Hua et al., 2011; Vasconcelos et al., 2010; Hua et al., 2015; Khosravian et al., 2015b; Wang and Tayebi, 2017; Wang and Tayebi, 2020]. Define the matrix $M := \sum_{i=1}^N k_i(p_i - p_c)(p_i - p_c)^\top$ with $k_i > 0, i = 1, 2, \dots, N$, $k_c := \sum_{i=1}^N k_i$ and $p_c := \frac{1}{k_c} \sum_{i=1}^N k_i p_i$. The matrix M can be rewritten as $M = A_1 - k_c p_c p_c^\top$ with $A_1 := \sum_{i=1}^N k_i p_i p_i^\top$. Assumption 4.1 guarantees that it is always possible to have the matrix M positive semi-definite with no more than one zero eigenvalue, through an appropriate choice of the gains k_i .

4.3 Hybrid observers design using bias-free measurement

4.3.1 Continuous observer and undesired equilibra

Let $\hat{X} := \mathcal{T}_{\text{SE}_2(3)}(\hat{R}, \hat{v}, \hat{p}) \in \text{SE}_2(3)$ be the estimate of the state X , where \hat{R} denotes the estimate of the attitude R , \hat{v} denotes the estimate of the linear velocity v and \hat{p} denotes the estimate of the position p . Define the right-invariant estimation error as $\tilde{X} := X \hat{X}^{-1} = \mathcal{T}_{\text{SE}_2(3)}(\tilde{R}, \tilde{v}, \tilde{p})$ with $\tilde{R} := R \hat{R}^\top$, $\tilde{v} := v - \tilde{R}\hat{v}$ and $\tilde{p} := p - \tilde{R}\hat{p}$. Note that the right-invariant estimation error on $\text{SE}_2(3)$ leads to the right-invariant estimation error on $\text{SO}(3)$ and the geometric estimation errors of the position and linear velocity.

Consider the following time-invariant continuous observer:

$$\dot{\hat{X}} = f(\hat{X}, \omega, a) - \Delta \hat{X}, \quad (4.7)$$

$$\Delta := -\text{Ad}_{X_c} \left(\mathbb{P}_{\text{se}_2(3)}(X_c^{-1}(r - \hat{X}b)K_n r^\top X_c^{-\top} \mathcal{K}) \right) \quad (4.8)$$

where $\hat{X}(0) \in \text{SE}_2(3)$ and $X_c := \mathcal{T}_{\text{SE}_2(3)}(I_3, 0, p_c) \in \text{SE}_2(3)$ with p_c defined before. The gain parameters are given by

$$K_n = \text{diag}(k_1, \dots, k_n), \quad \mathcal{K} = \begin{bmatrix} k_R I_3 & 0_{3 \times 1} & 0_{3 \times 1} \\ 0_{1 \times 3} & 0 & 0 \\ 0_{1 \times 3} & k_v & k_p \end{bmatrix} \quad (4.9)$$

with $k_R, k_p, k_v, k_i > 0, i = 1, 2, \dots, N$.

Remark 4.1 Note that the proposed continuous observer is designed on the matrix Lie group $\text{SE}_2(3)$ directly, which is different from most of the existing Kalman-type filters. The observer has two parts: the term $f(\hat{X}, \omega, a)$ relying on the measurements of ω and a , and an innovation term Δ designed in terms of the estimated state \hat{X} and landmark measurements.

Remark 4.2 A homogeneous transformation matrix $X_c \in \text{SE}_2(3)$ is introduced in the innovation term Δ , which intends to transform the inertial vectors to a specific frame. Considering the transformation $\bar{r}_i = X_c^{-1}r_i, i = 1, 2, \dots, N$, the innovation term Δ defined in (4.8) can be simplified as $\Delta = -\text{Ad}_{X_c}(\mathbb{P}_{\text{se}_2(3)}((\bar{r} - X_c^{-1}\hat{X}b)K_n \bar{r}^\top \mathcal{K}))$ with $\bar{r} = [\bar{r}_1, \dots, \bar{r}_N]$. Choosing $X_c = \mathcal{T}_{\text{SE}_2(3)}(I_3, 0, p_c)$ with $p_c := \frac{1}{k_c} \sum_{i=1}^N k_i p_i$ and $k_c = \sum_{i=1}^N k_i$, leads to a nice decoupling property in the closed-loop dynamics, which will be discussed later. Similar techniques can be found in Chapter 3.

Let $\tilde{y}_i := p_i - \hat{p} - \tilde{R}y_i = (I_3 - \tilde{R}^\top)p_i + \tilde{R}^\top\tilde{p}$ for all $i = 1, 2, \dots, N$. From the definitions of r, b and K_n , one obtains

$$\begin{aligned} X_c^{-1}(r - \hat{X}b)K_n r^\top X_c^{-\top} &= X_c^{-1} \sum_{i=1}^N k_i(r_i - \hat{X}b_i)r_i^\top X_c^{-\top} \\ &= \begin{bmatrix} \sum_{i=1}^N k_i \tilde{y}_i(p_i - p_c)^\top & 0_{3 \times 1} & \sum_{i=1}^N k_i \tilde{y}_i \\ 0_{1 \times 3} & 0 & 0 \\ 0_{1 \times 3} & 0 & 0 \end{bmatrix}, \end{aligned}$$

where we made use of the fact $(r - \hat{X}b)K_n r^\top = \sum_{i=1}^N k_i(r_i - \hat{X}b_i)r_i^\top$. Then, from the definitions of matrix \mathcal{K} , the Adjoint map $\text{Ad}_X(\cdot)$ and the projection map $\mathbb{P}_{\mathfrak{se}_2(3)}(\cdot)$, the expression of Δ defined in (4.8) becomes

$$\Delta = - \begin{bmatrix} k_R \mathbb{P}_{\mathfrak{so}(3)}(\Delta_R) & k_v \Delta_p & k_p \Delta_p - k_R \mathbb{P}_{\mathfrak{so}(3)}(\Delta_R)p_c \\ 0_{1 \times 3} & 0 & 0 \\ 0_{1 \times 3} & 0 & 0 \end{bmatrix} \quad (4.10)$$

where $\Delta_R := \sum_{i=1}^N k_i \tilde{y}_i(p_i - p_c)^\top$ and $\Delta_p := \sum_{i=1}^N k_i \tilde{y}_i$. Recall that $\tilde{y}_i = (I_3 - \tilde{R}^\top)p_i + \tilde{R}^\top\tilde{p}$, then one can show that

$$\Delta_R = \sum_{i=1}^n k_i \tilde{y}_i(p_i - p_c)^\top = (I_3 - \tilde{R})^\top M \quad (4.11)$$

$$\Delta_p = \sum_{i=1}^n k_i \tilde{y}_i = k_c \tilde{R}^\top (\tilde{p} - (I_3 - \tilde{R})p_c) \quad (4.12)$$

where we made use of the facts $\tilde{y}_i = (I_3 - \tilde{R}^\top)p_i + \tilde{R}^\top\tilde{p}$, $k_c = \sum_{i=1}^n k_i$, $\sum_{i=1}^n k_i p_i = k_c p_c$ and $M = \sum_{i=1}^n k_i p_i p_i^\top - k_c p_c p_c^\top$. It is important to mention that $\Delta_R = (I_3 - \tilde{R}^\top) \sum_{i=1}^n k_i p_i p_i^\top + k_c \tilde{R}^\top \tilde{p} p_c^\top$ when choosing $X_c = I_5$. This implies that the position estimation error \tilde{p} will affect the attitude estimation error \tilde{R} when the weighted center of landmarks p_c is not located at the origin (*i.e.*, $p_c \neq 0$).

Similar to Section 3.5, we introduce a new position estimation error $\tilde{p}_e := \tilde{p} - (I - \tilde{R})p_c$. In view of (2.86), (4.7) and (4.10), one has the following closed-loop system:

$$\begin{cases} \dot{\tilde{R}} = \tilde{R}(-k_R \mathbb{P}_{\mathfrak{so}(3)}(M \tilde{R})) \\ \dot{\tilde{p}}_e = -k_p k_c \tilde{p}_e + \tilde{v} \\ \dot{\tilde{v}} = -k_v k_c \tilde{p}_e + (I_3 - \tilde{R})\mathbf{g} \end{cases} \quad (4.13)$$

where we made use of the facts $\mathbb{P}_{\mathfrak{so}(3)}(\Delta_R) = \mathbb{P}_{\mathfrak{so}(3)}((I_3 - \tilde{R}^\top)M) = \mathbb{P}_{\mathfrak{so}(3)}(M \tilde{R})$ and $\dot{\tilde{p}}_e = \dot{\tilde{v}} - k_R \tilde{R} \mathbb{P}_{\mathfrak{so}(3)}(\Delta_R)p_c$. It is clear that $\mathcal{T}_{\mathsf{SE}_2(3)}(\tilde{R}, \tilde{v}, \tilde{p}) = I_5$ if and only if $\mathcal{T}_{\mathsf{SE}_2(3)}(\tilde{R}, \tilde{v}, \tilde{p}_e) = I_5$. Note that the geometric errors \tilde{v} and \tilde{p}_e considered here are different from the linear errors (*i.e.*, $v - \hat{v}$ and $p - \hat{p}$) considered in the classical EKF-based navigation filters. The modified geometric errors lead to an interesting decoupling property for the closed-loop system, where the dynamics of \tilde{R} are not dependent on \tilde{p}_e and \tilde{v} as shown in the first equation of (4.13).

Proposition 4.1 Consider the closed-loop dynamics (4.13). Let Ψ be the set of undesired equilibrium points (i.e., all the equilibrium points except I_5) of the closed-loop dynamics, which is given by

$$\begin{aligned} \Psi := & \left\{ \mathcal{T}_{\text{SE}_2(3)}(\tilde{R}, \tilde{v}, \tilde{p}_e) \in \text{SE}_2(3) \mid \tilde{R} = \mathcal{R}_a(\pi, u), u \in \mathcal{E}(M), \right. \\ & \left. \tilde{p}_e = \frac{1}{k_c k_v} (I - \tilde{R}) \mathbf{g}, \tilde{v} = k_c k_p \tilde{p}_e \right\}. \end{aligned} \quad (4.14)$$

Proof The proof of Proposition 4.1 is straightforward. From Lemma 2.3, the set of equilibrium points of the first equation in (4.13) is given by $\Psi_M := \{I_3\} \cup \{\tilde{R} \in \text{SO}(3) : \tilde{R} = \mathcal{R}_a(\pi, u), u \in \mathcal{E}(M)\}$. Note that $\Psi_M / \{I_3\}$ denotes the set of undesired equilibrium points of the rotational error dynamics. Substituting $\tilde{R} \in \Psi_M$ into the identities $\dot{\tilde{v}} = 0$ and $\dot{\tilde{p}}_e = 0$, one can easily verify that $\tilde{p}_e = \frac{1}{k_c k_v} (I - \tilde{R}) \mathbf{g}$ and $\tilde{v} = k_c k_p \tilde{p}_e$.

Remark 4.3 From the dynamics of \tilde{R} in (4.13), it is easy to verify that the equilibrium point I_3 is almost globally asymptotically stable [Mahony et al., 2008]. It is important to mention that, due to the topology of the Lie group $\text{SO}(3)$ as mentioned in Section 3.3, it is impossible to achieve robust and global stability results with smooth (or even discontinuous) state observers. Hence, the best stability result one can achieve with the continuous observer (4.7)-(4.8) is AGAS. This motivates the design of hybrid observers leading to robust and global stability results as shown in the next section.

4.3.2 Fixed-gain hybrid observer design

Define the following real-valued cost function $\Upsilon : \text{SE}_2(3) \times \mathbb{R}^{5 \times n} \times \mathbb{R}^{5 \times n} \rightarrow \mathbb{R}_{\geq 0}$

$$\Upsilon(\hat{X}, r, b) := \frac{1}{2} \sum_{i=1}^N k_i \|(r_i - r_c) - \hat{X}(b_i - b_c)\|^2 \quad (4.15)$$

where $r_c := \sum_{i=1}^N \frac{k_i}{k_c} r_i = [p_c^\top \ 0 \ 1]^\top$ and $b_c := \sum_{i=1}^N \frac{k_i}{k_c} b_i = [y_c^\top \ 0 \ 1]^\top$ with $y_c := \sum_{i=1}^N \frac{k_i}{k_c} y_i = R^\top(p_c - p)$. From the definitions of p_c , k_c and M , one can rewrite $\Upsilon(\hat{X}, r, b)$ as $\Upsilon(\hat{X}, r, b) = \frac{1}{2} \sum_{i=1}^N k_i \|(p_i - p_c) - \hat{R}(y_i - y_c)\|^2 = \text{tr}((I_3 - \hat{R})M)$. Given a non-empty and finite transformation set $\mathbb{Q} \subset \text{SE}_2(3)$, let us define the real-valued function $\mu_{\mathbb{Q}} : \text{SE}_2(3) \times \mathbb{R}^{5 \times n} \times \mathbb{R}^{5 \times n} \rightarrow \mathbb{R}$ as

$$\mu_{\mathbb{Q}}(\hat{X}, r, b) := \Upsilon(\hat{X}, r, b) - \min_{X_q \in \mathbb{Q}} \Upsilon(X_q^{-1} \hat{X}, r, b). \quad (4.16)$$

The flow set \mathcal{F}_o and jump set \mathcal{J}_o are defined as follows:

$$\mathcal{F}_o := \{\hat{X} \in \text{SE}_2(3) \mid \mu_{\mathbb{Q}}(\hat{X}, r, b) \leq \delta\}, \quad (4.17)$$

$$\mathcal{J}_o := \{\hat{X} \in \text{SE}_2(3) \mid \mu_{\mathbb{Q}}(\hat{X}, r, b) \geq \delta\}, \quad (4.18)$$

with some $\delta > 0$. The sets \mathcal{F}_o and \mathcal{J}_o are closed, and $\mathcal{F}_o \cup \mathcal{J}_o = \text{SE}_2(3)$. The transformation set $\mathbb{Q} \subset \text{SE}_2(3)$ is given by

$$\mathbb{Q} := \{X = \mathcal{T}_{\text{SE}_2(3)}(R, v, p) \mid R = \mathcal{R}_a(\theta, u), u \in \mathbb{U}, p = (I_3 - R)p_c, v = 0\}, \quad (4.19)$$

with a constant $\theta \in (0, \pi]$ and a set of finite unit vectors $\mathbb{U} \subset \mathbb{S}^2$, which can be chosen as per one of the following two approaches:

- 1) A superset of the eigenbasis set of M , *i.e.*, $\mathbb{U} \supseteq \mathbb{E}(M)$, if $\lambda_1^M \geq \lambda_2^M \geq \lambda_3^M > 0$ or $\lambda_1^M > \lambda_2^M > \lambda_3^M = 0$.
- 2) A set that contains any three orthogonal unit vectors in \mathbb{R}^3 , if $\text{tr}(M) - 2\lambda_{\max}^M > 0$.

Note that approach 1) considers the case where the matrix M is positive definite or positive semi-definite with distinct eigenvalues, however it requires the information about the eigenvectors of M . Note also that approach 2) does not need any information about the eigenvectors of M , but it requires a strong condition $\text{tr}(M) - 2\lambda_{\max}^M > 0$.

We propose the following hybrid observer:

$$\mathcal{H}_1^o : \begin{cases} \dot{\hat{X}} = f(\hat{X}, \omega, a) - \Delta \hat{X} & \hat{X} \in \mathcal{F}_o \\ \hat{X}^+ = X_q^{-1} \hat{X}, \quad X_q \in \gamma(\hat{X}) & \hat{X} \in \mathcal{J}_o \end{cases} \quad (4.20)$$

$$\Delta := -\text{Ad}_{X_c}(\mathbb{P}_{\mathfrak{se}_2(3)}(X_c^{-1}(r - \hat{X}b)K_n r^\top X_c^{-\top} \mathcal{K})), \quad (4.21)$$

where $\hat{X}(0) \in \text{SE}_2(3)$ and the map $\gamma : \text{SE}_2(3) \rightrightarrows \text{SE}_2(3)$ is defined by

$$\gamma(\hat{X}) := \left\{ X_q \in \mathbb{Q} \mid X_q = \arg \min_{X_q \in \mathbb{Q}} \Upsilon(X_q^{-1} \hat{X}, r, b) \right\}. \quad (4.22)$$

We define the extended space and state as $\mathcal{S}_1^c := \text{SE}_2(3) \times \text{SO}(3) \times \mathbb{R}^3 \times \mathbb{R}^3 \times \mathbb{R}_{\geq 0}$ and $x_1^c := (\hat{X}, \tilde{R}, \tilde{p}_e, \tilde{v}, t)$, respectively. In view of (4.13) and (4.19)-(4.22), one obtains the following hybrid closed-loop system:

$$\mathcal{H}_1^c : \begin{cases} \dot{x}_1^c = F_1(x_1^c) & x_1^c \in \mathcal{F}_1^c \\ x_1^{c+} = G_1(x_1^c) & x_1^c \in \mathcal{J}_1^c \end{cases} \quad (4.23)$$

with $\mathcal{F}_1^c := \{x_1^c \in \mathcal{S}_1^c : \hat{X} \in \mathcal{F}_o\}$, $\mathcal{J}_1^c := \{x_1^c \in \mathcal{S}_1^c : \hat{X} \in \mathcal{J}_o\}$, and

$$F_1(x_1^c) = \begin{pmatrix} f(\hat{X}, \omega, a) - \Delta \hat{X} \\ \tilde{R}(-k_R \mathbb{P}_{\mathfrak{so}(3)}(M \tilde{R})) \\ -k_c k_p \tilde{p}_e + \tilde{v} \\ -k_c k_v \tilde{p}_e + (I - \tilde{R})\mathbf{g} \\ 1 \end{pmatrix}, \quad G_1(x_1^c) = \begin{pmatrix} X_q^{-1} \hat{X} \\ RR_q \\ \tilde{p}_e \\ \tilde{v} \\ t \end{pmatrix}.$$

where we made use of the facts: $\tilde{R}^+ = R(R_q^\top \tilde{R}) = \tilde{R}R_q$, $\tilde{p}^+ = p - \tilde{R}R_q R_q^\top (\hat{p} - (I_3 - R_q)p_c) = \tilde{p} + \tilde{R}(I_3 - R_q)p_c$, $\tilde{p}_e^+ = \tilde{p}_e^+ - (I_3 - \tilde{R}R_q)p_c = \tilde{p} - (I_3 - \tilde{R})p_c = \tilde{p}_e$ and $\tilde{v}^+ = \tilde{v}$. Note that the sets $\mathcal{F}_1^c, \mathcal{J}_1^c$ are closed, and $\mathcal{F}_1^c \cup \mathcal{J}_1^c = \mathcal{S}_1^c$. Note also that the closed-loop system (4.23) satisfies the hybrid basic conditions given in Section 2.5.1 and is autonomous by taking ω and a as functions of t .

The main idea behind our hybrid observer is the introduction of a resetting mechanism to avoid the undesired equilibrium points of the closed-loop system (4.23) in the flow set \mathcal{F}_1^c , *i.e.*, all the undesired equilibrium points of the closed-loop system belong to the jump set \mathcal{J}_1^c . The innovation term Δ and the transformation set \mathbb{Q} are designed to guarantee a decrease of a Lyapunov function in both flow set \mathcal{F}_1^c and jump set \mathcal{J}_1^c .

Proposition 4.2 Consider the hybrid dynamics \mathcal{H}_1^c defined in (4.23). Consider the transformation set \mathbb{Q} defined in (4.19) with \mathbb{U} chosen as per Lemma 3.3. Then, there exists a constant $\Delta_M^* > 0$ as per Lemma 3.3 such that for all $\delta < (1 - \cos \theta)\Delta_M^*$, one has $\text{SE}_2(3) \times \Psi \times \mathbb{R}_{\geq 0} \subseteq \mathcal{J}_1^c$.

See Appendix C.1 for the proof. Proposition 4.2 provides a choice for the gap δ , ensuring that the set of undesired equilibrium points of the flow dynamics of (4.23) is a subset of the jump set \mathcal{J}_1^c .

Let us define the set $\mathcal{A}_1 := \{(\hat{X}, \tilde{R}, \tilde{p}_e, \tilde{v}, t) \in \mathcal{S}_1^c : \tilde{R} = I_3, \tilde{p}_e = 0_{3 \times 1}, \tilde{v} = 0_{3 \times 1}\}$. Now, one can state one of our main results.

Theorem 4.1 Consider the hybrid closed-loop system (4.23). Suppose that Assumption 4.1 holds. Let $k_i > 0, i = 1, 2, \dots, N$, and choose the set \mathbb{U} as per Lemma 3.3 and $\delta < (1 - \cos \theta)\Delta_M^*$ with Δ_M^* defined in (3.14). Then, the number of discrete jumps is finite and the set \mathcal{A}_1 is uniformly GES.

Proof See Appendix C.2

Remark 4.4 In view of (4.10), (4.19), (4.20) and (4.22), the proposed hybrid observer can be explicitly expressed, in terms of the available measurements, as follows:

$$\left. \begin{array}{l} \dot{\hat{R}} = \hat{R}\omega^\times + k_R \mathbb{P}_{\mathfrak{so}(3)}(\Delta_R)\hat{R} \\ \dot{\hat{p}} = \hat{v} + k_R \mathbb{P}_{\mathfrak{so}(3)}(\Delta_R)(\hat{p} - p_c) + k_p \Delta_p \\ \dot{\hat{v}} = \mathbf{g} + \hat{R}a + k_R \mathbb{P}_{\mathfrak{so}(3)}(\Delta_R)\hat{v} + k_v \Delta_p \end{array} \right\} \hat{X} \in \mathcal{F}_o$$

$$\left. \begin{array}{l} \hat{R}^+ = R_q^\top \hat{R} \\ \hat{p}^+ = R_q^\top (\hat{p} - (I_3 - R_q)p_c) \\ \hat{v}^+ = R_q^\top \hat{v} \end{array} \right\} \hat{X} \in \mathcal{J}_o$$

where $R_q \in \mathcal{R}_a(\theta, \mathbb{U})$ with $R_q = \min_{R_q \in \mathcal{R}_a(\theta, \mathbb{U})} \sum_{i=1}^N k_i \|(p_i - p_c) - R_q^\top \hat{R}(y_i - y_c)\|^2$, Δ_R and Δ_p are defined as per (4.10).

4.3.3 Variable-gain hybrid observer design

In this subsection, we provide a different version of the hybrid observer \mathcal{H}_1^o using variable gains relying on the solution of a CRE. Let us define the following gain map $\mathbb{P}_K : \mathbb{R}^{5 \times 5} \rightarrow \mathfrak{se}_2(3)$ inspired by [Khosravian et al., 2015b], such that for all $A_1 \in \mathbb{R}^{3 \times 3}, a_2, \dots, a_5 \in \mathbb{R}^3$ and $a_6, \dots, a_9 \in \mathbb{R}$, one has

$$\mathbb{P}_K \left(\begin{bmatrix} A_1 & a_2 & a_3 \\ a_4^\top & a_6 & a_7 \\ a_5^\top & a_8 & a_9 \end{bmatrix} \right) = \begin{bmatrix} k_R \mathbb{P}_{\mathfrak{so}(3)}(A_1) & K_v a_2 & K_p a_3 \\ 0_{1 \times 3} & 0 & 0 \\ 0_{1 \times 3} & 0 & 0 \end{bmatrix}. \quad (4.24)$$

where $K := (k_R, K_p, K_v)$ with $k_R > 0$ and $K_p, K_v \in \mathbb{R}^{3 \times 3}$ to be designed. Then, we propose the following hybrid observer.

$$\mathcal{H}_2^o : \left\{ \begin{array}{ll} \dot{\hat{X}} = f(\hat{X}, \omega, a) - \Delta \hat{X} & \hat{X} \in \mathcal{F}_o \\ \hat{X}^+ = X_q^{-1} \hat{X}, \quad X_q \in \gamma(\hat{X}) & \hat{X} \in \mathcal{J}_o \end{array} \right. \quad (4.25)$$

$$\Delta := -\text{Ad}_{X_c}(\mathbb{P}_{\mathcal{K}}(X_c^{-1}(r - \hat{X}b)K_n r^\top X_c^{-\top})), \quad (4.26)$$

where $\hat{X}(0) \in \text{SE}_2(3)$. The map γ is defined in (4.22) and the flow and jump sets $\mathcal{F}_o, \mathcal{J}_o$ are defined in (4.17) and (4.18), respectively. The gain map $\mathbb{P}_{\mathcal{K}}$ is given by (4.24). Note that the main difference between the hybrid observers \mathcal{H}_1^o and \mathcal{H}_2^o is the innovation term Δ . Instead of using constant scalar gains k_v, k_p as in the observer \mathcal{H}_1^o , the new observer \mathcal{H}_2^o uses variable matrix gains K_v, K_p to be designed later in this subsection.

In view of (2.86), and (4.24)-(4.26), one has the following closed-loop system in the flows:

$$\begin{cases} \dot{\tilde{R}} = \tilde{R}(-k_R \mathbb{P}_{\mathfrak{so}(3)}(M \tilde{R})) \\ \dot{\tilde{p}_e} = -k_c \tilde{R} K_p \tilde{R}^\top \tilde{p}_e + \tilde{v} \\ \dot{\tilde{v}} = -k_c \tilde{R} K_v \tilde{R}^\top \tilde{p}_e + (I_3 - \tilde{R})g \end{cases} \quad (4.27)$$

Define the new variable $\mathbf{x} := [(R^\top \tilde{p}_e)^\top, (R^\top \tilde{v})^\top] \in \mathbb{R}^6$. Note that $\|\mathbf{x}\|^2 = \|\tilde{p}_e\|^2 + \|\tilde{v}\|^2$, which implies that $\tilde{p}_e = \tilde{v} = 0_{3 \times 1}$ if and only if $\mathbf{x} = 0_{6 \times 1}$. Let $K := k_c [\tilde{R}^\top K_p^\top \tilde{R} \tilde{R}^\top K_v^\top \tilde{R}]^\top \in \mathbb{R}^{6 \times 3}$ and $\nu = [0_{1 \times 3} \ g^\top (R - \hat{R})]^\top \in \mathbb{R}^6$. From (4.27) one obtains the dynamics of \mathbf{x} as

$$\dot{\mathbf{x}} = A(t)\mathbf{x} - KC\mathbf{x} + \nu, \quad (4.28)$$

with

$$A(t) := \begin{bmatrix} -\omega(t)^\times & I_3 \\ 0_{3 \times 3} & -\omega(t)^\times \end{bmatrix}, \quad C := [I_3 \ 0_{3 \times 3}]. \quad (4.29)$$

Note that the dynamics of \mathbf{x} are linear time-varying and ν can be viewed as a perturbation term. The variable-gain matrix K can be updated as $K = PC^\top Q(t)$, with P being the solution of the CRE (2.116) with $P(0) \in \mathbb{R}^{6 \times 6}$ being a symmetric positive definite matrix, and $Q(t) \in \mathbb{R}^{6 \times 6}, V(t) \in \mathbb{R}^{6 \times 6}$ being strictly positive definite matrices.

Lemma 4.1 *The pair $(A(t), C)$ defined in (4.29) is uniformly observable.*

See Appendix C.3 for the proof. Given $V(t)$ and $Q(t)$ strictly positive definite, from Lemma 2.10, there exist two constants $p_m, p_M > 0$ such that $p_m I_6 \leq P(t) \leq p_M I_6$.

Remark 4.5 *Let $K_1, K_2 \in \mathbb{R}^{3 \times 3}$ such that $[K_1^\top, K_2^\top]^\top = K = PC^\top Q(t)$. Then, the gain matrices K_p and K_v can be computed as*

$$K_p = \frac{1}{k_c} \hat{R} K_1 \hat{R}^\top, \quad K_v = \frac{1}{k_c} \hat{R} K_2 \hat{R}^\top. \quad (4.30)$$

For the sake of simplicity, one can choose the weights $k_i > 0, i = 1, 2, \dots, N$ such that $k_c = \sum_{i=1}^N k_i = 1$.

Define the extended space $\mathcal{S}_2^c := \text{SE}_2(3) \times \text{SO}(3) \times \mathbb{R}^6 \times \mathbb{R}_{\geq 0}$ and the extended state $x_2^c := (\hat{X}, \tilde{R}, \mathbf{x}, t)$. In view of (4.19), (4.22), (4.25)–(4.28) and (2.116), one obtains the following hybrid closed-loop system:

$$\mathcal{H}_2^c : \begin{cases} \dot{x}_2^c = F_2(x_2^c) & x_2^c \in \mathcal{F}_2^c \\ x_2^{c+} = G_2(x_2^c) & x_2^c \in \mathcal{J}_2^c \end{cases} \quad (4.31)$$

where the flow and jump sets are defined as $\mathcal{F}_2^c := \{(\hat{X}, \tilde{R}, \mathbf{x}, t) \in \mathcal{S}_2^c : \hat{X} \in \mathcal{F}_o, \}$ and $\mathcal{J}_2^c := \{(\hat{X}, \tilde{R}, \mathbf{x}, t) \in \mathcal{S}_2^c : \hat{X} \in \mathcal{J}_o\}$, and the flow and jump maps are given by

$$F_2(x_2^c) = \begin{pmatrix} f(\hat{X}, \omega, a) - \Delta \hat{X} \\ \tilde{R}(-k_R \mathbb{P}_{\mathfrak{so}(3)}(M \tilde{R})) \\ Ax - KCx + \nu \\ 1 \end{pmatrix}, G_2(x_2^c) = \begin{pmatrix} X_g^{-1} \hat{X} \\ RR_q \\ \mathbf{x} \\ t \end{pmatrix}.$$

Note that the sets $\mathcal{F}_2^c, \mathcal{J}_2^c$ are closed, and $\mathcal{F}_2^c \cup \mathcal{J}_2^c = \mathcal{S}_2^c$. Note also that the closed-loop system (4.31) satisfies the hybrid basic conditions given in Section 2.5.1 and is autonomous by taking ω, a, A and K as functions of t .

Let us define the set $\mathcal{A}_2 := \{(\hat{X}, \tilde{R}, \mathbf{x}, t) \in \mathcal{S}_2^c : \tilde{R} = I_3, \|\mathbf{x}\| = 0, \}$. Now, one can state the following result:

Theorem 4.2 Consider the inertial navigation system (4.4)-(4.5) with the hybrid observer (4.25)-(4.26). Suppose that Assumption 4.1 holds. Let $k_i > 0, i = 1, 2, \dots, N$, choose the set \mathbb{U} as per Lemma 3.3, and choose $\delta < (1 - \cos \theta) \Delta_M^*$ with Δ_M^* defined in (3.14). Let $k_R > 0$, and $Q(t)$ and $V(t)$ be strictly positive definite. Then, the number of discrete jumps is finite and the set \mathcal{A}_2 is uniformly GES.

Proof See Appendix C.4.

4.4 Hybrid observers design using biased angular velocity

4.4.1 Fixed-gain hybrid observer design

In the previous section, nonlinear hybrid observers have been designed using non-biased angular velocity measurements. In this section, we consider the case where the angular velocity measurements contain an unknown constant or slowly varying bias. Let b_ω be the constant unknown angular velocity bias, such that $\omega_y = \omega + b_\omega$. Define \hat{b}_ω as the estimate of b_ω and $\tilde{b}_\omega := \hat{b}_\omega - b_\omega$ as the estimation error.

We propose the following hybrid nonlinear observer for inertial navigation with biased angular velocity:

$$\mathcal{H}_3^o : \left\{ \begin{array}{l} \dot{\hat{X}} = f(\hat{X}, \omega_y - \hat{b}_\omega, a) - \Delta \hat{X} \\ \dot{\hat{b}}_\omega = -k_\omega \hat{R}^\top \psi_{\mathfrak{so}(3)}(\Delta_R) \\ \hat{X}^+ = X_q^{-1} \hat{X}, \quad X_q \in \gamma(\hat{X}) \\ \hat{b}_\omega^+ = \hat{b}_\omega \end{array} \right\} \begin{array}{l} (\hat{X}, \hat{b}_\omega) \in \mathcal{F}_o \times \mathbb{R}^3 \\ (\hat{X}, \hat{b}_\omega) \in \mathcal{J}_o \times \mathbb{R}^3 \end{array} \quad (4.32)$$

$$\Delta := -\text{Ad}_{X_c}(\mathbb{P}(X_c^{-1}(r - \hat{X}b)K_n r^\top X_c^{-\top} \mathcal{K})), \quad (4.33)$$

where $\hat{X}(0) \in \text{SE}_2(3)$, $\hat{b}_\omega(0) \in \mathbb{R}^3$, $k_\omega > 0$, K_n and \mathcal{K} are given by (4.9) and Δ_R is given in (4.10). The map γ is defined in (4.22) and the flow and jump sets $\mathcal{F}_o, \mathcal{J}_o$ are defined in (4.17) and (4.18), respectively.

Consider the extended space and state as $\mathcal{S}_3^c := \mathcal{S}_1^c \times \mathbb{R}^3 \times \mathbb{R}^3$ and $x_3^c := (x_1^c, \hat{b}_\omega, \tilde{b}_\omega)$. Let us define the set $\mathcal{A}_3 := \{(x_1^c, \hat{b}_\omega, \tilde{b}_\omega) \in \mathcal{S}_3^c : x_1^c \in \mathcal{A}_1, \tilde{b}_\omega = 0_{3 \times 1}\}$. Let $|x_3^c|_{\mathcal{A}_3} \geq 0$ denote the distance to the set \mathcal{A}_3 such that $|x_3^c|_{\mathcal{A}_3}^2 := \inf_{y=(\bar{X}, I_3, 0, 0, \bar{t}, \bar{b}_\omega, 0) \in \mathcal{A}_3} (\|\bar{X} - \hat{X}\|_F^2 + |\tilde{R}|_I^2 + \|\tilde{p}_e\|^2 + \|\tilde{v}\|^2 + \|\bar{t} - t\|^2 + \|\bar{b}_\omega - \hat{b}_\omega\|^2 + \|\tilde{b}_\omega\|^2) = |\tilde{R}|_I^2 + \|\tilde{p}_e\|^2 + \|\tilde{v}\|^2 + \|\tilde{b}_\omega\|^2$.

Before stating our next result, the following assumption is made:

Assumption 4.2 *The state X and angular velocity ω are uniformly bounded.*

In practical applications, due the limited motion of the vehicles, the attitude, pose, linear velocity and angular velocity are naturally bounded. Hence, Assumption 4.2 is practical and reasonable.

Theorem 4.3 *Consider the inertial navigation system (4.4)-(4.5) with the hybrid observer (4.32)-(4.33). Suppose that Assumption 4.1 and Assumption 4.2 hold. Let $k_i > 0, i = 1, 2, \dots, N$, and choose the set \mathbb{U} as per Lemma 3.3 and $\delta < (1 - \cos \theta)\Delta_M^*$ with Δ_M^* defined in (3.14). Let $k_R, k_p, k_v, k_\omega > 0$. Then, for any initial condition $x_3^c(0, 0) \in \mathcal{S}_3^c$ the number of discrete jumps is finite, and the solution of $x_3^c(t, j)$ is complete and there exist $\kappa, \lambda_F > 0$ (depending on the initial conditions) such that*

$$|x_3^c(t, j)|_{\mathcal{A}_3}^2 \leq \kappa \exp(-\lambda_F(t + j)) |x_3^c(0, 0)|_{\mathcal{A}_3}^2, \quad (4.34)$$

for all $(t, j) \in \text{dom}x_3^c$.

Proof See Appendix C.5.

Remark 4.6 Note that the parameters λ_F and κ depend on the initial conditions, which is different from Theorem 4.1. This non-uniform type of exponential stability is a consequence of the angular velocity bias (see, for instance, the hybrid observers on $\text{SO}(3)$ in [Berkane et al., 2017b] and the hybrid observers on $\text{SE}(3)$ in Chapter 3).

4.4.2 Variable-gain hybrid observer design

We propose the following Riccati-based hybrid nonlinear observer for inertial navigation with biased angular velocity:

$$\mathcal{H}_4^o : \left\{ \begin{array}{l} \dot{\hat{X}} = f(\hat{X}, \omega_y - \hat{b}_\omega, a) - \Delta \hat{X} \\ \dot{\hat{b}}_\omega = -k_\omega \hat{R}^\top \psi_{\mathfrak{so}(3)}(\Delta_R) \\ \hat{X}^+ = X_q^{-1} \hat{X}, \quad X_q \in \gamma(\hat{X}) \\ \hat{b}_\omega^+ = \hat{b}_\omega \end{array} \right\} \begin{array}{l} (\hat{X}, \hat{b}_\omega) \in \mathcal{F}_o \times \mathbb{R}^3 \\ (\hat{X}, \hat{b}_\omega) \in \mathcal{J}_o \times \mathbb{R}^3 \end{array} \quad (4.35)$$

$$\Delta := -\text{Ad}_{X_c}(\mathbb{P}_{\mathcal{K}}(X_c^{-1}(r - \hat{X}b)K_n r^\top X_c^{-\top})), \quad (4.36)$$

where $\hat{X}(0) \in \text{SE}_2(3)$, $\hat{b}_\omega(0) \in \mathbb{R}^3$, $k_\omega > 0$, K_n is given by (4.9) and Δ_R is given in (4.10). The gain map $\mathbb{P}_{\mathcal{K}}$ is given by (4.24). The map γ is defined in (4.22) and the flow and jump sets $\mathcal{F}_o, \mathcal{J}_o$ are defined in (4.17) and (4.18), respectively.

In view of (4.4), (4.10), and (4.35)-(4.36), one has the following closed-loop system in the flows:

$$\begin{cases} \dot{\tilde{R}} = \tilde{R}((\hat{R}\tilde{b}_\omega)^\times - k_R \mathbb{P}_{\mathfrak{so}(3)}(M\tilde{R})) \\ \dot{\tilde{b}}_\omega = -k_\omega \hat{R}^\top \psi_{\mathfrak{so}(3)}(M\tilde{R}) \\ \dot{\tilde{p}}_e = -k_c \tilde{R} K_p \tilde{R}^\top \tilde{p}_e + \tilde{v} - (R\tilde{b}_\omega)^\times (p - p_c - \tilde{p}_e) \\ \dot{\tilde{v}} = -k_c \tilde{R} K_v \tilde{R}^\top \tilde{p}_e + (I_3 - \tilde{R})\mathbf{g} - (R\tilde{b}_\omega)^\times (v - \tilde{v}) \end{cases} \quad (4.37)$$

In view of (4.37), from the definition of \mathbf{x} and matrix K , one has the dynamics of \mathbf{x} as

$$\dot{\mathbf{x}} = A(t)\mathbf{x} - KC\mathbf{x} + \nu, \quad (4.38)$$

where the matrix C is defined in (4.29), $\nu = [((R^\top(p - p_c))^\times \tilde{b}_\omega)^\top, ((R^\top v)^\times \tilde{b}_\omega + (I_3 - \tilde{R})\mathbf{g})^\top]^\top$, and

$$A(t) := \begin{bmatrix} -(\omega_y - \hat{b}_\omega)^\times & I_3 \\ 0_{3 \times 3} & -(\omega_y - \hat{b}_\omega)^\times \end{bmatrix}. \quad (4.39)$$

The gain matrix K can be updated by $K = PC^\top Q(t)$, with P being the solution of the CRE (2.116) with $P(0) \in \mathbb{R}^{6 \times 6}$ being a symmetric positive definite matrix, and $Q(t) \in \mathbb{R}^{3 \times 3}, V(t) \in \mathbb{R}^{6 \times 6}$ being strictly positive definite matrices. Note that the matrices K_p and K_v can be easily obtained from (4.30).

Lemma 4.2 *The pair $(A(t), C)$ with $A(t)$ defined in (4.39) and C defined in (4.29) is uniformly observable.*

The proof of Lemma 4.2 can be conducted using similar steps as in the proof of Lemma 4.1, by introducing the matrices

$$\begin{aligned} T(t) &= \text{blkdiag}(\bar{R}(t), \bar{R}(t), \bar{R}(t)), \\ S(t) &= \text{blkdiag}((- \omega_y(t) + \hat{b}_\omega(t))^\times, (- \omega_y(t) + \hat{b}_\omega(t))^\times, (- \omega_y(t) + \hat{b}_\omega(t))^\times), \end{aligned}$$

and the constant matrix $\bar{A} = A(t) - S(t)$ with the rotation matrix $\bar{R}(t)$ generated by $\dot{\bar{R}}(t) = (- \omega_y(t) + \hat{b}_\omega(t))^\times \bar{R}(t)$ and $\bar{R}(0) \in \text{SO}(3)$. Therefore, given $V(t)$ and $Q(t)$ strictly positive definite, from Lemma 2.10 it follows that the solution of $P(t)$ is well-defined on $\mathbb{R}_{\geq 0}$ and there exist two constants $p_m, p_M > 0$ such that $p_m I_6 \leq P(t) \leq p_M I_6$.

Define the extended space and state as $\mathcal{S}_4^c := \mathcal{S}_2^c \times \mathbb{R}^3 \times \mathbb{R}^3$ and $x_4^c := (x_2^c, \hat{b}_\omega, \tilde{b}_\omega)$. Define the set $\mathcal{A}_4 := \{(x_2^c, \hat{b}_\omega, \tilde{b}_\omega) \in \mathcal{S}_4^c : x_2^c \in \mathcal{A}_2, \tilde{b}_\omega = 0_{3 \times 1}\}$. Let $|x_4^c|_{\mathcal{A}_4} \geq 0$ denote the distance to the set \mathcal{A}_4 such that $|x_4^c|_{\mathcal{A}_4}^2 := \inf_{y=(\bar{X}, I_3, 0, \bar{t}, \bar{b}_\omega, 0) \in \mathcal{A}_4} (\|\bar{X} - \hat{X}\|_F^2 + |\bar{R}|_I^2 + \|\mathbf{x}\|^2 + \|\bar{t} - t\|^2 + \|\bar{b}_\omega - \hat{b}_\omega\|^2 + \|\tilde{b}_\omega\|^2) = |\bar{R}|_I^2 + \|\mathbf{x}\|^2 + \|\tilde{b}_\omega\|^2$. Now, one can state the following result:

Theorem 4.4 *Consider the hybrid observer (4.35)-(4.36) for the system (4.4)-(4.5). Suppose that Assumption 4.1 and Assumption 4.2 hold. Let $k_i > 0, i = 1, 2, \dots, N$, and choose the set \mathbb{U} as per Lemma 3.3 and $\delta < (1 - \cos\theta)\Delta_M^*$ with Δ_M^* defined in (3.14). Let $k_R > 0, k_\omega > 0$, $Q(t)$ and $V(t)$ be strictly positive definite. Then, for any initial condition $x_4^c(0, 0) \in \mathcal{S}_4^c$ the number of discrete jumps is finite, and the solution of*

$x_4^c(t, j)$ is complete and there exist $\kappa, \lambda_F > 0$ (depending on the initial conditions) such that

$$|x_4^c(t, j)|_{\mathcal{A}_4}^2 \leq \kappa \exp(-\lambda_F(t + j)) |x_4^c(0, 0)|_{\mathcal{A}_4}^2, \quad (4.40)$$

for all $(t, j) \in \text{dom}x_4^c$.

Proof See Appendix C.6.

4.5 Hybrid observer design using biased angular velocity and linear acceleration

In this section, we consider the case where both the angular velocity and linear acceleration measurements are biased. Let b_a be the unknown acceleration bias such that $a_y = a + b_a$. Define \hat{b}_a as the estimate of b_a and $\tilde{b}_a := \hat{b}_a - b_a$ as the estimation error.

We propose the following Riccati-based hybrid nonlinear observer for inertial navigation:

$$\mathcal{H}_5^o : \left\{ \begin{array}{l} \dot{\hat{X}} = f(\hat{X}, \omega_y - \hat{b}_\omega, a_y - \hat{b}_a) - \Delta \hat{X} \\ \dot{\hat{b}}_\omega = -k_\omega \hat{R}^\top \psi_{\mathfrak{so}(3)}(\Delta_R) \\ \dot{\hat{b}}_a = -\hat{R}^\top K_a \Delta_p \\ \hat{X}^+ = X_q^{-1} \hat{X}, \quad X_q \in \gamma(\hat{X}) \\ \hat{b}_\omega^+ = \hat{b}_\omega \\ \hat{b}_a^+ = \hat{b}_a \end{array} \right\} \begin{array}{l} (\hat{X}, \hat{b}_\omega, \hat{b}_a) \in \mathcal{F}_o \times \mathbb{R}^3 \times \mathbb{R}^3 \\ (\hat{X}, \hat{b}_\omega, \hat{b}_a) \in \mathcal{J}_o \times \mathbb{R}^3 \times \mathbb{R}^3 \end{array} \quad (4.41)$$

$$\Delta := -\text{Ad}_{X_c}(\mathbb{P}_K(X_c^{-1}(r - \hat{X}b)K_n r^\top X_c^{-\top})), \quad (4.42)$$

where $\hat{X}(0) \in \text{SE}_2(3)$, $\hat{b}_\omega(0), \hat{b}_a(0) \in \mathbb{R}^3$, $k_\omega > 0$, K_n is given by (4.9) and the innovation terms Δ_R, Δ_p are given in (4.10). The gain map \mathbb{P}_K is given by (4.24). The map γ is defined in (4.22) and the flow and jump sets $\mathcal{F}_o, \mathcal{J}_o$ are defined in (4.17) and (4.18), respectively. In view of (4.4), (4.10), and (4.41)-(4.42), one has the following closed-loop system in the flows:

$$\left\{ \begin{array}{l} \dot{\tilde{R}} = \tilde{R}((\tilde{R}\tilde{b}_\omega)^\times - k_R \mathbb{P}_{\mathfrak{so}(3)}(M\tilde{R})) \\ \dot{\tilde{b}}_\omega = -k_\omega \tilde{R}^\top \psi_{\mathfrak{so}(3)}(M\tilde{R}) \\ \dot{\tilde{p}}_e = -k_c \tilde{R} K_p \tilde{R}^\top \tilde{p}_e + \tilde{v} - (R\tilde{b}_\omega)^\times(p - p_c - \tilde{p}_e) \\ \dot{\tilde{v}} = -k_c \tilde{R} K_v \tilde{R}^\top \tilde{p}_e + R\tilde{b}_a + (I_3 - \tilde{R})\mathbf{g} - (R\tilde{b}_\omega)^\times(v - \tilde{v}) \\ \dot{\tilde{b}}_a = -k_c \tilde{R}^\top K_a \tilde{R}^\top \tilde{p}_e \end{array} \right. \quad (4.43)$$

Define the new variable $\mathbf{x} := [(R^\top \tilde{p}_e)^\top, (R^\top \tilde{v})^\top, \tilde{b}_a^\top]^\top \in \mathbb{R}^9$. Note that $\|\mathbf{x}\|^2 = \|\tilde{p}_e\|^2 + \|\tilde{v}\|^2 + \|\tilde{b}_a\|^2$ and $\|\mathbf{x}\| = 0$ if and only if $\|\tilde{p}_e\| = \|\tilde{v}\| = \|\tilde{b}_a\| = 0$. In view of (4.43), one has the following dynamics of \mathbf{x} :

$$\dot{\mathbf{x}} = A(t)\mathbf{x} - KC\mathbf{x} + \nu, \quad (4.44)$$

with $L := k_c [\hat{R}^\top K_p^\top \hat{R}, \hat{R}^\top K_v \hat{R}, \hat{R}^\top K_a \hat{R}]^\top \in \mathbb{R}^{9 \times 3}$, $\nu := [((R^\top(p-p_c))^\times \tilde{b}_\omega)^\top, ((R^\top v)^\times \tilde{b}_\omega + (I_3 - \tilde{R})g)^\top, 0_{1 \times 3}]^\top \in \mathbb{R}^9$, and

$$\begin{aligned} A(t) &:= \begin{bmatrix} -(\omega_y - \hat{b}_\omega)^\times & I_3 & 0_{3 \times 3} \\ 0_{3 \times 3} & -(\omega_y - \hat{b}_\omega)^\times & I_3 \\ 0_{3 \times 3} & 0_{3 \times 3} & 0_{3 \times 3} \end{bmatrix}, \\ C &:= [I_3 \ 0_{3 \times 3} \ 0_{3 \times 3}]. \end{aligned} \quad (4.45)$$

The gain matrix K can be updated by $K = PC^\top Q(t)$, with P being the solution of the CRE (2.116) with $P(0) \in \mathbb{R}^{9 \times 9}$ being a symmetric positive definite matrix, and $Q(t) \in \mathbb{R}^{3 \times 3}, V(t) \in \mathbb{R}^{9 \times 9}$ being strictly positive definite matrices. Let $K_1, K_2, K_3 \in \mathbb{R}^{3 \times 3}$ such that $[K_1^\top, K_2^\top, K_3^\top]^\top = K = PC^\top Q(t)$. Then, the gain matrices K_p, K_v and K_a can be computed as

$$K_p = \frac{1}{k_c} \hat{R} K_1 \hat{R}^\top, K_v = \frac{1}{k_c} \hat{R} K_2 \hat{R}^\top, K_a = \frac{1}{k_c} \hat{R} K_3 \hat{R}^\top.$$

The following assumption is needed in the observability proof of the next lemma.

Assumption 4.3 *The time-derivative of ω is uniformly bounded.*

Lemma 4.3 *The pair $(A(t), C)$ defined in (4.45) is uniformly observable under Assumption 4.2 and Assumption 4.3.*

See Appendix C.7 for the proof. Therefore, given $V(t)$ and $Q(t)$ strictly positive definite, from Lemma 2.10 one can show that the solution of $P(t)$ is well-defined on $\mathbb{R}_{\geq 0}$ and there exist two constants $p_m, p_M > 0$ such that $p_m I_9 \leq P(t) \leq p_M I_9$.

Define the extended space and state as $\mathcal{S}_5^c := \text{SE}_2(3) \times \text{SO}(3) \times \mathbb{R}^9 \times \mathbb{R}_{\geq 0} \times \mathbb{R}^3 \times \mathbb{R}^3 \times \mathbb{R}^3$ and $x_5^c := (\hat{X}, \tilde{R}, \mathbf{x}, t, \hat{b}_\omega, \tilde{b}_\omega, \hat{b}_a, \tilde{b}_a)$. Define the set $\mathcal{A}_5 := \{(\hat{X}, \tilde{R}, \mathbf{x}, t, \hat{b}_\omega, \tilde{b}_\omega, \hat{b}_a, \tilde{b}_a) \in \mathcal{S}_5^c : \tilde{R} = I_3, \mathbf{x} = 0, \hat{b}_\omega = 0, \tilde{b}_a = 0\}$. Let $|x_5^c|_{\mathcal{A}_5} \geq 0$ denote the distance to the set \mathcal{A}_5 such that $|x_5^c|_{\mathcal{A}_5}^2 := \inf_{y=(\bar{X}, I_3, 0, \bar{t}, \bar{b}_\omega, 0, \bar{b}_a, 0) \in \mathcal{A}_5} (\|\bar{X} - \hat{X}\|_F^2 + |\bar{R}|_I^2 + \|\mathbf{x}\|^2 + \|\bar{t} - t\|^2 + \|\bar{b}_\omega - \hat{b}_\omega\|^2 + \|\bar{b}_a - \hat{b}_a\|^2 + \|\tilde{b}_a\|^2) = |\tilde{R}|_I^2 + \|\mathbf{x}\|^2 + \|\tilde{b}_\omega\|^2 + \|\tilde{b}_a\|^2$.

Now, one can state the following result:

Theorem 4.5 *Consider the hybrid observer (4.41)-(4.42) for the system (4.4)-(4.5). Suppose that Assumption 4.1 - Assumption 4.3 hold. Let $k_i > 0, i = 1, 2, \dots, N$, and choose the set \mathbb{U} as per Lemma 3.3 and $\delta < (1 - \cos \theta) \Delta_M^*$ with Δ_M^* defined in (3.14). Let $k_R > 0, k_\omega > 0$, and $Q(t), V(t)$ be strictly positive definite. Then, for any initial condition $x_5^c(0, 0) \in \mathcal{S}_5^c$ the number of discrete jumps is finite, and the solution of $x_5^c(t, j)$ is complete and there exist $\kappa, \lambda_F > 0$ (depending on the initial conditions) such that*

$$|x_5^c(t, j)|_{\mathcal{A}_5}^2 \leq \kappa \exp(-\lambda_F(t + j)) |x_5^c(0, 0)|_{\mathcal{A}_5}^2, \quad (4.46)$$

for all $(t, j) \in \text{dom} x_5^c$.

Remark 4.7 The proof of Theorem 4.5 can be conducted using similar steps as in the proof of Theorem 4.4, which is omitted here. In view of (4.19), (4.22), (4.41)-(4.44) and (2.116), one obtains the following hybrid closed-loop system:

$$\mathcal{H}_5^c : \begin{cases} \dot{x}_5^c = F_5(x_5^c) & x_5^c \in \mathcal{F}_5^c \\ x_5^{c+} = G_5(x_5^c) & x_5^c \in \mathcal{J}_5^c \end{cases} \quad (4.47)$$

where the flow and jump sets are defined as: $\mathcal{F}_5^c := \{(\hat{X}, \tilde{R}, \mathbf{x}, t, \hat{b}_\omega, \tilde{b}_\omega, \hat{b}_a, \tilde{b}_a) \in \mathcal{S}_5^c : \hat{X} \in \mathcal{F}_o\}$ and $\mathcal{J}_5^c := \{(\hat{X}, \tilde{R}, \mathbf{x}, t, \hat{b}_\omega, \tilde{b}_\omega, \hat{b}_a, \tilde{b}_a) \in \mathcal{S}_5^c : \hat{X} \in \mathcal{J}_o\}$ with \mathcal{F}_o and \mathcal{J}_o given in (4.17) and (4.18), respectively. The flow and jump maps are given by

$$F_5(x_5^c) = \begin{pmatrix} f(\hat{X}, \omega_y - \hat{b}_\omega, a_y - \hat{b}_a) - \Delta \hat{X} \\ \tilde{R}((\hat{R}\tilde{b}_\omega)^\times - k_R \mathbb{P}_{\mathfrak{so}(3)}(M\tilde{R})) \\ Ax - KCx + \nu \\ 1 \\ -k_\omega \hat{R}^\top \psi_{\mathfrak{so}(3)}(M\tilde{R}) \\ -k_\omega \hat{R}^\top \psi_{\mathfrak{so}(3)}(M\tilde{R}) \\ -k_c \hat{R}^\top K_a \tilde{R}^\top \tilde{p}_e \\ -k_c \hat{R}^\top K_a \tilde{R}^\top \tilde{p}_e \end{pmatrix}, \quad G_5(x_5^c) = \begin{pmatrix} (X_g^{-1} \hat{X}) \\ (\tilde{R} R_q) \\ \mathbf{x} \\ t \\ \hat{b}_\omega \\ \tilde{b}_\omega \\ \hat{b}_a \\ \tilde{b}_a \end{pmatrix}.$$

Note that the sets $\mathcal{F}_5^c, \mathcal{J}_5^c$ are closed, and $\mathcal{F}_5^c \cup \mathcal{J}_5^c = \mathcal{S}_5^c$. Note also that the closed-loop system (4.47) satisfies the hybrid basic conditions given Section 2.5.1 and is autonomous by taking ω_y, a_y, A and K as functions of t .

4.6 Simulation results

In this section, simulation results are presented to illustrate the performance of the proposed hybrid observers. We make use of the HyEQ Toolbox in Matlab [Sanfelice et al., 2013]. We refer to the continuous inertial navigation observer (*i.e.*, observer \mathcal{H}_3^o without jumps) as ‘CINO’, the fixed-gain hybrid inertial navigation observer \mathcal{H}_3^o as ‘HINO’, the CRE-based variable-gain hybrid inertial navigation observer \mathcal{H}_4^o as ‘HINO-CRE’, and the CRE-based variable-gain hybrid inertial navigation observer \mathcal{H}_5^o as ‘HINO-CRE2’.

We consider an autonomous vehicle moving on a 10-meter diameter circle at 10-meter height, on the trajectory: $p(t) = 10[\cos(0.8t), \sin(0.8t), 1]$. Consider the initial rotation as $R(0) = I_3$ and the angular velocity as $\omega(t) = [\sin(0.3\pi), 0, 0.1]^\top$. Six landmarks are randomly selected such that Assumption 4.1 holds. We consider the same initial conditions for each observer as: $\hat{R}(0) = \mathcal{R}_a(0.99\pi, u), u \in \mathcal{E}(M), \hat{v}(0), \hat{p}(0) = \hat{b}_\omega = 0_{3 \times 1}$. We consider the gain parameters $k_i = 1/6, i = 1, 2, \dots, 6, k_R = 1, k_v, k_p = 3, k_w = 1$. For the hybrid design, we choose $\mathbb{U} = \mathcal{E}(M), \theta = 0.8\pi$, and $\delta = 0.3(1 - \cos\theta)\Delta_M^*$ with Δ_M^* designed as per Lemma 3.3. Two sets of simulation are presented: the first one considers biased angular velocity measurements and the second one considers biased angular velocity and linear acceleration. The matrix parameters for the first CRE are chosen as $P(0) = 0.5I_5, V(t) = I_6, Q(t) = 10I_3$, and for the second CRE are chosen as $P(0) = I_9, V(t) = 0.05I_9, Q(t) = 10I_3$.

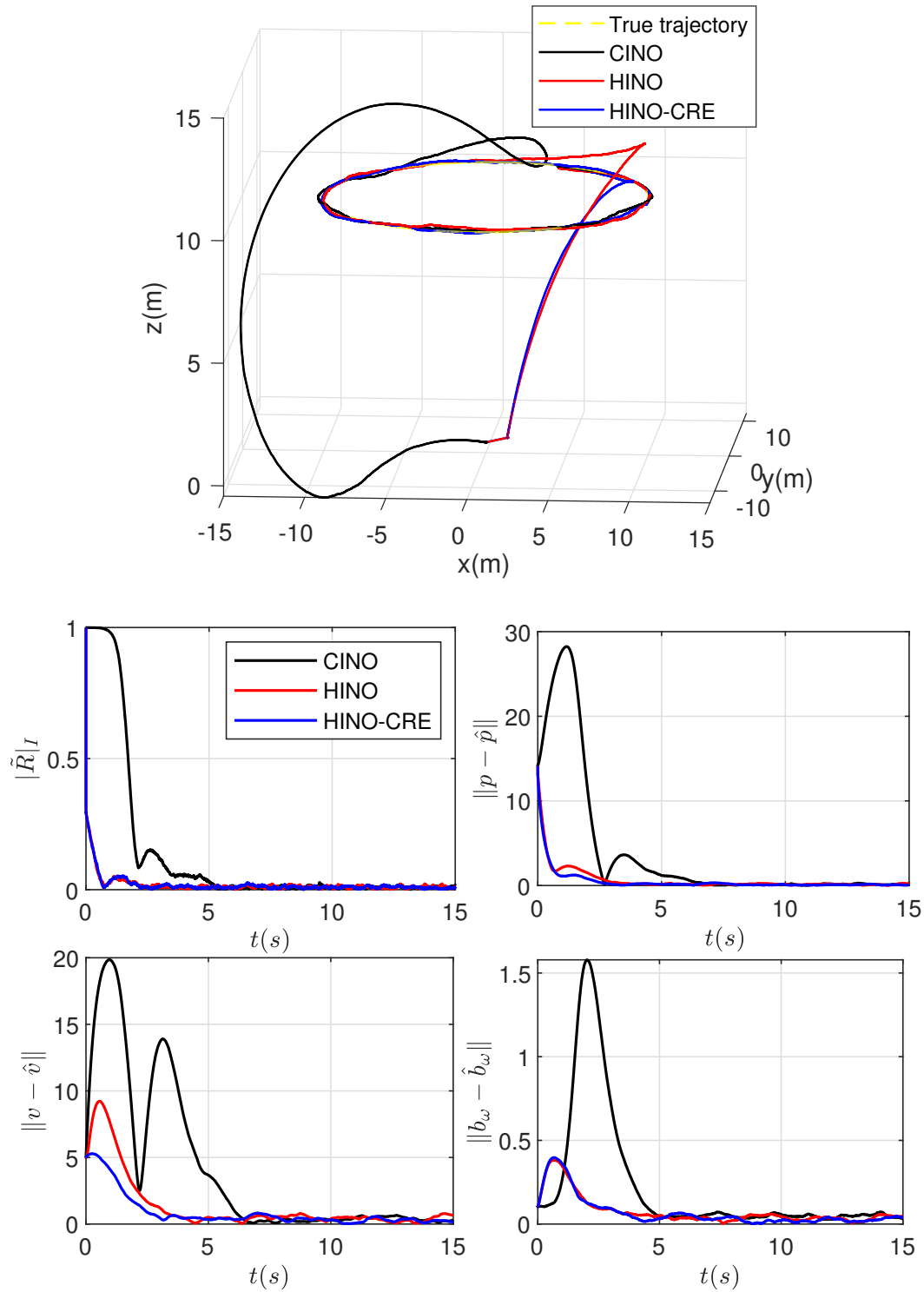


Figure 4.1: Simulation results with biased angular velocity $b_\omega = [-0.1 \ 0.02 \ 0.02]^\top$ and additive white Gaussian noise of 0.4 variance in the measurements of ω and a , and 0.1 variance in the landmark position measurements.

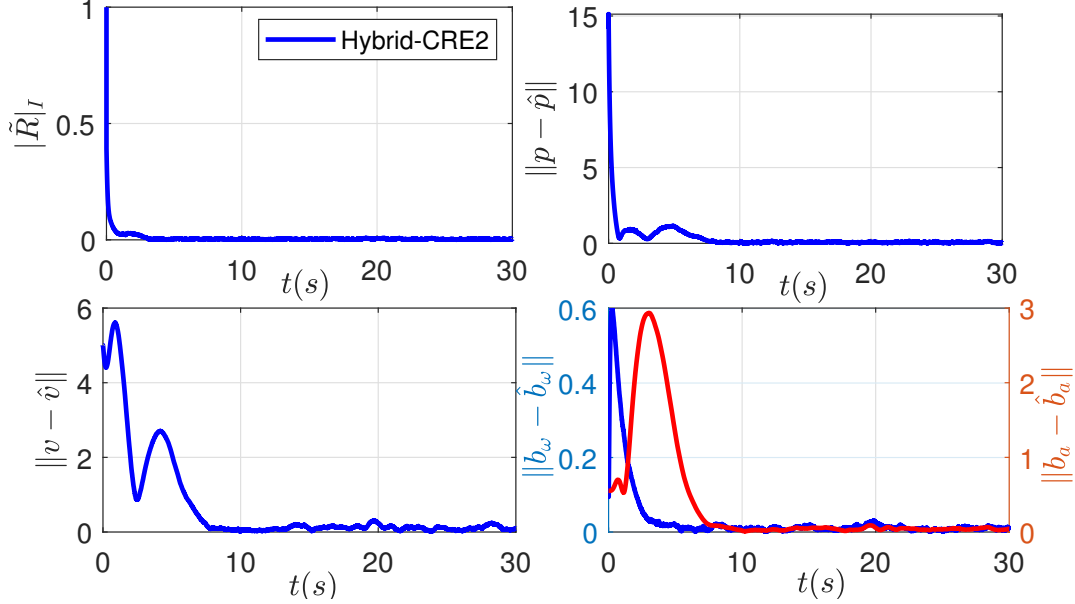


Figure 4.2: Simulation results with biased angular velocity $b_\omega = [-0.1 \ 0.02 \ 0.02]^\top$ and linear acceleration $b_a = [-0.01 \ 0.55 \ 0.07]^\top$, additive white Gaussian noise of 0.1 variance in the angular velocity, linear acceleration and landmark position measurements.

Simulation results are shown in Figure 4.1 and Figure 4.2. As one can see, the proposed hybrid observers exhibit fast convergence when the initial conditions are large. Simulation results also illustrate the good performances of the proposed hybrid observers in the presence of biases in the angular velocity and linear acceleration.

4.7 Experimental results

To further validate the performance of our proposed hybrid observers, we applied our algorithms to real data from the EuRoC dataset [Burri et al., 2016], where the trajectories are generated by a real flight of a quadrotor. This dataset includes a set of stereo images, IMU measurements and ground truth. The sampling rate of the IMU measurements from ADIS16448 is 200Hz and the sampling rate of the stereo images from MT9V034 is 20Hz. The ground truth of the states are obtained by a nonlinear least-squares batch solution using the Vicon pose and IMU measurements. More details about the EuRoC dataset can be found in [Burri et al., 2016].

4.7.1 Experimental setting

The images are undistorted with the camera parameters calibrated using Stereo Camera Calibrator App in MATLAB. The features are tracked via the Kanade-Lucas-Tomasi (KLT) tracker using minimum eigenvalue feature detection [Shi and Tomasi, 1994], which are shown in Figure 4.3. Since no physical landmarks are available in the EuRoC dataset, a set of ‘virtual’ landmarks are generated from the stereo images and the ground truth pose

at the beginning. More precisely, the coordinate of the i -th landmark expressed in the inertial frame is calculated as $p_i = R_G y_i + p_G$, where R_G, p_G are the ground truth rotation and position of the vehicle, y_i denotes the current three-dimensional position of the i -th point-feature generated from the current stereo images. For the sake of efficiency, we limit the maximum number of detected and tracked point-features to a certain number (60 in our experiments). It is quite unrealistic to track the same set of point-features through a long time image sequence. Hence, when the number of visible point-features is less than a certain threshold (6 in our experiments), a new set of point-features is generated using current stereo images and ground truth again. The three-dimensional coordinates of the point-features from stereo images expressed in the camera frame (cam0) are transformed to the frame attached to the vehicle using the calibration matrix provided in the dataset. To remove matched point-feature outliers the technique proposed in [Hua et al., 2018] has been used by choosing the thresholds $S = 30, D = 6$.

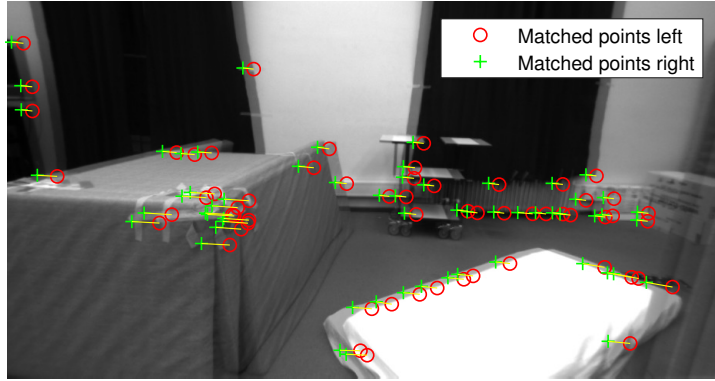


Figure 4.3: Example of features detection and tracking in the left and right images from a stereo camera using the MATLAB Computer Vision System Toolbox. Pictures come from the EuRoc dataset [Burri et al., 2016].

4.7.2 Realtime implementation

In practice, the IMU measurements can be obtained at a high rate, while the landmark measurements are often obtained, for example with stereo cameras, at a much lower rate. Taking into account this fact, we define a strictly increasing sequence $\{t_k\}_{k \in \mathbb{N} \setminus \{0\}}$ as the time-instants when the landmark measurements are obtained. Inspired by the work of continuous-discrete Kalman filter and extended Kalman filter in [Lewis et al., 2007, page 194] and [Kulikov and Kulikova, 2014], we implement our hybrid observer HINO-CRE2 as shown in Algorithm 1. The proposed algorithm has two parts: the states are continuously updated from IMU when no measurements of landmarks are received (*i.e.*, $t \in (t_{k-1}, t_k)$); when the measurements arrive (*i.e.*, $t = t_k$) the state variables are updated using the landmark measurements. This type of continuous-discrete observers for inertial navigation has also been considered in [Barrau and Bonnabel, 2017; Hua et al., 2018]. The CRE is continuously integrated from the time t_{k-1} to the next time instant t_k when the new landmark measurements arrive, and then a numerical discretization method is

Algorithm 1 Continuous-discrete algorithm of HINO-CRE2

Initialization: $\hat{X}(t_0) \in \text{SE}_2(3)$, $\hat{b}_\omega(t_0) \in \mathbb{R}^3$, $\hat{b}_a(t_0) \in \mathbb{R}^3$, $P(t_0) \in \mathbb{R}^{9 \times 9} > 0$.

Output: $\hat{X}(t)$, $\hat{b}_\omega(t)$, $\hat{b}_a(t)$ for all $t \geq t_0$

1: **for** $1 \leq k \leq n$ **do**

2: **while** $t_{k-1} \leq t \leq t_k$ **do**

3: Integrate the following equations:

$$\begin{cases} \dot{\hat{X}} &= f(\hat{X}, \omega_y - \hat{b}_\omega, a_y - \hat{b}_a) \\ \dot{\hat{b}}_\omega &= 0_{3 \times 1} \\ \dot{\hat{b}}_a &= 0_{3 \times 1} \\ \dot{P} &= A(t)P + PA(t)^\top + V(t) \end{cases}$$

4: **end while**

5: Set $\hat{X}_{k|k-1} = \hat{X}(t_k)$, $\hat{b}_{\omega,k|k-1} = \hat{b}_\omega(t_k)$, $\hat{b}_{a,k|k-1} = \hat{b}_a(t_k)$ and $P_{k|k-1} = P(t_k)$

6: Compute the gain matrices

$$\begin{cases} K_k &= P_{k|k-1}C^\top(CP_{k|k-1}C^\top + Q(t)^{-1})^{-1} \\ K_p &= \frac{1}{k_c}\hat{R}_{k|k-1}K_{1,k}\hat{R}_{k|k-1}^\top \\ K_v &= \frac{1}{k_c}\hat{R}_{k|k-1}K_{2,k}\hat{R}_{k|k-1}^\top \\ K_a &= \frac{1}{k_c}\hat{R}_{k|k-1}K_{3,k}\hat{R}_{k|k-1}^\top \end{cases}$$

from $K_k = [K_{1,k}^\top, K_{2,k}^\top, K_{3,k}^\top]^\top$ and $\hat{X}_{k|k-1} = \mathcal{T}_{\text{SE}_2(3)}(\hat{R}_{k|k-1}, \hat{v}_{k|k-1}, \hat{p}_{k|k-1})$

7: Compute the innovation terms Δ_k in (4.42) with K_p and K_v , $\Delta_{R,k}$ in (4.11) and $\Delta_{p,k}$ in (4.12)

8: Update the state estimates as

$$\begin{cases} \hat{X}_{k|k} &= \exp(-\Delta_k)\hat{X}_{k|k-1} \\ \hat{b}_{\omega,k|k} &= \hat{b}_{\omega,k|k-1} - k_\omega\hat{R}_{k|k-1}^\top\psi_{\mathfrak{so}(3)}(\Delta_{R,k}) \\ \hat{b}_{a,k|k} &= \hat{b}_{a,k|k-1} - \hat{R}_{k|k-1}^\top K_a \Delta_{p,k} \\ P_{k|k} &= P_{k|k-1} - K_k C P_{k|k-1} \end{cases}$$

9: **if** $(\mu_{\mathbb{Q}}(\hat{X}_{k|k}, r, b_k) \geq \delta)$ **then**

10: Reset the state $\hat{X}_{k|k} = X_q^{-1}\hat{X}_{k|k}$, $X_q \in \gamma(\hat{X}_{k|k})$

11: **end if**

12: Set $\hat{X}(t_k) = \hat{X}_{k|k}$, $\hat{b}_\omega(t_k) = \hat{b}_{\omega,k|k}$, $\hat{b}_a(t_k) = \hat{b}_{a,k|k}$ and $P(t_k) = P_{k|k}$

13: **end for**

applied at the instant of time t_k . A first-order numerical discretization method is applied to the dynamics of the estimated angular velocity bias \hat{b}_ω and linear acceleration bias \hat{b}_a . However, an exponential map based discrete update of \hat{X} has been considered, *i.e.*, $\hat{X}_{k|k} = \exp(-\Delta_k) \hat{X}_{k|k-1}$, which guarantees that $\hat{X}_{k|k} \in \text{SE}_2(3)$. Note that the estimated state \hat{X} is reset once the condition $\mu_{\mathbb{Q}}(\hat{X}, r, b) \geq \delta$ (*i.e.*, $\hat{X} \in \mathcal{J}_o$) is satisfied. Algorithm 1 can be easily adjusted to other observers proposed in this chapter.

4.7.3 Results

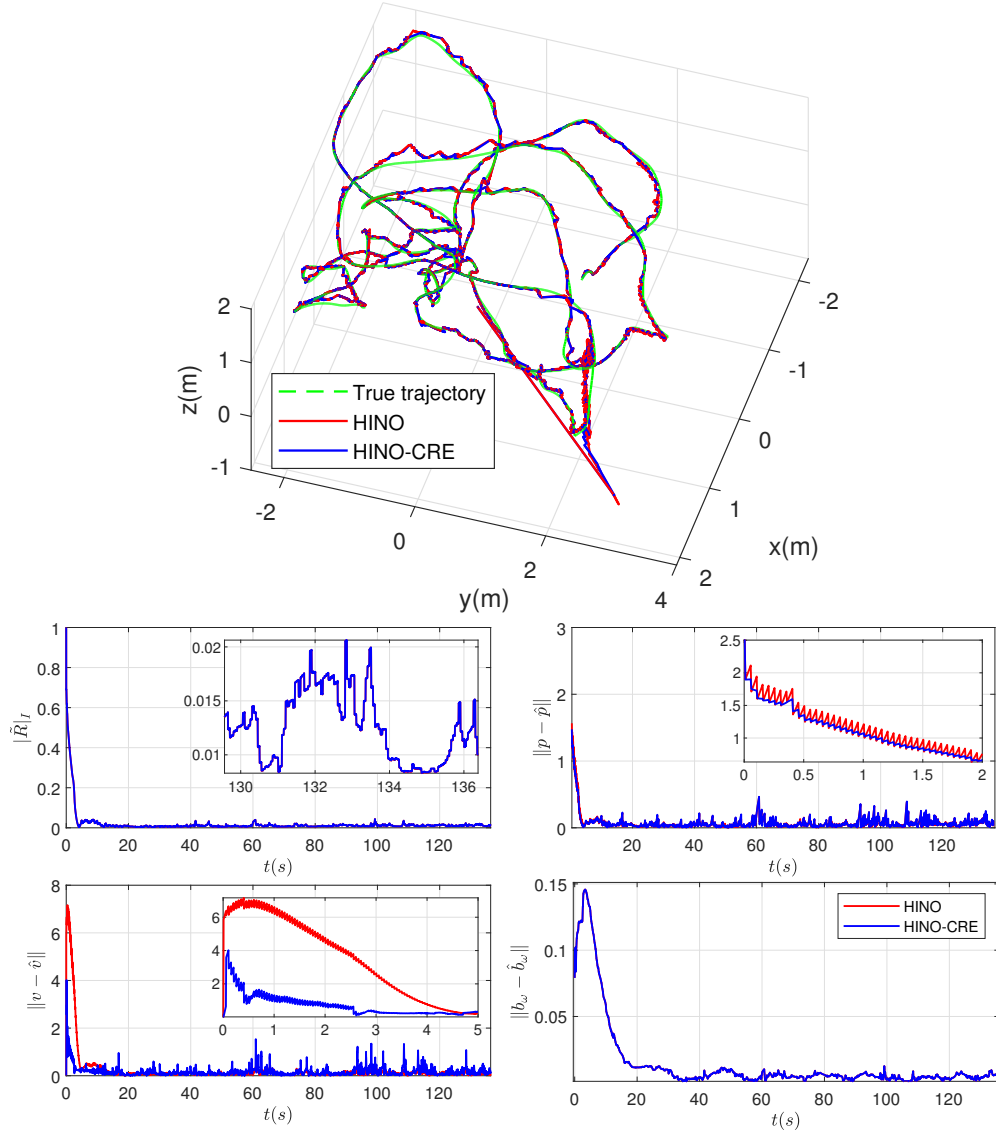


Figure 4.4: Experimental results using biased gyro and unbiased accelerometer measurements from the dataset V1_01_easy. The true and estimated trajectories are shown in the left plot. The estimation errors of rotation, position, velocity and IMU bias are shown in right plot.

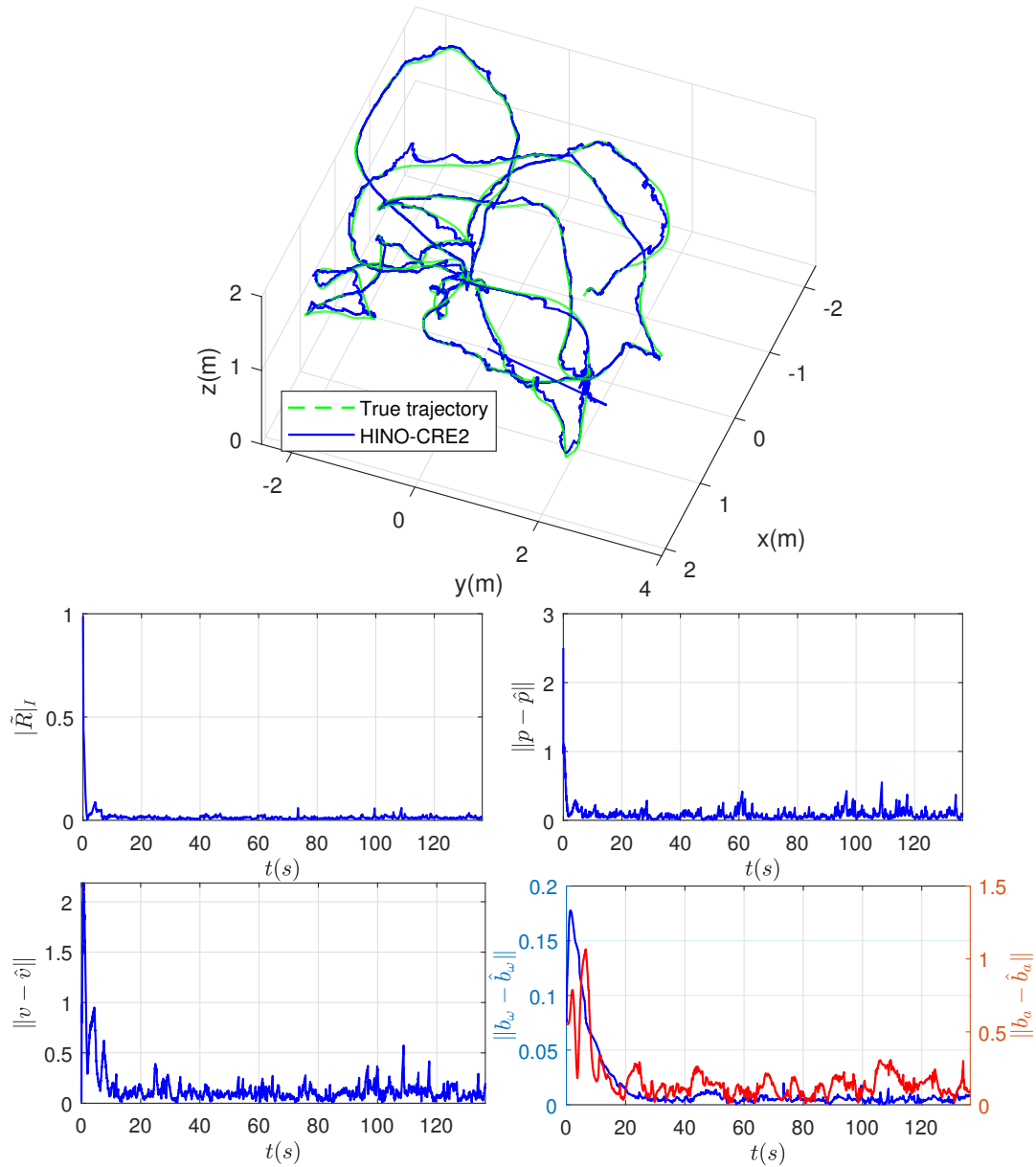


Figure 4.5: Experimental results using biased gyro and accelerometer measurements from the dataset V1_01_easy. The true and estimated trajectories are shown in the left plot. The estimation errors of rotation, position, velocity and IMU bias are shown in right plot.

Two sets of experiments have been presented with large initial conditions: $\hat{R}(0) = \exp(0.99\pi e_3^\times)R_G$ and $\hat{p}(0) = \hat{v}(0) = \hat{b}_\omega(0) = \hat{b}_a(0) = 0$. The gain parameters are carefully tuned with a trade-off between the convergence rate and the noise at steady state. Note that higher gains result in faster convergence but amplify noise at steady-state. As one can see, in the first plot of Figure 4.4 and Figure 4.5, the estimates provided by both observers HINO and HINO-CRE, using the biased gyro and unbiased accelerometer measurements from IMU and stereo vision, converge to the vicinity of the ground truth after a few seconds. In the second plot of Figure 4.4 and Figure 4.5, the estimates (including accelerometer-bias) provided by observer HINO-CRE2, using the biased IMU measurements and stereo vision, also converge to the vicinity of the ground truth after a few seconds. Note that the ground truth pose is used to validate the performance of the proposed algorithms and also to generate the virtual landmarks in the experiments due to the lack of physical landmarks.

4.8 Conclusions

In this chapter, we addressed the state estimation problem of the inertial navigation systems using IMU and landmark position measurements. The observer design relies on a resetting mechanism motivated from the previous chapter, where all undesired equilibrium points are avoided in the flows, and a decrease of the Lyapunov function after each jump is ensured. The proposed nonlinear geometric hybrid observers are designed on the matrix Lie group $\text{SE}_2(3)$, with global exponential stability guarantees.

We proposed two hybrid observers in Theorem 4.1 and Theorem 4.2, respectively, using bias-free angular velocity and linear acceleration measurements. The first observer relies on fixed gains, while the second one uses variable gains depending on the solution of a CRE. Based on a conceptually similar approach, these results are extended in Theorem 4.3 and 4.4 to handle biased angular velocity measurements. To handle the case of biased angular velocity and linear acceleration measurements, we proposed a new variable-gain hybrid observer in Theorem 4.5 with global exponential stability guarantees. All the proposed observers in this chapter are endowed with strong stability properties (*i.e.*, global exponential stability). Simulation and experimental results are provided to illustrate the performance of the proposed observers.

Chapter 5

Hybrid State Estimation for Inertial Navigation Using Intermittent Measurements

5.1 Introduction

In this chapter, we are interested in the problem of simultaneous estimation of the attitude, position and linear velocity of a rigid body using continuous IMU measurements and intermittent landmark position measurements. In practical applications, the landmark position measurements are obtained, usually via a vision system, at a much lower rate than IMU measurements. Therefore, the stability is not guaranteed if one tries to implement continuous-time observers in applications involving intermittent measurements combining sensors with different bandwidth characteristics (such as IMU and vision systems), and as such, the observers proposed in the previous chapter needs to be carefully redesigned. In the literature, most of the existing results are based on (discrete) Kalman-type filter such as extended Kalman filters (EKF) and unscented Kalman filters (UKF) [Mourikis and Roumeliotis, 2007; Mourikis et al., 2009], and the invariant Extended Kalman Filter (IEKF) [Barrau and Bonnabel, 2017]. It is well known that these Kalman-type filters, relying on local linearizations, suffer from large computational overhead and lack of strong stability guarantees.

Motivated by the recent work in [Ferrante et al., 2016; Li et al., 2017; Sferlazza et al., 2019; Berkane and Tayebi, 2017b; Berkane and Tayebi, 2019], two types of hybrid nonlinear observers for inertial navigation systems, with and without the knowledge of the gravity vector, relying on continuous angular velocity and linear acceleration measurements, and intermittent landmark measurements. For each observer, we provide two different design approaches for the gain parameters; a fixed-gain approach relying on an infinite-dimensional optimization, and a variable-gain approach relying on a continuous-discrete Riccati equation. The proposed observers are endowed with strong stability guarantees and do not rely on linearizations compared to the recent work in [Barrau and Bonnabel, 2017; Hamel and Samson, 2018]. In fact, the proposed observers do not have any restrictions on the initial conditions of the position and linear velocity. Moreover, the

first hybrid observer proposed here does not require the knowledge of the gravity vector, which was not considered in [Barrau and Bonnabel, 2017; Wang and Tayebi, 2020]. Unlike the results of [Berkane and Tayebi, 2017b; Berkane and Tayebi, 2019], the estimated attitude from our hybrid observers is continuous, which is desirable in practice, especially when dealing with observer-controller implementations. These results of the this chapter have been published in [Wang and Tayebi, 2019c].

5.2 Problem formulation

Consider a rigid body system, navigating in a three-dimensional space, modeled as (2.83)-(2.85), *i.e.*,

$$\dot{R} = R\omega^\times, \quad (5.1)$$

$$\dot{p} = v, \quad (5.2)$$

$$\dot{v} = g + Ra, \quad (5.3)$$

where $g \in \mathbb{R}^3$ denotes the gravity vector, $\omega \in \mathbb{R}^3$ denotes the angular velocity expressed in the body-frame, and $a \in \mathbb{R}^3$ is the body-frame “apparent acceleration” capturing all non-gravitational force applied to the rigid body expressed in the body-frame. We assume that the measurements of ω and a are continuously available.

We consider a family of N landmarks with $p_i \in \mathbb{R}^3$ being the position of the i -th landmark expressed in the inertial frame \mathcal{I} . The landmark measurements expressed in the body-fixed frame \mathcal{B} are denoted as

$$y_i := R^\top(p_i - p), \quad i = 1, 2, \dots, N. \quad (5.4)$$

Note that the landmark measurements can be directly constructed, for instance, using bearing measurements generated from a stereo vision system as (2.98). The following assumptions are needed in our observers design:

Assumption 5.1 *Assume that there exist at least three non-collinear landmarks among the $N \geq 3$ measurable landmarks at each instant of time.*

Note that Assumption 5.1 is commonly used in the problem of pose estimation on $\text{SE}(3)$ using landmark measurements [Vasconcelos et al., 2010; Hua et al., 2015; Khosravian et al., 2015b; Wang and Tayebi, 2017; Wang and Tayebi, 2019a].

Assumption 5.2 *We assume that the landmark measurements are available at some instant of time $t_j, j \in \mathbb{N}_{>0}$, and there exist constants $0 < T_m \leq T_M$ such that $T_m \leq t_{j+1} - t_j \leq T_M$ for all $j \in \mathbb{N}_{>0}$.*

Assumption 5.2 gives upper and lower bound on the time differences of two consecutive landmark measurements. Note that $T_m > 0$ is required to be strictly positive to avoid the Zeno behaviors. Note also that one has regular (*i.e.*, periodic) measurements if $T_m = T_M$.

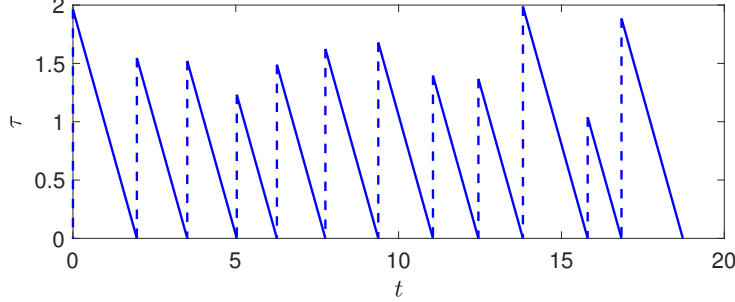


Figure 5.1: An example of the solution of the timer τ with $T_m = 1$ and $T_M = 2$.

Due to the impulsive nature of such intermittent measurements, the sampling events can be modeled by a decreasing timer τ that has the following hybrid dynamics:

$$\begin{cases} \dot{\tau} = -1 & \tau \in [0, T_M] \\ \tau^+ \in [T_m, T_M] & \tau \in \{0\} \end{cases} \quad (5.5)$$

with $\tau(0) \in [0, T_M]$. Note that τ decreases to zero continuously when there is not landmark measurements, and upon reaching zero (*i.e.*, landmark measurements are available) it is reset to a value between T_m and T_M . An example of the solution of the timer τ is shown in Figure 5.1.

The following lemma is useful in the subsequent developments:

Lemma 5.1 Define $p_c = \frac{1}{k_c} \sum_{i=1}^N k_i p_i$ and $k_c = \sum_{i=1}^N k_i$ with $k_i > 0, i = 1, 2, \dots, N$. Then, for each $\bar{R} \in \text{SO}(3), \bar{p} \in \mathbb{R}^3$ one has

$$\sum_{i=1}^N k_i (p_i - p_c)^\times (p_i - \bar{p} - \bar{R}y_i) = 2\psi_{\mathfrak{so}(3)}(MR\bar{R}^\top) \quad (5.6)$$

$$\sum_{i=1}^N k_i (p_i - \bar{p} - \bar{R}y_i) = k_c (\bar{R}R^\top(p - p_c) - (\bar{p} - p_c)) \quad (5.7)$$

where y_i denotes the measurement of landmark p_i defined in (5.4), and $M := \sum_{i=1}^N k_i(p_i - p_c)(p_i - p_c)^\top = \sum_{i=1}^N k_i p_i p_i^\top - k_c p_c p_c^\top$.

See the proof in Appendix D.2. Given at least three non-collinear landmarks $p_i, i = 1, 2, \dots, N$, it is always possible to guarantee that the matrix M is positive semidefinite and has no more than one zero eigenvalue, through an appropriate choice of the gains $k_i, i = 1, 2, \dots, N$.

Given constant matrices $A \in \mathbb{R}^{n \times n}, C \in \mathbb{R}^{m \times n}$ and $K \in \mathbb{R}^{n \times m}$, for each $P \in \mathbb{R}^{n \times n}$, we define the following real-valued matrix mapping $\Xi_P : [0, T_M] \rightarrow \mathbb{R}^{n \times n}$ as

$$\Xi_P(\tau) := (I - KC)^\top \hat{\Phi}(\tau)^\top P \hat{\Phi}(\tau) (I - KC) - P, \quad (5.8)$$

where $\hat{\Phi}(\tau) = \exp(A\tau)$. Let $A(t) \in \mathbb{R}^{n \times n}, C(t) \in \mathbb{R}^{m \times n}$, and $V(t), Q(t) \in \mathbb{R}^{n \times n}$ be the matrix-valued functions of time t , which are continuous and bounded for all $t \geq 0$. Then, we consider the CDRE (2.119)-(2.120) with $P(0)$ being a symmetric positive definite matrix and $Q(t), V(t)$ being positive definite matrices.

5.3 Observers design with unknown gravity vector

In this section, we assume that the gravity vector is unknown. Define $\hat{\mathbf{g}} \in \mathbb{R}^3$ as the estimate of the gravity vector \mathbf{g} . Let $\hat{R} \in \text{SO}(3)$ denote the estimate of the attitude R , $\hat{p} \in \mathbb{R}^3$ denote the estimate of the position p , and $\hat{v} \in \mathbb{R}^3$ denote the estimate of velocity v . Let us introduce an auxiliary variable $\eta \in \mathbb{R}^3$. We propose the following hybrid nonlinear observer:

$$\begin{array}{ll} \dot{\hat{R}} = \hat{R}(\omega + \hat{R}^\top \eta)^\times & \hat{R}^+ = \hat{R} \\ \dot{\eta} = 0_{3 \times 1} & \eta^+ = \sigma_R \\ \dot{\hat{p}} = \eta^\times(\hat{p} - p_c) + \hat{v} & \hat{p}^+ = \hat{p} + \hat{R}K_p\hat{R}^\top \sigma_p \\ \dot{\hat{v}} = \eta^\times\hat{v} + \hat{r} + \hat{R}a & \hat{v}^+ = \hat{v} + \hat{R}K_v\hat{R}^\top \sigma_p \\ \dot{\hat{\mathbf{g}}} = \eta^\times\hat{\mathbf{g}} & \hat{\mathbf{g}}^+ = \hat{\mathbf{g}} + \hat{R}K_g\hat{R}^\top \sigma_p \end{array} \quad (5.9)$$

$\underbrace{\hspace{10em}}_{\tau \in [0, T_M]} \qquad \underbrace{\hspace{10em}}_{\tau \in \{0\}}$

where $\hat{R}(0) \in \text{SO}(3)$, $\hat{p}(0), \hat{v}(0), \hat{\mathbf{g}}(0) \in \mathbb{R}^3$ and $\eta(0) = 0_{3 \times 1}$. The gain matrices $K_p, K_v, K_g \in \mathbb{R}^{3 \times 3}$ will be designed later, and the innovation terms σ_R and σ_p are given as

$$\sigma_R = \frac{k_R}{2} \sum_{i=1}^N k_i (p_i - p_c)^\times (p_i - \hat{p} - \hat{R}y_i) \quad (5.10)$$

$$\sigma_p = \sum_{i=1}^N k_i (p_i - \hat{p} - \hat{R}y_i) \quad (5.11)$$

with $k_R > 0, k_i > 0, \forall i = 1, 2, \dots, N$, the measurement y_i given in (5.4), and p_c defined as per Lemma 5.1. The structure of this observer is given by Figure 5.2.

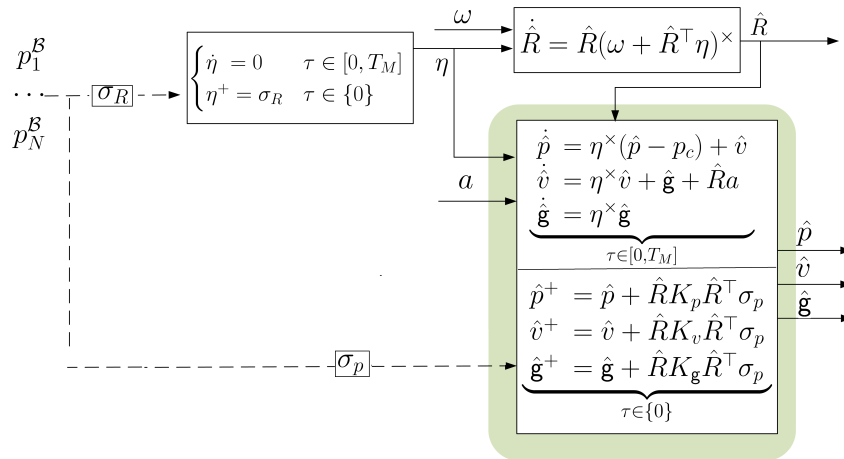


Figure 5.2: Nonlinear observer (5.9) with gravity vector estimation

Remark 5.1 *The variables $\hat{R}, \eta, \hat{p}, \hat{v}$ and $\hat{\mathbf{g}}$ are continuously integrated when no landmark measurements are received (i.e., $t \in [t_{j-1}, t_j], \forall j \in \mathbb{N}_{>0}$), and updated via appropriate*

jumps once the landmark measurements are received (i.e., $t = t_j, j \in \mathbb{N}_{>0}$). It should be pointed out that the estimated rotation \hat{R} from the hybrid observer (5.9) is continuous, leading to an interesting difference with respect to the results in [Berkane and Tayebi, 2017b; Barrau and Bonnabel, 2017; Berkane and Tayebi, 2019].

Define the geometric estimation errors: $\tilde{R} = R\hat{R}^\top$, $\tilde{v} = v - \tilde{R}\hat{v}$, $\tilde{p} = p - \tilde{R}\hat{p} - (I - \tilde{R})p_c$, and $\tilde{\mathbf{g}} = \mathbf{g} - \tilde{R}\hat{\mathbf{g}}$. From the identities (5.6) and (5.7) given in Lemma 5.1, the innovation terms σ_R defined in (5.10) and σ_p defined in (5.11) can be rewritten as

$$\sigma_R = k_R \psi_{\mathfrak{so}(3)}(M\tilde{R}), \quad \sigma_p = k_c \tilde{R}^\top \tilde{p} \quad (5.12)$$

with k_c defined in Lemma 5.1. In view of (5.1)-(5.3), (5.9) and (5.12), the closed-loop dynamics of the estimation errors are given as follows:

$$\begin{array}{ll} \dot{\tilde{R}} &= \tilde{R}(-\eta)^\times & \tilde{R}^+ &= \tilde{R} \\ \dot{\eta} &= 0_{3 \times 1} & \eta^+ &= k_R \psi_{\mathfrak{so}(3)}(M\tilde{R}) \\ \dot{\tilde{p}} &= \tilde{v} & \tilde{p}^+ &= \tilde{p} - k_c R K_p R^\top \tilde{p} \\ \dot{\tilde{v}} &= \tilde{\mathbf{g}} & \tilde{v}^+ &= \tilde{v} - k_c R K_v R^\top \tilde{p} \\ \dot{\tilde{\mathbf{g}}} &= 0_{3 \times 1} & \tilde{\mathbf{g}}^+ &= \tilde{\mathbf{g}} - k_c R K_g R^\top \tilde{p} \end{array} \quad \underbrace{\tau \in [0, T_M]}_{\tau \in \{0\}} \quad (5.13)$$

In the following subsections, we provide two design approaches; a fixed-gain design relying on an infinite-dimensional optimization and a variable-gain design relying on a CDRE, for the proposed hybrid observer (5.9).

5.3.1 Fixed-gain design

In this subsection, we consider constant gain matrices K_p, K_v and K_g . Let $K_p = k_p I_3, K_v = k_v I_3$, and $K_g = k_g I_3$ with some constant scalars k_p, k_v and k_g to be designed. Let us introduce the new vector $\mathbf{x} := [\tilde{p}^\top, \tilde{v}^\top, \tilde{\mathbf{g}}^\top]^\top \in \mathbb{R}^9$. From (5.13), one has the following dynamics:

$$\begin{cases} \dot{\mathbf{x}} = A\mathbf{x}, & \tau \in [0, T_M] \\ \mathbf{x}^+ = (I - KC)\mathbf{x}, & \tau \in \{0\} \end{cases} \quad (5.14)$$

where the matrices A, K and C are given by

$$A = \begin{bmatrix} 0_{3 \times 3} & I_3 & 0_{3 \times 3} \\ 0_{3 \times 3} & 0_{3 \times 3} & I_3 \\ 0_{3 \times 3} & 0_{3 \times 3} & 0_{3 \times 3} \end{bmatrix}, \quad K := k_c \begin{bmatrix} k_p I_3 \\ k_v I_3 \\ k_g I_3 \end{bmatrix}, \quad C = [I_3, \ 0_{3 \times 3}, \ 0_{3 \times 3}]. \quad (5.15)$$

Define the extended space $\mathcal{U} := \text{SO}(3) \times \mathbb{R}^3$. We introduce the new state $x_1 = (\tilde{R}, \eta, \mathbf{x}, \tau) \in \mathcal{U} \times \mathbb{R}^9 \times [0, T_M]$. From (5.13) and (5.14), one obtains the hybrid closed-loop system $\mathcal{H}_1 = (F_1, G_1, \mathcal{F}_1, \mathcal{J}_1)$ as

$$\mathcal{H}_1 : \begin{cases} \dot{x}_1 = F_1(x_1) & x_1 \in \mathcal{F}_1 \\ x_1^+ \in G_1(x_1) & x_1 \in \mathcal{J}_1 \end{cases} \quad (5.16)$$

with the flow and jump maps defined as

$$F_1(x_1) = \left(\tilde{R}(-\eta)^\times, 0_{3 \times 1}, Ax, -1 \right) \quad (5.17)$$

$$G_1(x_1) = \left(\tilde{R}, k_R \psi_{\mathfrak{so}(3)}(M\tilde{R}), (I - KC)\mathbf{x}, [T_m, T_M] \right) \quad (5.18)$$

$$\mathcal{F}_1 = \mathcal{U} \times \mathbb{R}^9 \times [0, T_M] \quad (5.19)$$

$$\mathcal{J}_1 = \mathcal{U} \times \mathbb{R}^9 \times \{0\} \quad (5.20)$$

Note that the flow set \mathcal{F}_1 and jump set \mathcal{J}_1 of \mathcal{H}_1 are closed, and $\mathcal{F}_1 \cup \mathcal{J}_1 = \mathcal{U} \times \mathbb{R}^9 \times [0, T_M]$. Moreover, the flow map F_1 and jump map G_1 is outer semicontinuous and locally bounded. Therefore, the hybrid system \mathcal{H}_1 satisfies the hybrid basic conditions given in Section 2.5.1.

Let $\bar{M} := \frac{1}{2}(\text{tr}(M)I_3 - M)$ be a positive definite matrix, where M is defined in Lemma 5.1, and define $\varsigma_M := \lambda_m^{\bar{M}}/\lambda_M^{\bar{M}} = (\text{tr}(M) - \lambda_M^M)/(\text{tr}(M) - \lambda_m^M)$. Let us define the following closed set:

$$\mathcal{A} := \{(\tilde{R}, \eta, \mathbf{x}, \tau) \in \mathcal{U} \times \mathbb{R}^9 \times [0, T_M] \mid \tilde{R} = I_3, \eta = 0_{3 \times 1}, \mathbf{x} = 0_{9 \times 1}\}. \quad (5.21)$$

Now, one can state the following result:

Theorem 5.1 Consider the hybrid dynamical system (5.16)-(5.20). Let Assumption 5.1 and Assumption 5.2 hold. Suppose that the matrix \bar{M} is positive definite, and there exists a positive definite symmetric matrix P satisfying $\Xi_P(\tau) < 0, \forall \tau \in [T_m, T_M]$, with $\Xi_P(\tau)$ defined in (5.8) and matrices A, K and C given in (5.15). Then, for any $|\tilde{R}(0)|_I < \sqrt{\varsigma_M}$, there exist a constant $k_R^* > 0$ such that, for every $0 < k_R < k_R^*$, the set \mathcal{A} is exponentially stable.

Proof See Appendix D.3.

Remark 5.2 Recall the matrix M defined in Lemma 5.1. To increase the basin of attraction for the attitude estimation error, it is always possible to have $\varsigma_M = 1$ (i.e., $M = kI_3$ with some $k > 0$) by tuning the weights $k_i, i = 1, \dots, N$, when there exist at least four non-coplanar landmarks. Moreover, when there exist three non-collinear landmarks, it is still possible to make $\varsigma_M = 1$ as in [Tayebi et al., 2013].

Remark 5.3 The optimization problem $\Xi_P(\tau) < 0, \forall \tau \in [T_m, T_M]$ can be solved using the polytopic embedding technique proposed in [Ferrante et al., 2016] and the finite-dimensional LMI approach proposed in the recent work [Sferlazza et al., 2019]. A complete procedure for solving this infinite-dimensional optimization problem, adapted from the work in [Sferlazza et al., 2019], is provided in Appendix D.1.

5.3.2 Variable-gain design

In this subsection, we consider time-varying gains related to the solutions of continuous-discrete Riccati equations. Consider the new vector $\mathbf{x} = [\tilde{p}^\top R, \tilde{v}^\top R, \tilde{g}^\top R]^\top \in \mathbb{R}^9$. Then, from (5.1) and (5.9), the dynamics of \mathbf{x} are given by

$$\begin{cases} \dot{\mathbf{x}} = A(t)\mathbf{x}, & \tau \in [0, T_M] \\ \mathbf{x}^+ = (I - KC(t))\mathbf{x}, & \tau \in \{0\} \end{cases} \quad (5.22)$$

where the matrices $A(t)$, K and $C(t)$ are given by

$$A(t) = \begin{bmatrix} -\omega^\times & I_3 & 0_{3 \times 3} \\ 0_{3 \times 3} & -\omega^\times & I_3 \\ 0_{3 \times 3} & 0_{3 \times 3} & -\omega^\times \end{bmatrix}, K = k_c \begin{bmatrix} K_p \\ K_v \\ K_g \end{bmatrix}, \quad C(t) = [I_3 \ 0_{3 \times 3} \ 0_{3 \times 3}]. \quad (5.23)$$

The gain matrix K is designed as

$$K = PC(t)^\top (C(t)PC(t)^\top + Q(t))^{-1}, \quad (5.24)$$

where P is the solution of the CDRE (2.119)-(2.120) with matrices $(A(t), C(t))$ given by (5.23) and matrices $Q(t)$ and $V(t)$ being uniformly positive definite.

Introducing the new state $x_2 = (\tilde{R}, \eta, \mathbf{x}, \tau) \in \mathcal{U} \times \mathbb{R}^9 \times [0, T_M]$, from (5.13) and (5.22), one obtains the following hybrid closed-loop system $\mathcal{H}_2 = (F_2, G_2, \mathcal{F}_2, \mathcal{J}_2)$:

$$\mathcal{H}_2 : \begin{cases} \dot{x}_2 = F_2(x_2) & x_2 \in \mathcal{F}_2 \\ x_2^+ \in G_2(x_2) & x_2 \in \mathcal{J}_2 \end{cases} \quad (5.25)$$

with the flow and jump maps defined as

$$F_2(x_2) = \left(\tilde{R}(-\eta)^\times, 0_{3 \times 1}, A(t)\mathbf{x}, -1 \right) \quad (5.26)$$

$$G_2(x_2) = \left(\tilde{R}, k_R \psi_{\mathfrak{so}(3)}(M\tilde{R}), (I - KC(t))\mathbf{x}, [T_m, T_M] \right) \quad (5.27)$$

$$\mathcal{F}_2 := \mathcal{U} \times \mathbb{R}^9 \times [0, T_M] \quad (5.28)$$

$$\mathcal{J}_2 := \mathcal{U} \times \mathbb{R}^9 \times \{0\} \quad (5.29)$$

Note that the flow set \mathcal{F}_2 and jump set \mathcal{J}_2 of \mathcal{H}_2 are closed, and $\mathcal{F}_2 \cup \mathcal{J}_2 = \mathcal{U} \times \mathbb{R}^9 \times [0, T_M]$. Moreover, the flow map F_2 and jump map G_2 is outer semicontinuous and locally bounded. Therefore, the hybrid system \mathcal{H}_2 satisfies the hybrid basic conditions given in Section 2.5.1.

Now, one can state the following result:

Theorem 5.2 *Consider the hybrid dynamical system (5.25)-(5.29). Let Assumption 5.1 and Assumption 5.2 hold. Suppose that the matrix \bar{M} is positive definite, and the conditions given in Lemma 2.12 are satisfied. Choose the gain K as (5.24) with P being the solution of CDRE (2.119)-(2.120) and matrices $(A(t), C(t))$ defined in (5.23). Then, for any $|\tilde{R}(0)|_I < \sqrt{\varsigma_M}$, there exist a constant $k_R^* > 0$ such that, for any $0 < k_R < k_R^*$, the set \mathcal{A} is exponentially stable.*

Proof See Appendix D.4.

5.4 Observers design with known gravity vector

In this section, we provide different observers in the case where the gravity vector \mathbf{g} is known, which is reasonable in many practical applications. With the knowledge of the gravity vector \mathbf{g} , the number of the estimated states is reduced. On one hand, it reduces the cost of computation, while, on the other hand, it increases the difficulty of the stability analysis. To this end, we will need the following technical lemma:

Lemma 5.2 Consider two continuously differentiable functions $\mathcal{V}_1 : \mathcal{U} \rightarrow \mathbb{R}_{\geq 0}$ and $\mathcal{V}_2 : \mathbb{R}^n \rightarrow \mathbb{R}_{\geq 0}$ such that the following inequalities hold:

$$\underline{\alpha}_1 \|\zeta\|^2 \leq \mathcal{V}_1(\zeta) \leq \bar{\alpha}_1 \|\zeta\|^2, \quad \forall \zeta \in \mathcal{U} \quad (5.30)$$

$$\dot{\mathcal{V}}_1 \leq -\lambda_1 \mathcal{V}_1 \quad (5.31)$$

$$\underline{\alpha}_2 \|\mathbf{x}\|^2 \leq \mathcal{V}_2(\mathbf{x}) \leq \bar{\alpha}_2 \|\mathbf{x}\|^2, \quad \forall \mathbf{x} \in \mathbb{R}^n \quad (5.32)$$

$$\dot{\mathcal{V}}_2 \leq -\lambda_2 \mathcal{V}_2 + \beta \|\zeta\| \|\mathbf{x}\| \quad (5.33)$$

where $\underline{\alpha}_1, \bar{\alpha}_1, \underline{\alpha}_2, \bar{\alpha}_2, \lambda_1, \lambda_2, \beta$ are strictly positive real scalars. Then, the following inequality holds:

$$\varepsilon \dot{\mathcal{V}}_1 + \dot{\mathcal{V}}_2 \leq -\lambda (\varepsilon \mathcal{V}_1 + \mathcal{V}_2) \quad (5.34)$$

with some $\varepsilon > \frac{\beta^2}{2\lambda_1\lambda_2\underline{\alpha}_1\underline{\alpha}_2}$ and $\lambda = \min\{\frac{\lambda_1}{2}, (\lambda_2 - \frac{\beta^2}{2\varepsilon\lambda_1\underline{\alpha}_1\underline{\alpha}_2})\}$.

Proof See the proof in Appendix D.5.

We propose the following hybrid nonlinear observer:

$$\begin{array}{ll} \dot{\hat{R}} = \hat{R}(\omega + \hat{R}^\top \eta)^\times & \hat{R}^+ = \hat{R} \\ \dot{\eta} = 0_{3 \times 1} & \eta^+ = \sigma_R \\ \underbrace{\dot{\hat{p}} = \eta^\times(\hat{p} - p_c) + \hat{v}}_{\tau \in [T_m, T_M]} & \underbrace{\hat{p}^+ = \hat{p} + \hat{R}K_p \hat{R}^\top \sigma_p}_{\tau \in \{0\}} \\ \dot{\hat{v}} = \eta^\times \hat{v} + \mathbf{g} + \hat{R}\mathbf{a} & \underbrace{\hat{v}^+ = \hat{v} + \hat{R}K_v \hat{R}^\top \sigma_p}_{\tau \in \{0\}} \end{array} \quad (5.35)$$

where $\hat{R}(0) \in \text{SO}(3)$, $\hat{p}(0), \hat{v}(0) \in \mathbb{R}^3$ and $\eta(0) = 0_{3 \times 1}$. The gain matrices $K_p, K_v \in \mathbb{R}^{3 \times 3}$ will be designed later, and the innovation terms σ_R and σ_p are given in (5.10) and (5.11), respectively. The structure of this observer is given by Figure 5.3.

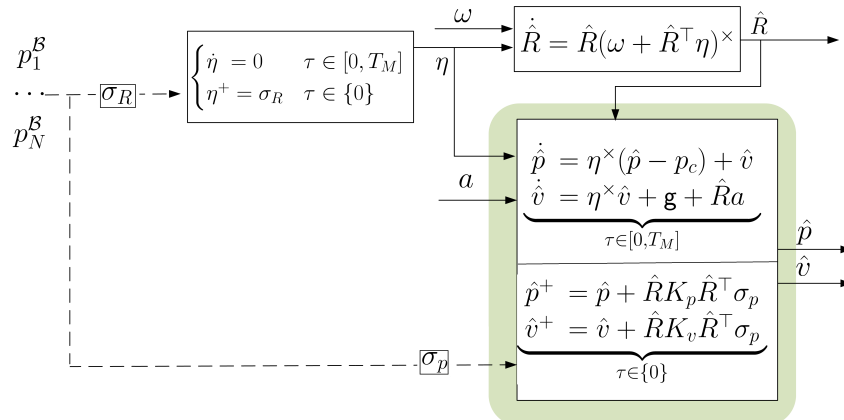


Figure 5.3: Nonlinear observer (5.35) without gravity vector estimation

In view of (5.1)-(5.3), (5.12) and (5.35), the dynamics of the estimation errors are given by

$$\begin{array}{ll} \dot{\tilde{R}} = \tilde{R}(-\eta)^{\times} & \tilde{R}^+ = \tilde{R} \\ \dot{\eta} = 0_{3 \times 1} & \eta^+ = k_R \psi_{\mathfrak{so}(3)}(M \tilde{R}) \\ \dot{\tilde{p}} = \tilde{v} & \tilde{p}^+ = \tilde{p} - k_c R K_p R^{\top} \tilde{p} \\ \underbrace{\dot{\tilde{v}} = (I - \tilde{R})g}_{\tau \in [0, T_M]} & \underbrace{\tilde{v}^+ = \tilde{v} - k_c R K_v R^{\top} \tilde{p}}_{\tau \in \{0\}} \end{array} \quad (5.36)$$

where M is defined in Lemma 5.1.

5.4.1 Fixed-gain design

Consider the variable $\mathbf{x} = [\tilde{p}^{\top}, \tilde{v}^{\top}]^{\top} \in \mathbb{R}^6$, and choose $K_p = k_p I_3$ and $K_v = k_v I_3$ with some positive scalars $k_p, k_v > 0$. From (5.36), the hybrid dynamics of \mathbf{x} are given by

$$\begin{cases} \dot{\mathbf{x}} = A\mathbf{x} + \delta_g, & \tau \in [0, T_M] \\ \mathbf{x}^+ = (I - KC)\mathbf{x}, & \tau \in \{0\} \end{cases} \quad (5.37)$$

where $\delta_g = [0_{1 \times 3}, g^{\top}(I_3 - \tilde{R})]^{\top}$, and the matrices A, K and C are given by

$$A = \begin{bmatrix} 0_{3 \times 3} & I_3 \\ 0_{3 \times 3} & 0_{3 \times 3} \end{bmatrix}, K = k_c \begin{bmatrix} k_p I_3 \\ k_v I_3 \end{bmatrix}, C = [I_3 \ 0_{3 \times 3}]. \quad (5.38)$$

Note that the main difference of (5.37) with respect to (5.14), is the additional term δ_g induced by the gravity.

Let $x_3 = (\tilde{R}, \eta, \mathbf{x}, \tau) \in \mathcal{U} \times \mathbb{R}^6 \times [0, T_M]$. From (5.36) and (5.37), one obtains the hybrid closed-loop system $\mathcal{H}_3 = (F_3, G_3, \mathcal{F}_3, \mathcal{J}_3)$ as follows:

$$\mathcal{H}_3 : \begin{cases} \dot{x}_3 = F_3(x_3) & x_3 \in \mathcal{F}_3 \\ x_3^+ \in G_3(x_3) & x_3 \in \mathcal{J}_3 \end{cases} \quad (5.39)$$

with the flow and jump maps defined as

$$F_3(x_3) = \left(\tilde{R}(-\eta)^{\times}, 0_{3 \times 1}, A\mathbf{x} + \delta_g, -1 \right) \quad (5.40)$$

$$G_3(x_3) = \left(\tilde{R}, k_R \psi_{\mathfrak{so}(3)}(M \tilde{R}), (I - KC)\mathbf{x}, [T_m, T_M] \right) \quad (5.41)$$

$$\mathcal{F}_3 := \mathcal{U} \times \mathbb{R}^6 \times [0, T_M] \quad (5.42)$$

$$\mathcal{J}_3 := \mathcal{U} \times \mathbb{R}^6 \times \{0\} \quad (5.43)$$

One can show that the hybrid system \mathcal{H}_3 satisfies the hybrid basic conditions given in Section 2.5.1. Let us introduce the following closed set:

$$\bar{\mathcal{A}} := \{(\tilde{R}, \eta, \mathbf{x}, \tau) \in \mathcal{U} \times \mathbb{R}^6 \times [0, T_M] \mid \tilde{R} = I_3, \eta = 0_{3 \times 1}, \mathbf{x} = 0_{6 \times 1}\}. \quad (5.44)$$

Now, one can state the following result:

Theorem 5.3 Consider the hybrid dynamical system (5.39)-(5.43). Let Assumption 5.1 and Assumption 5.2 hold. Suppose that the matrix \bar{M} is positive definite, and there exists a positive definite symmetric matrix P satisfying $\Xi_P(\tau) < 0, \forall \tau \in [T_m, T_M]$, with $\Xi_P(\tau)$ defined in (5.8) and matrices A, K and C given in (5.38). Then, for any $|\tilde{R}(0)|_I < \sqrt{\zeta_M}$, there exist a constant $k_R^* > 0$, such that for any $k_R < k_R^*$ the set $\bar{\mathcal{A}}$ is exponentially stable.

Proof See Appendix D.6.

5.4.2 Variable-gain design

Let $\mathbf{x} = [\tilde{p}^\top R, \tilde{v}^\top R]^\top \in \mathbb{R}^6$ and $x_4 = (\tilde{R}, \eta, \mathbf{x}, \tau)$. From (5.1) and (5.36), the hybrid dynamics of \mathbf{x} are given by

$$\begin{cases} \dot{\mathbf{x}} = A(t)\mathbf{x} + \bar{\delta}_g, & \tau \in [0, T_M] \\ \mathbf{x}^+ = (I - KC(t))\mathbf{x}, & \tau \in \{0\} \end{cases}$$

where $\bar{\delta}_g = [0_{1 \times 3} \ g^\top (R - \hat{R})]^\top$, and the matrices $A(t), K$ and $C(t)$ are given by

$$A(t) = \begin{bmatrix} -\omega^\times & I_3 \\ 0_{3 \times 3} & -\omega^\times \end{bmatrix}, K = k_c \begin{bmatrix} K_p \\ K_v \end{bmatrix}, C(t) = [I_3 \ 0_{3 \times 3}]. \quad (5.45)$$

Let us design the gain matrix K as

$$K = PC(t)^\top (C(t)PC(t)^\top + Q(t))^{-1} \quad (5.46)$$

where P is the solution of the CDRE (2.119)-(2.120) with matrices $(A(t), C(t))$ given by (5.45) and matrices $Q(t), V(t) \in \mathbb{R}^{6 \times 6}$ being uniformly positive definite.

From (5.36) and (5.45), one obtains the following hybrid closed-loop system $\mathcal{H}_4 = (F_4, G_4, \mathcal{F}_4, \mathcal{J}_4)$:

$$\mathcal{H}_4 : \begin{cases} \dot{x}_4 = F_4(x_4) & x_4 \in \mathcal{F}_4 \\ x_4^+ \in G_4(x_4) & x_4 \in \mathcal{J}_4 \end{cases} \quad (5.47)$$

with the following flow and jump maps:

$$F_4(x_4) = \left(\tilde{R}(-\eta)^\times, 0_{3 \times 1}, A(t)\mathbf{x} + \bar{\delta}_g, -1 \right) \quad (5.48)$$

$$G_4(x_4) = \left(\tilde{R}, k_R \psi_{\mathfrak{so}(3)}(M\tilde{R}), (I - KC(t))\mathbf{x}, [T_m, T_M] \right) \quad (5.49)$$

$$\mathcal{F}_4 := \mathfrak{U} \times \mathbb{R}^6 \times [0, T_M] \quad (5.50)$$

$$\mathcal{J}_4 := \mathfrak{U} \times \mathbb{R}^6 \times \{0\} \quad (5.51)$$

One can show that the hybrid system \mathcal{H}_4 satisfies the hybrid basic conditions given in Section 2.5.1. Now, one can state the following result:

Theorem 5.4 Consider the hybrid dynamical system (5.47)-(5.51). Let Assumption 5.1 and Assumption 5.2 hold. Suppose that the matrix \bar{M} is positive definite, and the conditions given in Lemma 2.12 are satisfied. Choose the gain K as (5.24) with P being the solution to the CDRE (2.119)-(2.120) and matrices $(A(t), C(t))$ defined in (5.45). Then, for any $|\tilde{R}(0)|_I < \sqrt{\zeta_M}$, there exist a constant $k_R^* > 0$, such that for any $k_R < k_R^*$ the set $\bar{\mathcal{A}}$ is exponentially stable.

Proof See Appendix D.7.

5.5 Simulation results

In this section, simulation results are presented to illustrate the performance of the proposed hybrid observers. We refer to the hybrid inertial navigation observer (5.9) with fixed gain as ‘HINO1-F’, the hybrid inertial navigation observer (5.9) with variable gain as ‘HINO1-V’, the hybrid inertial navigation observer (5.35) with fixed gain as ‘HINO2-F’, and the hybrid inertial navigation observer (5.35) with variable gain as ‘HINO2-V’. Moreover, we refer to the invariant observer proposed in [Barrau and Bonnabel, 2017] as ‘IEKF’.

Consider an autonomous vehicle moving on the ‘8’-shape trajectory given by $p(t) = 10[\sin(t), \sin(t)\cos(t), 1]^\top$, with the initial rotation $R(0) = I_3$ and the angular velocity $\omega(t) = [\sin(0.3\pi), 0.1, \cos(0.3\pi)]^\top$. The same initial conditions are considered for each observer as: $\hat{R}(0) = \mathcal{R}_a(0.1\pi, u)$ with $u \in \mathbb{S}^2$, $\hat{v}(0) = \hat{p}(0) = \hat{g}(0) = 0_{3 \times 1}$, and $P(0) = I$. Eight landmarks are randomly selected on the ground such that Assumption 5.1 holds. We consider continuous IMU measurements and intermittent landmark position measurements with $T_m = 0.1$ and $T_M = 0.2$. Moreover, additive white Gaussian noise has been considered with the variances $n_y = 0.1$, $n_a = 0.1$ and $n_\omega = 0.01$ in the landmark position measurements, acceleration a and angular velocity w , respectively. The gain parameters are taken as $k_i = 1/8$, $i = 1, 2, \dots, 8$ and $k_R = 1.2$. In addition, we chose

$$V(t) = \text{diag}(n_w^2 I_3, (n_w^2 + n_a^2) I_3, n_w^2 I_3), Q(t) = n_y^2 I_3$$

for HINO1-V, and

$$V(t) = \text{diag}(n_w^2 I_3, (n_w^2 + n_a^2) I_3), Q(t) = n_y^2 I_3$$

for HINO2-V. For the HINO1-F and HINO2-F, we pick $k_p = 0.5$, $k_v = 1.0$ and $k_g = 0.6$, such that, for both observers, there exists a matrix P satisfying $\Xi_P(\tau) < 0$, $\forall \tau \in [T_m, T_M]$. For the IEKF, we choose the parameters \hat{Q}_t and \hat{N}_t in equation (35) in [Barrau and Bonnabel, 2017] as suggested in the paper.

Simulation results are shown in Figure 5.4. As one can see, the estimates from the proposed hybrid observers and IEKF converge, after a few seconds, to the vicinity of the real state. Interestingly, from the observation in the simulation, the computations of our observers HINO2-F and HINO2-V are significantly faster than the computations required by IEKF. This is mainly due to the fact that the IEKF [Barrau and Bonnabel, 2017, Eqn. (35)] requires the computation of the inverse of a potentially high-dimensional matrix $S \in \mathbb{R}^{3N \times 3N}$, when the number of landmarks N is large.

5.6 Experimental results

To further validate the performance of our proposed hybrid observers, we applied our algorithms to real data from the EuRoc dataset given in Section 4.7. The IMU measurements are obtained at the rate of 200Hz, while, the measurements of the stereo camera are obtained approximately at the rate of 20Hz. In our experiments, the numerical integration of the estimated attitude is performed as follows: $\hat{R}_{k+1} = \hat{R}_k \exp(\omega_k^\times \Delta_T)$ with

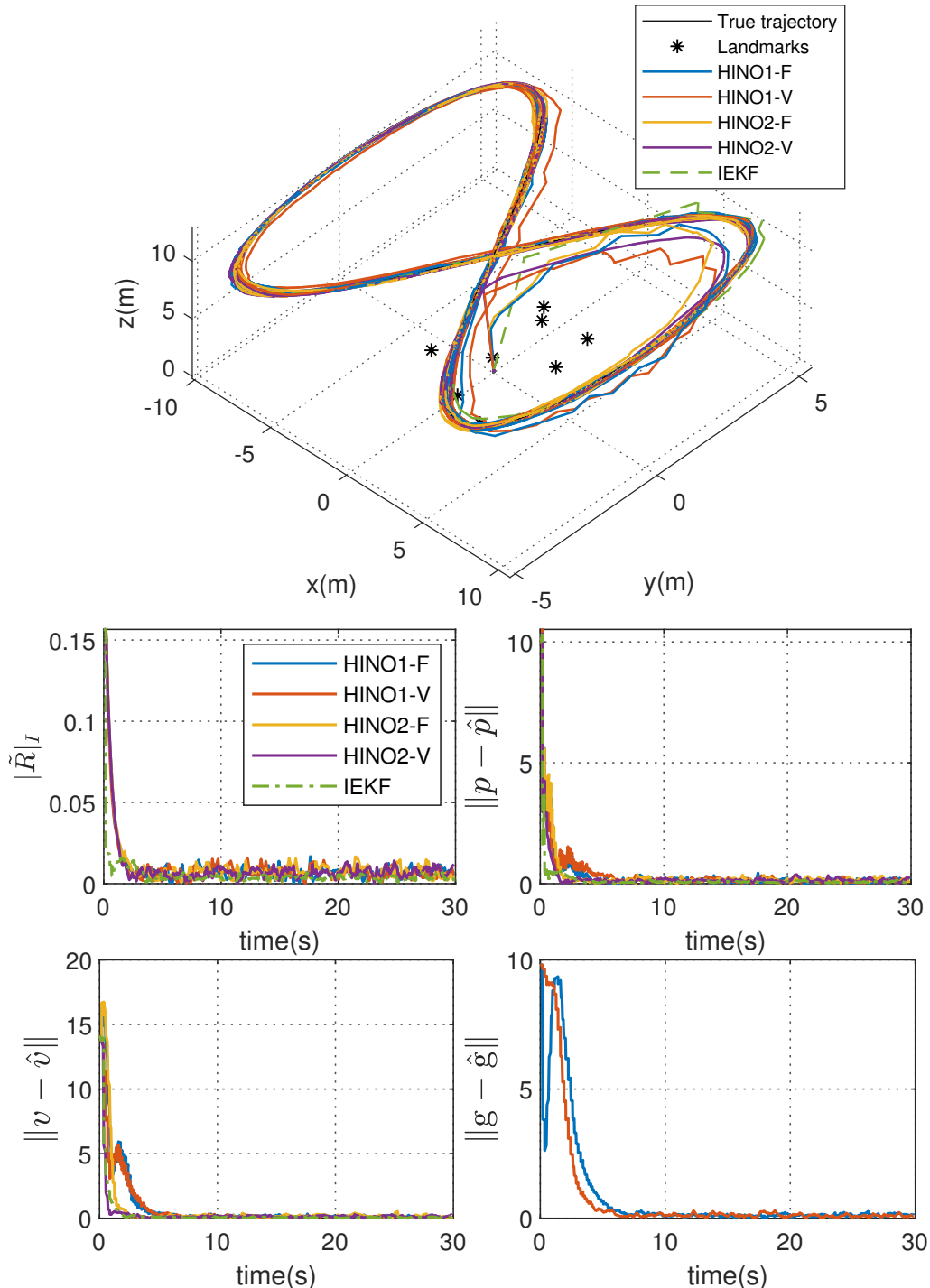


Figure 5.4: Simulation results using intermittent landmark measurements. The true and estimated trajectories are shown in the top. The estimation errors of rotation, position, linear velocity and gravity vector are shown in the bottom.

$\Delta_T := t_{k+1} - t_k, \forall k \in \mathbb{N}_{>0}$ and the sequence $\{t_k\}_{k \in \mathbb{N}_{>0}}$ denoting the time instants of the IMU measurements, while a first-order numerical discretization method is applied for the integration of the other variables such as \hat{p}, \hat{v}, η and \hat{g} .

Three sets of experiments have been performed with the initial conditions: $\hat{R}(0) = \exp(0.1\pi u^\times)R_G$ with $u \in \mathbb{S}^2$, $\hat{p}(0) = \hat{v}(0) = 0_{3 \times 1}$, and $\eta(0) = \hat{g}(0) = 0_{3 \times 1}$. The gain parameters are tuned such that all the observers have a similar performance, which is a trade-off between the convergence rate and the noise at steady state. Note that higher gains result in faster convergence but amplify noise at steady-state. As one can see in Figure 5.5 - Figure 5.7, the estimates provided by all the proposed hybrid observers and IEKF, using the high rate IMU measurements and low rate stereo vision measurements, converge after a few seconds, to the vicinity of the ground truth. Note that the ground truth pose is used to validate the performance of the proposed algorithms and also to generate the virtual landmarks in the experiments, as explained in Section 4.7.1, due to the lack of physical landmarks.

5.7 Conclusion

In this chapter, we addressed the full state estimation problem for inertial navigation systems using continuous IMU measurements and intermittent landmark position measurements. Hybrid inertial navigation observers relying on continuous angular velocity and linear acceleration, and intermittent landmark position measurements, have been proposed. Different versions have been developed depending on whether the gravity vector is known or not and whether the observer gains are constant or time-varying. All the proposed observers are endowed with exponential stability guarantees. This is, to the best of our knowledge, the first work dealing with inertial navigation observers design, using intermittent measurements, with strong stability guarantees. Simulation and experimental results, illustrating the performance of the proposed hybrid nonlinear observers, have been provided.

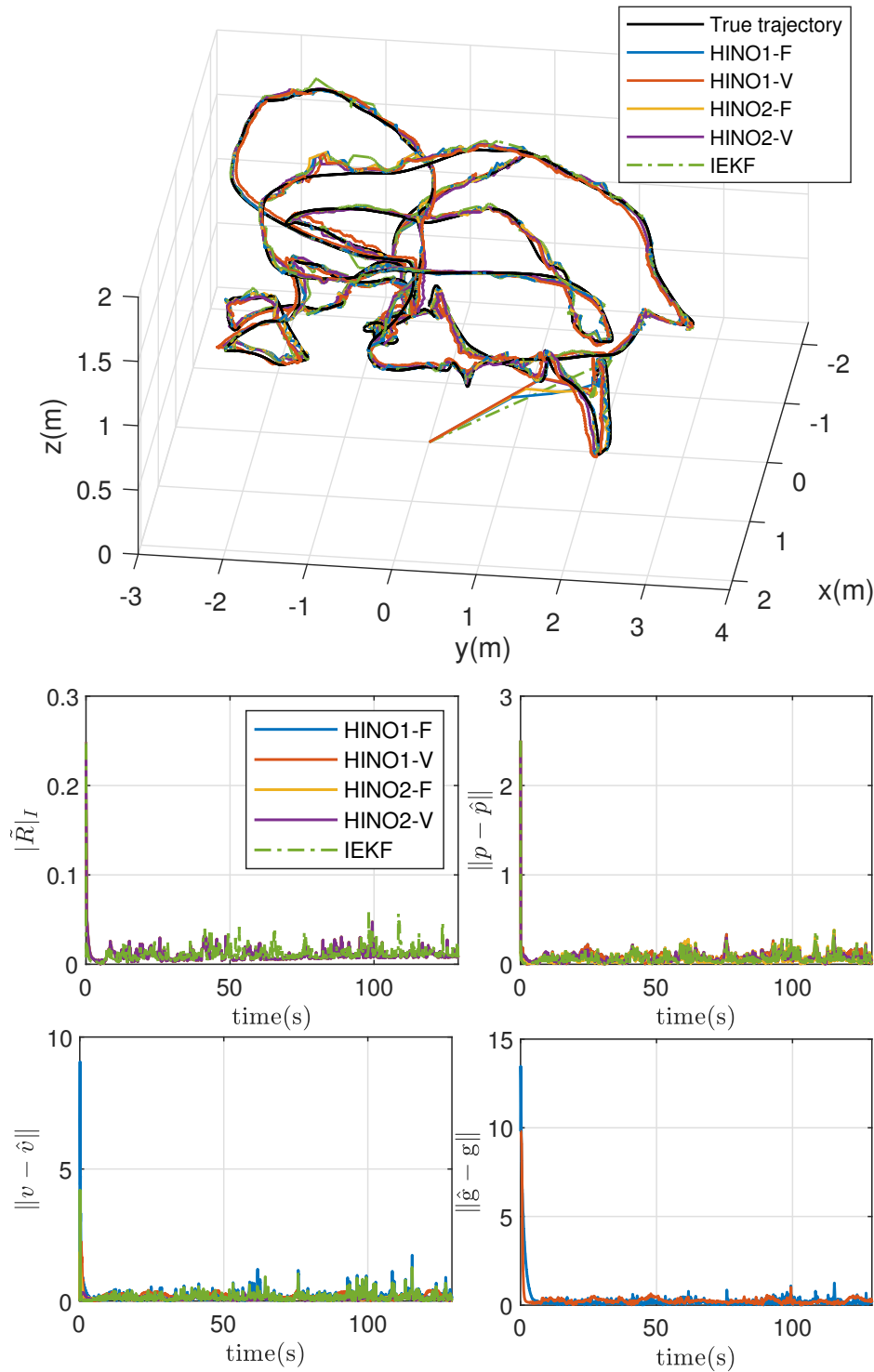


Figure 5.5: Experimental results using dataset V1_01_easy. The true (groundtruth) and estimated trajectories are shown in the top. The estimation errors of rotation, position, velocity and gravity vector are shown in the bottom.

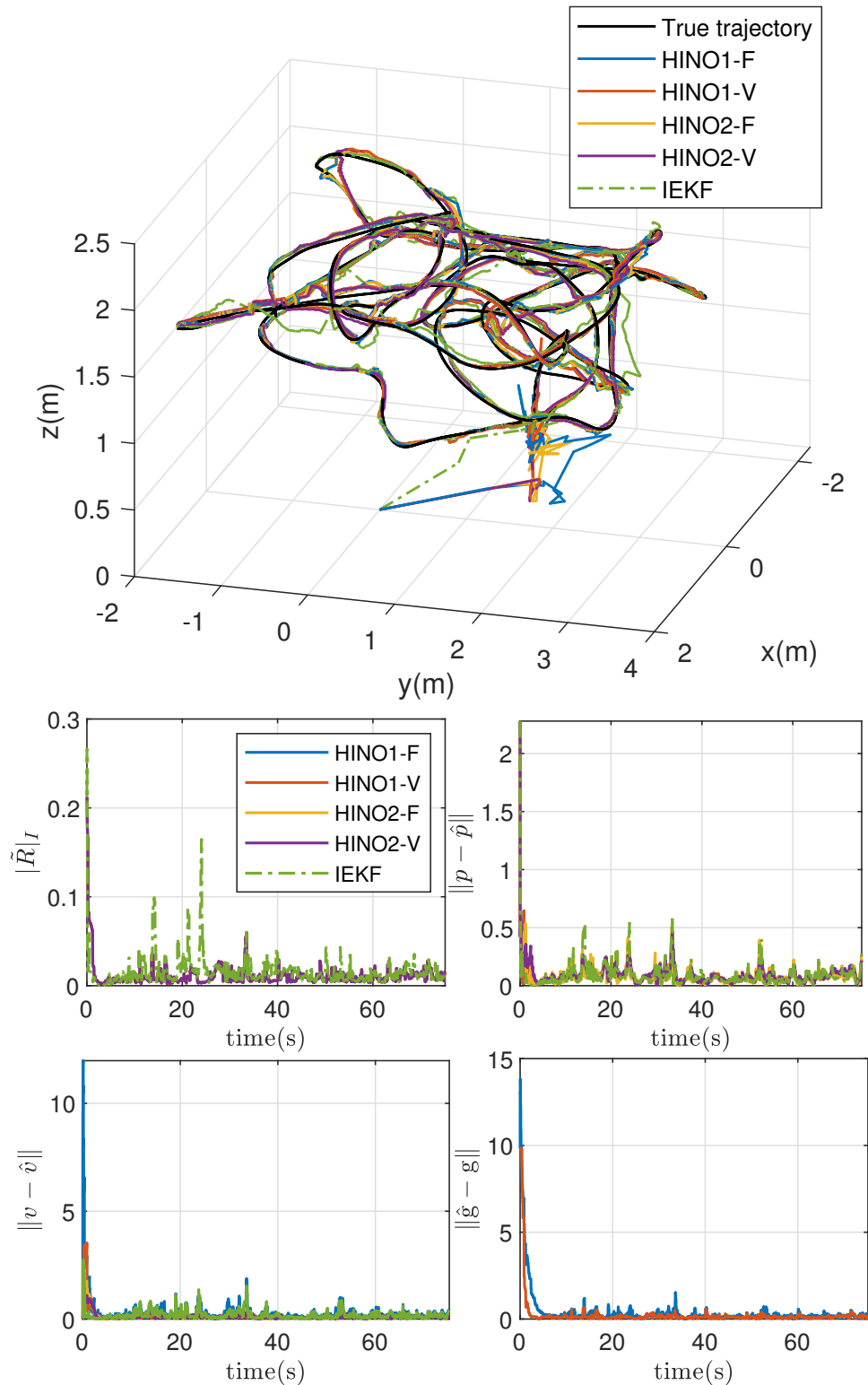


Figure 5.6: Experimental results using dataset V1_02_medium. The true (groundtruth) and estimated trajectories are shown in the top. The estimation errors of rotation, position, velocity and gravity vector are shown in the bottom.

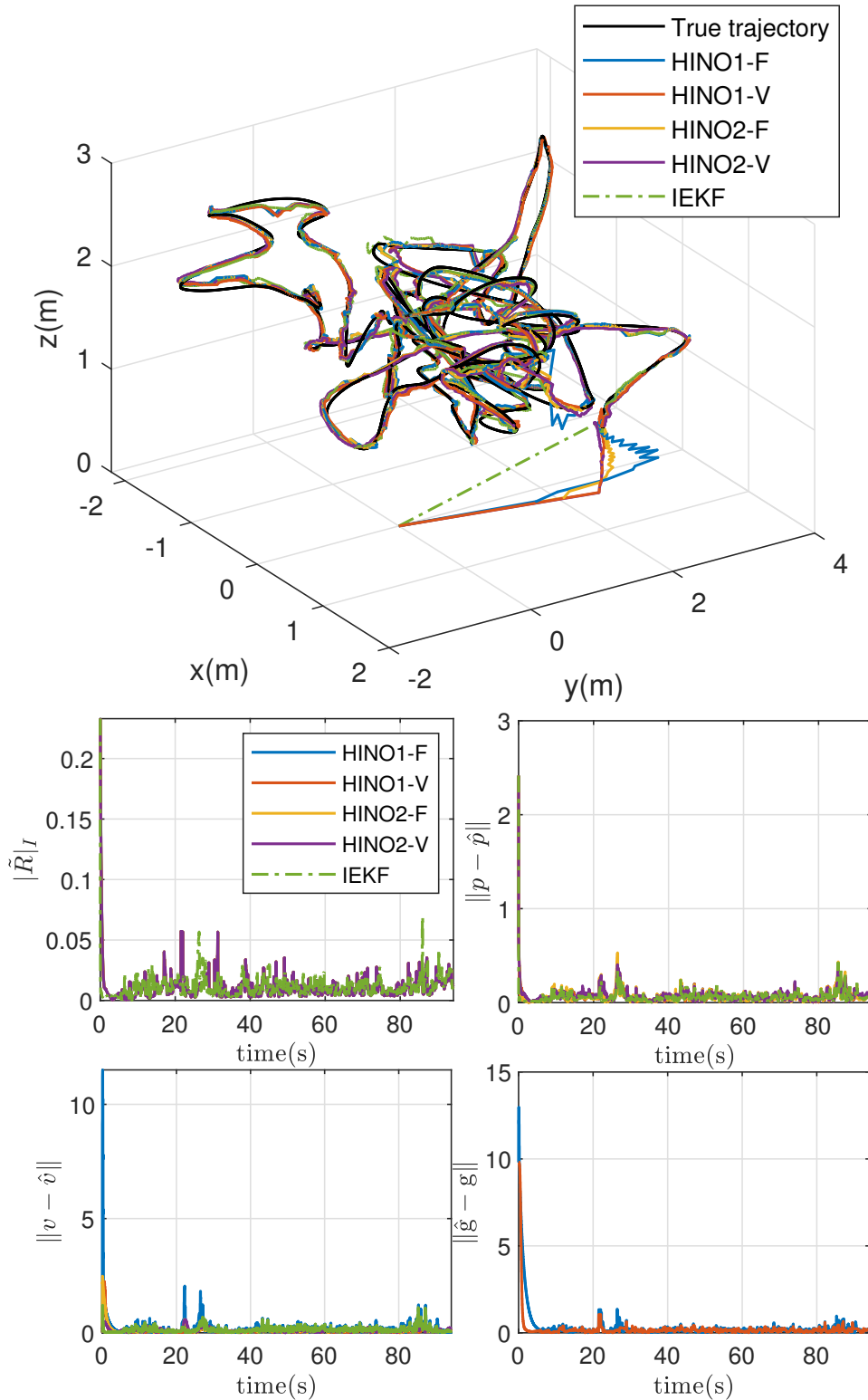


Figure 5.7: Experimental results using dataset V1_03_difficult. The true (groundtruth) and estimated trajectories are shown in the top. The estimation errors of rotation, position, velocity and gravity vector are shown in the bottom.

Chapter 6

Nonlinear Observers for Inertial Navigation Using Stereo Bearing Measurements

6.1 Introduction

In this chapter, we consider the problem of simultaneous estimation of the attitude, position and linear velocity for INSs using IMU and stereo bearing measurements. A vision aided INS, combining an IMU and onboard cameras, is an interesting alternative for autonomous navigation in GPS-denied environments [Rehbinder and Ghosh, 2003; Hamel and Samson, 2017]. In practice, inertial-vision systems either use a single camera, known as monocular vision [George and Sukkarieh, 2007; Chowdhary, 2013; Qin et al., 2018], or two cameras, known as stereo vision [Matthies and Shafer, 1987; Kriegman et al., 1989]. In fact, vision systems do not directly provide three-dimensional landmarks positions [Le Bras et al., 2017], and as such, additional algorithms are needed to obtain the three-dimensional body-frame landmark positions [Hartley and Zisserman, 2003; Corke, 2017]. From the model of a pinhole camera, the measurements obtained from images can be seen as a set of bearing vectors (unit vectors pointing to the landmarks from the optical center of the camera expressed in the camera frame). Therefore, it is of great interest to design observers for autonomous navigation systems using directly the bearing measurements provided by vision systems [Pachter and Porter, 2004; Baldwin et al., 2009; Le Bras et al., 2017; Hamel and Samson, 2018; Hamel and Samson, 2017]. In the literature, most of the existing results, relying on bearing measurements, are Kalman-type filters with local stability guarantees.

Motivated by the recent work in [Hamel and Samson, 2018; Le Bras et al., 2017; Hamel and Samson, 2017], a generic stability result for a class of nonlinear time-varying systems evolving on $\text{SO}(3) \times \mathbb{R}^n$, guaranteeing almost global asymptotic stability and local exponential stability, has been derived. Based on this, two observers for INS, depending on the number of available landmarks, are proposed using IMU and stereo bearing measurements. These observers are then extended to handle biased accelerometer measurements. Finally, to handle the case of biased IMU measurements, these results are

further extended using some high gain conditions. Unlike the results of [Hamel and Samson, 2018; Le Bras et al., 2017; Hamel and Samson, 2017], stereo bearing measurements are considered in this work to provide full-state (including attitude, position and linear velocity) estimation for INSs. One of the main contribution of our work is that the proposed observers guarantee almost global asymptotic stability and local exponential stability in the cases of non-biased IMU measurements and biased-accelerometer-only IMU measurements. This is distinct from the classical KF-based filters where only local stability is guaranteed. Numerical simulation are provided to illustrate the performance of the proposed observers. These results appeared in our work [Wang and Tayebi, 2019b].

6.2 Problem formulation

Consider the following kinematic equations of a rigid body:

$$\dot{R} = R\omega^\times, \quad (6.1a)$$

$$\dot{p} = v, \quad (6.1b)$$

$$\dot{v} = g + Ra, \quad (6.1c)$$

where $g \in \mathbb{R}^3$ denotes the gravity vector, $\omega \in \mathbb{R}^3$ denotes the body-frame angular velocity expressed in frame \mathcal{B} , and $a \in \mathbb{R}^3$ denotes the body-frame “apparent acceleration” capturing all non-gravitational forces applied to the rigid body expressed in the body-frame. We assume that the rigid body system is equipped with an IMU, which provides the measurements of the angular velocity ω and acceleration a .

Consider a family of N landmarks available for measurement. Let p_i be the position of the i -th landmark expressed in frame \mathcal{I} and $p_i^\mathcal{B} := R^\top(p_i - p)$ be the position of the i -th landmark expressed in frame \mathcal{B} . Consider \mathcal{C}_L and \mathcal{C}_R as the frames attached to the optical center of the left camera and the right camera, respectively. Let (R_{cL}, p_L) and (R_{cR}, p_R) denote the homogeneous transformation from the body-fixed frame to the left and right camera frames, respectively. The model of the bearing vectors obtained from a stereo vision system is given as follows:

$$\mathbf{x}_i^s := \frac{R_{cs}^\top(p_i^\mathcal{B} - p_s)}{\|p_i^\mathcal{B} - p_s\|}, \quad s \in \{L, R\}, i = 1, 2, \dots, N. \quad (6.2)$$

Note that the bearing measurement \mathbf{x}_i^s is not linear with respect to the landmark position $p_i^\mathcal{B}$, and only partial position information is available in each bearing. An example of the stereo bearing measurements is shown Figure 6.1.

Remark 6.1 Note that $p_i^{\mathcal{C}_s} = R_{cs}^\top(p_i^\mathcal{B} - p_s)$ denotes the position of the i -th landmark, w.r.t. the left or right camera frame. Let (u_i^s, v_i^s) be the coordinates of the i -th landmark, w.r.t. the center of the image in pixels obtained from the left or right camera. The bearing measurements of the i -th landmark can be written in terms of the pixel measurement as $\mathbf{x}_i^s = \frac{1}{\|\mathcal{K}^{-1}z_i^s\|}\mathcal{K}^{-1}z_i^s \in \mathbb{S}^2$ with $\mathcal{K} \in \mathbb{R}^{3 \times 3}$ denoting the intrinsic matrices of the camera and $z_i^s = [u_i^s, v_i^s, 1]^\top \in \mathbb{R}^3$.

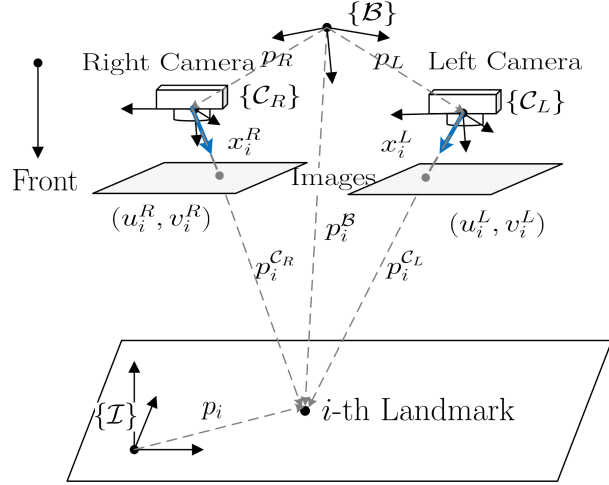


Figure 6.1: An illustration of the stereo vision system. The stereo bearing vectors are highlighted in blue arrows.

Assumption 6.1 *There exists a constant $c_p > 0$ such that $\|p_i\| \leq c_p$ for all $i = 1, 2, \dots, N$.*

Assumption 6.1 implies that the landmarks position can not be infinite, which is reasonable in practice. The knowledge on the value of c_p is not assumed. This assumption implies that the stereo bearing vectors x_i^R and x_i^L are not collinear.

6.3 Nonlinear observers design with non-biased IMU measurements

6.3.1 AGAS for a class of nonlinear systems on $\text{SO}(3) \times \mathbb{R}^n$

Let $A(t) \in \mathbb{R}^{n \times n}$ and $C(t) \in \mathbb{R}^{m \times n}$ be continuous and bounded matrix-valued functions. Consider a generalized nonlinear time-varying system on $\text{SO}(3) \times \mathbb{R}^n$ as

$$\begin{cases} \dot{\tilde{R}} = \tilde{R}(k_R \sigma_R)^\times \\ \dot{x} = A(t)x - K(t)y \\ y = C(t)x \end{cases} \quad (6.3)$$

with $(\tilde{R}, x) \in \text{SO}(3) \times \mathbb{R}^n$ the system state, $y \in \mathbb{R}^m$ the system output. The term σ_R is given as follows:

$$\sigma_R = -\psi_{\mathfrak{so}(3)}(M\tilde{R}) + \phi(x, t) \quad (6.4)$$

where $\phi(x, t) \in \mathbb{R}^3$, $M \in \mathbb{R}^{3 \times 3}$ and $K(t) = PC^\top(t)Q(t)$ with P being the solution to the CRE (2.116). Note that the dynamics of \tilde{R} and x are decoupled if $\phi(x, t) = 0, \forall x \in \mathbb{R}^n, t \geq 0$. In this chapter, we consider the case where $\phi(x, t)$ satisfies the following assumption:

Assumption 6.2 *There exists a constant $c_\phi > 0$ such that $\|\phi(x, t)\| \leq c_\phi \|x\|$ for all $x \in \mathbb{R}^n$ and $t \geq 0$.*

The following assumptions are needed in the proof of the following main result:

Assumption 6.3 *Matrix $M = M^\top$ is positive semi-definite with distinct eigenvalues.*

Assumption 6.4 *The pair $(A(t), C(t))$ in (6.3) is uniformly observable.*

Theorem 6.1 *Consider the nonlinear time-varying system (6.3)-(6.4). Suppose that Assumption 6.2 - Assumption 6.4 are satisfied. Then, the following statements hold:*

i) *The set of equilibrium points of system (6.3) is given by*

$$\Psi := (I_3, 0) \cup \{(\tilde{R}, x) \in \text{SO}(3) \times \mathbb{R}^n : \tilde{R} = \mathcal{R}_\alpha(\pi, v), v \in \mathcal{E}(M), x = 0\}. \quad (6.5)$$

ii) *The desired equilibrium $(I_3, 0)$ is AGAS and the other three undesired equilibria are unstable.*

iii) *There exist a constant $\kappa^* > 0$ such that the desired equilibrium $(I_3, 0)$ is exponentially stable if*

$$\text{tr}((I - \tilde{R}(0))M) + \kappa x(0)^\top P(0)^{-1}x(0) \leq \varepsilon_R,$$

where $\kappa > \kappa^*$ and $\varepsilon_R \in (0, 2(\text{tr}(M) - \lambda_{\max}^M))$.

Proof See Appendix E.1.

Theorem 6.1 provides AGAS and local exponential stability results for a class of systems on $\text{SO}(3) \times \mathbb{R}^n$. Note that the topological obstruction to global asymptotic stability of this class of systems is mainly due to the topological obstruction on $\text{SO}(3)$. In the following subsections, Two nonlinear observers for INS using IMU and direct stereo bearing measurements are presented.

6.3.2 Observer design using stereo bearing measurements

Let \hat{R} and \hat{p} be the estimates of the attitude R , and the position p , respectively. We define the attitude estimation error as $\tilde{R} := R\hat{R}^\top$, and the geometric position estimation error as $\tilde{p} := R^\top(p - p_1) - \hat{R}^\top(\hat{p} - p_1)$. Similar to Section 3.5, the term p_1 is used here to translate the inertial frame. In fact, $\tilde{p} = R^\top p - \hat{R}^\top \hat{p} = R^\top(p - \tilde{R}\hat{p})$ as long as $p_1 = 0$, i.e., the origin of the inertial frame is located at p_1 . Define \hat{p}_i as the estimate of p_i and $\tilde{p}_i := R^\top(p_i - p_1) - \hat{R}^\top(\hat{p}_i - p_1)$ as the landmark estimation errors for $i = 2, \dots, N$. Then, we introduce the following vectors:

$$y_i = \nu_i^R + \nu_i^L, \quad \forall i = 1, 2, \dots, N \quad (6.6)$$

where for each $s \in \{L, R\}$, $\nu_1^s := R_{cs} \pi_{\mathbf{x}_1^s} R_{cs}^\top (\hat{R}^\top(p_1 - \hat{p}) - p_s)$ and $\nu_i^s := R_{cs} \pi_{\mathbf{x}_i^s} R_{cs}^\top (\hat{R}^\top(\hat{p}_i - \hat{p}) - p_s)$ for $i = 2, \dots, N$. Let $p_i^{C_s} = R_{cs}^\top (R^\top(p_i - p) - p_s)$ denote the measurement of the

i -th landmark expressed in the s -camera frame. From the definitions of the projection operator π_x and the bearing vector \mathbf{x}_i^s , one has $\pi_{\mathbf{x}_i^s} p_i^{C_s} = 0$. Making use of the definitions of \tilde{p} and \tilde{p}_i , for each $s \in \{L, R\}$, one can show that $\nu_1^s = R_{cs} \pi_{\mathbf{x}_1^s} (R_{cs}^\top (\hat{R}^\top (p_1 - \hat{p}) - p_s) - p_i^{C_s}) = R_{cs} \pi_{\mathbf{x}_1^s} R_{cs}^\top \tilde{p}$ and $\nu_i^s = R_{cs} \pi_{\mathbf{x}_i^s} (R_{cs}^\top (\hat{R}^\top (\hat{p}_i - \hat{p}) - p_s) - p_i^{C_s}) = R_{cs} \pi_{\mathbf{x}_i^s} R_{cs}^\top (\tilde{p} - \tilde{p}_i)$. Then, one can rewrite (6.6) in terms of the estimation errors as

$$y_i = \begin{cases} \Pi_i \tilde{p} & i = 1 \\ \Pi_i (\tilde{p} - \tilde{p}_i), & i = 2, \dots, N, \end{cases} \quad (6.7)$$

where $\Pi_i := R_{cR} \pi_{\mathbf{x}_i^R} R_{cR}^\top + R_{cL}^\top \pi_{\mathbf{x}_i^L} R_{cL}^\top, \forall i = 1, 2, \dots, N$. The choice of the virtual output y_i defined in (6.6) leads to a nice linear relationship with respect to the estimation errors \tilde{p} and \tilde{p}_i as shown in (6.7). This allows us to obtain a linear time-varying error dynamics for which the design of the gains can be carried out via a CRE. In practice, one can always have $R_{cR} \approx R_{cL}$ through a proper design. Hence, in this paper, we assume that $R_{cR} = R_{cL}$. From Assumption 6.1, the stereo bearing vectors \mathbf{x}_i^R and \mathbf{x}_i^L are not collinear. This implies that the matrix Π_i is (uniformly) positive definite for all $i = 1, 2, \dots, N$. Let us introduce the following output

$$y = [y_1^\top, y_2^\top, \dots, y_N^\top]^\top \in \mathbb{R}^{3N}. \quad (6.8)$$

Let \hat{v} and $\hat{\mathbf{g}}$ be the estimates of the linear velocity v and the gravity vector \mathbf{g} , respectively. We propose the following nonlinear observer:

$$\begin{aligned} \Sigma_1 : \quad & \dot{\hat{R}} = \hat{R}(\omega - k_R \hat{R}^\top \sigma_R)^\times \\ \Sigma_2 : \quad & \begin{cases} \dot{\hat{p}} = \hat{v} - k_R \sigma_R^\times (\hat{p} - p_1) + \hat{R} K_p y \\ \dot{\hat{v}} = \hat{\mathbf{g}} + \hat{R} a - k_R \sigma_R^\times \hat{v} + \hat{R} K_v y \\ \dot{\hat{\mathbf{g}}} = -k_R \sigma_R^\times \hat{\mathbf{g}} + \hat{R} K_g y \\ \dot{\hat{p}}_i = -k_R \sigma_R^\times (\hat{p}_i - p_1) + \hat{R} K_i y, \quad i = 2, \dots, N \end{cases}, \end{aligned} \quad (6.9)$$

where $k_R > 0$, the gain matrices $K_p, K_v, K_g, K_2, \dots, K_N \in \mathbb{R}^{3 \times 3N}$ to be designed later via a CRE, and the term σ_R is given by

$$\sigma_R := \rho_0 m_I^\times \hat{R} m_B + \rho_1 \mathbf{g}^\times \hat{\mathbf{g}} + \sum_{i=2}^N \rho_i \bar{p}_i^\times (\hat{p}_i - p_1) \quad (6.10)$$

with $\bar{p}_i := p_i - p_1$ and $\rho_i \geq 0$ for all $i = 0, 1, \dots, N$. Note that the innovation term (6.10) is given in a general manner. One can set ρ_i to zero when the associated information is not available. For example, one chooses $\rho_0 = 0$ when the magnetometer measurements are not available. The structure of this observer is given by Figure 6.2. The position, velocity, gravity vector and landmark positions are estimated using ω, a and stereo bearing measurements. The attitude is thereafter estimated using the angular velocity, the magnetometer measurements, the estimated gravity vector, and landmark positions estimates.

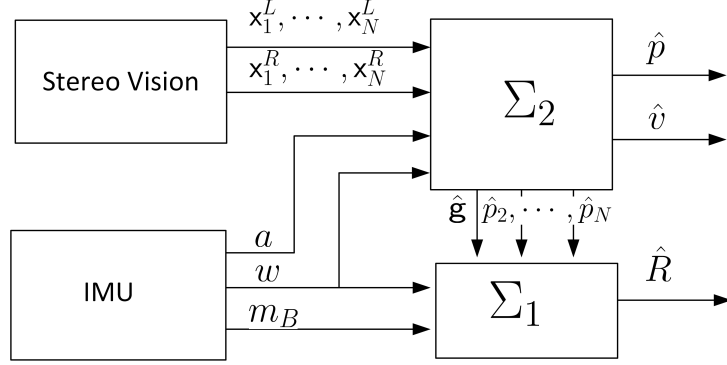


Figure 6.2: Nonlinear observer (6.9) using non-biased IMU and stereo bearing measurements

Define the velocity estimation error as $\tilde{v} := R^\top v - \hat{R}^\top \hat{v}$ and the gravity vector estimation error as $\tilde{\mathbf{g}} := R^\top \mathbf{g} - \hat{R}^\top \hat{\mathbf{g}}$. In view of (6.1a)-(6.1c) and (6.9), one obtains the following closed-loop system:

$$\dot{\hat{R}} = \tilde{R}(k_R \sigma_R)^\times, \quad (6.11a)$$

$$\dot{\tilde{p}} = -\omega^\times \tilde{p} + \tilde{v} - K_p y, \quad (6.11b)$$

$$\dot{\tilde{p}}_i = -\omega^\times \tilde{p}_i - K_i y, \quad i = 2, \dots, N \quad (6.11c)$$

$$\dot{\tilde{v}} = -\omega^\times \tilde{v} + \tilde{\mathbf{g}} - K_v y, \quad (6.11d)$$

$$\dot{\tilde{\mathbf{g}}} = -\omega^\times \tilde{\mathbf{g}} - K_{\mathbf{g}} y, \quad (6.11e)$$

Define the new variable $x := [\tilde{p}^\top, \tilde{p}_2^\top, \dots, \tilde{p}_N^\top, \tilde{v}^\top, \tilde{\mathbf{g}}^\top]^\top \in \mathbb{R}^{6+3N}$. In view of (6.8) and (6.11a)-(6.11e), the dynamics of x and the output y can be written in the form of (6.3) with

$$A = \begin{bmatrix} -\omega^\times & 0_{3 \times 3} & \cdots & 0_{3 \times 3} & I_3 & 0_{3 \times 3} \\ 0_{3 \times 3} & -\omega^\times & \cdots & 0_{3 \times 3} & 0_{3 \times 3} & 0_{3 \times 3} \\ \vdots & \vdots & \ddots & \vdots & \vdots & \vdots \\ 0_{3 \times 3} & 0_{3 \times 3} & \cdots & -\omega^\times & 0_{3 \times 3} & 0_{3 \times 3} \\ 0_{3 \times 3} & 0_{3 \times 3} & \cdots & 0_{3 \times 3} & -\omega^\times & I_3 \\ 0_{3 \times 3} & 0_{3 \times 3} & \cdots & 0_{3 \times 3} & 0_{3 \times 3} & -\omega^\times \end{bmatrix}, \quad (6.12)$$

$$C = \begin{bmatrix} \Pi_1 & 0_{3 \times 3} & \cdots & 0_{3 \times 3} & 0_{3 \times 3} & 0_{3 \times 3} \\ \Pi_2 & -\Pi_2 & \cdots & 0_{3 \times 3} & 0_{3 \times 3} & 0_{3 \times 3} \\ \vdots & \vdots & \ddots & \vdots & \vdots & \vdots \\ \Pi_N & 0_{3 \times 3} & \cdots & -\Pi_N & 0_{3 \times 3} & 0_{3 \times 3} \end{bmatrix}. \quad (6.13)$$

The gain matrix K is chosen as

$$[K_p^\top, K_2^\top, \dots, K_N^\top, K_v^\top, K_{\mathbf{g}}^\top]^\top := K = PC^\top Q(t)$$

where $P \in \mathbb{R}^{(6+3N) \times (6+3N)}$ is the solution to the CRE (2.116). Using the facts $\hat{\mathbf{g}} = \hat{R}(R^\top \mathbf{g} - \tilde{\mathbf{g}}) = \tilde{R}^\top \mathbf{g} - \hat{R}\tilde{\mathbf{g}}$ and $\hat{p}_i - p_1 = \hat{R}(R^\top(p_i - p_1) - \tilde{p}_i) = \tilde{R}^\top \bar{p}_i - \hat{R}\tilde{p}_i$, one can

show that $\mathbf{g}^\times \hat{\mathbf{g}} = \mathbf{g}^\times \tilde{R}^\top \mathbf{g} - \mathbf{g}^\times \hat{R} \tilde{\mathbf{g}}$ and $\bar{p}_i^\times (\hat{p}_i - p_1) = \bar{p}_i^\times \tilde{R}^\top \bar{p}_i - \bar{p}_i^\times \hat{R} \tilde{p}_i$. Then, from (2.46), one can rewrite the term σ_R as (6.4) where $\phi(x, t) = -\Gamma(t)x$ with $\Gamma(t) := [0_{3 \times 3}, \rho_2 \bar{p}_2^\times \hat{R}(t), \dots, \rho_N \bar{p}_N^\times \hat{R}(t), 0_{3 \times 3}, \rho_1 \mathbf{g}^\times \hat{R}(t)]$, and

$$M := \rho_0 m_I m_I^\top + \rho_1 \mathbf{g} \mathbf{g}^\top + \sum_{i=2}^N \rho_i \bar{p}_i \bar{p}_i^\top \quad (6.14)$$

Making use of the fact $\|\Gamma\| \leq \rho_1 \|\mathbf{g}\| + \sum_{i=2}^N \rho_i \|\bar{p}_i\| := c_\phi$, one can show that $\|\phi(x, t)\| \leq c_\phi \|x\|$. This implies that the Assumption 6.2 is satisfied for σ_R given in (6.10).

Lemma 6.1 *Consider the matrix M defined in (6.14) with $\rho_i \geq 0, i = 0, 1, \dots, N$. Then, the matrix M has three distinct eigenvalues if*

- 1) $N \geq 1$ and vectors m_I and \mathbf{g} are not collinear;
- 2) $N \geq 2$ and there exist at least one landmark p_i such that $p_i - p_1$ and \mathbf{g} are not collinear;
- 3) $N \geq 3$ and there exist at least three non-collinear landmarks.

Remark 6.2 *Given at least two non-collinear vectors, including the inertial vectors and the vectors generated by landmarks, one can verify that the matrix M is positive semi-definite with no more than one zero eigenvalue. Moreover, it is always possible to guarantee that the matrix M has three distinct eigenvalues through an appropriate choice of the gains $\rho_i \geq 0, i = 0, 1, \dots, N$.*

Remark 6.3 *At least three non-collinear landmarks are common in the full-state estimation problem of inertial-vision navigation systems with inertial vision systems, for example [Barrau and Bonnabel, 2017; Wang and Tayebi, 2018b; Wang and Tayebi, 2020]. Thanks to the knowledge of the gravity vector and its estimate, the number of landmarks can be reduced to 2 in our design. Moreover, with the magnetometer measurements, only one landmark is required in the observer (6.9) .*

Lemma 6.2 *The pair (A, C) defined in (6.12) and (6.13) is uniformly observable.*

Proof See Appendix E.2.

6.3.3 Simplified observer for $N > 3$ landmarks

It is noted that, in the previous subsection, the dimension of the estimated state increases as the number of landmarks increases. This means that the computation time could be large when the number of landmarks is large. To solve this problem, a simplified observer for the case of $N > 3$ landmarks is presented in this subsection.

Let e_1, e_2, e_3 be the standard basis vectors of the linear space \mathbb{R}^3 , that is, e_i has all entries equal to zero except for the i -th entry which is equal to 1. Then, for each landmark $p_i = [p_{i,1}, p_{i,2}, p_{i,3}]^\top$, one verifies that $p_i = \sum_{j=1}^3 p_{i,j} e_j$. Let $\hat{e}_1, \hat{e}_2, \hat{e}_3$ be the estimates of

e_1, e_2, e_3 , respectively. Define the new position estimation error $\tilde{p} = R^\top p - \hat{R}^\top \hat{p}$ and the basis vectors estimation error $\tilde{e}_j = R^\top e_j - \hat{R}^\top \hat{e}_j$. Let us introduce the following vectors:

$$y_i = \nu_i^R + \nu_i^L, \quad i = 1, 2, \dots, N \quad (6.15)$$

where for each $i = 1, 2, \dots, N$ and $s \in \{L, R\}$, $\nu_i^s := R_{cs} \pi_{x_i^s} R_{cs}^\top (\hat{R}^\top (\hat{p}_i - \hat{p}) - p_s)$, with $\hat{p}_i = \sum_{j=1}^3 p_{i,j} \hat{e}_j$. Note that the difference of the vector ν_i^s , with respect to the one in the previous subsection, is the vector \hat{p}_i constructed from the estimates $\hat{e}_1, \hat{e}_2, \hat{e}_3$. In this case, only three basis vectors will be estimated no matter the number of landmarks. This is a very efficient way when the number of landmark is very large. Making use of the fact $\pi_{x_i^s} R_{cs}^\top (R^\top (p_i - p) - p_s) = 0$, one has $\nu_i^s = R_{cs} \pi_{x_i^s} R_{cs}^\top (R^\top p - \hat{R}^\top \hat{p} - (R^\top p_i - \hat{R}^\top \hat{p}_i))$. Then, one can rewrite (6.15) in terms of the estimation errors as

$$y_i = \Pi_i \tilde{p} - \sum_{j=1}^3 p_{i,j} \Pi_i \tilde{e}_j, \quad i = 1, 2, \dots, N \quad (6.16)$$

with $\Pi_i = R_{cR} \pi_{x_i^R} R_{cR}^\top + R_{cL}^\top \pi_{x_i^L} R_{cL}^\top$ being positive definite for all $t \geq 0$ from Assumption 6.1. Note that, with the new choice of the the output y_i , the linear relationship with respect to estimation errors \tilde{p} and \tilde{e}_j still holds as (6.7). Then, we introduce the following output

$$y = [y_1^\top, y_2^\top, \dots, y_N^\top]^\top \in \mathbb{R}^{3N}. \quad (6.17)$$

We propose the following nonlinear observer

$$\begin{aligned} \Sigma_1 : & \begin{cases} \dot{\hat{R}} = \hat{R}(\omega - k_R \hat{R}^\top \sigma_R)^\times \\ \dot{\hat{p}} = \hat{v} - k_R \sigma_R^\times \hat{p} + \hat{R} K_p y \\ \dot{\hat{v}} = \hat{g} + \hat{R} a - k_R \sigma_R^\times \hat{v} + \hat{R} K_v y \\ \dot{\hat{g}} = -k_R \sigma_R^\times \hat{g} + \hat{R} K_g y \\ \dot{\hat{e}}_i = -k_R \sigma_R^\times \hat{e}_i + \hat{R} K_i y, \quad i = 1, 2, 3 \end{cases} \\ \Sigma_2 : & \begin{cases} \dot{\hat{R}} = \hat{R}(\omega - k_R \hat{R}^\top \sigma_R)^\times \\ \dot{\hat{p}} = \hat{v} - k_R \sigma_R^\times \hat{p} + \hat{R} K_p y \\ \dot{\hat{v}} = \hat{g} + \hat{R} a - k_R \sigma_R^\times \hat{v} + \hat{R} K_v y \\ \dot{\hat{g}} = -k_R \sigma_R^\times \hat{g} + \hat{R} K_g y \\ \dot{\hat{e}}_i = -k_R \sigma_R^\times \hat{e}_i + \hat{R} K_i y, \quad i = 1, 2, 3 \end{cases} \end{aligned} \quad (6.18)$$

where $k_R > 0$, the gain matrices $K_p, K_v, K_g, K_i \in \mathbb{R}^{3 \times 3N}, i = 1, 2, 3$ to be designed later, and the term σ_R is given by

$$\sigma_R := \rho_0 m_I^\times \hat{R} m_B + \rho_1 g^\times \hat{g} + \sum_{i=1}^3 \rho_{i+1} e_i^\times \hat{e}_i \quad (6.19)$$

with $\rho_i \geq 0$, for all $i = 0, 1, \dots, 4$. The structure of this observer is given by Figure 6.3. The position, velocity, gravity vector and axis vectors are estimated using ω, a and stereo bearing measurements. The attitude is thereafter estimated using the angular velocity and magnetometer measurements, as well as the estimated basis vectors and gravity.

Define the new variable $x := [\tilde{p}^\top, \tilde{e}_1^\top, \tilde{e}_2^\top, \tilde{e}_3^\top, \tilde{v}^\top, \tilde{g}^\top]^\top \in \mathbb{R}^{18}$. In view of (6.1a)-(6.1c), (6.18), one obtains the following closed-loop system (6.3) with

$$A = \begin{bmatrix} -\omega^\times & 0_{3 \times 3} & 0_{3 \times 3} & 0_{3 \times 3} & I_3 & 0_{3 \times 3} \\ 0_{3 \times 3} & -\omega^\times & 0_{3 \times 3} & 0_{3 \times 3} & 0_{3 \times 3} & 0_{3 \times 3} \\ 0_{3 \times 3} & 0_{3 \times 3} & -\omega^\times & 0_{3 \times 3} & 0_{3 \times 3} & 0_{3 \times 3} \\ 0_{3 \times 3} & 0_{3 \times 3} & 0_{3 \times 3} & -\omega^\times & 0_{3 \times 3} & 0_{3 \times 3} \\ 0_{3 \times 3} & 0_{3 \times 3} & 0_{3 \times 3} & 0_{3 \times 3} & -\omega^\times & I_3 \\ 0_{3 \times 3} & -\omega^\times \end{bmatrix} \quad (6.20)$$

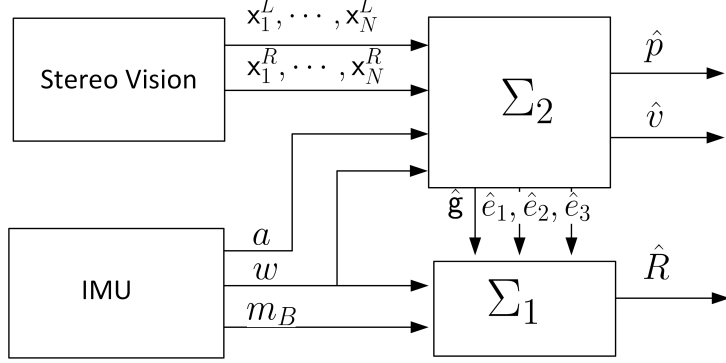


Figure 6.3: Simplified nonlinear observer (6.18) using non-biased IMU and stereo bearing measurements

$$C = \begin{bmatrix} \Pi_1 & -p_{11}\Pi_1 & -p_{12}\Pi_1 & -p_{13}\Pi_1 & 0_{3 \times 3} & 0_{3 \times 3} \\ \Pi_2 & -p_{21}\Pi_2 & -p_{22}\Pi_2 & -p_{23}\Pi_2 & 0_{3 \times 3} & 0_{3 \times 3} \\ \vdots & \vdots & \vdots & \vdots & \vdots & \vdots \\ \Pi_N & -p_{N1}\Pi_N & -p_{N2}\Pi_N & -p_{N3}\Pi_N & 0_{3 \times 3} & 0_{3 \times 3} \end{bmatrix} \quad (6.21)$$

The gain matrix K is chosen as

$$[K_p^\top, K_1^\top, K_2^\top, K_3^\top, K_v^\top, K_g^\top]^\top := K = PC^\top Q(t)$$

where P is the solution to the CRE (2.116). Using the fact $\hat{e}_i = \hat{R}(R^\top e_i - \tilde{e}_i) = \tilde{R}^\top e_i - \hat{R}\tilde{e}_i$, one obtains $e_i^\times \hat{e}_i = e_i^\times \tilde{R}^\top e_i - e_i^\times \hat{R}\tilde{e}_i$. Then, from (2.46) one can rewrite σ_R as (6.4) where $\phi(x, t) = -\Gamma(t)x$ with $\Gamma(t) = [0_{3 \times 3}, \rho_2 e_1^\times \hat{R}(t), \rho_3 e_2^\times \hat{R}(t), \rho_4 e_3^\times \hat{R}(t), 0_{3 \times 3}, \rho_1 g^\times \hat{R}(t)] \in \mathbb{R}^{3 \times 18}$, and

$$M := \rho_0 m_I m_I^\top + \rho_1 g g^\top + \sum_{i=1}^3 \rho_{i+1} e_i e_i^\top \quad (6.22)$$

Making use of the fact $\|\Gamma\| \leq \rho_1 \|g\| + \sum_{i=2}^4 \rho_i \|e_i\| := c_\phi$, one can show that $\|\phi(x, t)\| \leq c_\phi \|x\|$.

Lemma 6.3 *The pair $(A(t), C(t))$ defined in (6.20) and (6.21) is uniformly observable.*

Proof See Appendix E.3.

6.4 Nonlinear observers design with biased IMU measurements

6.4.1 Biased accelerometer measurements only

In this subsection, we consider the case where the acceleration measurements contain an unknown constant bias. Let b_a be the unknown acceleration bias such that $a_y = a + b_a$.

Define \hat{b}_a as the estimation of b_a and $\tilde{b}_a := \hat{b}_a - b_a$ as the estimation error. We propose the following observer modified from (6.9) as

$$\begin{aligned} \Sigma_1 : & \begin{cases} \dot{\hat{R}} = \hat{R}(\omega - k_R \hat{R}^\top \sigma_R)^\times \\ \dot{\hat{p}} = \hat{v} - k_R \sigma_R^\times (\hat{p} - p_1) + \hat{R} K_p y \\ \dot{\hat{v}} = \hat{g} + \hat{R}(a_y - \hat{b}_a) - k_R \sigma_R^\times \hat{v} + \hat{R} K_v y \\ \dot{\hat{g}} = -k_R \sigma_R^\times \hat{g} + \hat{R} K_g y \\ \dot{\hat{b}}_a = -K_a y \\ \dot{\hat{p}}_i = -k_R \sigma_R^\times (\hat{p}_i - p_1) + \hat{R} K_i y, \quad i = 2, \dots, N, \end{cases} \\ \Sigma_2 : & \begin{cases} \dot{\hat{R}} = \hat{R}(\omega - k_R \hat{R}^\top \sigma_R)^\times \\ \dot{\hat{p}} = \hat{v} - k_R \sigma_R^\times (\hat{p} - p_1) + \hat{R} K_p y \\ \dot{\hat{v}} = \hat{g} + \hat{R}(a_y - \hat{b}_a) - k_R \sigma_R^\times \hat{v} + \hat{R} K_v y \\ \dot{\hat{g}} = -k_R \sigma_R^\times \hat{g} + \hat{R} K_g y \\ \dot{\hat{b}}_a = -K_a y \\ \dot{\hat{p}}_i = -k_R \sigma_R^\times (\hat{p}_i - p_1) + \hat{R} K_i y, \quad i = 2, \dots, N, \end{cases} \end{aligned} \quad (6.23)$$

where $k_R > 0$, the gain matrices $K_p, K_v, K_g, K_a, K_i \in \mathbb{R}^{3 \times 3N}, i = 1, 2, \dots, N$ to be designed later via a CRE, and the term σ_R is given by (6.10). Similar to the previous section, one verifies that Assumption 6.2 and Assumption 6.3 are satisfied.

Let $x := [\tilde{p}^\top, \tilde{p}_2^\top, \dots, \tilde{p}_N^\top, \tilde{v}^\top, \tilde{g}^\top, \tilde{b}_a^\top]^\top \in \mathbb{R}^{9+3N}$. In view of (6.1a)-(6.1c), (6.23), one obtains the dynamics of x and the output y in the compact form (6.3) with

$$A = \begin{bmatrix} -\omega^\times & 0_{3 \times 3} & \cdots & 0_{3 \times 3} & I_3 & 0_{3 \times 3} & 0_{3 \times 3} \\ 0_{3 \times 3} & -\omega^\times & \cdots & 0_{3 \times 3} & 0_{3 \times 3} & 0_{3 \times 3} & 0_{3 \times 3} \\ \vdots & \vdots & \ddots & \vdots & \vdots & \vdots & \vdots \\ 0_{3 \times 3} & 0_{3 \times 3} & \cdots & -\omega^\times & 0_{3 \times 3} & 0_{3 \times 3} & 0_{3 \times 3} \\ 0_{3 \times 3} & 0_{3 \times 3} & \cdots & 0_{3 \times 3} & -\omega^\times & I_3 & I_3 \\ 0_{3 \times 3} & 0_{3 \times 3} & \cdots & 0_{3 \times 3} & 0_{3 \times 3} & -\omega^\times & 0_{3 \times 3} \\ 0_{3 \times 3} & 0_{3 \times 3} & \cdots & 0_{3 \times 3} & 0_{3 \times 3} & 0_{3 \times 3} & 0_{3 \times 3} \end{bmatrix} \quad (6.24)$$

$$C = \begin{bmatrix} \Pi_1 & 0_{3 \times 3} & \cdots & 0_{3 \times 3} & 0_{3 \times 3} & 0_{3 \times 3} & 0_{3 \times 3} \\ \Pi_2 & -\Pi_2 & \cdots & 0_{3 \times 3} & 0_{3 \times 3} & 0_{3 \times 3} & 0_{3 \times 3} \\ \vdots & \vdots & \ddots & \vdots & \vdots & \vdots & \vdots \\ \Pi_N & 0_{3 \times 3} & \cdots & -\Pi_N & 0_{3 \times 3} & 0_{3 \times 3} & 0_{3 \times 3} \end{bmatrix}. \quad (6.25)$$

The gain matrix K is chosen as

$$[K_p^\top, K_2^\top, \dots, K_N^\top, K_v^\top, K_g^\top, K_a^\top]^\top := K = PC^\top Q(t)$$

where P is the solution to the CRE (2.116). The term σ_R can be easily rewritten as (6.4) where $\phi(x, t) = -\Gamma(t)x$ with $\Gamma(t) = [0_{3 \times 3}, \rho_2 \bar{p}_2^\times \hat{R}(t), \dots, \rho_N \bar{p}_N^\times \hat{R}(t), 0_{3 \times 3}, \rho_1 g^\times \hat{R}(t), 0_{3 \times 3}]$ and M defined in (6.14). One can show that $\|\phi(x, t)\| \leq c_\phi \|x\|$ with $c_\phi := \rho_1 \|g\| + \sum_{i=2}^N \rho_i \|\bar{p}_i\|$, which implies that Assumption 6.2 is satisfied for σ_R given in (6.10).

Lemma 6.4 Consider the pair (A, C) defined in (6.24) and (6.25). Assume that $\omega, \dot{\omega}, \ddot{\omega}$ and $\dot{\omega}$ exist and are uniformly bounded. Then, the inequality (2.111) holds for all $t \geq 0$, if there exist constants $\bar{\delta}, \bar{\mu} > 0$ such that

$$\int_t^{t+\bar{\delta}} \|\omega(\tau) \times \dot{\omega}(\tau)\| d\tau > \bar{\mu}, \quad \forall t \geq 0. \quad (6.26)$$

Proof See Appendix E.4.

Remark 6.4 In practice, it is reasonable to assume that $\omega, \dot{\omega}, \ddot{\omega}$ and $\ddot{\omega}$ are uniformly bounded. The persistence of excitation condition (6.26) is required to generate sufficient motion such that the gravity vector and accelerometer bias can be estimated separately. This can be verified by the fourth and fifth equations in (6.23).

For the case of $N > 3$, we propose the following nonlinear observer modified from (6.18) as

$$\begin{aligned} \Sigma_1 : \quad & \begin{cases} \dot{\hat{R}} = \hat{R}(\omega - k_R \hat{R}^\top \sigma_R)^\times \\ \dot{\hat{p}} = \hat{v} - k_R \sigma_R^\times \hat{p} + \hat{R} K_p y \\ \dot{\hat{v}} = \hat{g} + \hat{R}(a_y - \hat{b}_a) - k_R \sigma_R^\times \hat{v} + \hat{R} K_v y \\ \dot{\hat{g}} = -k_R \sigma_R^\times \hat{g} + \hat{R} K_g y \\ \dot{\hat{b}}_a = -K_a y \\ \dot{\hat{e}}_i = -k_R \sigma_R^\times \hat{e}_i + \hat{R} K_i y, \quad i = 1, 2, 3 \end{cases} \\ \Sigma_2 : \quad & \begin{cases} \dot{\hat{R}} = \hat{R}(\omega - k_R \hat{R}^\top \sigma_R)^\times \\ \dot{\hat{p}} = \hat{v} - k_R \sigma_R^\times \hat{p} + \hat{R} K_p y \\ \dot{\hat{v}} = \hat{g} + \hat{R}(a_y - \hat{b}_a) - k_R \sigma_R^\times \hat{v} + \hat{R} K_v y \\ \dot{\hat{g}} = -k_R \sigma_R^\times \hat{g} + \hat{R} K_g y \\ \dot{\hat{b}}_a = -K_a y \\ \dot{\hat{e}}_i = -k_R \sigma_R^\times \hat{e}_i + \hat{R} K_i y, \quad i = 1, 2, 3 \end{cases} \end{aligned} \quad (6.27)$$

where $k_R > 0$, the gain matrices $K_p, K_v, K_g, K_a, K_i \in \mathbb{R}^{3 \times 3N}, i = 1, 2, 3$ to be designed later via a CRE, and the term σ_R is given by (6.19).

Let $x := [\tilde{p}^\top, \tilde{e}_1^\top, \tilde{e}_2^\top, \tilde{e}_3^\top, \tilde{v}^\top, \tilde{g}^\top, \tilde{b}_a^\top]^\top \in \mathbb{R}^{21}$. In view of (6.1a)-(6.1c), (6.27), one obtains the following close-loop system (6.3) with

$$A = \begin{bmatrix} -\omega^\times & 0_{3 \times 3} & 0_{3 \times 3} & 0_{3 \times 3} & I_3 & 0_{3 \times 3} & 0_{3 \times 3} \\ 0_{3 \times 3} & -\omega^\times & 0_{3 \times 3} & 0_{3 \times 3} & 0_{3 \times 3} & 0 & 0_{3 \times 3} \\ 0_{3 \times 3} & 0_{3 \times 3} & -\omega^\times & 0_{3 \times 3} & 0_{3 \times 3} & 0_{3 \times 3} & 0_{3 \times 3} \\ 0_{3 \times 3} & 0_{3 \times 3} & 0_{3 \times 3} & -\omega^\times & 0_{3 \times 3} & 0_{3 \times 3} & 0_{3 \times 3} \\ 0_{3 \times 3} & 0_{3 \times 3} & 0_{3 \times 3} & 0_{3 \times 3} & -\omega^\times & I_3 & I_3 \\ 0_{3 \times 3} & -\omega^\times & 0_{3 \times 3} \\ 0_{3 \times 3} & 0_{3 \times 3} \end{bmatrix} \quad (6.28)$$

$$C = \begin{bmatrix} \Pi_1 & -p_{11}\Pi_1 & -p_{12}\Pi_1 & -p_{13}\Pi_1 & 0_{3 \times 3} & 0_{3 \times 3} & 0_{3 \times 3} \\ \Pi_2 & -p_{21}\Pi_2 & -p_{22}\Pi_2 & -p_{23}\Pi_2 & 0_{3 \times 3} & 0_{3 \times 3} & 0_{3 \times 3} \\ \vdots & \vdots & \vdots & \vdots & \vdots & \vdots & \vdots \\ \Pi_N & -p_{N1}\Pi_N & -p_{N2}\Pi_N & -p_{N3}\Pi_N & 0_{3 \times 3} & 0_{3 \times 3} & 0_{3 \times 3} \end{bmatrix} \quad (6.29)$$

The gain matrix K is chosen as

$$[K_p^\top, K_1^\top, K_2^\top, K_3^\top, K_v^\top, K_g^\top, K_a^\top]^\top := K = PC^\top Q(t)$$

where P is the solution to the CRE (2.116). One can rewrite σ_R as (6.4) where $\phi(x, t) = -\Gamma(t)x$ with $\Gamma(t) = [0_{3 \times 3}, \rho_2 e_1^\times \hat{R}(t), \rho_3 e_2^\times \hat{R}(t), \rho_4 e_3^\times \hat{R}(t), 0_{3 \times 3}, \rho_1 g^\times \hat{R}(t), 0_{3 \times 3}] \in \mathbb{R}^{3 \times 21}$, and M defined in (6.22). Making use of the fact $\|\Gamma\| \leq \rho_1 \|g\| + \sum_{i=2}^N \rho_i \|\bar{p}_i\| := c_\phi$, one can show that $\|\phi(x, t)\| \leq c_\phi \|x\|$.

Lemma 6.5 Consider the pair (A, C) defined in (6.28) and (6.29). Suppose that $\omega, \dot{\omega}, \ddot{\omega}$ and $\ddot{\omega}$ exist and are uniformly bounded, and at least four non-coplanar landmarks are available. Then, inequality (2.111) holds for all $t \geq 0$ if condition (6.26) is satisfied.

Proof See Appendix E.5.

6.4.2 Biased accelerometer and gyroscope measurements

In this subsection, we consider the case where both the acceleration and gyroscope measurements contain unknown constant biases. Let b_ω be the unknown acceleration bias such that $\omega_y = \omega + b_\omega$. Define \hat{b}_ω as the estimation of b_ω and $\tilde{b}_\omega := \hat{b}_\omega - b_\omega$ as the estimation error. We propose the following nonlinear observer modified from (6.27) as

$$\begin{aligned} \Sigma_1 : & \begin{cases} \dot{\hat{R}} = \hat{R}(\omega_y - \hat{b}_\omega - k_R \hat{R}^\top \sigma_R)^\times \\ \dot{\hat{b}}_\omega = \mathbf{P}_\delta^\epsilon(\hat{b}_\omega, k_\omega \hat{R}^\top \sigma_R) \\ \dot{\hat{p}} = \hat{v} - k_R \sigma_R^\times \hat{p} + \hat{R} K_p y \\ \dot{\hat{v}} = \mathbf{g} + \hat{R}(a_y - \hat{b}_a) - k_R \sigma_R^\times \hat{v} + \hat{R} K_v y \\ \dot{\hat{b}}_a = -K_a y \\ \dot{\hat{e}}_i = -k_R \sigma_R^\times \hat{e}_i + \hat{R} K_i y, \quad i = 1, 2, 3 \end{cases} \\ \Sigma_2 : & \begin{cases} \dot{\hat{p}} = \hat{v} - k_R \sigma_R^\times \hat{p} + \hat{R} K_p y \\ \dot{\hat{v}} = \mathbf{g} + \hat{R}(a_y - \hat{b}_a) - k_R \sigma_R^\times \hat{v} + \hat{R} K_v y \\ \dot{\hat{b}}_a = -K_a y \\ \dot{\hat{e}}_i = -k_R \sigma_R^\times \hat{e}_i + \hat{R} K_i y, \quad i = 1, 2, 3 \end{cases} \end{aligned} \quad (6.30)$$

where $K_R, k_\omega > 0$, the gain matrices $K_p, K_v, K_a, K_i \in \mathbb{R}^{3 \times 3N}$, $i = 1, 2, 3$ to be designed later via a CRE, and the term σ_R is given by

$$\sigma_R := \rho_0 m_I^\times \hat{R} m_B + \sum_{i=1}^3 \rho_i e_i^\times \text{sat}_{c_e}(\hat{e}_i) \quad (6.31)$$

where the saturation function sat_{c_e} is defined as $\text{sat}_{c_e}(\hat{e}_i) = \min\{1, c_e/\|\hat{e}_i\|\}\hat{e}_i$ with some scalar $c_e > 1$. Note that $\text{sat}_{c_e}(\hat{e}_i)$ is reduced to \hat{e}_i when $\|\hat{e}_i\| \leq c_e$. In this case, σ_R can be rewritten as (6.4) where $M = \rho_0 m_I m_I^\top + \sum_{i=1}^3 \rho_i e_i e_i^\top$, and $\phi(x, t) = -\Gamma(t)x$ with $\Gamma(t) = [0_{3 \times 3}, \rho_1 e_1^\times \hat{R}(t), \rho_2 e_2^\times \hat{R}(t), \rho_3 e_3^\times \hat{R}(t), 0_{3 \times 3}, 0_{3 \times 3}]$. Then, one shows $\|\phi(x, t)\| \leq c_\phi \|x\|$ with $c_\phi := \sum_{i=1}^3 \rho_i$, which implies that Assumption 6.2 is satisfied for σ_R given in (6.31). The projection map is given in (3.75). The structure of this observer is given by Figure 6.4. The position, velocity, accelerometer bias and basis vectors are estimated using biased IMU and stereo bearing measurements. The attitude is then estimated using the angular velocity and magnetometer measurements, as well as the estimated basis vectors.

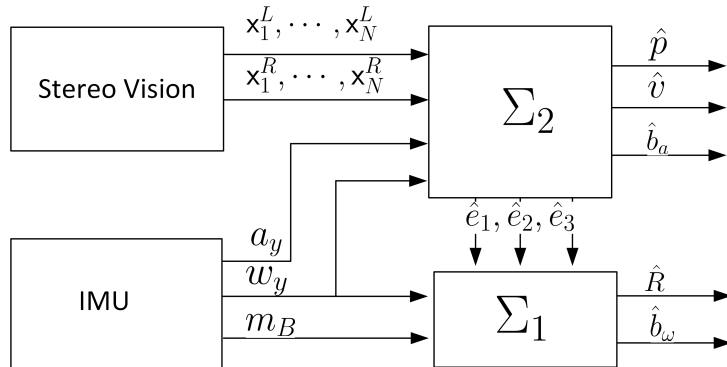


Figure 6.4: Nonlinear observer (6.30) using biased IMU and stereo bearing measurements

Remark 6.5 The projection map $\mathbf{P}_\delta^\epsilon(\cdot, \cdot)$ was introduced to guarantee that \hat{b}_ω is uniformly bounded. Moreover, since $\|\text{sat}_{c_e}(\hat{e}_i)\| < c_e$ for all $\hat{e}_i \in \mathbb{R}^3$, one can show that

$\|\mathbf{P}_\delta^\epsilon(\hat{b}_\omega, k_\omega \hat{R}^\top \sigma_R)\| \leq k_\omega \|\sigma_R\| < k_\omega (\rho_0 \|m_I\|^2 + \sum_{i=1}^3 \rho_i c_e)$. This implies that the first-order derivative of \hat{b}_ω is bounded for all $t \geq 0$. The boundedness of \hat{b}_ω and its first-order derivative will be used later to show the existence of the solution P to the CRE (2.116).

Remark 6.6 It is noted that the estimate of the gravity is not considered in this case. This is due to the difficulties it introduces, with respect to the existence of the solution to the CRE (2.116) when the gyro and accelerometer biases are considered simultaneously. From a simple extension of Lemma 6.4 and 6.5, the second and third derivatives of $(\omega_y - \hat{b}_\omega)$ are required to be bounded if the estimate of the gravity vector is included as the observer (6.27). However, it is difficult to show the boundedness of the second and third derivatives of \hat{b}_ω since σ_R contains \hat{e}_i whose dynamics depend on the solution of the CRE.

Define the new variable $x := [\tilde{p}^\top, \tilde{e}_1^\top, \tilde{e}_2^\top, \tilde{e}_3^\top, \tilde{v}^\top, \tilde{b}_a^\top]^\top \in \mathbb{R}^{18}$. In view of (6.1a)-(6.1c) and (6.30), one obtains the following closed-loop system:

$$\begin{cases} \dot{\tilde{R}} = \tilde{R}(\hat{R}\tilde{b}_\omega + k_R \sigma_R)^\times \\ \dot{\tilde{b}}_\omega = \mathbf{P}_\delta^\epsilon(\hat{b}_\omega, k_\omega \hat{R}^\top \sigma_R) \\ \dot{x} = A(t)x - Ky + \varphi(\tilde{R}, \tilde{b}_\omega, t) \\ y = C(t)x \end{cases} \quad (6.32)$$

with $\varphi(\tilde{R}, \tilde{b}_\omega, t) = [p^\top R \tilde{b}_\omega^\times, e_1^\top R \tilde{b}_\omega^\times, e_2^\top R \tilde{b}_\omega^\times, e_3^\top R \tilde{b}_\omega^\times, v^\top R \tilde{b}_\omega^\times + g^\top(I - \tilde{R})^\top, 0_{1 \times 3}]^\top$, and

$$A = \begin{bmatrix} -\hat{\omega}_y^\times & 0_{3 \times 3} & 0_{3 \times 3} & 0_{3 \times 3} & I_3 & 0_{3 \times 3} \\ 0_{3 \times 3} & -\hat{\omega}_y^\times & 0_{3 \times 3} & 0_{3 \times 3} & 0_{3 \times 3} & 0_{3 \times 3} \\ 0_{3 \times 3} & 0_{3 \times 3} & -\hat{\omega}_y^\times & 0_{3 \times 3} & 0_{3 \times 3} & 0_{3 \times 3} \\ 0_{3 \times 3} & 0_{3 \times 3} & 0_{3 \times 3} & -\hat{\omega}_y^\times & 0_{3 \times 3} & 0_{3 \times 3} \\ 0_{3 \times 3} & 0_{3 \times 3} & 0_{3 \times 3} & 0_{3 \times 3} & -\hat{\omega}_y^\times & I_3 \\ 0_{3 \times 3} & 0_{3 \times 3} \end{bmatrix} \quad (6.33)$$

$$C = \begin{bmatrix} \Pi_1 & -p_{11}\Pi_1 & -p_{12}\Pi_1 & -p_{13}\Pi_1 & 0_{3 \times 3} & 0_{3 \times 3} \\ \Pi_2 & -p_{21}\Pi_2 & -p_{22}\Pi_2 & -p_{23}\Pi_2 & 0_{3 \times 3} & 0_{3 \times 3} \\ \vdots & \vdots & \vdots & \vdots & \vdots & \vdots \\ \Pi_N & -p_{N1}\Pi_N & -p_{N2}\Pi_N & -p_{N3}\Pi_N & 0_{3 \times 3} & 0_{3 \times 3} \end{bmatrix} \quad (6.34)$$

where $\hat{\omega}_y := \omega_y - \hat{b}_\omega = \omega - \tilde{b}_\omega$. The gain matrix K is chosen as

$$[K_p^\top, K_2^\top, \dots, K_N^\top, K_v^\top, K_g^\top, K_a^\top]^\top := K = PC^\top Q(t)$$

where P is the solution of the CRE (2.116).

Assumption 6.5 There exist constants $c_p, c_v, c_\omega, c_{\dot{\omega}} > 0$ such that $\|p(t)\| \leq c_p$, $\|v(t)\| \leq c_v$, $\|\omega(t)\| \leq c_\omega$ and $\|\dot{\omega}(t)\| \leq c_{\dot{\omega}}$ for all $t \geq 0$.

Lemma 6.6 Consider the pair (A, C) defined in (6.33) and (6.34). Suppose that Assumption 6.5 holds and at least four non-coplanar landmarks are available. Then, inequality (2.111) holds for all $t \geq 0$.

From Assumption 6.5 and the boundedness of \hat{b}_ω and its first-order derivative, it is easy to verify that A and its first-order derivative are uniformly bounded. Then, the proof of Lemma 6.6 can be conducted using similar steps as in the proof of Lemma 6.5, which is omitted here. Given the facts that the pair $(A(t), C(t))$ is uniformly observable and the matrix-valued functions $V(t) \in \mathbb{R}^{n \times n}$ and $Q(t) \in \mathbb{R}^{m \times m}$ are positive definite matrices, one can show that the conditions in Lemma 2.10 are satisfied, and hence there exist positive constants $0 < p_m \leq p_M < \infty$ such that $p_m I_n \leq P(t) \leq p_M I_n$ for all $t > \delta$.

Define $\varsigma(t) = [\|\tilde{R}(t)\|_I, \|\tilde{b}_\omega(t)\|, \|x(t)\|]^\top \in \mathbb{R}^3$. Now, one can state the following result:

Theorem 6.2 Consider the nonlinear time-varying system (6.32) with (6.31) and (6.33)-(6.34). Suppose that Assumption 6.5 holds. For each $\varepsilon_R < 1$ and for all initial conditions $|\tilde{R}(0)|_I \leq \varepsilon_R$, $\|\tilde{b}_\omega(0)\| < 2c_b + \delta$, $x(0) \in \mathbb{R}^{18}$, there exist $k_R^* > 0$ and $v_m^* > 0$ such that, for all $k_R \geq k_R^*$ and $V(t) \geq v_m^* I$, $\varsigma(t)$ is bounded and

$$\|\varsigma(t)\| \leq \kappa \exp(-\lambda(t - T)) \|\varsigma(T)\|, \quad \forall t \geq T, \quad (6.35)$$

for some positive scalars κ, λ, T .

Proof See Appendix E.6.

Theorem 6.2 shows that, with an appropriate tuning of the gains, the proposed observer (6.30) guarantees exponential convergence of the estimation errors (after a finite time). It is important to mention that the high gain conditions, provided in the proof, are rather conservative, and simulation has shown that the proposed observer (6.30) has a large region of attraction without high gains. Note that observer (6.23) can also be easily extended to handle biased accelerometer and gyroscope measurements, which is omitted here.

In practice, the IMU measurements can be obtained at a high rate, while the vision measurements are often obtained at a much lower rate. Hence, the IMU measurements can be seen as continuous measurements and stereo bearing measurements can be seen as intermittent measurements. Taking into account this fact, the proposed observer (6.30) can be implemented as in Algorithm 2. Similar to Algorithm 1 in Section 4.7, this Algorithm contains two parts: a continuous integration of the state using IMU measurements when the stereo bearing measurements are not available, and a discrete correction to the estimated linear state is applied when the vision measurements arrive. Moreover, between two consecutive stereo bearing measurements, the continuous part of Algorithm 1 can be discretized using first order numerical integrations for vectors, and the following numerical integration for the rotation matrix, $\hat{R}_{\kappa+1} = \hat{R}_\kappa \exp(dT(\omega_{y,\kappa} - \hat{b}_{\omega,\kappa} - k_R \hat{R}_\kappa^\top \sigma_R)^\times)$ with dT being the sampling period of the IMU measurements. The Algorithm 2 can be easily modified for other observers proposed in this chapter which are omitted here.

Algorithm 2 Continuous-discrete implementation algorithm

Initialization: Set $k = 0, t_0 = 0, \|\hat{R}(t_0)\| \leq \varepsilon_R, \|\hat{b}_\omega(t_0)\| < \delta, \hat{p}(t_0) \in \mathbb{R}^3, \hat{v}(t_0) \in \mathbb{R}^3, \hat{b}_a(t_0) \in \mathbb{R}^3, \hat{e}_i(t_0) \in \mathbb{R}^3, i = 1, 2, 3, P(t_0) \in \mathbb{R}^{21 \times 21} > 0$. Choose $Q, V > 0$.

Output: State $\hat{R}(t), \hat{b}_\omega(t), \hat{p}(t), \hat{v}(t), \hat{g}(t), \hat{b}_a(t)$ for all $t \geq t_0$

1: **while** Simulation time not exceeded **do**

2: Set $k = k + 1$

3: **while** $t_{k-1} \leq t \leq t_k$ **do**

4: Compute σ_R in (6.19)

5: Integrate the following equations:

$$\begin{cases} \dot{\hat{R}} &= \hat{R}(\omega_y - \hat{b}_\omega - k_R \hat{R}^\top \sigma_R)^\times \\ \dot{\hat{b}}_\omega &= \mathbf{P}_\delta^\epsilon(\hat{b}_\omega, k_\omega \hat{R}^\top \sigma_R) \\ \dot{\hat{p}} &= \hat{v} - k_R \sigma_R^\times \hat{p} \\ \dot{\hat{v}} &= \mathbf{g} + \hat{R}(a_y - \hat{b}_a) - k_R \sigma_R^\times \hat{v} \\ \dot{\hat{b}}_a &= 0 \\ \dot{\hat{e}}_i &= -k_R \sigma_R^\times \hat{e}_i, \quad i = 1, 2, 3 \\ \dot{P} &= AP + PA^\top + V \end{cases}$$

6: **end while**

7: Set $P_{k|k-1} = P(t_k)$ and $\mathcal{S}_{k|k-1} = \mathcal{S}(t_k)$ for each $\mathcal{S} \in \{\hat{R}, \hat{b}_\omega, \hat{p}, \hat{v}, \hat{b}_a, \hat{e}_1, \hat{e}_2, \hat{e}_3\}$

8: Compute the gain matrices

$$\begin{aligned} [K_{p,k}^\top, K_{1,k}^\top, K_{2,k}^\top, K_{3,k}^\top, K_{v,k}^\top, K_{a,k}^\top]^\top &:= K_k \\ &= P_{k|k-1} C^\top (C P_{k|k-1} C^\top + Q^{-1})^{-1} \end{aligned}$$

9: Obtain stereo bearing measurements x_i^L, x_i^R for each $i = 1, 2, \dots$

10: Compute the output y in (6.17).

11: Update the state estimates as

$$\begin{cases} \hat{p}_{k|k} &= \hat{p}_{k|k-1} + \hat{R} K_{p,k} y \\ \hat{v}_{k|k} &= \hat{v}_{k|k-1} + \hat{R} K_{v,k} y \\ \hat{b}_{a,k|k} &= \hat{b}_{a,k|k-1} - K_{a,k} y \\ \hat{e}_{i,k|k} &= \hat{e}_{i,k|k-1} + \hat{R} K_{i,k} y, \quad i = 1, 2, 3 \\ P_{k|k} &= (I - K_k C) P_{k|k-1} \end{cases}$$

12: Set $P(t_k) = P_{k|k}$ and $\mathcal{S}(t_k) = \mathcal{S}_{k|k}$ for each $\mathcal{S} \in \{\hat{R}, \hat{b}_\omega, \hat{p}, \hat{v}, \hat{b}_a, \hat{e}_1, \hat{e}_2, \hat{e}_3\}$

13: **end while**

6.5 Simulation results

6.5.1 Simulation with continuous and noise-free measurements

In this simulation, we consider an autonomous vehicle moving on the ‘8’-shape trajectory described by $p(t) = 10[\sin(t), \sin(t)\cos(t), 1]^\top$, with the initial attitude $R(0) = I_3$ and angular velocity $\omega(t) = [-\cos(2t), 1, \sin(2t)]^\top$. The gravity and magnetic vectors, expressed in the inertial frame, are given as $\mathbf{g} = [0, 0, -9.81]^\top$ and $\mathbf{m}_I = [0.8, 0.6, 0]^\top$, respectively. There are 10 randomly selected non-coplanar landmarks. The stereo bearing measurements are generated from (6.2). The accelerometer bias is given as $\mathbf{b}_a = [-0.0209, 0.1216, 0.0788]^\top$.

Four observers are considered in this simulation. We refer to the observer (6.23) using the knowledge of the gravity vector, magnetometer measurements and stereo bearing measurements of one landmark as ‘SBINO1’, the observer (6.23) using magnetometer measurements and stereo bearing measurements of two landmarks as ‘SBINO2’, the observer (6.23) using stereo bearing measurements of $N \geq 3$ landmarks as ‘SBINO3’, and the observer (6.27) as ‘SBINO4’. The same initial conditions are considered for each observer as: $\hat{R}(0) = \mathcal{R}_a(0.5\pi, u)$ with $u \in \mathbb{S}^2$, $\hat{v}(0) = \hat{p}(0) = \hat{\mathbf{g}}(0) = \hat{\mathbf{b}}_a(0) = 0_{3 \times 1}$, and $P(0) = I$. The parameters of each observer are taken as $k_R = 8$, $\rho_0 = 0.5/\|\mathbf{g}\|^2$, $\rho_1 = \rho_2 = \dots = \rho_{10} = 0.5$ ($\rho_i = 0$ when it is not used in the design of σ_R), and $Q = 10^5 I$, $V = 10^{-6} I$ for each CRE. Simulation results are shown in Figure 6.5. As one can see, the estimated states from all the observers converge, after a few seconds, to the vicinity of the real states.

6.5.2 Simulation using real IMU data from the EuRoc dataset

To further validate the performance of our proposed observers, we consider a real trajectory (generated by a real flight of a quadrotor) and real (biased and noisy) IMU measurements from the EuRoc dataset [Burri et al., 2016]. We consider $N = 25$ randomly selected landmarks such that there are at least four non-coplanar landmarks. In this simulation, the stereo bearing measurements are generated from (6.2) and $p_i^B = R_G^\top(p_i - p_G)$ with the ground truth rotation R_G and position p_G . Additional noise in the bearing measurements is considered as [Hamel and Samson, 2018]

$$x_i^s = \frac{\text{sign}(x_{i,3}^s)}{d_{x_i^s}}(x_{i,1}^s/x_{i,3}^s + n_{i,1}, x_{i,2}^s/x_{i,3}^s + n_{i,1}, 1), \quad (6.36)$$

$$d_{x_i^s} = \|x_{i,1}^s/x_{i,3}^s + n_{i,1}, x_{i,2}^s/x_{i,3}^s + n_{i,2}, 1\|, \quad (6.37)$$

with $s \in \{L, R\}$, $i = 1, 2, \dots, N$ and $n_{i,1}, n_{i,2}$ being uncorrelated zero-mean uniformly distributed noise inputs with a maximum deviation of 0.005. The calibration matrix R_{cL}, R_{cR}, p_L, p_R are provided in the dataset. The initial conditions for the observer (6.27) are given as $\hat{R}(0) = \mathcal{R}_a(0.2\pi, u^\times)R_G(0)$ with $u \in \mathbb{S}^2$, $\hat{p}(0) = \hat{v}(0) = \hat{\mathbf{b}}_a(0) = 0$, and $\hat{e}_i(0) = e_i$ for all $i = 1, 2, 3$. The parameters are taken as $k_R = k_\omega = 2$, $\rho_0 = 0$, $\rho_1 = \rho_2 = \rho_3 = 0.5$, $P(0) = I_{18}$, $V(t) = 10^{-5} I_{18}$, $Q(t) = 10^5 \text{blkdiag}(\Pi_1^{-\top} \Pi_1^{-1}, \Pi_2^{-\top} \Pi_2^{-1}, \dots, \Pi_N^{-\top} \Pi_N^{-1})$. The simulation results are given in Figure 6.6. As one can see, the estimates converge to

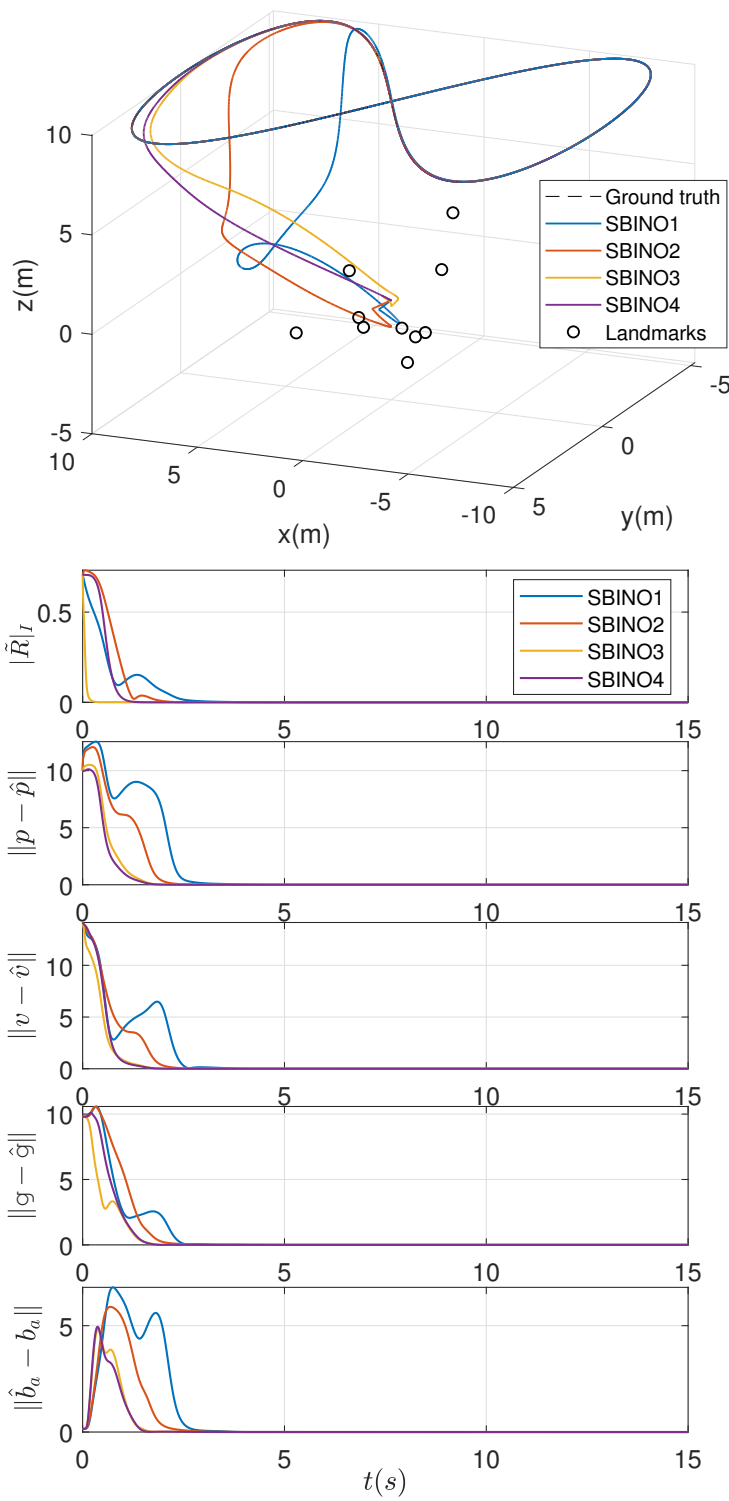


Figure 6.5: Simulations results using ideal IMU measurements.

the vicinity of the ground truth after a few seconds with large initial errors of position, velocity and gravity vector. It is important to mention that, due to the limited field of view of the cameras, the number of visible landmarks are not fixed, especially when the motion of the vehicle is large. It is difficult to show the existence of a solution of the CRE when the dimension of the matrix C changes frequently. Hence, it is still an open problem to design an observer with rigorous stability guarantees, and proper parameters Q and V , that ensures ‘optimal’ solutions (in terms of measurement noise) to the CRE where the visible landmarks are not fixed.

6.6 Conclusion

In this chapter, the problem of attitude, position and linear velocity estimation for inertial navigation relying on IMU and stereo bearing measurements has been addressed. First, a stability result for a generic class of nonlinear time-varying systems on $\mathbf{SO}(3) \times \mathbb{R}^n$ has been derived. This stability result has been exploited to develop two nonlinear navigation observers. These observers are then extended to handle biased accelerometer and gyroscope measurements. Numerical results using simulated landmark measurements together with IMU data from the EuRoc dataset have been provided to illustrate the performance of the proposed observers. An interesting direction of future work would be applying the hybrid techniques to handle the case where the visible landmarks are not fixed.

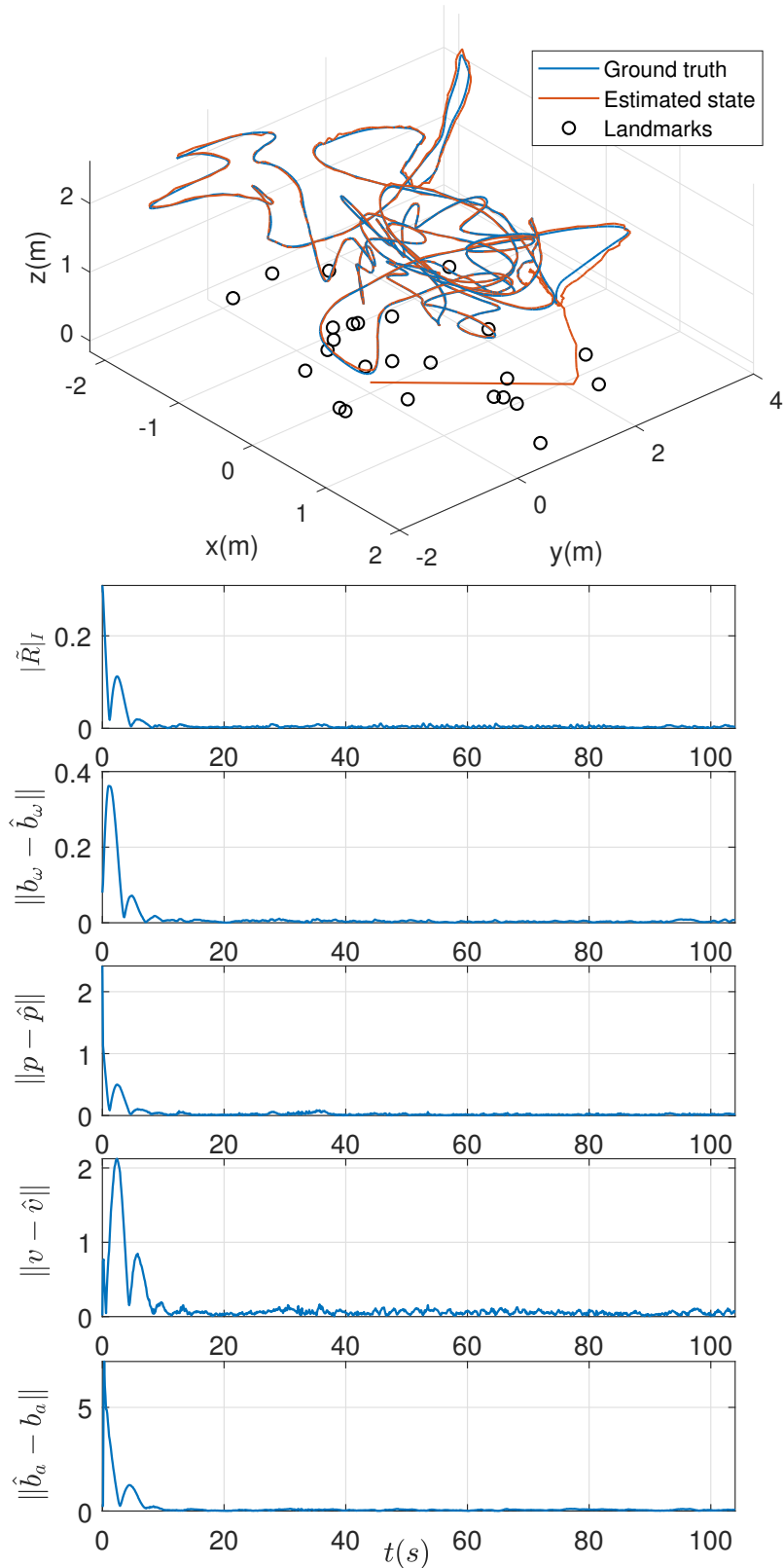


Figure 6.6: Simulations results using real IMU measurements from the EuRoc dataset V1_03_difficult.

Chapter 7

Conclusions

Summary

In this thesis, we explored the topics of state estimation for autonomous navigation systems. We considered the pose estimation problem on the Lie group $\text{SE}(3)$ using inertial and landmark position measurement. Then, we considered the pose and linear velocity estimation problem for INSs using continuous landmark position measurements, intermittent landmark position measurements and stereo bearing measurements, respectively.

With regards to the pose estimation on $\text{SE}(3)$, we proposed a generic hybrid pose and velocity-bias estimation scheme on $\text{SE}(3) \times \mathbb{R}^6$ with global asymptotic (exponential) stability guarantees. The main feature of this hybrid estimation scheme is the new observer-state jump mechanism that adjusts the observer state through appropriate jumps in the direction of a decreasing potential function on $\text{SE}(3)$ when the pose estimation error is in the neighborhood of an undesired critical point of this potential function. Then, an explicit hybrid observer for pose and velocity-bias estimation, using inertial and landmark position measurements, was derived. To remove the coupling between the rotational and translational error dynamics, in the bias-free case, the explicit hybrid observer was re-designed. Moreover, this modified hybrid observer was further extended to a practically implementable version with fully decoupled rotational and translational error dynamics in the presence of biased linear and angular velocities.

Concerning the full-state (pose and linear velocity) estimation problem for INSs, we proposed three different estimation schemes based on the type of measurements used, *i.e.*, continuous landmark position measurements, intermittent landmark position measurements, and stereo bearing measurements. In fact, globally exponentially stable nonlinear geometric hybrid observers on $\text{SE}_2(3)$ using ideal IMU and landmark position measurements have been proposed. These results have been extended to handle biased IMU measurements with GES guarantees. Moreover, two hybrid nonlinear observers for INSs, with strong stability guarantees, have been developed using continuous IMU measurements and intermittent landmark position measurements. Finally, the full-state estimation problem, with AGAS guarantees, relying directly on stereo bearing measurements has been addressed.

Perspectives

There are still several issues related to the state estimation problem for INSs, and the proposed solutions in this work constitute a good platform for several future extensions. In this dissertation, we assume that the landmark positions are obtained from vision systems, such as stereo-vision systems. However, it is interesting to explore the extension of the proposed algorithms using intermittent monocular-bearing measurements and to conduct an in-depth study on the observability constraints related to the use of a single camera. There are very few results in the literature dealing with this problem, for example [[Hamel and Samson, 2018](#); [Chowdhary, 2013](#); [Qin et al., 2018](#)].

In this dissertation, it is assumed that the number of landmarks is fixed and all the landmarks are time-invariant. However, in practice, it is quite unrealistic to track the same set of landmarks all the time, especially when the motion of the vehicle is large. On the other hand, the location of the landmarks may be time-varying, such as the case where they are attached to a moving object. There are a few interesting results on $\text{SO}(3)$ using time-varying reference vectors, for instance [[Grip et al., 2012](#); [Trumpf et al., 2012](#)]. However, due to the complexity of the INS dynamics, it is still a challenging task to design full-state observers with strong stability guarantees, when the number of landmarks is not fixed or/and the positions of landmarks are time-varying.

The Simultaneous Localization and Mapping (SLAM) is a very popular and practical problem in robotics. It consists of building a map of an unknown environment while keeping track of the vehicle's location [[Durrant-Whyte and Bailey, 2006](#); [Bailey and Durrant-Whyte, 2006](#)]. Recently, geometric nonlinear observers for SLAM from a Lie group perspective, with strong stability guarantees, have made their appearance in the literature [[Barrau and Bonnabel, 2015](#); [Mahony and Hamel, 2017](#); [Zlotnik and Forbes, 2018](#); [Wang and Tayebi, 2018a](#)]. The design of monocular-vision based geometric SLAM algorithms, with strong stability guarantees, in dynamic environments, is an interesting problem yet to be solved.

Bibliography

- Absil, P.-A., Mahony, R., and Sepulchre, R. (2009). *Optimization algorithms on matrix manifolds*. Princeton University Press.
- Adams, J. C., Gregorwich, W., Capots, L., and Liccardo, D. (2001). Ultra-wideband for navigation and communications. In *2001 IEEE Aerospace Conference Proceedings (Cat. No. 01TH8542)*, volume 2, pp. 2–785. IEEE.
- Aplevich, J. D. (2000). *The essentials of linear state-space systems*. Wiley New York.
- Bailey, T. and Durrant-Whyte, H. (2006). Simultaneous localization and mapping (SLAM): Part II. *IEEE Robotics & Automation Magazine*, 13(3):108–117.
- Baldwin, G., Mahony, R., and Trumpf, J. (2009). A nonlinear observer for 6 DOF pose estimation from inertial and bearing measurements. In *Proceedings of the IEEE International Conference on Robotics and Automation*, pp. 2237–2242.
- Baldwin, G., Mahony, R., Trumpf, J., Hamel, T., and Cheviron, T. (2007). Complementary filter design on the Special Euclidean group $\text{SE}(3)$. In *Proceedings of the European Control Conference (ECC)*, pp. 3763–3770.
- Bar-Itzhack, I. and Oshman, Y. (1985). Attitude determination from vector observations: quaternion estimation. *IEEE Transactions on Aerospace and Electronic Systems*, 32(1):128–136.
- Barczyk, M. (2012). *Nonlinear state estimation and modeling of a helicopter UAV*. PhD thesis, University of Alberta.
- Barczyk, M. and Lynch, A. F. (2013). Invariant observer design for a helicopter UAV aided inertial navigation system. *IEEE Transactions on Control Systems Technology*, 21(3):791–806.
- Barrau, A. and Bonnabel, S. (2014a). Intrinsic filtering on Lie groups with applications to attitude estimation. *IEEE Transactions on Automatic Control*, 60(2):436–449.
- Barrau, A. and Bonnabel, S. (2014b). Invariant particle filtering with application to localization. In *Proceedings the 53rd IEEE Annual Conference on Decision and Control (CDC)*, pp. 5599–5605.

- Barrau, A. and Bonnabel, S. (2015). An EKF-SLAM algorithm with consistency properties. *arXiv preprint*. arXiv:1510.06263.
- Barrau, A. and Bonnabel, S. (2017). The invariant extended Kalman filter as a stable observer. *IEEE Transactions on Automatic Control*, 62(4):1797–1812.
- Batista, P., Silvestre, C., and Oliveira, P. (2012a). Globally exponentially stable cascade observers for attitude estimation. *Control Engineering Practice*, 20(2):148–155.
- Batista, P., Silvestre, C., and Oliveira, P. (2012b). Sensor-based globally asymptotically stable filters for attitude estimation: Analysis, design, and performance evaluation. *IEEE Transactions on Automatic Control*, 57(8):2095–2100.
- Batista, P., Silvestre, C., Oliveira, P., and Cardeira, B. (2010). Accelerometer calibration and dynamic bias and gravity estimation: Analysis, design, and experimental evaluation. *IEEE transactions on control systems technology*, 19(5):1128–1137.
- Berkane, S. (2017). *Hybrid Attitude Control and Estimation On SO(3)*. PhD thesis, University of Western Ontario.
- Berkane, S., Abdessameud, A., and Tayebi, A. (2016). A globally exponentially stable hybrid attitude and gyro-bias observer. In *Proceedings of the 55th IEEE Conference on Decision and Control (CDC)*, pp. 308–313.
- Berkane, S., Abdessameud, A., and Tayebi, A. (2017a). Hybrid attitude and gyro-bias observer design on $\text{SO}(3)$. *IEEE Transactions on Automatic Control*, 62(11):6044–6050.
- Berkane, S., Abdessameud, A., and Tayebi, A. (2017b). Hybrid global exponential stabilization on $\text{SO}(3)$. *Automatica*, 81:279–285.
- Berkane, S. and Tayebi, A. (2017a). Attitude and gyro bias estimation using GPS and IMU measurements. In *Proceedings of the 56th IEEE Conference on Decision and Control (CDC)*, pp. 2402–2407. IEEE.
- Berkane, S. and Tayebi, A. (2017b). Attitude observer using synchronous intermittent vector measurements. In *Proceedings of the 56th IEEE Conference on Decision and Control (CDC), Melbourne, Australia*, pp. 3027–3032.
- Berkane, S. and Tayebi, A. (2017c). Construction of synergistic potential functions on $\text{SO}(3)$ with application to velocity-free hybrid attitude stabilization. *IEEE Transactions on Automatic Control*, 62(1):495–501.
- Berkane, S. and Tayebi, A. (2019). Attitude estimation with intermittent measurements. *Automatica*, 105:415–421.
- Bloch, A. M. (2003). Nonholonomic mechanics. In *Nonholonomic mechanics and control*, pp. 207–276. Springer.

- Bonnabel, S., Martin, P., and Rouchon, P. (2008). Symmetry-preserving observers. *IEEE Transactions on Automatic Control*, 53(11):2514–2526.
- Bonnabel, S., Martin, P., and Rouchon, P. (2009a). Non-linear symmetry-preserving observers on Lie groups. *IEEE Transactions on Automatic Control*, 54(7):1709–1713.
- Bonnabel, S., Martin, P., and Salaün, E. (2009b). Invariant Extended Kalman filter: theory and application to a velocity-aided attitude estimation problem. In *Proceedings of the 48th IEEE Conference on Decision and Control and the 28th Chinese Control Conference (CDC/CCC)*, pp. 1297–1304. IEEE.
- Bray, D. (2003). *Dynamic positioning*, volume 9. Oilfield Publications Limited.
- Bristeau, P.-J., Petit, N., and Praly, L. (2010). Design of a navigation filter by analysis of local observability. In *49th IEEE Conference on Decision and Control (CDC)*, pp. 1298–1305. IEEE.
- Britting, K. R. (1971). Inertial navigation systems analysis.
- Bryne, T. H., Hansen, J. M., Rogne, R. H., Sokolova, N., Fossen, T. I., and Johansen, T. A. (2017). Nonlinear observers for integrated INS/GNSS navigation: implementation aspects. *IEEE Control Systems Magazine*, 37(3):59–86.
- Bucy, R. S. (1967). Global theory of the Riccati equation. *Journal of computer and system sciences*, 1(4):349–361.
- Bucy, R. S. (1972). The Riccati equation and its bounds. *Journal of computer and system sciences*, 6(4):343–353.
- Burri, M., Nikolic, J., Gohl, P., Schneider, T., Rehder, J., Omari, S., Achtelik, M., and Siegwart, R. (2016). The EuRoC micro aerial vehicle datasets. *The International Journal of Robotics Research*.
- Chen, C.-T. (1999). *Linear system theory and design*. Oxford University Press, Inc., 3 edition.
- Chen, S. (2011). Kalman filter for robot vision: a survey. *IEEE Transactions on Industrial Electronics*, 59(11):4409–4420.
- Chowdhary, A. D. W. E. N. J. M. K. F. D. G. (2013). Autonomous flight in GPS-denied environments using monocular vision and inertial sensors. *Journal of Aerospace Information Systems*, 10(4):172–186.
- Corke, P. (2017). *Robotics, vision and control: fundamental algorithms in MATLAB® second, completely revised*, volume 118. Springer.
- Crassidis, J. L., Markley, F. L., and Cheng, Y. (2007). Survey of nonlinear attitude estimation methods. *Journal of Guidance, Control, and Dynamics*, 30(1):12–28.

- DeSouza, G. N. and Kak, A. C. (2002). Vision for mobile robot navigation: A survey. *IEEE transactions on pattern analysis and machine intelligence*, 24(2):237–267.
- Deyst, J. and Price, C. (1968). Conditions for asymptotic stability of the discrete minimum-variance linear estimator. *IEEE Transactions on Automatic Control*, 13:702–705.
- Do Carmo, M. P. (1992). *Riemannian geometry*. Birkhauser.
- Durrant-Whyte, H. and Bailey, T. (2006). Simultaneous localization and mapping: part I. *IEEE robotics & automation magazine*, 13(2):99–110.
- Ferrante, F., Gouaisbaut, F., Sanfelice, R. G., and Tarbouriech, S. (2016). State estimation of linear systems in the presence of sporadic measurements. *Automatica*, 73:101–109.
- Foster, C. C. and Elkaim, G. H. (2008). Extension of a two-step calibration methodology to include nonorthogonal sensor axes. *Aerospace and Electronic Systems, IEEE Transactions on*, 44(3):1070–1078.
- George, M. and Sukkarieh, S. (2007). Inertial navigation aided by monocular camera observations of unknown features. In *Proceedings 2007 IEEE International Conference on Robotics and Automation*, pp. 3558–3564. IEEE.
- Gezici, S., Tian, Z., Giannakis, G. B., Kobayashi, H., Molisch, A. F., Poor, H. V., and Sahinoglu, Z. (2005). Localization via ultra-wideband radios: a look at positioning aspects for future sensor networks. *IEEE signal processing magazine*, 22(4):70–84.
- Goebel, R., Sanfelice, R. G., and Teel, A. R. (2009). Hybrid dynamical systems. *IEEE Control Systems*, 29(2):28–93.
- Goebel, R., Sanfelice, R. G., and Teel, A. R. (2012). *Hybrid Dynamical Systems: modeling, stability, and robustness*. Princeton University Press.
- Grant, M., Boyd, S., and Ye, Y. (2009). CVX: Matlab software for disciplined convex programming.
- Grewal, M. S., Weill, L. R., and Andrews, A. P. (2007). *Global positioning systems, inertial navigation, and integration*. John Wiley & Sons.
- Grip, H. F., Fossen, T. I., Johansen, T. A., and Saberi, A. (2012). Attitude estimation using biased gyro and vector measurements with time-varying reference vectors. *IEEE Transactions on Automatic Control*, 57(5):1332–1338.
- Grip, H. F., Fossen, T. I., Johansen, T. A., and Saberi, A. (2013). Nonlinear observer for GNSS-aided inertial navigation with quaternion-based attitude estimation. In *American Control Conference (ACC), 2013*, pp. 272–279. IEEE.
- Hamel, T. and Samson, C. (2017). Position estimation from direction or range measurements. *Automatica*, 82:137–144.

- Hamel, T. and Samson, C. (2018). Riccati observers for the non-stationary PnP problem. *IEEE Transactions on Automatic Control*, 63(3):726–741.
- Hartley, R. and Zisserman, A. (2003). *Multiple view geometry in computer vision*. Cambridge university press.
- Hesch, J. A. and Roumeliotis, S. I. (2011). A direct least-squares (DLS) method for PnP. In *2011 International Conference on Computer Vision*, pp. 383–390. IEEE.
- Holm, D. D., Schmah, T., and Stoica, C. (2009). *Geometric mechanics and symmetry: from finite to infinite dimensions*, volume 12. Oxford University Press.
- Hua, M.-D. and Allibert, G. (2018). Riccati observer design for pose, linear velocity and gravity direction estimation using landmark position and IMU measurements. In *2018 IEEE Conference on Control Technology and Applications (CCTA)*, pp. 1313–1318. IEEE.
- Hua, M.-D., Ducard, G., Hamel, T., Mahony, R., and Rudin, K. (2014). Implementation of a nonlinear attitude estimator for aerial robotic vehicles. *IEEE Transactions on Control Systems Technology*, 22(1):201–213.
- Hua, M.-D., Hamel, T., Mahony, R., and Trumpf, J. (2015). Gradient-like observer design on the Special Euclidean group $\text{SE}(3)$ with system outputs on the real projective space. In *Proceedings of the 54th IEEE Annual Conference on Decision and Control (CDC)*, pp. 2139–2145.
- Hua, M.-D., Hamel, T., and Samson, C. (2017). Riccati nonlinear observer for velocity-aided attitude estimation of accelerated vehicles using coupled velocity measurements. In *Proceedings of the 56th IEEE Annual Conference on Decision and Control (CDC)*, pp. 2428–2433.
- Hua, M.-D., Manerikar, N., Hamel, T., and Samson, C. (2018). Attitude, linear velocity and depth estimation of a camera observing a planar target using continuous homography and inertial data. In *Proceedings of IEEE International Conference on Robotics and Automation (ICRA)*, pp. 1429–1435. IEEE.
- Hua, M.-D., Martin, P., and Hamel, T. (2016). Stability analysis of velocity-aided attitude observers for accelerated vehicles. *Automatica*, 63:11–15.
- Hua, M.-D., Zamani, M., Trumpf, J., Mahony, R., and Hamel, T. (2011). Observer design on the Special Euclidean group $\text{SE}(3)$. In *Proceedings of the 50th IEEE Conference on Decision and Control and European Control Conference (CDC-ECC)*, pp. 8169–8175.
- Ioannou, P. A. and Sun, J. (1995). *Robust adaptive control*. Prentice-Hall Englewood Cliffs, NJ.
- Janabi-Sharifi, F. and Marey, M. (2010). A kalman-filter-based method for pose estimation in visual servoing. *IEEE transactions on Robotics*, 26(5):939–947.

- Khosravian, A., Trumpf, J., Mahony, R., and Hamel, T. (2015a). Recursive attitude estimation in the presence of multi-rate and multi-delay vector measurements. In *2015 American Control Conference (ACC)*, pp. 3199–3205. IEEE.
- Khosravian, A., Trumpf, J., Mahony, R., and Lageman, C. (2015b). Observers for invariant systems on Lie groups with biased input measurements and homogeneous outputs. *Automatica*, 55:19–26.
- Koditschek, D. E. (1989). The application of total energy as a Lyapunov function for mechanical control systems. in *Dynamics and Control of Multibody Systems*, ser. *Contemporary Mathematics*, J. E. Marsden, P. S. Krishnaprasad, and J. C. Simo, Eds. Providence, RI: Amer. Math. Soc., 97:131.
- Kriegman, D. J., Triendl, E., and Binford, T. O. (1989). Stereo vision and navigation in buildings for mobile robots. *IEEE Transactions on Robotics and Automation*, 5(6):792–803.
- Kulikov, G. Y. and Kulikova, M. V. (2014). Accurate numerical implementation of the continuous-discrete extended Kalman filter. *IEEE Transactions on Automatic Control*, 59(1):273–279.
- Lageman, C., Trumpf, J., and Mahony, R. (2010). Gradient-like observers for invariant dynamics on a Lie group. *IEEE Transactions on Automatic Control*, 55(2):367–377.
- Le Bras, F., Hamel, T., Mahony, R., and Samson, C. (2017). Observers for position estimation using bearing and biased velocity information. In *Sensing and Control for Autonomous Vehicles*, pp. 3–23. Springer.
- Lefferts, E. J., Markley, F. L., and Shuster, M. D. (1982). Kalman filtering for spacecraft attitude estimation. *Journal of Guidance, Control, and Dynamics*, 5(5):417–429.
- Lewis, F. L., Xie, L., and Popa, D. (2007). *Optimal and robust estimation: with an introduction to stochastic control theory*. Boca Raton, FL: CRC press, 2 edition.
- Li, Y., Phillips, S., and Sanfelice, R. G. (2017). Robust distributed estimation for linear systems under intermittent information. *IEEE Transactions on Automatic Control*, 63(4):973–988.
- Ljusternik, L. and Schnirelmann, L. (1934). *Méthodes topologiques dans les problèmes variationnels*. Paris, France: Hermann.
- Mahony, R. and Hamel, T. (2017). A geometric nonlinear observer for simultaneous localisation and mapping. In *Proceedings of the 56th IEEE Annual Conference on Decision and Control (CDC)*, pp. 2408–2415.
- Mahony, R., Hamel, T., and Pflimlin, J.-M. (2008). Nonlinear complementary filters on the Special Orthogonal group. *IEEE Transactions on automatic control*, 53(5):1203–1218.

- Markley, F. L. (1988). Attitude determination using vector observations and the singular value decomposition. *The Journal of the Astronautical Sciences*, 36(3):245–258.
- Markley, F. L. (2003). Attitude error representations for kalman filtering. *Journal of guidance, control, and dynamics*, 26(2):311–317.
- Matthies, L. and Shafer, S. (1987). Error modeling in stereo navigation. *IEEE Journal on Robotics and Automation*, 3(3):239–248.
- Mayhew, C. G. and Teel, A. R. (2011a). Hybrid control of rigid-body attitude with synergistic potential functions. In *Proceedings of the American Control Conference (ACC)*, pp. 287–292.
- Mayhew, C. G. and Teel, A. R. (2011b). Synergistic potential functions for hybrid control of rigid-body attitude. In *Proceedings of American Control Conference*, pp. 875–880.
- Mayhew, C. G. and Teel, A. R. (2013). Synergistic hybrid feedback for global rigid-body attitude tracking on $\text{SO}(3)$. *IEEE Transactions on Automatic Control*, 58(11):2730–2742.
- Moeini, A. and Namvar, M. (2016). Global attitude/position estimation using landmark and biased velocity measurements. *IEEE Transactions on Aerospace and Electronic Systems*, 52(2):852–862.
- Morse, M. (1934). *The calculus of variations in the large*, volume 18. American Mathematical Soc.
- Mourikis, A. I. and Roumeliotis, S. I. (2007). A multi-state constraint Kalman filter for vision-aided inertial navigation. In *Proceedings 2007 IEEE International Conference on Robotics and Automation*, pp. 3565–3572. IEEE.
- Mourikis, A. I., Trawny, N., Roumeliotis, S. I., Johnson, A. E., Ansar, A., and Matthies, L. (2009). Vision-aided inertial navigation for spacecraft entry, descent, and landing. *IEEE Transactions on Robotics*, 25(2):264–280.
- Nikolic, J., Rehder, J., Burri, M., Gohl, P., Leutenegger, S., Furgale, P. T., and Siegwart, R. (2014). A synchronized visual-inertial sensor system with FPGA pre-processing for accurate real-time SLAM. In *Robotics and Automation (ICRA), 2014 IEEE International Conference on*, pp. 431–437. IEEE.
- Ohya, I., Kosaka, A., and Kak, A. (1998). Vision-based navigation by a mobile robot with obstacle avoidance using single-camera vision and ultrasonic sensing. *IEEE transactions on robotics and automation*, 14(6):969–978.
- Olivares, A., Olivares, G., Gorri, J., and Ramirez, J. (2009). High-efficiency low-cost accelerometer-aided gyroscope calibration. In *2009 International Conference on Test and Measurement*, volume 1, pp. 354–360. IEEE.

- Pachter, M. and Porter, A. (2004). Bearings-only measurements for INS aiding: The three-dimensional case. In *Proceedings of the 2004 American Control Conference*, volume 6, pp. 5363–5368. IEEE.
- Palais, R. S. and Terng, C.-L. (2006). *Critical point theory and submanifold geometry*, volume 1353. Springer.
- Panahandeh, G. and Jansson, M. (2014). Vision-aided inertial navigation based on ground plane feature detection. *IEEE/ASME transactions on mechatronics*, 19(4):1206–1215.
- Qin, T., Li, P., and Shen, S. (2018). Vins-mono: A robust and versatile monocular visual-inertial state estimator. *IEEE Transactions on Robotics*, 34(4):1004–1020.
- Quan, L. and Lan, Z. (1999). Linear n-point camera pose determination. *IEEE Transactions on pattern analysis and machine intelligence*, 21(8):774–780.
- Rehbinder, H. and Ghosh, B. K. (2003). Pose estimation using line-based dynamic vision and inertial sensors. *IEEE Transactions on Automatic Control*, 48(2):186–199.
- Roberts, A. and Tayebi, A. (2011). On the attitude estimation of accelerating rigid-bodies using GPS and IMU measurements. In *Proceedings of the IEEE CDC-ECC, Orlando, FL, USA, December 12-15*, pp. 8088–8093.
- Sachs, J. (2013). *Handbook of ultra-wideband short-range sensing: theory, sensors, applications*. John Wiley & Sons.
- Sanfelice, R., Copp, D., and Nanez, P. (2013). A toolbox for simulation of hybrid systems in Matlab/Simulink: Hybrid Equations (HyEQ) Toolbox. In *Proceedings of the 16th international conference on Hybrid systems: computation and control*, pp. 101–106. ACM.
- Sanfelice, R. G., Goebel, R., and Teel, A. R. (2007). Invariance principles for hybrid systems with connections to detectability and asymptotic stability. *IEEE Transactions on Automatic Control*, 52(12):2282–2297.
- Santoso, F., Garratt, M. A., and Anavatti, S. G. (2016). Visual–inertial navigation systems for aerial robotics: Sensor fusion and technology. *IEEE Transactions on Automation Science and Engineering*, 14(1):260–275.
- Scandaroli, G. G. (2013). *Visuo-inertial data fusion for pose estimation and self-calibration*. PhD thesis, Université Nice Sophia Antipolis.
- Sferlazza, A., Tarbouriech, S., and Zaccarian, L. (2019). Time-varying sampled-data observer with asynchronous measurements. *IEEE Transactions on Automatic Control*, 64(2):869–876.
- Shi, J. and Tomasi, C. (1994). Good features to track. In *Proc. of IEEE conf. on Computer Vision and Pattern Recognition*, pp. 593–600. IEEE.

- Shuster, M. D. (1993). A survey of attitude representations. *Navigation*, 8(9):439–517.
- Shuster, M. D. and Oh, S. (1981). Three-axis attitude determination from vector observations. *Journal of Guidance, Control, and Dynamics*, 4(1):70–77.
- Tayebi, A. and McGilvray, S. (2006). Attitude stabilization of a VTOL quadrotor aircraft. *IEEE Transactions on Control Systems Technology*, 14(3):562–571.
- Tayebi, A., Roberts, A., and Benallegue, A. (2013). Inertial vector measurements based velocity-free attitude stabilization. *IEEE Transactions on Automatic Control*, 58(11):2893–2898.
- Teel, A. R., Forni, F., and Zaccarian, L. (2013). Lyapunov-based sufficient conditions for exponential stability in hybrid systems. *IEEE Transactions on Automatic Control*, 58(6):1591–1596.
- Trumpf, J., Mahony, R., Hamel, T., and Lageman, C. (2012). Analysis of non-linear attitude observers for time-varying reference measurements. *IEEE Transactions on Automatic Control*, 57(11):2789–2800.
- Vasconcelos, J. F., Cunha, R., Silvestre, C., and Oliveira, P. (2010). A nonlinear position and attitude observer on $\text{SE}(3)$ using landmark measurements. *Systems & Control Letters*, 59(3):155–166.
- Wahba, G. (1965). A least squares estimate of satellite attitude. *SIAM review*, 7(3):409–409.
- Wang, J. and Wilson, W. J. (1992). 3D relative position and orientation estimation using Kalman filter for robot control. In *Proceedings 1992 IEEE International Conference on Robotics and Automation*, pp. 2638–2645. IEEE.
- Wang, M. and Tayebi, A. (2017). Globally asymptotically stable hybrid observers design on $\text{SE}(3)$. In *Proceedings of the 56th IEEE Annual Conference on Decision and Control (CDC)*, pp. 3033–3038.
- Wang, M. and Tayebi, A. (2018a). Geometric nonlinear observer design for SLAM on a matrix Lie group. In *Proceedings of the 57th IEEE conf. on decision and control (CDC)*, pp. 1488–1493.
- Wang, M. and Tayebi, A. (2018b). A globally exponentially stable nonlinear hybrid observer for 3D inertial navigation. In *Proceedings of the 57th IEEE Annual Conference on Decision and Control (CDC)*, pp. 1367–1372.
- Wang, M. and Tayebi, A. (2018c). On the design of hybrid pose and velocity-bias observers on lie group $\text{SE}(3)$. *Internal technical report*. arXiv:1805.00897v2.
- Wang, M. and Tayebi, A. (2019a). Hybrid pose and velocity-bias estimation on $\text{SE}(3)$ using inertial and landmark measurements. *IEEE Transactions on Automatic Control*, 64(8):3399–3406.

- Wang, M. and Tayebi, A. (2019b). Nonlinear observers for stereo-vision-aided inertial navigation. In *Proceedings of the 58th IEEE Annual Conference on Decision and Control (CDC)*, pp. 2516–2521.
- Wang, M. and Tayebi, A. (2019c). Nonlinear state estimation for inertial navigation systems with intermittent measurements. *Submitted to Automatica*.
- Wang, M. and Tayebi, A. (2020). Hybrid nonlinear observers for inertial navigation using landmark measurements. *IEEE Transactions on Automatic Control, accepted*. arXiv:1906.04689v1.
- Wu, T.-H., Kaufman, E., and Lee, T. (2015). Globally asymptotically stable attitude observer on $\text{SO}(3)$. In *Proceedings of the 54th IEEE Conference on Decision and Control (CDC)*, pp. 2164–2168.
- Wu, Y. and Hu, Z. (2006). PnP problem revisited. *Journal of Mathematical Imaging and Vision*, 24(1):131–141.
- Yuan, Q. and Chen, I.-M. (2013). 3-D localization of human based on an inertial capture system. *IEEE Transactions on Robotics*, 29(3):806–812.
- Zhou, Y., Law, C. L., Guan, Y. L., and Chin, F. (2010). Indoor elliptical localization based on asynchronous UWB range measurement. *IEEE Transactions on Instrumentation and Measurement*, 60(1):248–257.
- Zlotnik, D. E. and Forbes, J. R. (2018). Gradient-based observer for simultaneous localization and mapping. *IEEE Transactions on Automatic Control*, 63(12):4338–4344.
- Zwirello, L., Li, X., Zwick, T., Ascher, C., Werling, S., and Trommer, G. F. (2013). Sensor data fusion in UWB-supported inertial navigation systems for indoor navigation. In *2013 IEEE International Conference on Robotics and Automation*, pp. 3154–3159. IEEE.

Appendix A

Proofs of Chapter 2

A.1 Proof of Lemma 2.4

Let $r = (r_v^\top, r_s)^\top, b = (b_v^\top, b_s)^\top \in \mathbb{R}^4$ with $r_v, b_v \in \mathbb{R}^3$ and $r_s, b_s \in \mathbb{R}$. From the definition of wedge product defined in (2.65), one can easily verify that

$$\begin{aligned} r \wedge r &= \begin{bmatrix} r_v \times r_v \\ r_s r_v - r_s r_v \end{bmatrix} = 0 \\ b \wedge r &= \begin{bmatrix} b_v \times r_v \\ b_s r_v - r_s b_v \end{bmatrix} = - \begin{bmatrix} r_v \times b_v \\ r_s b_v - b_s r_v \end{bmatrix} = -r \wedge b \end{aligned}$$

where we made use of the fact that $r_v \times r_v = 0$ in (2.15) and $r_v \times b_v = -b_v \times r_v$ in (2.17). This implies (2.66) and (2.67). Let $R \in \text{SO}(3), p \in \mathbb{R}^3$ such that $g = \mathcal{T}_{\text{SE}(3)}(R, p)$. Then one can show that

$$\begin{aligned} &(I - g)rr^\top \\ &= \begin{bmatrix} I - R & -p \\ 0 & 0 \end{bmatrix} \begin{bmatrix} r_v r_v^\top & r_v r_s \\ r_s r_v^\top & r_s r_s \end{bmatrix} \\ &= \begin{bmatrix} (I - R)r_v r_v^\top - r_s p r_v^\top & (I - R)r_s r_v - r_s r_s p \\ 0 & 0 \end{bmatrix} \\ &= \begin{bmatrix} r_v r_v^\top - (Rr_v + r_w p)r_v^\top & r_w r_v - r_w(Rr_v + r_w p) \\ 0 & 0 \end{bmatrix} \end{aligned}$$

From the definition of $\psi_{\mathfrak{se}(3)}(\cdot)$ defined in (2.57), one deduces

$$\begin{aligned} \psi_{\mathfrak{se}(3)}((I - g)rr^\top) &= \left[\begin{array}{c} \psi_{\mathfrak{so}(3)}(r_v r_v^\top - (Rr_v + r_w p)r_v^\top) \\ \frac{1}{2}(r_w r_v - r_w(Rr_v + r_w p)) \end{array} \right] \\ &= \frac{1}{2} \begin{bmatrix} (Rr_v + r_w p) \times r_v \\ r_w r_v - r_w(Rr_v + r_w p) \end{bmatrix} \\ &= \frac{1}{2}(gr) \wedge r \end{aligned}$$

where we made use of the facts $\psi_{\mathfrak{so}(3)}(r_v r_v^\top) = 0$ and $\psi_{\mathfrak{so}(3)}((Rr_v + r_w p)r_v^\top) = \frac{1}{2}r_v \times (Rr_v + r_w p) = -\frac{1}{2}(Rr_v + r_w p) \times r_v$ in (2.31). Hence, one concludes (2.68). Using the facts:

$$gr = \begin{bmatrix} Rr_v + r_s p \\ r_s \end{bmatrix}, \quad gb = \begin{bmatrix} Rb_v + b_s p \\ b_s \end{bmatrix}$$

and from (2.65), one can show that

$$\begin{aligned} (gb) \wedge (gr) &= \begin{bmatrix} (Rb_v + b_s p) \times (Rr_v + r_s p) \\ b_s(Rr_v + r_s p) - r_s(Rb_v + b_s p) \end{bmatrix} \\ &= \begin{bmatrix} (Rb_v) \times (Rr_v) + (Rb_v) \times (r_s p) + (b_s p) \times (Rr_v) + (b_s p) \times (r_s p) \\ b_s(Rr_v + r_s p) - r_s(Rb_v + b_s p) \end{bmatrix} \\ &= \begin{bmatrix} R(b_v \times r_v) - r_s p \times (Rb_v) + b_s p \times (Rr_v) \\ b_s Rr_v - r_s Rb_v \end{bmatrix} \\ &= \begin{bmatrix} R & p \times R \\ \mathbf{0}_{3 \times 3} & R \end{bmatrix} \begin{bmatrix} b_v \times r_v \\ b_s r_v - r_s b_v \end{bmatrix}. \end{aligned} \quad (\text{A.1})$$

where we made use of the facts $(Rb_v) \times (Rr_v) = R(b_v \times r_v)$, $(Rb_v) \times (r_s p) = -r_s p \times (Rb_v)$ and $(b_s p) \times (r_s p) = 0$. Recall the definition of Ad_g^* in (2.63), one has

$$\text{Ad}_{g^{-1}}^* = \begin{bmatrix} (R^\top)^\top & -(R^\top)^\top (-R^\top p)^\times \\ \mathbf{0}_{3 \times 3} & (R^\top)^\top \end{bmatrix} = \begin{bmatrix} R & p \times R \\ \mathbf{0}_{3 \times 3} & R \end{bmatrix}. \quad (\text{A.2})$$

where we made use of the facts $g^{-1} = \mathcal{T}_{\mathsf{SE}(3)}(R^\top, -R^\top p)$ and $R(R^\top p)^\times = p^\times R$ in (2.25). In view of (A.1) and (A.2), one concludes (2.69). This completes the proof.

A.2 Proof of Lemma 2.5

Let $A = \begin{bmatrix} A_1 & a_2 \\ a_3 & a_4 \end{bmatrix}$ with $A_1 \in \mathbb{R}^{3 \times 3}$, $a_2, a_3^\top \in \mathbb{R}^3$ and $a_4 \in \mathbb{R}$, and $g = \mathcal{T}_{\mathsf{SE}(3)}(R, p)$ with $R \in \text{SO}(3)$, $p \in \mathbb{R}^3$. The first two properties can be verified straighted as

$$\begin{aligned} MA &= \begin{bmatrix} M_1 & m_2 \\ \mathbf{0}_{1 \times 3} & 0 \end{bmatrix} \begin{bmatrix} A_1 & a_2 \\ a_3 & a_4 \end{bmatrix} = \begin{bmatrix} M_1 A_1 + m_2 a_3 & M_1 a_2 + m_2 a_4 \\ \mathbf{0}_{1 \times 3} & 0 \end{bmatrix} \in \mathcal{M}_0^4, \\ gM &= \begin{bmatrix} R & p \\ \mathbf{0}_{1 \times 3} & 1 \end{bmatrix} \begin{bmatrix} M_1 & m_2 \\ \mathbf{0}_{1 \times 3} & 0 \end{bmatrix} = \begin{bmatrix} RM_1 & Rm_2 \\ \mathbf{0}_{1 \times 3} & 0 \end{bmatrix} \in \mathcal{M}_0^4. \end{aligned} \quad (\text{A.3})$$

Recall that $g^{-1} = \mathcal{T}_{\mathsf{SE}(3)}(R^\top, -R^\top p)$ and $g^{-\top} = (g^{-1})^\top$, then one has

$$g^{-\top} M = \begin{bmatrix} R & 0 \\ -p^\top R & 1 \end{bmatrix} \begin{bmatrix} M_1 & m_2 \\ \mathbf{0}_{1 \times 3} & 0 \end{bmatrix} = \begin{bmatrix} RM_1 & Rm_2 \\ -p^\top R M_1 & -p^\top R m_2 \end{bmatrix}$$

Using the definition of $\mathbb{P}_{\mathfrak{se}(3)}(\cdot)$ in (2.56), one obtains

$$\mathbb{P}_{\mathfrak{se}(3)}(gM) = \begin{bmatrix} \mathbb{P}_{\mathfrak{so}(3)}(RM_1) & Rm_2 \\ \mathbf{0}_{1 \times 3} & 0 \end{bmatrix} = \mathbb{P}_{\mathfrak{se}(3)}(g^{-\top} M).$$

This gives (2.72). Using the facts

$$\begin{aligned} g^\top g &= \begin{bmatrix} R^\top & \mathbf{0}_{3 \times 1} \\ p^\top & 1 \end{bmatrix} \begin{bmatrix} R & p \\ \mathbf{0}_{1 \times 3} & 1 \end{bmatrix} = \begin{bmatrix} I_3 & R^\top p \\ p^\top R & 1 + p^\top p \end{bmatrix} \\ M\bar{M}^\top &= \begin{bmatrix} M_1 & m_2 \\ \mathbf{0}_{1 \times 3} & 0 \end{bmatrix} \begin{bmatrix} \bar{M}_1^\top & \mathbf{0}_{3 \times 1} \\ \bar{m}_2^\top & 0 \end{bmatrix} = \begin{bmatrix} M_1\bar{M}_1^\top + m_2\bar{m}_2^\top & \mathbf{0}_{3 \times 1} \\ \mathbf{0}_{1 \times 3} & 0 \end{bmatrix}, \end{aligned}$$

one can show that

$$\begin{aligned} \text{tr}(g^\top g M \bar{M}^\top) &= \text{tr} \left(\begin{bmatrix} I_3 & R^\top p \\ p^\top R & 1 + p^\top p \end{bmatrix} \begin{bmatrix} M_1\bar{M}_1^\top + m_2\bar{m}_2^\top & \mathbf{0}_{3 \times 1} \\ \mathbf{0}_{1 \times 3} & 0 \end{bmatrix} \right) \\ &= \text{tr}(M_1\bar{M}_1^\top + m_2\bar{m}_2^\top) = \text{tr}(M\bar{M}^\top). \end{aligned}$$

This implies (2.73). Applying the fact that

$$g^\top g M = \begin{bmatrix} I_3 & R^\top p \\ p^\top R & 1 + p^\top p \end{bmatrix} \begin{bmatrix} M_1 & m_2 \\ \mathbf{0}_{1 \times 3} & 0 \end{bmatrix} = \begin{bmatrix} M_1 & m_2 \\ p^\top R M_1 & p^\top R m_2 \end{bmatrix},$$

and the definition of $\psi_{\mathfrak{se}(3)}(\cdot)$ in (2.57), one can easily show that

$$\psi_{\mathfrak{se}(3)}(g^\top g M) = \psi_{\mathfrak{se}(3)} \left(\begin{bmatrix} M_1 & m_2 \\ p^\top R M_1 & p^\top R m_2 \end{bmatrix} \right) = \begin{bmatrix} \psi_{\mathfrak{so}(3)}(M_1) \\ \frac{1}{2}m_2 \end{bmatrix} = \psi_{\mathfrak{se}(3)}(g^\top g M).$$

This implies (2.74). Moreover, substituting

$$\begin{aligned} g^\top M g^{-\top} &= \begin{bmatrix} R^\top & \mathbf{0}_{3 \times 1} \\ p^\top & 1 \end{bmatrix} \begin{bmatrix} M_1 & m_2 \\ \mathbf{0}_{1 \times 3} & 0 \end{bmatrix} \begin{bmatrix} R & 0 \\ -p^\top R & 1 \end{bmatrix} \\ &= \begin{bmatrix} R^\top M_1 & R^\top m_2 \\ p^\top M_1 & p^\top m_2 \end{bmatrix} \begin{bmatrix} R & 0 \\ -p^\top R & 1 \end{bmatrix} \\ &= \begin{bmatrix} R^\top M_1 R - R^\top m_2 p^\top R & R^\top m_2 \\ * & * \end{bmatrix}, \end{aligned}$$

into the definition of $\psi_{\mathfrak{se}(3)}(\cdot)$ in (2.57), one has

$$\begin{aligned} \psi_{\mathfrak{se}(3)}(g^\top M g^{-\top}) &= \begin{bmatrix} \psi_{\mathfrak{so}(3)}(R^\top M_1 R - R^\top m_2 p^\top R) \\ \frac{1}{2}R^\top m_2 \end{bmatrix} \\ &= \begin{bmatrix} R^\top \psi_{\mathfrak{so}(3)}(M_1) - \frac{1}{2}R^\top p^\times m_2 \\ \frac{1}{2}R^\top m_2 \end{bmatrix} \\ &= \begin{bmatrix} R^\top & -R^\top p^\times \\ \mathbf{0}_{3 \times 3} & R^\top \end{bmatrix} \begin{bmatrix} \psi_{\mathfrak{so}(3)}(M_1) \\ \frac{1}{2}m_2 \end{bmatrix} \end{aligned}$$

where made use of the facts $\psi_{\mathfrak{so}(3)}(R^\top M_1 R) = R^\top \psi_{\mathfrak{so}(3)}(M_1)$ from (2.29) and $\psi_{\mathfrak{so}(3)}(R^\top m_2 p^\top R) = \frac{1}{2}(R^\top p) \times (R^\top m_2) = \frac{1}{2}R^\top(p \times m_2) = \frac{1}{2}R^\top p^\times m_2$ from (2.24) and (2.31). Applying that the results of Ad_g^* and $\psi_{\mathfrak{se}(3)}(M)$, one concludes (2.75). This completes the proof.

A.3 Proof of Lemma 2.6

From the definitions of x_i^L and x_i^R defined in (2.96), one has the following identities:

$$\begin{aligned} x_i^L \times x_i^R &= \frac{p_i^{C_L} \times (p_i^{C_L} + b_{LR})}{\|p_i^{C_L}\| \|p_i^{C_L} + b_{LR}\|} = \frac{p_i^{C_L} \times b_{LR}}{\|p_i^{C_L}\| \|p_i^{C_L} + b_{LR}\|} \\ b_{LR} \times x_i^L &= \frac{b_{LR} \times p_i^{C_L}}{\|p_i^{C_L}\|} \\ b_{LR} \times x_i^R &= \frac{b_{LR} \times (p_i^{C_L} + b_{LR})}{\|p_i^{C_L} + b_{LR}\|} = \frac{b_{LR} \times p_i^{C_L}}{\|p_i^{C_L} + b_{LR}\|} \end{aligned}$$

Hence, one can show that

$$\|p_i^{C_L}\| = \frac{\|b_{LR} \times x_i^R\|}{\|x_i^L \times x_i^R\|}, \quad \|p_i^{C_L} + b_{LR}\| = \frac{\|b_{LR} \times x_i^L\|}{\|x_i^L \times x_i^R\|}$$

Since $p_i^{C_L} = \|p_i^{C_L}\| x_i^L$ and $p_i^{C_L} + b_{LR} = p_i^{C_R} = \|p_i^{C_L} + b_{LR}\| x_i^R$, one deduces that $p_i^{C_L} = \frac{\|b_{LR} \times x_i^R\|}{\|x_i^L \times x_i^R\|} x_i^L$ and $p_i^{C_L} = \frac{\|b_{LR} \times x_i^L\|}{\|x_i^L \times x_i^R\|} x_i^R - b_{LR}$ and thus also

$$p_i^{C_L} = \frac{x_i^L \|b_{LR} \times x_i^R\| + x_i^R \|b_{LR} \times x_i^L\|}{2 \|x_i^L \times x_i^R\|} - \frac{1}{2} b_{LR} \quad (\text{A.4})$$

Applying the fact $p_i^{C_L} := R_{cL}^\top (p_i^B - p_L)$, i.e., $p_i^B = R_{cL} p_i^{C_L} + p_L$, one has (2.98). This completes the proof.

A.4 Proof of Lemma 2.7

Since $\bar{\Phi}(t, \tau)$ is the state transition matrix associated to \bar{A} , one can easily verify that

$$\begin{aligned} \Phi(t, t) &= T(t) \bar{\Phi}(t, t) T^{-1}(t) = T(t) T^{-1}(t) = I_n \\ \Phi^{-1}(t, \tau) &= T(\tau) \bar{\Phi}^{-1}(t, \tau) T^{-1}(t) = T(\tau) \bar{\Phi}(\tau, t) T^{-1}(t) = \Phi(\tau, t) \\ \Phi(t_3, t_2) \Phi(t_2, t_1) &= T(t_3) \bar{\Phi}(t_3, t_2) T^{-1}(t_2) T(t_2) \bar{\Phi}(t_2, t_1) T^{-1}(t_1) \\ &= T(t_3) \bar{\Phi}(t_3, t_2) \bar{\Phi}(t_2, t_1) T^{-1}(t_1) \\ &= T(t_3) \bar{\Phi}(t_3, t_1) T^{-1}(t_1) \\ &= \Phi(t_3, t_1) \end{aligned}$$

Applying the facts $\dot{T}(t) = S(t)T(t)$ and $T(t)\bar{A} = \bar{A}T(t)$, one can further show that

$$\begin{aligned} \frac{d}{dt} \Phi(t, \tau) &= \dot{T}(t) \bar{\Phi}(t, \tau) T^{-1}(\tau) + T(t) \frac{d}{dt} \bar{\Phi}(t, \tau) T^{-1}(\tau) \\ &= S(t) T(t) \bar{\Phi}(t, \tau) T^{-1}(\tau) + T(t) \bar{A} \bar{\Phi}(t, \tau) T^{-1}(\tau) \\ &= S(t) T(t) \bar{\Phi}(t, \tau) T^{-1}(\tau) + \bar{A} T(t) \bar{\Phi}(t, \tau) T^{-1}(\tau) \\ &= A(t) T(t) \bar{\Phi}(t, \tau) T^{-1}(\tau) \\ &= A(t) \Phi(t, \tau) \end{aligned}$$

Therefore, one can conclude that $\Phi(t, \tau)$ is the state transition matrix associated to $A(t)$. This completes the proof.

A.5 Proof of Lemma 2.11

The proof of this lemma is motivated by [Hamel and Samson, 2017, Lemma 2.5]. To prove that $P(t)$ is well-defined for all $t \geq 0$ and positive definite, it is sufficient to show that neither the eigenvalues of P nor the eigenvalues of P^{-1} , can tend to infinity in finite time with positive definite initial condition (*i.e.*, $P(0) > 0$). This implies that none of the eigenvalues of P can either reach zero or tend to infinity in finite time. Let $(\lambda(t), v(t))$ be one pair of the eigenvalues and eigenvectors of $P(t)$ such that $Pv = \lambda v$ and $v \in \mathbb{S}^{n-1}$. Taking the time-derivative on both sides of $Pv = \lambda v$, one has

$$\dot{P}v + P\dot{v} = \dot{\lambda}v + \lambda\dot{v}$$

Since $\|v\| = 1$, one verifies that $v^\top \dot{v} = 0$. Then, one has

$$\dot{\lambda} = v^\top \dot{P}v + v^\top P\dot{v} = v^\top \dot{P}v + \lambda v^\top \dot{v} = v^\top \dot{P}v$$

where we made use of the fact that $v^\top P = \lambda v^\top$. From (2.119)-(2.120), one has the dynamics of λ as

$$\dot{\lambda} = \lambda v^\top Av + \lambda v^\top A^\top v + v^\top Vv, \quad (\text{A.5})$$

$$\lambda^+ = \lambda - \lambda^2 v^\top C^\top (CPC^\top + Q^{-1})^{-1} Cv, \quad (\text{A.6})$$

Let a be the upper bounded of $\|A\|$ and v be the upper bound of $\|V\|$. Using the fact $C^\top (CPC^\top + Q^{-1})^{-1} C \geq 0$, one has

$$\begin{aligned} \dot{\lambda} &\leq 2a\lambda + v \\ \lambda^+ &\leq \lambda \end{aligned}$$

Recall the definition of the solution to a hybrid system, one has the solution of λ as $\lambda(t, j)$ with $t \in [t_j, t_{j+1}]$. Then, one can show that

$$\lambda(t, j) \leq \left(\lambda(0, 0) + \frac{v}{2a} \right) e^{2at} - \frac{v}{2a} \quad (\text{A.7})$$

for all $j \in \mathbb{N}$ and $t \in [t_j, t_{j+1}]$.

On the other hand, let $(\bar{\lambda}(t), v(t))$ be one pair of the eigenvalues and eigenvectors of $P^{-1}(t)$ such that $P^{-1}v = \bar{\lambda}v$ and $v \in \mathbb{S}^{n-1}$. One can show that $\dot{\bar{\lambda}} = v^\top \dot{P}^{-1}v$. From (2.119)-(2.120), one has the following dynamics:

$$\dot{P}^{-1} = -P^{-1}A - A^\top P^{-1} - P^{-1}VP^{-1} \quad (\text{A.8})$$

$$(P^+)^{-1} = P^{-1} + C^\top QC, \quad (\text{A.9})$$

where we made use of the fact $\dot{P}^{-1} = -P^{-1}\dot{P}P^{-1}$ and

$$(P + PC^\top RCP)^{-1} = P^{-1} - C^\top (R^{-1} + CPC^\top)^{-1}C = P^{-1} + C^\top QC,$$

with $R = -(CPC^\top + Q^{-1})^{-1}$ from the property of matrix inversion (2.7). Then, the dynamics of $\bar{\lambda}$ is given by

$$\dot{\bar{\lambda}} = -\bar{\lambda}v^\top Av - \bar{\lambda}v^\top A^\top v - \bar{\lambda}^2 v^\top Vv, \quad (\text{A.10})$$

$$\bar{\lambda}^+ = \bar{\lambda} + v^\top C^\top Q C v, \quad (\text{A.11})$$

Let q be the upper bound of $\|C^\top Q C\|$. Then, one obtains

$$\begin{aligned}\dot{\bar{\lambda}} &\leq 2a\bar{\lambda}, \\ \bar{\lambda}^+ &= \bar{\lambda} + q\end{aligned}$$

Then, one can show that

$$\bar{\lambda}(t, j) \leq \bar{\lambda}(0, 0)e^{2at} + \sum_{i=0}^j q e^{2a(t-t_i)} \quad (\text{A.12})$$

for all $j \in \mathbb{N}$ and $t \in [t_j, t_{j+1})$. Hence, from (A.7) and (A.12), it is clear that $\lambda, \bar{\lambda}$ can not grow to infinity in finite time for any $P(0)$ being positive definite. It follows that the solution of P is well defined on $\mathbb{R}_{\geq 0}$. This completes the proof.

Appendix B

Proofs of Chapter 3

B.1 Proof of Lemma 3.1

From the definition of \mathbb{A} , one can show that

$$\mathbb{A} = \sum_{i=1}^n k_i r_i r_i^\top = \begin{bmatrix} \sum_{i=1}^{n_1} k_i p_i^\mathcal{I} (p_i^\mathcal{I})^\top + \sum_{j=1}^{n_2} k_{j+n_1} v_j^\mathcal{I} (v_j^\mathcal{I})^\top & \sum_{i=1}^{n_1} k_i p_i^\mathcal{I} \\ \sum_{i=1}^{n_1} k_i (p_i^\mathcal{I})^\top & \sum_{i=1}^{n_1} k_i \end{bmatrix},$$

which implies:

$$\begin{aligned} A &:= \sum_{i=1}^{n_1} k_i p_i^\mathcal{I} (p_i^\mathcal{I})^\top + \sum_{j=1}^{n_2} k_{j+n_1} v_j^\mathcal{I} (v_j^\mathcal{I})^\top \\ b &:= \sum_{i=1}^{n_1} k_i p_i^\mathcal{I} \quad d := \sum_{i=1}^{n_1} k_i. \end{aligned}$$

From Assumption 3.1, there exists at least one $k_i > 0$ for all $i = 1, 2, \dots, n_1$. Hence, one has $d > 0$. Let $\alpha_i = k_i / (\sum_{i=1}^{n_1} k_i)$, it is easy to verify that $p_c^\mathcal{I} = \sum_{i=1}^{n_1} \alpha_i p_i^\mathcal{I} = bd^{-1}$. In view of (3.8) and (3.9), one has

$$\begin{aligned} M &= A - bb^\top d^{-1} \\ &= \sum_{i=1}^{n_1} k_i p_i^\mathcal{I} (p_i^\mathcal{I})^\top + \sum_{i=1}^{n_2} k_{j+n_1} v_i^\mathcal{I} (v_i^\mathcal{I})^\top - \left(\sum_{i=1}^{n_1} k_i p_i^\mathcal{I} \right) \left(\sum_{i=1}^{n_1} k_i p_i^\mathcal{I} \right)^\top \left(\sum_{i=1}^{n_1} k_i \right)^{-1} \\ &= \sum_{i=1}^{n_1} k_i p_i^\mathcal{I} (p_i^\mathcal{I})^\top - \sum_{i=1}^{n_1} k_i p_c^\mathcal{I} (p_c^\mathcal{I})^\top + \sum_{i=1}^{n_2} k_{j+n_1} v_i^\mathcal{I} (v_i^\mathcal{I})^\top. \end{aligned}$$

Substituting $p_i^\mathcal{I} = \bar{v}_i^\mathcal{I} + p_c^\mathcal{I}$ from (3.8) and $\sum_{i=1}^{n_1} k_i \bar{v}_i^\mathcal{I} = 0$, one obtains

$$\begin{aligned} M &= \sum_{i=1}^{n_1} k_i (\bar{v}_i^\mathcal{I} + p_c^\mathcal{I}) (\bar{v}_i^\mathcal{I} + p_c^\mathcal{I})^\top - \sum_{i=1}^{n_1} k_i p_c^\mathcal{I} (p_c^\mathcal{I})^\top + \sum_{i=1}^{n_2} k_{j+n_1} v_i^\mathcal{I} (v_i^\mathcal{I})^\top \\ &= \sum_{i=1}^{n_1} k_i (\bar{v}_i^\mathcal{I}) (\bar{v}_i^\mathcal{I})^\top + \sum_{i=1}^{n_2} k_{j+n_1} v_i^\mathcal{I} (v_i^\mathcal{I})^\top. \end{aligned}$$

It is straightforward to verify that M is positive semi-definite. Then, one can further show that

$$\bar{M} = \frac{1}{2} \sum_{i=1}^{n_1} k_i ((\bar{v}_i^{\mathcal{I}})^{\times})^2 + \frac{1}{2} \sum_{j=1}^{n_2} k_{j+n_1} ((v_j^{\mathcal{I}})^{\times})^2. \quad (\text{B.1})$$

From lemma 2 in [Tayebi et al., 2013], one can conclude that \bar{M} is positive definite. This completes the proof.

B.2 Proof of Lemma 3.2

From the definition of \mathbb{A} in (3.9) as per Lemma 3.1, one obtains

$$\begin{aligned} \sum_{i=1}^n k_i \|r_i - g^{-1}r_i\|^2 &= \text{tr}((I_4 - g^{-1})\mathbb{A}(I_4 - g^{-1})^{\top}) \\ &= \text{tr}(g^{\top}g(I_4 - g^{-1})\mathbb{A}(I_4 - g^{-1})^{\top}) \\ &= \text{tr}((I_4 - g)\mathbb{A}(I_4 - g)^{\top}), \end{aligned}$$

where property (2.73) and the facts $(I_4 - g^{-1}) \in \mathcal{M}_0^4$ and $(I_4 - g^{-1})\mathbb{A} \in \mathcal{M}_0^4$ have been used. Furthermore, using the fact $(\bar{g}^{-1}g^{-1}r_i) \wedge (\bar{g}^{-1}r_i) = \text{Ad}_{\bar{g}^{-1}}^*((g^{-1}r_i) \wedge r_i)$, one verifies that

$$\begin{aligned} \psi_{\mathfrak{se}(3)}(\mathbb{P}_{\mathfrak{se}(3)}((I_4 - g^{-1})\mathbb{A})) &= \sum_{i=1}^n k_i \psi_{\mathfrak{se}(3)}((I_4 - g^{-1})r_i r_i^{\top}) = \frac{1}{2} \sum_{i=1}^n k_i (g^{-1}r_i) \wedge r_i \\ \text{Ad}_{g_1}^* \sum_{i=1}^n k_i (\bar{g}g^{-1}r_i) \wedge r_i &= \sum_{i=1}^n k_i (g^{-1}r_i) \wedge (\bar{g}^{-1}r_i). \end{aligned}$$

This completes the proof.

B.3 Proof of Lemma 3.3

Let (λ_v^M, v) denote the pair of eigenvalue and eigenvector of the matrix M , i.e., $Mv = \lambda_v^M v$. Then, one has

$$\Delta_M(u_q, v) = \text{tr}(M) - u_q^{\top} M u_q - 2\lambda_v^M (1 - (u_q^{\top} v)^2). \quad (\text{B.2})$$

- 1) For the sake of analysis, let $\mathbb{E}(M) = \{v_1, v_2, v_3\}$ with v_1, v_2, v_3 are three orthogonal eigenvector of M . Using the fact $\mathbb{E}(M) \subseteq \mathbb{U}$, for any $v \in \mathcal{E}(M)$ one has

$$\max_{u_q \in \mathbb{U}} \Delta_M(u_q, v) \geq \max_{u_q \in \mathbb{E}(M)} \Delta_M(u_q, v).$$

- a) For the case $M = \lambda_1^M I_3$, for any $v \in \mathcal{E}(M)$ and $u_q \in \mathbb{E}(M)$, from (B.2) one has

$$\Delta_M(u_q, v) = \text{tr}(M) - u_q^{\top} M u_q - 2\lambda_1^M (1 - (u_q^{\top} v)^2)$$

$$= 2\lambda_1^M(u_q^\top v)^2, \quad q = 1, 2, 3.$$

Using the fact $\sum_{q=1}^3 (u_q^\top v)^2 = 1$ for any $v \in \mathbb{S}^2$, one has $\max_{u_q \in \mathbb{U}} (u_q^\top v)^2 \geq \frac{1}{3}$ which implies $\max_{u_q \in \mathbb{U}} u_q^\top W_v u_q \geq \frac{2}{3}\lambda_1^M$. Then, for any $v \in \mathcal{E}(M)$, one can show that

$$\Delta_M^* = \min_{v \in \mathcal{E}(M)} \max_{u_q \in \mathbb{U}} \Delta(u_q, v) \geq \frac{2}{3}\lambda_1^M. \quad (\text{B.3})$$

b) For the case $\lambda_1^M = \lambda_2^M \neq \lambda_3^M > 0$, without loss of generality let $\mathcal{E}(M) = \{v_3\} \cup \mathcal{S}_{12}$ with $\mathcal{S}_{12} := \text{span}\{v_1, v_2\} \cap \mathbb{S}^2$. Then, if $v = v_3$, from (B.2) one has

$$\begin{aligned} \Delta(u_q, v) &= \text{tr}(M) - u_q^\top M u_q - 2\lambda_3^M(1 - (u_q^\top v_3)^2) \\ &= \begin{cases} \text{tr}(M) - \lambda_1^M - 2\lambda_3^M, & u_q \in \{v_1, v_2\} \\ \text{tr}(M) - \lambda_3^M, & u_q = v_3 \end{cases}. \end{aligned}$$

Consequently, one has

$$\max_{u_q \in \mathbb{U}} \Delta(u_q, v) = 2\lambda_{12}^M, \quad v = v_3. \quad (\text{B.4})$$

If $v \in \mathcal{S}_{12}$, one has

$$\begin{aligned} \Delta(u_q, v) &= \text{tr}(M) - u_q^\top M u_q - 2\lambda_1^M(1 - (u_q^\top v)^2) \\ &= \begin{cases} \lambda_3^M - \lambda_1^M + 2\lambda_1^M(u_q^\top v)^2 & u_q \in \{v_1, v_2\} \\ 0, & u_q = v_3 \end{cases}. \end{aligned}$$

Using the fact that u_1 and u_2 are orthogonal, one has $\sum_{q=1}^2 (u_q^\top v)^2 = 1$ for any $v \in \mathcal{S}_{12}$. Then, one has

$$\max_{u_q \in \mathbb{U}} \Delta(u_q, v) \geq \lambda_3^Q, \quad v \in \mathcal{S}_{12}. \quad (\text{B.5})$$

Hence, in view of (B.4) and (B.5), one obtains

$$\min_{v \in \mathcal{E}(M)} \max_{u_q \in \mathbb{U}} \Delta(u_q, v) \geq \min \{2\lambda_{12}^M, \lambda_3^Q\}. \quad (\text{B.6})$$

c) If M has three distinct eigenvalues $\lambda_i^M \neq \lambda_j^M, i \neq j = 1, 2, 3$, then, for each $v_s \in \mathcal{E}(M)$, one has

$$\begin{aligned} \Delta(u_q, v_s) &= \text{tr}(M) - u_q^\top M u_q - 2v_s^\top M v_s(1 - (u_q^\top v_s)^2) \\ &= \begin{cases} \text{tr}(M) - u_q^\top M u_q - 2v_s^\top M v_s & q \neq s \\ \text{tr}(M) - u_s^\top M u_s & q = s \end{cases}. \end{aligned}$$

Since $\text{tr}(M) - u_q^\top M u_q \geq \text{tr}(M) - u_q^\top M u_q - 2v_s^\top M v_s$, one obtains

$$\max_{u_q \in \mathbb{U}} \Delta(u_q, v_s) = \text{tr}(M) - \lambda_s^M, \quad \forall v_s \in \mathcal{E}(M).$$

Hence, one has

$$\min_{v \in \mathcal{E}(M)} \max_{u \in \mathbb{U}} \Delta(u_q, v) = \text{tr}(M) - \lambda_{\max}^M. \quad (\text{B.7})$$

From (B.3), (B.6) and (B.7), one concludes (3.15).

- 2) If $\text{tr}(M) - 2\lambda_{\max}^M > 0$, let u_1, u_2, u_3 be any orthonormal basis in \mathbb{R}^3 and $\{u_1, u_2, u_3\} \subseteq \mathbb{U}$. Then, for any $v \in \mathcal{E}(M)$, $u_q \in \mathbb{U}$, one has

$$\Delta(u_q, v) = \text{tr}(M) - u_q^\top M u_q - 2\lambda_v^M (1 - (u_q^\top v)^2).$$

Using the facts $\sum_{q=1}^3 (u_q^\top v)^2 = 1$ for any $v \in \mathbb{S}^2$ and $\sum_{q=1}^3 u_q^\top M u_q = \text{tr}(M)$, one has

$$\begin{aligned} \frac{1}{3} \sum_{q=1}^3 \Delta(u_q, v) &= \frac{1}{3} \left(3\text{tr}(M) - \sum_{q=1}^3 u_q^\top M u_q - 2\lambda_v^M \left(3 - \sum_{q=1}^3 (u_q^\top v)^2 \right) \right) \\ &= \frac{1}{3} (2\text{tr}(M) - 4\lambda_v^M), \end{aligned}$$

which implies that $\max_{u_q \in \mathbb{U}} \Delta(u_q, v) \geq \frac{2}{3} (\text{tr}(M) - 2\lambda_v^M)$. Then, for any $v \in \mathcal{E}(M)$, one can show that

$$\min_{v \in \mathcal{E}(M)} \max_{u_q \in \mathbb{U}} \Delta(u_q, v) \geq \frac{2}{3} (\text{tr}(M) - 2\lambda_{\max}^M).$$

which gives (3.16).

This completes the proof.

B.4 Proof of Proposition 3.1

. In view of (2.53), one can show that

$$\begin{aligned} \dot{\mathcal{U}}(\tilde{g}) &= \left\langle \nabla_{\tilde{g}} \mathcal{U}, \tilde{g}(\text{Ad}_{\hat{g}}(\tilde{b}_\xi - k_\beta \beta))^\wedge \right\rangle_{\tilde{g}} \\ &= \langle \langle \tilde{g}^{-1} \nabla_{\tilde{g}} \mathcal{U}, (\text{Ad}_{\hat{g}}(\tilde{b}_\xi - k_\beta \beta))^\wedge \rangle \rangle. \end{aligned} \quad (\text{B.8})$$

Let us consider the following real-valued function on $\text{SE}(3) \times \mathbb{R}^6$,

$$V(\tilde{g}, \tilde{b}_\xi) = \mathcal{U}(\tilde{g}) + \tilde{b}_\xi \Gamma^{-1} \tilde{b}_\xi \quad (\text{B.9})$$

From the definition of the potential function, one can verify that V is positive definite with respect to the equilibrium point $(I_4, 0)$. Taking the time derivative of V , along the trajectories of (3.21)-(3.22), one has

$$\begin{aligned} \dot{V} &= \langle \langle \tilde{g}^{-1} \nabla_{\tilde{g}} \mathcal{U}, (\text{Ad}_{\hat{g}}(\tilde{b}_\xi - k_\beta \beta))^\wedge \rangle \rangle - 2\tilde{b}_\xi^\top \sigma_b \\ &= -k_\beta \langle \langle \tilde{g}^{-1} \nabla_{\tilde{g}} \mathcal{U}, (\psi_{\mathfrak{se}(3)}(\tilde{g}^{-1} \nabla_{\tilde{g}} \mathcal{U}))^\wedge \rangle \rangle + \langle \langle \tilde{g}^{-1} \nabla_{\tilde{g}} \mathcal{U}, \text{Ad}_{\hat{g}}(\tilde{b}_\xi^\wedge) \rangle \rangle - 2\tilde{b}_\xi^\top \sigma_b \end{aligned}$$

$$\begin{aligned}
&\leq -k_\beta \langle \langle \tilde{g}^{-1} \nabla_{\tilde{g}} \mathcal{U}, (\psi_{\mathfrak{se}(3)}(\tilde{g}^{-1} \nabla_{\tilde{g}} \mathcal{U}))^\wedge \rangle \rangle + \langle \langle \text{Ad}_{\hat{g}}^*(\tilde{g}^{-1} \nabla_{\tilde{g}} \mathcal{U}), \tilde{b}_\xi^\wedge \rangle \rangle - 2\tilde{b}_\xi^\top \sigma_b \\
&= -2k_\beta \|\psi_{\mathfrak{se}(3)}(\tilde{g}^{-1} \nabla_{\tilde{g}} \mathcal{U})\|^2 + 2\tilde{b}_\xi^\top \text{Ad}_{\hat{g}}^* \psi_{\mathfrak{se}(3)}(\tilde{g}^{-1} \nabla_{\tilde{g}} \mathcal{U}) - 2\tilde{b}_\xi^\top \sigma_b \\
&= -2k_\beta \|\psi_{\mathfrak{se}(3)}(\tilde{g}^{-1} \nabla_{\tilde{g}} \mathcal{U})\|^2,
\end{aligned} \tag{B.10}$$

where we made use of the fact $\text{Ad}_{\hat{g}} \text{Ad}_{\hat{g}^{-1}} = I_6$, (2.61), (2.62), (2.58), and the definitions of β, σ_b . Thus, V is non-increasing for all $t \geq 0$ and the estimation errors $(\tilde{g}, \tilde{b}_\xi)$ are bounded. There exist a constant $\mu > 0$ and a set $\mathcal{D}_\mu := \{(\tilde{g}, \tilde{b}_\xi) \in \text{SE}(3) \times \mathbb{R}^6 \mid V(\tilde{g}, \tilde{b}_\xi) < \mu\}$, such that $(\tilde{g}(t), \tilde{b}_\xi(t)) \in \mathcal{D}_\mu, \forall t \geq 0$ if $(\tilde{g}(0), \tilde{b}_\xi(0)) \in \mathcal{D}_\mu$. Applying LaSalle's invariance theorem, one concludes that that $(\tilde{g}, \tilde{b}_\xi)$ must converge to the largest invariant subset of $\mathcal{W} \cap \mathcal{D}_\mu$

$$\mathcal{W} = \{(\tilde{g}, \tilde{b}_\xi) \in \text{SE}(3) \times \mathbb{R}^6 \mid \tilde{g} \in C_{\text{SE}(3)} \mathcal{U}, \tilde{b}_\xi \in \mathbb{R}^6\}.$$

One can easily verify that $(I_4, 0) \in \mathcal{W} \cap \mathcal{D}_\mu$. Choose μ small enough such that $\mathcal{W} \cap \mathcal{D}_\mu = \{(\tilde{g}, \tilde{b}_\xi) \in \text{SE}(3) \times \mathbb{R}^6 \mid \tilde{g} = I_4, \tilde{b}_\xi \Gamma^{-1} \tilde{b}_\xi < \mu\}$. Hence the solution of \tilde{g} must converge to I_4 . For $\tilde{g} \equiv I_4$, it follows that $\dot{\tilde{g}} \equiv 0$ and $\beta \equiv 0$. Using the facts $\dot{\tilde{g}} \equiv 0$ and $\beta \equiv 0$, one can conclude from (3.21) that $\tilde{b}_\xi \equiv 0$. Therefore, the solutions of $(\tilde{g}, \tilde{b}_\xi)$ must converge to the equilibrium $(I_4, 0)$. Finally, the equilibrium $(I_4, 0)$ is locally asymptotically stable. This completes the proof.

B.5 Proof of Theorem 3.1

Let us consider the following real-valued function on \mathcal{S} ,

$$V(x) = \mathcal{U}(\tilde{g}) + \tilde{b}_\xi^\top \Gamma^{-1} \tilde{b}_\xi. \tag{B.11}$$

Similar to (B.10), the time derivative of V , along the flows of trajectories of (3.30), is given by

$$\begin{aligned}
\dot{V} &= \left\langle \nabla_{\tilde{g}} \mathcal{U}, \tilde{g} (\text{Ad}_{\hat{g}}(\tilde{b}_\xi - k_\beta \beta))^\wedge \right\rangle_{\tilde{g}} - 2\tilde{b}_\xi^\top \sigma_b \\
&= \langle \langle \tilde{g}^{-1} \nabla_{\tilde{g}} \mathcal{U}, (\text{Ad}_{\hat{g}}(\tilde{b}_\xi - k_\beta \beta))^\wedge \rangle \rangle - 2\tilde{b}_\xi^\top \sigma_b \\
&= -2k_\beta \|\psi_{\mathfrak{se}(3)}(\tilde{g}^{-1} \nabla_{\tilde{g}} \mathcal{U})\|^2,
\end{aligned} \tag{B.12}$$

Then, for any $x \in \mathcal{F}_c$, V is non-increasing along the flows of (3.30). For any $x \in \mathcal{J}_c$, one can show that

$$\begin{aligned}
V(x^+) - V(x) &= \mathcal{U}(\tilde{g}^+) - \mathcal{U}(\tilde{g}) \\
&\leq \min_{g_q \in \mathbb{Q}} \mathcal{U}(\tilde{g} g_q) - \mathcal{U}(\tilde{g}) \leq -\delta,
\end{aligned} \tag{B.13}$$

which implies that V is strictly decreasing over the jumps of (3.30). Applying the hybrid invariance principle in Theorem 2.1, it follows that the set $\bar{\mathcal{A}}$ is stable.

Next we are going to show the asymptotic stability and finite number of jumps. From (B.12) and (B.13), one can verify that

$$0 \leq V(x(t, j)) \leq V(x(t, j-1)) - \delta \leq V(x(0, 0)) - \delta j, \tag{B.14}$$

where $(t, j), (t, j - 1) \in \text{dom } x$ with $(t, j) \succeq (t, j - 1)$. This leads to $j \leq J := \left\lceil \frac{V(x(0,0))}{\delta} \right\rceil$, where, $\lceil \cdot \rceil$ denotes the ceiling function. Hence, one concludes that the number of jumps is finite and it is linked to the initial conditions.

In view of (B.14), it follows from Theorem 2.1 that x must converge to the largest invariant subset of $\mathcal{F}_c \cap \mathcal{W}$ with

$$\mathcal{W} = \{x \in \mathcal{S} \mid \tilde{g} \in C_{\text{SE}(3)}\mathcal{U}\} = C_{\text{SE}(3)}\mathcal{U} \times \mathbb{R}^3 \times \text{SE}(3) \times \mathbb{R}^6 \times \mathbb{R}_{\geq 0},$$

where we made use of the definition of $C_{\text{SE}(3)}\mathcal{U}$. From the definition of \mathcal{F}_c and condition (3.31), one can verify that $\mathcal{X}_{\mathcal{U}} \times \mathbb{R}^6 \times \text{SE}(3) \times \mathbb{R}^6 \times \mathbb{R}_{\geq 0} \not\subseteq \mathcal{F}_c$ and $\mathcal{X}_{\mathcal{U}} \times \mathbb{R}^6 \times \text{SE}(3) \times \mathbb{R}^6 \times \mathbb{R}_{\geq 0} \subseteq \mathcal{J}_c$. Using the facts:

$$\begin{aligned} \mathcal{W} &= \mathcal{X}_{\mathcal{U}} \times \mathbb{R}^3 \times \text{SE}(3) \times \mathbb{R}^6 \times \mathbb{R}_{\geq 0} \cup \{I_4\} \times \mathbb{R}^6 \times \text{SE}(3) \times \mathbb{R}^6 \times \mathbb{R}_{\geq 0} \\ \mathcal{X}_{\mathcal{U}} \times \mathbb{R}^6 \times \text{SE}(3) \times \mathbb{R}^6 \times \mathbb{R}_{\geq 0} &\not\subseteq \mathcal{F}_c \\ \{I_4\} \times \mathbb{R}^6 \times \text{SE}(3) \times \mathbb{R}^6 \times \mathbb{R}_{\geq 0} &\subseteq \mathcal{F}_c, \end{aligned}$$

one has

$$\begin{aligned} \mathcal{F}_c \cap \mathcal{W} &= \mathcal{F}_c \cap (\mathcal{X}_{\mathcal{U}} \times \mathbb{R}^3 \times \text{SE}(3) \times \mathbb{R}^6 \times \mathbb{R}_{\geq 0} \cup \{I_4\} \times \mathbb{R}^6 \times \text{SE}(3) \times \mathbb{R}^6 \times \mathbb{R}_{\geq 0}) \\ &= (\mathcal{F}_c \cap \mathcal{X}_{\mathcal{U}} \times \mathbb{R}^3 \times \text{SE}(3) \times \mathbb{R}^6 \times \mathbb{R}_{\geq 0}) \cup (\mathcal{F}_c \cap \{I_4\} \times \mathbb{R}^6 \times \text{SE}(3) \times \mathbb{R}^6 \times \mathbb{R}_{\geq 0}) \\ &= \emptyset \cup \{I_4\} \times \mathbb{R}^6 \times \text{SE}(3) \times \mathbb{R}^6 \times \mathbb{R}_{\geq 0} \\ &= \{I_4\} \times \mathbb{R}^6 \times \text{SE}(3) \times \mathbb{R}^6 \times \mathbb{R}_{\geq 0} \end{aligned} \tag{B.15}$$

Hence the solution of x must converge to $\{I_4\} \times \mathbb{R}^6 \times \text{SE}(3) \times \mathbb{R}^6 \times \mathbb{R}_{\geq 0}$, i.e., the pose estimation error \tilde{g} must converge to I_4 . For $\tilde{g} \equiv I_4$, it follows that $\dot{\tilde{g}} \equiv 0$ and $\beta \equiv 0$. Using the facts $\dot{\tilde{g}} \equiv 0$ and $\beta \equiv 0$, one can conclude from (3.30) that $\dot{b}_\xi \equiv 0$. Therefore, the solutions of x must converge to $\bar{\mathcal{A}}$. Finally, the set $\bar{\mathcal{A}}$ is globally attractive and stable which shows that $\bar{\mathcal{A}}$ is GAS.

B.6 Proof of Theorem 3.2

Let us consider the following real-valued function $V : \mathcal{S} \rightarrow \mathbb{R}_{\geq 0}$ in (B.11). In view of (B.12) and (B.13), one obtains

$$\dot{V} = -2k_\beta \|\psi_{\text{se}(3)}(\tilde{g}^{-1} \nabla_{\tilde{g}} \mathcal{U})\|^2, \quad \forall x \in \mathcal{F}_c, \tag{B.16}$$

$$V(x^+) \leq V(x) - \delta, \quad \forall x \in \mathcal{J}_c. \tag{B.17}$$

These imply that V is non-increasing along the flows of (3.30) and strictly decreasing over the jumps of (3.30). Similar to (B.14), the number of jumps is no more than the finite value $J_{\max} := \lceil V(x(0,0))/\delta \rceil$. From the definitions of $C_{\text{SE}(3)}\mathcal{U}$ and $\mathcal{X}_{\mathcal{U}}$, one has $\|\psi_{\text{se}(3)}(\tilde{g}^{-1} \nabla_{\tilde{g}} \mathcal{U})\| = 0$ and $|\tilde{g}|_I \neq 0$ for all $\tilde{g} \in \mathcal{X}_{\mathcal{U}}$. From condition (3.33), one can show that $\mathcal{X}_{\mathcal{U}} \times \mathbb{R}^3 \times \text{SE}(3) \times \mathbb{R}^6 \times \mathbb{R}_{\geq 0} \not\subseteq \mathcal{F}_c$. Since $\mathcal{F}_c \cup \mathcal{J}_c = \mathcal{S}$, one concludes that $\mathcal{X}_{\mathcal{U}} \times \mathbb{R}^3 \times \text{SE}(3) \times \mathbb{R}^6 \times \mathbb{R}_{\geq 0} \subseteq \mathcal{J}_c$.

To show exponential stability, let us consider the following Lyapunov function candidate:

$$\mathcal{L}(x) = V(x) - z^\top U \tilde{b}_\xi, \quad (\text{B.18})$$

where $U := \text{diag}(\mu_1 I_3, \mu_2 I_3)$ with $\mu_1, \mu_2 > 0$ and $z := [\psi_{\mathfrak{so}(3)}(\tilde{R})^\top \hat{R}, \tilde{p}^\top R]^\top$. Let $e := [|\tilde{g}|_I, \|\tilde{b}_\omega\|, \|\tilde{b}_v\|]^\top$ and let e_i be the i -th elements of e . Letting $\psi_{\tilde{R}} := \psi_{\mathfrak{so}(3)}(\tilde{R})$, from (2.38) and (2.55) one verifies that $\|\psi_{\tilde{R}}\|^2 \leq \text{tr}(I_3 - R) = \frac{1}{2}\|I_3 - \tilde{R}\|_F^2 \leq \frac{1}{2}|\tilde{g}|_I^2 = \frac{1}{2}e_1^2$. From (3.32), one obtains

$$\begin{aligned} \mathcal{L} &\leq \alpha_2 e_1^2 + \frac{1}{k_\omega} e_2^2 + \frac{1}{k_v} e_3^2 + e_1 \left(\frac{\sqrt{2}\mu_1}{2} e_2 + \mu_2 e_3 \right) \\ \mathcal{L} &\geq \alpha_1 e_1^2 + \frac{1}{k_\omega} e_2^2 + \frac{1}{k_v} e_3^2 - e_1 \left(\frac{\sqrt{2}\mu_1}{2} e_2 + \mu_2 e_3 \right), \end{aligned}$$

which implies

$$e^\top \underbrace{\begin{bmatrix} \alpha_1 & \frac{-\sqrt{2}}{4}\mu_1 & \frac{-1}{2}\mu_2 \\ \frac{-\sqrt{2}}{4}\mu_1 & \frac{1}{k_\omega} & 0 \\ \frac{-1}{2}\mu_2 & 0 & \frac{1}{k_v} \end{bmatrix}}_{P_1} e \leq \mathcal{L}(x) \leq e^\top \underbrace{\begin{bmatrix} \alpha_2 & \frac{\sqrt{2}}{4}\mu_1 & \frac{1}{2}\mu_2 \\ \frac{\sqrt{2}}{4}\mu_1 & \frac{1}{k_\omega} & 0 \\ \frac{1}{2}\mu_2 & 0 & \frac{1}{k_v} \end{bmatrix}}_{P_2} e.$$

Using the fact $|x|_{\bar{\mathcal{A}}}^2 = |\tilde{g}|_I^2 + \|\tilde{b}_\xi\|^2 = \|e\|^2$, one obtains the following inequalities:

$$\lambda_{\min}^{P_1} |x|_{\bar{\mathcal{A}}}^2 \leq \mathcal{L}(x) \leq \lambda_{\max}^{P_2} |x|_{\bar{\mathcal{A}}}^2. \quad (\text{B.19})$$

From (3.30), one has

$$\dot{\tilde{R}} = \tilde{R}(-k_\beta \psi_\omega + \hat{R} \tilde{b}_\omega)^\times, \quad (\text{B.20})$$

$$\dot{\tilde{p}} = \tilde{R}(-k_\beta \psi_v + \hat{p}^\times \hat{R} \tilde{b}_\omega + \hat{R} \tilde{b}_v), \quad (\text{B.21})$$

$$\dot{\psi}_{\tilde{R}} = E(\tilde{R})(-k_\beta \psi_\omega + \hat{R} \tilde{b}_\omega), \quad (\text{B.22})$$

where $E(\tilde{R}) := \frac{1}{2}(\text{tr}(\tilde{R}) - \tilde{R}^\top)$. The arguments of ψ have been omitted for simplicity, and ψ_ω, ψ_v are given by $\psi := [\psi_\omega^\top, \psi_v^\top]^\top$. From Lemma 2.1, one has $\|E(\tilde{R})\|_F \leq \sqrt{3}$ and $v^\top(I_3 - E(\tilde{R}))v \leq 2|R|_I^2\|v\|^2 \leq 2|R|_I\|v\|^2 \leq \frac{\sqrt{2}}{2}\|I_3 - \tilde{R}\|_F\|v\|^2 \leq \frac{\sqrt{2}}{2}|\tilde{g}|_I\|v\|^2$ for all $v \in \mathbb{R}^3$. Define the constants $c_\omega := \sup_{t \geq 0} \|\omega(t)\|$ and $c_p := \sup_{t \geq 0} \|p(t)\|$. Since \tilde{b}_ω is bounded both in the flow and jump sets, there exists a constant $c_{b_\omega} := \sup_{(t,j) \geq (0,0)} \|\tilde{b}_\omega(t, j)\|$. In view of (B.20)-(B.22), the time-derivative of the cross term $\mathfrak{X} := z^\top U \tilde{b}_\xi = -\mu_1 \tilde{b}_\omega^\top \hat{R}^\top \psi_{\tilde{R}} - \mu_2 \tilde{p}^\top R \tilde{b}_v$ is obtained as

$$\begin{aligned} \dot{\mathfrak{X}} &= -\dot{z}^\top U \tilde{b}_\xi - z^\top \dot{U} \tilde{b}_\xi \\ &= -\mu_1 \tilde{b}_\omega^\top (\dot{\hat{R}}^\top \psi_{\tilde{R}} + \hat{R}^\top \dot{\psi}_{\tilde{R}}) - \mu_2 \tilde{b}_v^\top (R^\top \dot{\tilde{p}} + \hat{R}^\top \tilde{p}) - z^\top U \dot{\tilde{b}}_a \\ &= \mu_1 \tilde{b}_\omega^\top (\omega - \tilde{b}_\omega + k_\beta \psi_\omega)^\times \hat{R}^\top \psi_{\tilde{R}} - \mu_1 \tilde{b}_\omega^\top \hat{R}^\top E(\tilde{R})(-k_\beta \psi_\omega + \hat{R} \tilde{b}_\omega) + \mu_2 \tilde{b}_v^\top (\omega)^\times R^\top \tilde{p} \end{aligned}$$

$$\begin{aligned}
& -\mu_2 \tilde{b}_v^\top \hat{R}^\top (-k_\beta \psi_v + \hat{p}^\times \hat{R} \tilde{b}_\omega + \hat{R} \tilde{b}_v) - z^\top U \Gamma \text{Ad}_g^* \text{Ad}_{\tilde{g}^{-1}}^* \psi \\
& \leq -\mu_1 \|\tilde{b}_\omega\|^2 - \mu_2 \|\tilde{b}_v\|^2 + \mu_1 c_\omega \|\psi_{\tilde{R}}\| \|\tilde{b}_\omega\| + \mu_1 k_\beta \|\tilde{b}_\omega\| \|\psi_\omega\| \|\psi_{\tilde{R}}\| \\
& \quad + \mu_1 \tilde{b}_\omega^\top \hat{R}^\top (I_3 - E(\tilde{R})) \hat{R} \tilde{b}_\omega + \mu_1 k_\beta \|\tilde{b}_\omega\| \|E(\tilde{R})\|_F \|\psi_\omega\| + \mu_2 c_\omega \|\tilde{b}_v\| \|\tilde{p}\| \\
& \quad + \mu_2 k_\beta \|\tilde{b}_v\| \|\psi_v\| + \mu_2 c_{b_\omega} \|\tilde{b}_v\| \|\tilde{p}\| + \mu_2 c_p \|\tilde{b}_v\| \|\tilde{b}_\omega\| + k_\Gamma \|U\|_2 \|z\| \|\text{Ad}_g^*\|_F \|\text{Ad}_{\tilde{g}^{-1}}^* \psi\| \\
& \leq -\mu_1 \|\tilde{b}_\omega\|^2 - \mu_2 \|\tilde{b}_v\|^2 + 2\sqrt{\alpha_4} \mu_1 k_\beta \|\tilde{b}_\omega\| \|\tilde{g}\|_I + \frac{\sqrt{2}}{2} \mu_1 c_\omega \|\tilde{g}\|_I \|\tilde{b}_\omega\| \\
& \quad + \frac{\sqrt{2}}{2} \mu_1 c_{b_\omega} \|\tilde{g}\|_I \|\tilde{b}_\omega\| + \sqrt{3\alpha_4} \mu_1 k_\beta \|\tilde{b}_\omega\| \|\tilde{g}\|_I + \mu_2 c_\omega \|\tilde{b}_v\| \|\tilde{g}\|_I + \sqrt{\alpha_4} \mu_2 k_\beta \|\tilde{b}_v\| \|\tilde{g}\|_I \\
& \quad + \mu_2 c_{b_\omega} \|\tilde{b}_v\| \|\tilde{g}\|_I + \mu_2 c_p \|\tilde{b}_v\| \|\tilde{b}_\omega\| + k_\Gamma c_g \sqrt{\alpha_5} (u_1 + u_2) \|\tilde{g}\|_I^2 \\
& \leq -\mu_1 \|\tilde{b}_\omega\|^2 - \mu_2 \|\tilde{b}_v\|^2 + \mu_1 (\frac{\sqrt{2}}{2} c_\omega + 2\sqrt{\alpha_4} k_\beta + \frac{\sqrt{2}}{2} c_{b_\omega} + \sqrt{3\alpha_4} k_\beta) \|\tilde{g}\|_I \|\tilde{b}_\omega\| \\
& \quad + \mu_2 (c_\omega + \sqrt{\alpha_4} k_\beta + c_{b_\omega}) \|\tilde{b}_v\| \|\tilde{g}\|_I + \mu_2 c_p \|\tilde{b}_v\| \|\tilde{b}_\omega\| + k_\Gamma c_g \sqrt{\alpha_5} (u_1 + u_2) \|\tilde{g}\|_I^2,
\end{aligned}$$

where $k_\Gamma := \|\Gamma\|_F$, $c_g := \|\text{Ad}_g^*\|_F = \sqrt{6 + 2c_p^2}$, and the following facts have been used: $\|\tilde{g}\|_I^2 = \|I_3 - \tilde{R}\|^2 + \|\tilde{p}\|^2$, $\|\hat{p}\| = \|\hat{R}^\top(p - \tilde{p})\| \leq c_p + \|\tilde{p}\|$, $\|\psi_\omega\|^2 + \|\psi_v\|^2 \leq \alpha_4 \|\tilde{g}\|_I^2$, $\|z\| = \|\psi_{\tilde{R}}\| + \|\tilde{p}\| \leq \|\tilde{g}\|_I$, $\|U\|_2 \leq (\mu_1 + \mu_2)$ and Eq. (3.34). Let $c_1 := \frac{\sqrt{2}}{2} c_\omega + 2k_\beta \sqrt{\alpha_4} + \frac{\sqrt{2}c_{b_\omega}}{2} + k_\beta \sqrt{3\alpha_4}$, $c_2 := k_\beta \sqrt{\alpha_4} + c_{b_\omega} + c_\omega$, $c_3 := k_\Gamma \sqrt{\alpha_5} c_g$. Then, the time-derivative of \mathfrak{X} satisfies

$$\begin{aligned}
\dot{\mathfrak{X}} & \leq -\mu_1 \|\tilde{b}_\omega\|^2 - \mu_2 \|\tilde{b}_v\|^2 + \mu_1 c_1 \|\tilde{b}_\omega\| \|\tilde{g}\|_I + \mu_2 c_2 \|\tilde{b}_v\| \|\tilde{g}\|_I \\
& \quad + (\mu_1 c_3 + \mu_2 c_3) \|\tilde{g}\|_I^2 + \mu_2 c_p \|\tilde{b}_v\| \|\tilde{b}_\omega\|,
\end{aligned} \tag{B.23}$$

Consequently, in view of (B.12) and (B.23), one obtains

$$\begin{aligned}
\dot{\mathcal{L}} & \leq -2k_\beta \alpha_3 e_1^2 + (\mu_1 c_3 + \mu_2 c_3) e_1^2 - \mu_1 \|\tilde{b}_\omega\|^2 - \mu_2 \|\tilde{b}_v\|^2 \\
& \quad + \mu_1 c_1 \|\tilde{b}_\omega\| e_1 + \mu_2 c_2 \|\tilde{b}_v\| e_1 + \mu_2 c_p \|\tilde{b}_v\| \|\tilde{b}_\omega\| \\
& = -e^\top \begin{bmatrix} 2k_\beta \alpha_3 - \mu_1 c_3 - \mu_2 c_3 & -\frac{1}{2} \mu_1 c_1 & -\frac{1}{2} \mu_2 c_2 \\ -\frac{1}{2} \mu_1 c_1 & \mu_1 & -\frac{1}{2} \mu_2 c_p \\ -\frac{1}{2} \mu_2 c_2 & -\frac{1}{2} \mu_2 c_p & \mu_2 \end{bmatrix} e \\
& = -e_{12}^\top P_{31} e_{12} - e_{13}^\top P_{32} e_{13} - e_{23}^\top P_{33} e_{23},
\end{aligned}$$

where $e_{ij} := [e_i, e_j]^\top$, $i, j = 1, 2, 3$ with e_i denoting the i -th elements of e , and

$$\begin{aligned}
P_{31} & := \begin{bmatrix} k_\beta \alpha_3 - \mu_1 c_3 & -\frac{1}{2} \mu_1 c_1 \\ -\frac{1}{2} \mu_1 c_1 & \frac{1}{2} \mu_1 \end{bmatrix}, P_{32} := \begin{bmatrix} k_\beta \alpha_3 - \mu_2 c_3 & -\frac{1}{2} \mu_2 c_2 \\ -\frac{1}{2} \mu_2 c_2 & \frac{1}{2} \mu_2 \end{bmatrix}, \\
P_{33} & := \begin{bmatrix} \frac{1}{2} \mu_1 & -\frac{1}{2} \mu_2 c_p \\ -\frac{1}{2} \mu_2 c_p & \frac{1}{2} \mu_2 \end{bmatrix}.
\end{aligned}$$

To guarantee that the matrices P_1, P_2, P_{31}, P_{32} and P_{33} are positive definite, the parameters μ_1 and μ_2 are chosen as follows:

$$\begin{aligned}
\mu_1 & < \frac{2\sqrt{\alpha_1}}{\sqrt{k_\omega}}, \quad \mu_2 < \frac{\sqrt{2\alpha_1}}{\sqrt{k_v}} \quad \text{for } P_1, P_2 > 0 \\
\mu_1 & < \frac{k_\beta \alpha_3}{c_3 + \frac{1}{4} c_1^2}, \quad \mu_2 < \frac{k_\beta \alpha_3}{c_3 + \frac{1}{4} c_2^2} \quad \text{for } P_{31}, P_{32} > 0
\end{aligned}$$

$$\mu_2 < \frac{1}{c_p^2} \mu_1 \quad \text{for } P_{33} > 0$$

which are equivalent to

$$\begin{aligned} 0 < \mu_1 &< \min \left\{ \frac{2\sqrt{\alpha_1}}{\sqrt{k_\omega}}, \frac{k_\beta \alpha_3}{c_3 + \frac{1}{4} c_1^2} \right\} \\ 0 < \mu_2 &< \min \left\{ \frac{\sqrt{2\alpha_1}}{\sqrt{k_v}}, \frac{k_\beta \alpha_3}{c_3 + \frac{1}{4} c_2^2}, \frac{1}{c_p^2} \mu_1 \right\}. \end{aligned}$$

One concludes that

$$\dot{\mathcal{L}}(x) \leq -\lambda_F \mathcal{L}(x), \quad x \in \mathcal{F}_c, \quad (\text{B.24})$$

with $\lambda_F := \min\{\lambda_{\min}^{P_{31}}, \lambda_{\min}^{P_{32}}, \lambda_{\min}^{P_{33}}\}/\lambda_{\max}^{P_2}$. On the other hand, from (B.12) and (B.13), it is clear that \tilde{b}_ξ is bounded in the flow and jump sets. Hence, there exists a constant $c_{b_a} := \sup_{(t,j) \succeq (0,0)} \|\tilde{b}_\xi(t, j)\|$. Let $g_q = \mathcal{T}_{\mathsf{SE}(3)}(R_q, p_q) \in \mathbb{Q}$. Using the facts: $\tilde{R}^+ = \tilde{R}R_q$ and $\tilde{p}^+ = \tilde{p} + \tilde{R}p_q$, one has

$$\begin{aligned} \|z^+ - z\| &= \left\| \begin{bmatrix} (\hat{R}^+)^T \psi_{\mathfrak{so}(3)}(\tilde{R}^+) - \hat{R}^T \psi_{\mathfrak{so}(3)}(\tilde{R}) \\ R^T \tilde{p}^+ - R^T \tilde{p} \end{bmatrix} \right\| \\ &\leq \|R_q \psi_{\mathfrak{so}(3)}(\tilde{R}R_q) - \psi_{\mathfrak{so}(3)}(\tilde{R})\| + \|\tilde{p}^+ - \tilde{p}\| \\ &\leq \|R_q \psi_{\mathfrak{so}(3)}(\tilde{R}R_q)\| + \|\psi_{\mathfrak{so}(3)}(\tilde{R})\| + \|\tilde{R}p_q\| \\ &\leq 2 + \|p_q\| \end{aligned}$$

where we have made use of the fact $\|\psi_{\mathfrak{so}(3)}(R)\| \leq 1, \forall R \in \mathsf{SO}(3)$ in (2.47). Then, one can further show that

$$\begin{aligned} \mathcal{L}(x^+) - \mathcal{L}(x) &= V(x^+) - V(x) + (z^+)^T U \tilde{b}_\xi - z^T U \tilde{b}_\xi \\ &= V(x^+) - V(x) + \|(z^+) - z\| \|U \tilde{b}_\xi\| \\ &\leq -\delta + (\mu_1 + \mu_2)c_4, \end{aligned}$$

where $c_4 := (2 + \|p_q\|)c_{b_a}$. Choosing μ_1 and μ_2 such that

$$\begin{aligned} 0 < \mu_1 &< \min \left\{ \frac{2\sqrt{\alpha_1}}{\sqrt{k_\omega}}, \frac{k_\beta \alpha_3}{c_3 + \frac{1}{4} c_1^2}, \frac{\delta}{2c_4} \right\}, \\ 0 < \mu_2 &< \min \left\{ \frac{\sqrt{2\alpha_1}}{\sqrt{k_v}}, \frac{k_\beta \alpha_3}{c_3 + \frac{1}{4} c_2^2}, \frac{1}{c_p^2} \mu_1, \mu_1 \right\}, \end{aligned}$$

there exists a constant $0 < \delta^* \leq \delta - 2\mu_1 c_4 > 0$ such that

$$\mathcal{L}(x^+) \leq \mathcal{L}(x) - \delta^*, \quad x \in \mathcal{J}_c. \quad (\text{B.25})$$

In view of (B.24) and (B.25), it follows that $\mathcal{L}(t, j) \leq \exp(-\lambda_F t) \mathcal{L}(0, 0)$ for each $(t, j) \in \text{dom}x$. One verifies that $\mathcal{L}(x^+) \leq \exp(-\lambda_J) \mathcal{L}(x)$, with $\lambda_J := -\ln(1 - \delta^*/\mathcal{L}(0, 0))$. Consequently, one obtains

$$\mathcal{L}(t, j) \leq \exp(-2\lambda_J(t + j)) \mathcal{L}(0, 0), \quad (\text{B.26})$$

where $\lambda := \frac{1}{2} \min\{\lambda_F, \lambda_J\}$. From (B.19) and (B.26), for each $(t, j) \in \text{dom}x$ one has

$$|x(t, j)|_{\bar{\mathcal{A}}} \leq k \exp(-\lambda(t + j)) |x(0, 0)|_{\bar{\mathcal{A}}}, \quad (\text{B.27})$$

where $k := \sqrt{\lambda_{\max}^{P_2}/\lambda_{\min}^{P_1}}$. Since $\mathcal{F}_c \cup \mathcal{J}_c = \mathcal{S}$, the number of jumps is finite and there is no finite escape-time, one concludes that the solution to the hybrid system \mathcal{H} is complete as per Proposition 2.10 in [Goebel et al., 2012]. This completes the proof.

B.7 Proof of Lemma 3.4

Given $g = \mathcal{T}_{\text{SE}(3)}(R, p)$, $M = A - bb^\top d^{-1}$, from (3.9) one can verify that

$$\begin{aligned} \mathcal{U}(g) &= \frac{1}{2} \text{tr} \left(\begin{bmatrix} I_3 - R & -p \\ 0 & 0 \end{bmatrix} \begin{bmatrix} A & b \\ b^\top & d \end{bmatrix} \begin{bmatrix} I_3 - R & -p \\ 0 & 0 \end{bmatrix}^\top \right) \\ &= \frac{1}{2} \text{tr} ((I_3 - R)A(I_3 - R)^\top - 2(I_3 - R)bp^\top + dpp^\top) \\ &= \text{tr}(M(I_3 - R)) + \frac{1}{2}d \|p - (I_3 - R)bd^{-1}\|^2. \end{aligned}$$

The gradient $\nabla_g \mathcal{U}(g)$ can be computed using the differential of $\mathcal{U}(g)$ in an arbitrary tangential direction $gX \in T_g \text{SE}(3)$ with some $X \in \mathfrak{se}(3)$

$$d\mathcal{U}(g) \cdot gX = \langle \nabla_g \mathcal{U}(g), gX \rangle_g = \langle \langle g^{-1} \nabla_g \mathcal{U}(g), X \rangle \rangle. \quad (\text{B.28})$$

On the other hand, from the definition of the tangent map, one has

$$\begin{aligned} d\mathcal{U}(g) \cdot gX &= \text{tr}(-gX\mathbb{A}(I_4 - g)^\top) \\ &= \langle \langle g^\top(g - I_4)\mathbb{A}, X \rangle \rangle \\ &= \langle \langle \mathbb{P}_{\mathfrak{se}(3)}(g^\top(g - I_4)\mathbb{A}), X \rangle \rangle \\ &= \langle \langle \mathbb{P}_{\mathfrak{se}(3)}(g^{-1}(g - I_4)\mathbb{A}), X \rangle \rangle \\ &= \langle \langle \mathbb{P}_{\mathfrak{se}(3)}((I_4 - g^{-1})\mathbb{A}), X \rangle \rangle, \end{aligned} \quad (\text{B.29})$$

where the fact $(I_4 - g^{-1})\mathbb{A} \in \mathcal{M}_0^4$ and property (2.72) have been used. Hence, in view of (B.28) and (B.29), one can verify (3.37).

Using the fact $g\mathbb{P}((I_4 - g^{-1})\mathbb{A}) \in \mathcal{M}_0^4$, the identity $\nabla_g \mathcal{U}(g) = 0$ implies that $(I_4 - g^{-1})\mathbb{A} = \mathbb{A}(I_4 - g^{-1})^\top$, which can be further reduced as $\mathbb{A}g^\top = g\mathbb{A}$. Applying the matrix decomposition (2.8), one obtains

$$\begin{bmatrix} M & 0 \\ 0 & d \end{bmatrix} \begin{bmatrix} R & p - (I_3 - R)bd^{-1} \\ 0 & 1 \end{bmatrix}^\top = \begin{bmatrix} R & p - (I_3 - R)bd^{-1} \\ 0 & 1 \end{bmatrix} \begin{bmatrix} M & 0 \\ 0 & d \end{bmatrix}.$$

Consequently, one can further deduce that

$$RM = MR^\top, \quad p = (I_3 - R)bd^{-1}. \quad (\text{B.30})$$

From Lemma 2.3, one has the solution of (B.30) as

$$(R, p) \in \{(I_3, 0)\} \cup \{(R, p) : R = \mathcal{R}_a(\pi, v), p = (I_3 - \mathcal{R}_a(\pi, v))bd^{-1}, v \in \mathcal{E}(M)\},$$

which implies (3.38). This completes the proof.

B.8 Proof of Lemma 3.5

Let $p_e := p - (I_3 - R)bd^{-1}$. For the case $(I_3 - R)bd^{-1} = 0$, one has $\|I_3 - R\|_F^2 + \|p_e\|^2 = |g|_I^2$. For the case $(I_3 - R)bd^{-1} \neq 0$, there exists a positive scalar $0 < \varrho_1(R) < \|bd^{-1}\|$ such that $\|(I_3 - R)bd^{-1}\| = \varrho_1\|I_3 - R\|_F$. Let $\phi_1 := \angle(p, (I_3 - R)bd^{-1})$ with $\angle(\cdot, \cdot)$ denoting the angle between two vectors. Then, one has

$$\begin{aligned} & \|I_3 - R\|_F^2 + \|p_e\|^2 \\ &= (1 + \varrho_1^2)\|I_3 - R\|_F^2 + \|p\|^2 - 2\varrho_1 \cos \phi_1 \|p\| \|I_3 - R\|_F \\ &= [\|p\| \quad \|I_3 - R\|_F] \underbrace{\begin{bmatrix} 1 & -\varrho_1 \cos \phi_1 \\ -\varrho_1 \cos \phi_1 & 1 + \varrho_1^2 \end{bmatrix}}_{\Theta_1} \begin{bmatrix} \|p\| \\ \|I_3 - R\|_F \end{bmatrix}. \end{aligned}$$

which implies that

$$s_1|g|_I^2 \leq \|I_3 - R\|_F^2 + \|p_e\|^2 \leq s_2|g|_I^2, \quad (\text{B.31})$$

where $s_1 := \min\{1, \lambda_{\min}^{\Theta_1}\}$ and $s_2 := \max\{1, \lambda_{\max}^{\Theta_1}\}$. Note that the matrix Θ_1 is always positive definite. Using the facts $\bar{M} = \frac{1}{2}(\text{tr}(M)I_3 - M)$ and $\lambda_{\min}^{\bar{M}} > 0$ for any $R \in \text{SO}(3)$ one verifies that

$$\frac{1}{2}\lambda_{\min}^{\bar{M}}\|I_3 - R\|_F^2 \leq \text{tr}(M(I_3 - R)) \leq \frac{1}{2}\lambda_{\max}^{\bar{M}}\|I_3 - R\|_F^2. \quad (\text{B.32})$$

Then, from (3.36) one can show that

$$\begin{aligned} \mathcal{U}(g) &\geq \frac{1}{2}\lambda_{\min}^{\bar{M}}\|I_3 - R\|_F^2 + \frac{d}{2}\|p_e\|^2 \geq \alpha_1|g|_I^2, \\ \mathcal{U}(g) &\leq \frac{1}{2}\lambda_{\max}^{\bar{M}}\|I_3 - R\|_F^2 + \frac{d}{2}\|p_e\|^2 \leq \alpha_2|g|_I^2, \end{aligned}$$

with

$$\alpha_1 := \min \left\{ \frac{1}{2}\lambda_{\min}^{\bar{M}}, \frac{1}{2}d \right\} s_1, \quad \alpha_2 := \max \left\{ \frac{1}{2}\lambda_{\max}^{\bar{M}}, \frac{1}{2}d \right\} s_2. \quad (\text{B.33})$$

Using the fact

$$\begin{aligned} (I_4 - g^{-1})\mathbb{A} &= \begin{bmatrix} I - R^\top & R^\top p \\ 0 & 0 \end{bmatrix} \begin{bmatrix} A & b \\ b^\top & d \end{bmatrix} = \begin{bmatrix} (I - R^\top)A + R^\top pb^\top & (I - R^\top)b + R^\top pd \\ 0 & 0 \end{bmatrix} \\ &= \begin{bmatrix} (I_3 - R^\top)M + R^\top p_e b^\top & R^\top dp_e \\ 0 & 0 \end{bmatrix}, \end{aligned}$$

From (2.57), one verifies that

$$\psi_{\mathfrak{se}(3)}((I_4 - g^{-1})\mathbb{A}) = \frac{1}{2} \begin{bmatrix} 2\psi_{\mathfrak{so}(3)}(MR) + b^\times R^\top p_e \\ R^\top p_e d \end{bmatrix}. \quad (\text{B.34})$$

Hence, one can show that

$$\|\psi_{\mathfrak{se}(3)}((I_4 - g^{-1})\mathbb{A})\|^2$$

$$\begin{aligned}
&= \frac{1}{4} \|2\psi_{\mathfrak{so}(3)}(MR) + b^\times R^\top p_e\|^2 + \frac{1}{4} d^2 \|p_e\|^2 \\
&= \|\psi_{\mathfrak{so}(3)}(MR)\|^2 + \psi_{\mathfrak{so}(3)}(MR)^\top b^\times R^\top p_e + \frac{1}{4} \|b^\times R^\top p_e\|^2 + \frac{1}{4} d^2 \|p_e\|^2 \\
&\geq \|\psi_{\mathfrak{so}(3)}(MR)\|^2 - \|\psi_{\mathfrak{so}(3)}(MR)\| \|b^\times R^\top p_e\| + \frac{1}{4} \|b^\times R^\top p_e\|^2 + \frac{1}{4} d^2 \|p_e\|^2 \\
&= \|\psi_{\mathfrak{so}(3)}(MR)\|^2 - |\sin \phi_2| \|b\| \|\psi_{\mathfrak{so}(3)}(MR)\| \|p_e\| + \frac{1}{4} s_1 \|b\|^2 \|p_e\|^2 + \frac{1}{4} d^2 \|p_e\|^2 \\
&= [\|\psi_{\mathfrak{so}(3)}(MR)\| \quad \|p_e\|] \Theta_2 \begin{bmatrix} \|\psi_{\mathfrak{so}(3)}(MR)\| \\ \|p_e\| \end{bmatrix},
\end{aligned}$$

with

$$\Theta_2 := \begin{bmatrix} 1 & -\frac{1}{2} |\sin \phi_2| \|b\| \\ -\frac{1}{2} |\sin \phi_2| \|b\| & \frac{1}{4} (\sin^2 \phi_2 \|b\|^2 + d^2) \end{bmatrix},$$

where we used the facts $\|b^\times R^\top p_e\|^2 = p_e^\top R(b^\top b I_3 - b b^\top) R^\top p_e = \sin^2 \phi_2 \|b\|^2 \|p_e\|^2$ and $\phi_2 := \angle(b, R^\top p_e)$. It is straightforward to verify that the matrix Θ_2 is positive definite. Let $\lambda_{\min}^{\Theta_2}$ be the minimum eigenvalue of the matrix Θ_2 . One has

$$\begin{aligned}
\|\psi_{\mathfrak{se}(3)}((I_4 - g^{-1})\mathbb{A})\|^2 &= \frac{1}{4} \|2\psi_{\mathfrak{so}(3)}(MR) + b^\times R^\top p_e\|^2 + \frac{1}{4} d^2 \|p_e\|^2 \\
&\geq \lambda_{\min}^{\Theta_2} (\|\psi_{\mathfrak{so}(3)}(MR)\|^2 + \|p_e\|^2) \\
&= \lambda_{\min}^{\Theta_2} (\vartheta(M, R) \text{tr}(\underline{M}(I_3 - R)) + \|p_e\|^2) \\
&= \lambda_{\min}^{\Theta_2} \left(\frac{1}{2} \vartheta(M, R) \lambda_{\min}^{\underline{M}} \|I_3 - R\|_F^2 + \|p_e\|^2 \right),
\end{aligned}$$

where $\underline{M} := \text{tr}(\bar{M}^2) I_3 - 2\bar{M}^2$, and we made use of the fact $\|\psi_{\mathfrak{so}(3)}(MR)\|^2 = \vartheta(M, R) \text{tr}(\underline{M}(I_3 - R))$ with $\vartheta(M, R) := (1 - |R|_I^2 \cos^2(\angle(u, \bar{M}u)))$ and $u \in \mathbb{S}^2$ is the axis of the rotation R (see (2.38) in Lemma 2.1). For any $\mathcal{T}_{\mathsf{SE}(3)}(R, p) \in \mathsf{SE}(3)/\mathcal{X}_U$, one has $0 < \vartheta(M, R) \leq 1$. Hence, there exists a positive ϑ^* such that

$$\vartheta^* := \min_{\mathcal{T}_{\mathsf{SE}(3)}(R, p) \in \Upsilon} \left(1 - \frac{1}{8} \|I_3 - R\|_F^2 \cos^2(\angle(u, \bar{M}u)) \right).$$

Therefore, one obtains

$$\|\psi_{\mathfrak{se}(3)}((I_4 - g^{-1})\mathbb{A})\|^2 \geq \lambda_{\min}^{\Theta_2} \left(\frac{1}{2} \vartheta^* \lambda_{\min}^{\underline{M}} \|I_4 - R\|_F^2 + \|p_e\|^2 \right) \geq \alpha_3 |g|_I^2,$$

where

$$\alpha_3 := \lambda_{\min}^{\Theta_2} \min \left\{ 1, \frac{1}{2} \vartheta^* \lambda_{\min}^{\underline{M}} \right\} s_1. \tag{B.35}$$

Moreover, one can also show that

$$\|\psi_{\mathfrak{se}(3)}((I_4 - g^{-1})\mathbb{A})\|^2 = \frac{1}{4} \|2\psi_{\mathfrak{so}(3)}(MR) + b^\times R^\top p_e\|^2 + \frac{1}{4} d^2 \|p_e\|^2$$

$$\begin{aligned}
&\leq 2\|\psi_{\mathfrak{so}(3)}(MR)\|^2 + \frac{1}{2}\|b^\times R^\top p_e\|^2 + \frac{1}{4}d^2\|p_e\|^2 \\
&\leq 2\|\psi_{\mathfrak{so}(3)}(MR)\|^2 + \frac{1}{2}\|b\|^2\|p_e\|^2 + \frac{1}{4}d^2\|p_e\|^2 \\
&\leq \lambda_{\max}^M \|I_3 - R\|_F^2 + (\frac{1}{2}\|b\|^2 + \frac{1}{4}d^2)\|p_e\|^2 \\
&= \alpha_4 |g|_I^2.
\end{aligned}$$

where

$$\alpha_4 := \max \left\{ \left(\frac{1}{2}\|b\|^2 + \frac{1}{4}d^2 \right), \frac{1}{2}\lambda_{\max}^M \right\} s_2. \quad (\text{B.36})$$

From (B.34), one obtains

$$\begin{aligned}
\text{Ad}_{g^{-1}}^* \psi_{\mathfrak{se}(3)}((I_4 - g^{-1})\mathbb{A}) &= \frac{1}{2} \begin{bmatrix} R & p^\times R \\ 0 & R \end{bmatrix} \begin{bmatrix} 2\psi_{\mathfrak{so}(3)}(MR) + b^\times R^\top p_e \\ R^\top p_e d \end{bmatrix} \\
&= \frac{1}{2} \begin{bmatrix} 2R\psi_{\mathfrak{so}(3)}(MR) + Rb^\times R^\top p_e + dp^\times p_e \\ dp_e \end{bmatrix} \\
&= \frac{1}{2} \begin{bmatrix} 2R\psi_{\mathfrak{so}(3)}(MR) + (Rb + dp)^\times p_e \\ dp_e \end{bmatrix} \\
&= \frac{1}{2} \begin{bmatrix} 2R\psi_{\mathfrak{so}(3)}(MR) + b^\times p_e \\ dp_e \end{bmatrix},
\end{aligned}$$

where the facts $dp = dp_e + (I_3 - R)b$ and $p_e^\times p_e = 0$ have been used. One can further show that

$$\begin{aligned}
\|\text{Ad}_{g^{-1}}^* \psi_{\mathfrak{se}(3)}((I_4 - g^{-1})\mathbb{A})\|^2 &\leq 2\|\psi_{\mathfrak{so}(3)}(MR)\|^2 + \frac{1}{2}\|b^\times p_e\|^2 + \frac{1}{4}d\|p_e\|^2 \\
&\leq \lambda_{\max}^M \|I_3 - R\|_F^2 + (\frac{1}{2}\|b\|^2 + \frac{1}{4}d)\|p_e\|^2 \\
&\leq \alpha_4 |g|_I^2.
\end{aligned}$$

This completes the proof.

B.9 Proof of Proposition 3.2

Let $\tilde{g} = \mathcal{T}_{\mathbb{SE}(3)}(\tilde{R}, \tilde{p})$ with $\tilde{R} = \mathcal{R}_a(\theta, v)$, $\theta \in \mathbb{R}$ and $v \in \mathbb{S}^2$. In view of (3.9) and (3.43), one obtains

$$\mathcal{U}_1(\tilde{g}) = \text{tr}((I_3 - \tilde{R})M) + \frac{1}{2}d\|\tilde{p} - (I_3 - \tilde{R})bd^{-1}\|^2 \quad (\text{B.37})$$

$$= 2(1 - \cos \theta)v^\top \bar{M}v + \frac{1}{2}d\|\tilde{p} - (I_3 - \tilde{R})bd^{-1}\|^2 \quad (\text{B.38})$$

where the matrix \bar{M} is defined in Lemma 3.1. Under Assumption 3.1, one has $d > 0$ and \bar{M} is positive definite. Consequently, $\mathcal{U}_1(\tilde{g})$ has a unique global minimum at $\tilde{g} = I_4$, i.e.,

\mathcal{U}_1 is a potential function on $\text{SE}(3)$. From (B.37), for any $\tilde{g} = \mathcal{T}_{\text{SE}(3)}(\tilde{R}, \tilde{p}) \in \mathcal{X}_{\mathcal{U}_1}$ and $g_q = \mathcal{T}_{\text{SE}(3)}(R_q, p_q) \in \mathbb{Q}$, one has

$$\begin{aligned}\mathcal{U}_1(\tilde{g}g_q) &= \text{tr}((I_3 - \tilde{R}R_q)M) + \frac{1}{2}d\|p_q - (I_3 - R_q)bd^{-1}\|^2 \\ &= \text{tr}((I_3 - \tilde{R})M) + \text{tr}(\tilde{R}(I_3 - R_q)M) \\ &= \mathcal{U}_1(\tilde{g}) - (1 - \cos \theta^*)\Delta_M(u_q, v).\end{aligned}\quad (\text{B.39})$$

where $u_q \in \mathbb{U}$, $v \in \mathcal{E}(M)$, $\Delta_M(\cdot)$ is defined in (3.13). We also made use of the following facts: $p_q = (I_3 - R_q)bd^{-1}$, $\tilde{R} = \mathcal{R}_a(\pi, v) = 2vv^\top - I_3$, $R_q = \mathcal{R}_a(\theta^*, u_q)$. From (B.39), one can obtain

$$\begin{aligned}\mathcal{U}_1(\tilde{g}) - \min_{g_q \in \mathbb{Q}} \mathcal{U}_1(\tilde{g}g_q) &= (1 - \cos \theta^*) \max_{u_q \in \mathbb{U}} \Delta_M(u_q, v), \forall v \in \mathcal{E}(M) \\ &\geq (1 - \cos \theta^*) \min_{v \in \mathcal{E}(M)} \max_{u_q \in \mathbb{U}} \Delta_M(u_q, v) \\ &= (1 - \cos \theta^*)\Delta_M^* > \delta,\end{aligned}$$

which implies that $\mathcal{X}_{\mathcal{U}_1} \times \mathbb{R}^6 \times \text{SE}(3) \times \mathbb{R}^6 \times \mathbb{R}_{\geq 0} \subseteq \mathcal{J}_c$ from (3.29). In view of (3.3) and (3.46)-(3.48), one can write the hybrid closed-loop system as in (3.30). The proof is completed by using Lemma 3.4, Theorem 3.2 and the facts $\mathcal{X}_{\mathcal{U}_1} \times \mathbb{R}^6 \times \text{SE}(3) \times \mathbb{R}^6 \times \mathbb{R}_{\geq 0} \subseteq \mathcal{J}_c$ and $\mathcal{X}_{\mathcal{U}_1} \times \mathbb{R}^6 \times \text{SE}(3) \times \mathbb{R}^6 \times \mathbb{R}_{\geq 0} \not\subseteq \mathcal{F}_c$.

B.10 Proof of Theorem 3.3

As in Proposition 3.2, for any $\underline{g} \in \mathcal{X}_{\mathcal{U}_2}$, one verifies that

$$\begin{aligned}\mathcal{U}_2(\underline{g}) - \min_{g_q \in \mathbb{Q}} \mathcal{U}_2(g_c^{-1}\underline{g}g_qg_c) &= \mathcal{U}_2(\underline{g}) - \min_{g_q \in \mathbb{Q}} \mathcal{U}_2(\underline{g}g_c^{-1}g_qg_c) \\ &= \mathcal{U}_1(\underline{g}) - \min_{g_q \in \mathbb{Q}} \mathcal{U}_1(\underline{g}g_q) > \delta,\end{aligned}$$

which implies that $\mathcal{X}_{\mathcal{U}_2} \times \mathbb{R}^6 \times \text{SE}(3) \times \mathbb{R}^6 \times \mathbb{R}_{\geq 0} \subseteq \mathcal{J}'_c$. Let us consider the following real-valued function:

$$\mathcal{L}_R = \text{tr}(M(I - \tilde{R})) + \frac{1}{2k_\omega} \tilde{b}_\omega^\top \tilde{b}_\omega - \bar{\mu}_1 \psi_{\mathfrak{so}(3)}(\tilde{R})^\top \tilde{R} \tilde{b}_\omega, \quad (\text{B.40})$$

where $\bar{\mu}_1 > 0$. Let $\bar{e}_1 := [\|I_3 - \tilde{R}\|_F, \|\tilde{b}_\omega\|]^\top$. Following similar steps as in the proof of Theorem 3.2, it is clear that there exist a constant $c_{b_\omega} := \sup_{(t,j) \succeq (0,0)} \|\tilde{b}_\omega(t, j)\|$, and a constant $\bar{\mu}_1^*$ such that for all $\bar{\mu}_1 < \bar{\mu}_1^*$

$$\bar{c}_1 \|\bar{e}_1\|^2 \leq \mathcal{L}_R \leq \bar{c}_2 \|\bar{e}_1\|^2, \quad (\text{B.41})$$

$$\dot{\mathcal{L}}_R \leq -\bar{c}_3 \mathcal{L}_R, \quad x' \in \mathcal{F}'_c, \quad (\text{B.42})$$

for some positive constants \bar{c}_1, \bar{c}_2 and \bar{c}_3 . Let us consider the following real-valued function:

$$\mathcal{L}_p = \frac{d}{2} \underline{\tilde{p}}^\top \underline{\tilde{p}} + \frac{1}{k_v} \tilde{b}_v^\top \tilde{b}_v - \bar{\mu}_2 \underline{\tilde{p}}^\top \underline{R} \tilde{b}_v. \quad (\text{B.43})$$

Let $\bar{e}_2 := [\|\tilde{p}\|, \|\tilde{b}_v\|]^\top$. It is straightforward to show that

$$\bar{e}_2^\top \underbrace{\begin{bmatrix} \frac{d}{2} & -\frac{\bar{\mu}_2}{2} \\ -\frac{\bar{\mu}_2}{2} & \frac{1}{k_v} \end{bmatrix}}_{H_1} \bar{e}_2 \leq \mathcal{L}_p \leq \bar{e}_2^\top \underbrace{\begin{bmatrix} \frac{d}{2} & \frac{\bar{\mu}_2}{2} \\ \frac{\bar{\mu}_2}{2} & \frac{1}{k_v} \end{bmatrix}}_{H_2} \bar{e}_2. \quad (\text{B.44})$$

The time-derivative of \mathcal{L}_p along the trajectories of (3.72) and (3.74) is obtained as

$$\begin{aligned} \dot{\mathcal{L}}_p &= d\tilde{p}^\top \dot{\tilde{p}} + \frac{1}{k_v} \tilde{b}_v^\top \dot{\tilde{b}}_v - \bar{\mu}_2 \dot{\tilde{p}}^\top R \tilde{b}_v - \bar{\mu}_2 \tilde{p}^\top R \dot{\tilde{b}}_v - \bar{\mu}_2 \tilde{p}^\top \dot{R} \tilde{b}_v \\ &= -\frac{d^2}{2} k_\beta \tilde{p}^\top \tilde{p} + d\tilde{p}^\top \underline{R} \tilde{p}^\times \underline{R} \tilde{b}_\omega + \bar{\mu}_2 k_\beta \frac{d}{2} \tilde{p}^\top R \tilde{b}_v + \bar{\mu}_2 \tilde{b}_\omega^\top \hat{R}^\top \underline{p}^\times \underline{R}^\top R \tilde{b}_v - \bar{\mu}_2 \tilde{b}_v^\top \tilde{b}_v \\ &\quad + \frac{d}{2} k_v \bar{\mu}_2 \tilde{p}^\top R \hat{R}^\top \underline{R}^\top \tilde{p} - \bar{\mu}_2 \tilde{p}^\top R \omega^\times \tilde{b}_v \\ &\leq -\frac{d^2}{2} k_\beta \tilde{p}^\top \tilde{p} - \bar{\mu}_2 \tilde{b}_v^\top \tilde{b}_v + d\tilde{p}^\top \underline{R} (\underline{R}^\top \underline{p} - \underline{R}^\top \tilde{p})^\times \hat{R} \tilde{b}_\omega + \bar{\mu}_2 k_\beta \frac{d}{2} \|\tilde{p}\| \|\tilde{b}_v\| \\ &\quad + \bar{\mu}_2 \tilde{b}_\omega^\top \hat{R} (\underline{R}^\top \underline{p} - \underline{R}^\top \tilde{p})^\times \underline{R}^\top R \tilde{b}_v + \bar{\mu}_2 \frac{d}{2} k_v \|\tilde{p}\|^2 + \bar{\mu}_2 \|\omega\| \|\tilde{p}\| \|\tilde{b}_v\| \\ &\leq -\frac{d^2}{2} k_\beta \|\tilde{p}\|^2 - \bar{\mu}_2 \|\tilde{b}_v\|^2 + d\bar{c}_p \|\tilde{p}\| \|\tilde{b}_\omega\| + \bar{\mu}_2 k_\beta \frac{d}{2} \|\tilde{p}\| \|\tilde{b}_v\| + \bar{\mu}_2 \bar{c}_p \|\tilde{b}_\omega\| \|\tilde{b}_v\| \\ &\quad + \bar{\mu}_2 c_{b_\omega} \|\tilde{p}\| \|\tilde{b}_v\| + \bar{\mu}_2 \frac{d}{2} k_v \|\tilde{p}\|^2 + \bar{\mu}_2 c_\omega \|\tilde{p}\| \|\tilde{b}_v\|, \end{aligned}$$

where $\bar{c}_p := \|\underline{p}\| = \|p - bd^{-1}\|$, and the following facts have been used: $\underline{R} = \hat{R}$, $\underline{R} = R$ and $\hat{p} = \underline{R}^\top (p - \tilde{p})$. Let $\bar{c}_4 := \max\{d, \bar{\mu}_2\}$ and $\bar{c}_5 := k_\beta \frac{d}{2} + c_\omega + c_{b_\omega}$. Then, one has

$$\dot{\mathcal{L}}_p \leq -\bar{e}_2^\top \underbrace{\begin{bmatrix} \frac{d^2}{2} k_\beta - \bar{\mu}_2 \frac{d}{2} k_v & -\frac{1}{2} \bar{\mu}_2 \bar{c}_5 \\ -\frac{1}{2} \bar{\mu}_2 \bar{c}_5 & \bar{\mu}_2 \end{bmatrix}}_{H_3} \bar{e}_2 + \sqrt{2} \bar{c}_4 \bar{c}_p \|\tilde{b}_\omega\| \|\bar{e}_2\|.$$

To guarantee that the matrices H_1 , H_2 and H_3 are positive definite, it is sufficient to pick $\bar{\mu}_2$ such that $0 < \bar{\mu}_2 < \min \left\{ \frac{\sqrt{2d}}{\sqrt{k_v}}, \frac{k_\beta d^2}{dk_v + \frac{1}{2} \bar{c}_5^2} \right\}$. Hence, one has

$$\begin{aligned} \dot{\mathcal{L}}_p &\leq -\lambda_{\min}^{H_3} \|\bar{e}_2\|^2 + \sqrt{2} \bar{c}_4 \bar{c}_p \|\bar{e}_1\| \|\bar{e}_2\| \\ &\leq -\eta_2 \mathcal{L}_p + \eta_3 \sqrt{\mathcal{L}_R} \sqrt{\mathcal{L}_p}, \quad x' \in \mathcal{F}'_c, \end{aligned} \quad (\text{B.45})$$

where $\eta_2 := \lambda_{\min}^{H_3} / \lambda_{\max}^{H_2} > 0$, $\eta_3 := \sqrt{2} \bar{c}_4 \bar{c}_p / \sqrt{\lambda_{\min}^{H_1} \bar{c}_1} > 0$, and we made use of the fact $\|\tilde{b}_\omega\| \leq \|\bar{e}_1\| \leq \frac{1}{\sqrt{\bar{c}_1}} \sqrt{\mathcal{L}_R}$. Let $\zeta_1 := \sqrt{\mathcal{L}_R}$, $\zeta_2 := \sqrt{\mathcal{L}_p}$ and $\zeta := [\zeta_1, \zeta_2]^\top$. From (C.3) and (C.6), one obtains

$$\dot{\zeta} \leq -H_4 \zeta, \quad H_4 := \begin{bmatrix} \bar{c}_3 & 0 \\ -\frac{\eta_3}{2} & \frac{\eta_2}{2} \end{bmatrix}. \quad (\text{B.46})$$

One can easily verify that H_4 is positive definite. Let us consider the following Lyapunov function candidate:

$$\mathcal{L}'(x') = \mathcal{L}_R + \mathcal{L}_p = \|\zeta\|^2. \quad (\text{B.47})$$

Using the fact $|x'|_{\bar{\mathcal{A}}'}^2 = |\tilde{g}|_I^2 + \|\tilde{b}_\xi\|^2 = \|\bar{e}_1\|^2 + \|\bar{e}_2\|^2$, from (B.41), (C.3), (B.44) and (C.6), one has

$$\underline{\alpha}|x'|_{\bar{\mathcal{A}}'}^2 \leq \mathcal{L}'(x') \leq \bar{\alpha}|x'|_{\bar{\mathcal{A}}'}^2 \quad (\text{B.48})$$

$$\dot{\mathcal{L}}'(x') \leq -\zeta^\top H_4 \zeta \leq -\lambda'_F \mathcal{L}'(x'), \quad x' \in \mathcal{F}'_c, \quad (\text{B.49})$$

where $\lambda'_F := \lambda_{\min}^{H_4}$, $\underline{\alpha} := \min\{\bar{c}_1, \lambda_{\min}^{H_1}\}$ and $\bar{\alpha} := \max\{\bar{c}_2, \lambda_{\max}^{H_2}\}$. On the other hand, using the facts $\underline{\tilde{R}}^+ = \underline{\tilde{R}}R_q$, $\tilde{b}_\omega^+ = \tilde{b}_\omega$, $\tilde{b}_v^+ = \tilde{b}_v$ and $\underline{\tilde{p}}^+ = \underline{\tilde{p}}$, one has

$$\begin{aligned} \mathcal{L}(x'^+) - \mathcal{L}(x') &= \|\zeta^+\|^2 - \|\zeta\|^2 = \mathcal{L}_R^+ + \mathcal{L}_p^+ - \mathcal{L}_R - \mathcal{L}_p \\ &= \text{tr}(M(I - \underline{\tilde{R}}^+)) - \text{tr}(M(I - \underline{\tilde{R}})) - \bar{\mu}_1 \psi_{\mathfrak{so}(3)}(\underline{\tilde{R}})^\top \underline{\hat{R}} \tilde{b}_\omega + \bar{\mu}_1 \psi_{\mathfrak{so}(3)}(\underline{\tilde{R}}^+)^\top \underline{\hat{R}}^+ \tilde{b}_\omega^+ \\ &< -\delta + \bar{\mu}_1 (\|\psi_{\mathfrak{so}(3)}(\underline{\tilde{R}})\| + \|\psi_{\mathfrak{so}(3)}(\underline{\tilde{R}}R_q)\|) \|\tilde{b}_\omega\| \\ &\leq -\delta + 4\bar{\mu}_1 c_{b_\omega}. \end{aligned}$$

Choosing $\bar{\mu}_1 < \min\{\bar{\mu}_1^*, \delta/4c_{b_\omega}\}$ such that

$$\mathcal{L}(x'^+) \leq \mathcal{L}(x') - \bar{\delta}^*, \quad x' \in \mathcal{J}'_c, \quad (\text{B.50})$$

where $\bar{\delta}^* := -\delta + 4\bar{\mu}_1 c_{b_\omega} > 0$. In view of (B.49) and (B.50), one shows that $0 \leq j \leq J_{\max} := \lceil \mathcal{L}'(0, 0)/\bar{\delta}^* \rceil$ and $\mathcal{L}'(t, j) \leq \mathcal{L}'(0, 0) \exp(-\lambda'_F t)$. One can show that $\mathcal{L}'(x'^+) \leq \exp(-\lambda'_J) \mathcal{L}'(x')$, with $\lambda'_J := -\ln(1 - \bar{\delta}^*/\mathcal{L}'(0, 0))$. Consequently, one obtains

$$\mathcal{L}'(t, j) \leq \exp(-2\lambda'(t+j)) \mathcal{L}'(0, 0), \quad (\text{B.51})$$

where $\lambda' := \frac{1}{2} \min\{\lambda'_F, \lambda'_J\}$. From (B.48) and (B.51), for each $(t, j) \in \text{dom}x'$ one has

$$|x'(t, j)|_{\bar{\mathcal{A}}'} \leq k' \exp(-\lambda'(t+j)) |x'(0, 0)|_{\bar{\mathcal{A}}'}, \quad (\text{B.52})$$

where $k' := \sqrt{\bar{\alpha}/\underline{\alpha}}$. Using the same arguments as in the proof of Theorem 3.2, one can conclude that the solution to the hybrid system \mathcal{H}' is complete. This completes the proof.

Appendix C

Proofs of Chapter 4

C.1 Proof of Proposition 4.2

For each $x_1^c \in \text{SE}_2(3) \times \Psi \times \mathbb{R}^+$, let us rewrite $\tilde{R} = \mathcal{R}_a(\pi, v)$ with $v \in \mathcal{E}(M)$, and $R_q = \mathcal{R}_a(\theta, u_q)$ with $\theta \in (0, \pi]$ and $u_q \in \mathbb{U}$. In view of (4.15) and (4.16), one can show that

$$\begin{aligned}\mu_{\mathbb{Q}}(\hat{R}, r, b) &= \Upsilon(\hat{X}, r, b) - \min_{X_q = \mathcal{T}(R_q, p_q, v_q) \in \mathbb{Q}} \Upsilon(X_q^\top \hat{X}, r, b) \\ &= \text{tr}((I_3 - \tilde{R})M) - \min_{R_q \in \mathcal{R}_a(\theta, \mathbb{U})} \text{tr}((I_3 - \tilde{R}R_q)M) \\ &= \max_{R_q \in \mathcal{R}_a(\theta, \mathbb{U})} \text{tr}(\tilde{R}(I_3 - R_q)M) \\ &= (1 - \cos \theta) \max_{u_q \in \mathbb{U}} \Delta(u_q, v) \\ &\geq (1 - \cos \theta) \max_{u_q \in \mathcal{E}(M)} \Delta(u_q, v),\end{aligned}$$

where we made use of the fact $\max_{u_q \in \mathbb{U}} \Delta(u_q, v) \geq \max_{u_q \in \mathcal{E}(M)} \Delta(u_q, v)$ for any $v \in \mathbb{R}^3$ and the definition (3.13). From the definition of Δ_M^* given in (3.14) such that for any $x_1^c \in \text{SE}_2(3) \times \Psi \times \mathbb{R}^+$, one has

$$\begin{aligned}\mu_{\mathbb{Q}}(\hat{R}, r, b) &\geq (1 - \cos \theta) \min_{v \in \mathcal{E}(M)} \max_{u_q \in \mathcal{E}(M)} \Delta(u, v) \\ &\geq (1 - \cos \theta) \Delta_M^* > \delta,\end{aligned}$$

which gives $\text{SE}_2(3) \times \Psi \times \mathbb{R}^+ \subseteq \mathcal{J}_1^c$ from (4.18) and (4.23). This completes the proof.

C.2 Proof of Theorem 4.1

Consider the following real-valued function $\mathcal{L}_R : \text{SO}(3) \rightarrow \mathbb{R}^+$:

$$\mathcal{L}_R(\tilde{R}) = \text{tr}((I - \tilde{R})M). \quad (\text{C.1})$$

Let $\bar{M} := \frac{1}{2}(\text{tr}(M)I_3 - M)$, $\underline{M} := \text{tr}(\bar{M}^2)I - 2\bar{M}^2$ and $\bar{\underline{M}} := \frac{1}{2}(\text{tr}(\underline{M})I_3 - \underline{M})$. Applying the results in [Berkane et al., 2017b, Lemma 2], one obtains

$$4\lambda_m^{\bar{M}} |\tilde{R}|_I^2 \leq \mathcal{L}_R \leq 4\lambda_M^{\bar{M}} |\tilde{R}|_I^2, \quad (\text{C.2})$$

$$\dot{\mathcal{L}}_R \leq -\lambda_R |\tilde{R}|_I^2 \quad x_1^c \in \mathcal{F}_1^c \quad (\text{C.3})$$

where $\lambda_R := 4k_R \varrho_M \lambda_{\tilde{m}}$, and $\varrho_M := \min_{x_1^c \in \mathcal{F}_1^c} \alpha(M, \tilde{R})$ with $\alpha(\cdot, \cdot)$ defined as per Lemma 2.1. Moreover, one can verify that $\alpha(M, \tilde{R}) > 0$ for all $x_1^c \in \mathcal{F}_1^c$, which implies $\lambda_R > 0$ in the flows.

On the other hand, consider the following real-valued function $\mathcal{L}_p : \mathbb{R}^3 \times \mathbb{R}^3 \rightarrow \mathbb{R}^+$ as

$$\mathcal{L}_p(\tilde{p}_e, \tilde{v}) = \frac{1}{2} \|\tilde{p}_e\|^2 + \frac{1}{2k_c k_v} \|\tilde{v}\|^2 - \mu \tilde{p}_e^\top \tilde{v}. \quad (\text{C.4})$$

with some $\mu > 0$. Let $e_2 := [\|\tilde{p}_e\| \ \|\tilde{v}\|]^\top$. One verifies that

$$e_2^\top \underbrace{\begin{bmatrix} \frac{1}{2} & -\frac{\mu}{2} \\ -\frac{\mu}{2} & \frac{1}{2k_c k_v} \end{bmatrix}}_{P_1} e_2 \leq \mathcal{L}_p \leq e_2^\top \underbrace{\begin{bmatrix} \frac{1}{2} & \frac{\mu}{2} \\ \frac{\mu}{2} & \frac{1}{2k_c k_v} \end{bmatrix}}_{P_2} e_2, \quad (\text{C.5})$$

The time-derivative of \mathcal{L}_p along the flows of (4.23) is given by

$$\begin{aligned} \dot{\mathcal{L}}_p &= \tilde{p}_e^\top (-k_c k_p \tilde{p}_e + \tilde{v}) + \frac{1}{k_c k_v} \tilde{v}^\top (-k_c k_v \tilde{p}_e + (I - \tilde{R})\mathbf{g}) \\ &\quad - \mu (-k_c k_p \tilde{p}_e + \tilde{v})^\top \tilde{v} - \mu \tilde{p}_e^\top (-k_c k_v \tilde{p}_e + (I_3 - \tilde{R})\mathbf{g}) \\ &= -k_c k_p \tilde{p}_e^\top \tilde{p}_e + \mu k_c k_v \tilde{p}_e^\top \tilde{p}_e - \mu \tilde{v}^\top \tilde{v} + \mu k_c k_p \tilde{p}_e^\top \tilde{v} \\ &\quad + \frac{1}{k_c k_v} \tilde{v}^\top (I - \tilde{R})\mathbf{g} - \mu \tilde{p}_e^\top (I_3 - \tilde{R})\mathbf{g} \\ &\leq -(k_p - \mu k_v) k_c \|\tilde{p}_e\|^2 - \mu \|\tilde{v}\| + \mu k_c k_p \|\tilde{p}_e\| \|\tilde{v}\| \\ &\quad + \frac{\mathbf{g}}{k_c k_v} \|\tilde{v}\| \|I - \tilde{R}\|_F + \mu \mathbf{g} \|\tilde{p}_e\| \|I_3 - \tilde{R}\|_F. \end{aligned}$$

Let $c_1 := \max\{\frac{\mathbf{g}}{k_c k_v}, \mu \mathbf{g}\}$, one can further deduce that

$$\dot{\mathcal{L}}_p \leq -e_2^\top \underbrace{\begin{bmatrix} (k_p - \mu k_v) k_c & \frac{\mu k_c k_p}{2} \\ \frac{\mu k_c k_p}{2} & \mu \end{bmatrix}}_{P_3} e_2 + 4c_1 |\tilde{R}|_I \|e_2\| \quad (\text{C.6})$$

where we made use of the facts $\|I_3 - \tilde{R}\|_F^2 = 8|\tilde{R}|_I^2$ and $\|\tilde{v}\| + \|\tilde{p}_e\| \leq \sqrt{2(\|\tilde{v}\|^2 + \|\tilde{p}_e\|)^2} = \sqrt{2} \|e_2\|$. To guarantee that the matrices P_1, P_2 and P_3 are positive definite, it is sufficient to pick μ as

$$0 < \mu < \min \left\{ \frac{1}{\sqrt{k_c k_v}}, \frac{4k_p}{4k_v + k_c k_p^2} \right\}.$$

To show exponential stability, let us consider the following Lyapunov function candidate:

$$\mathcal{L}(x_1^c) := \mathcal{L}_R(\tilde{R}) + \varepsilon \mathcal{L}_p(\tilde{p}_e, \tilde{v}), \quad (\text{C.7})$$

with some $0 < \varepsilon$. Let $|x_1^c|_{\mathcal{A}_1} \geq 0$ denote the distance to the set \mathcal{A}_1 such that $|x_1^c|_{\mathcal{A}_1}^2 := \inf_{y=(\bar{X}, I_3, 0, 0, \bar{t}) \in \mathcal{A}_1} (\|\bar{X} - \hat{X}\|_F^2 + |\tilde{R}|_I^2 + \|\tilde{p}_e\|^2 + \|\tilde{v}\|^2 + \|\bar{t} - t\|^2) = |\tilde{R}|_I^2 + \|\tilde{p}_e\|^2 + \|\tilde{v}\|^2 = |\tilde{R}|_I^2 + \|e_2\|^2$. From (C.2) and (C.5), one has

$$\alpha |x_1^c|_{\mathcal{A}_1}^2 \leq \mathcal{L}(x_1^c) \leq \bar{\alpha} |x_1^c|_{\mathcal{A}_1}^2, \quad (\text{C.8})$$

where $\underline{\alpha} := \min\{4\lambda_m^{\bar{M}}, \varepsilon\lambda_m^{P_1}\}$, $\bar{\alpha} := \max\{4\lambda_M^{\bar{M}}, \varepsilon\lambda_M^{P_2}\}$. From (C.3) and (C.6), one has

$$\begin{aligned}\dot{\mathcal{L}}(x_1^c) &\leq -\lambda_R |\tilde{R}|_I^2 - \varepsilon\lambda_m^{P_3} \|e_2\|^2 + 4\varepsilon c_1 |\tilde{R}|_I \|e_2\| \\ &= -[|\tilde{R}|_I \quad \|e_2\|] \underbrace{\begin{bmatrix} \lambda_R & -2\varepsilon c_1 \\ -2\varepsilon c_1 & \varepsilon\lambda_m^{P_3} \end{bmatrix}}_{P_4} \begin{bmatrix} |\tilde{R}|_I \\ \|e_2\| \end{bmatrix} \\ &\leq -\lambda_F \mathcal{L}(x_1^c),\end{aligned}\tag{C.9}$$

where P_4 is positive definite by choosing $\varepsilon < \lambda_R \lambda_m^{P_3} / (4c_1^2)$, and $\lambda_F := \lambda_m^{P_4} / \bar{\alpha}$ with $\bar{\alpha}$ given in (C.8). In view of the jumps of (4.16)-(4.18), (4.23) and (C.1), one shows

$$\begin{aligned}\mathcal{L}(x_1^{c+}) - \mathcal{L}(x_1^c) &= \mathcal{L}_R(\tilde{R}^+) - \mathcal{L}_R(\tilde{R}) + \varepsilon \mathcal{L}_p(\tilde{p}_e^+, \tilde{v}^+) - \varepsilon \mathcal{L}_p(\tilde{p}_e, \tilde{v}) \\ &= -\Upsilon(\hat{X}, r, b) + \min_{X_q \in \mathbb{Q}} \Upsilon(X_q^\top \hat{X}, r, b) \\ &= -\mu_{\mathbb{Q}}(\hat{X}, r, b) \leq -\delta,\end{aligned}\tag{C.10}$$

where we made use of the facts: $\mathcal{L}_R = \Upsilon(\hat{X}, r, b)$, $\mathcal{L}_R^+ = \min_{X_q \in \mathbb{Q}} \Upsilon(X_q^\top \hat{X}, r, b)$ from (4.15)-(4.16), and $\mathcal{L}_p^+ = \mathcal{L}_p$ from $\tilde{p}_e = \tilde{p}_e$, $\tilde{v}^+ = \tilde{v}$. Using the facts $\mathcal{L}_R^+ - \mathcal{L}_R \leq -\delta$ and (C.3), one has $\mathcal{L}_R(\tilde{R}(t, j)) \leq \dots \leq \mathcal{L}_R(\tilde{R}(0, 0)) - j\delta$, where $(t, j) \in \text{dom}x_1^c$. From (C.2), one obtains $j \leq J := \lceil 4\lambda_M^{\bar{M}} / \delta \rceil$, where $\lceil \cdot \rceil$ denotes the ceiling function. Hence, one can conclude that the number of jumps is finite.

Since the solution of x_1^c is complete and the number of jumps is bounded, the hybrid time domain takes the form $\text{dom}x_1^c = \cup_{j=0}^{J-1} ([t_j, t_{j+1}] \times \{j\}) \cup ([t_J, +\infty) \times \{J\})$. In view of (C.9)-(C.10), one obtains

$$\begin{aligned}\mathcal{L}(x_1^c(t, j)) &\leq \exp(-\lambda_F(t - t_j)) \mathcal{L}(x_1^c(t_j, j)) \leq \exp(-\lambda_F t) \mathcal{L}(x_1^c(0, 0)) \\ &\leq \exp(\lambda_F J) \exp(-\lambda_F(t + j)) \mathcal{L}(x_1^c(0, 0)).\end{aligned}$$

Substituting (C.8), one concludes that for each $(t, j) \in \text{dom}x_1^c$,

$$|x_1^c(t, j)|_{\mathcal{A}_1}^2 \leq \kappa \exp(-\lambda_F(t + j)) |x_1^c(0, 0)|_{\mathcal{A}_1}^2,$$

where $\kappa := \exp(\lambda_F J) \bar{\alpha} / \underline{\alpha}$. This completes the proof.

C.3 Proof of Lemma 4.1

To show uniform observability, we need to explicitly calculate the state transition matrix $\Phi(t, \tau)$. Consider a time-varying rotation matrix $\bar{R}(t)$ with $\bar{R}(0) \in \text{SO}(3)$ and $\dot{\bar{R}}(t) = (-\omega(t))^\times \bar{R}(t)$. Note that $\bar{R}(t)$ does not have to be equal to $R(t)$. Let us introduce the matrices $T(t) = \text{blkdiag}(\bar{R}(t), \bar{R}(t))$, $S(t) = \text{blkdiag}((- \omega(t))^\times, (- \omega(t))^\times)$ and constant matrix $\bar{A} = A(t) - S(t)$. Then, one verifies that $\dot{T}(t) = S(t)T(t)$ and $T(t)\bar{A} = \bar{A}T(t)$. From Lemma 2.7, the state transition matrix $\Phi(t, \tau)$ associated to $A(t)$ can be expressed as

$$\Phi(t, \tau) = T(t)\bar{\Phi}(t, \tau)T^{-1}(\tau)\tag{C.11}$$

with $\bar{\Phi}(t, \tau) = \exp(\bar{A}(t - \tau))$ being the state transition matrix associated to \bar{A} . Using the facts $T^{-1}(\tau) = T^\top(\tau)$, $T^{-1}(\tau)C^\top = C^\top\bar{R}^\top(\tau)$ and $\bar{R}^\top(\tau)\bar{R}(\tau) = I_3$ one obtains

$$\begin{aligned} & \frac{1}{\delta} \int_t^{t+\delta} T(t)\bar{\Phi}(\tau, t)^\top T^{-1}(\tau)C^\top CT(\tau)\bar{\Phi}(\tau, t)T^{-1}(t)d\tau \\ &= T(t) \left(\frac{1}{\delta} \int_t^{t+\delta} \bar{\Phi}(\tau, t)^\top C^\top C\bar{\Phi}(\tau, t)d\tau \right) T^{-1}(t) \end{aligned} \quad (\text{C.12})$$

Note that the pair (\bar{A}, C) is (Kalman) observable, *i.e.*, $\text{rank}[C, C\bar{A}, \dots, C\bar{A}^6] = 6$. Therefore, from Lemma 2.10, there exist positive constants $\bar{\delta}, \bar{\mu}$ such that for all $t \geq 0$ one has $\bar{W}(t, t + \bar{\delta}) = \frac{1}{\bar{\delta}} \int_t^{t+\bar{\delta}} \bar{\Phi}(\tau, t)^\top C^\top C\bar{\Phi}(\tau, t)d\tau \geq \bar{\mu}I_6$. From (C.12), choosing $\delta \geq \bar{\delta}$ and $0 < \mu \leq \frac{\bar{\delta}}{\delta}\bar{\mu}$, one obtains the Observability Gramian as

$$W_O(t, t + \delta) \geq \frac{\bar{\delta}}{\delta} T(t)\bar{W}(t, t + \bar{\delta})T^{-1}(t) \geq \frac{\bar{\delta}}{\delta} I_6 \geq \mu I_6,$$

for all $t \geq 0$, which implies that $(A(t), C)$ is uniformly observable. This completes the proof.

C.4 Proof of Theorem 4.2

The proof of Theorem 4.2 is similar to the proof of Theorem 4.1. Consider the following Lyapunov function candidate:

$$\mathcal{L}(x_2^c) := \mathcal{L}_R(\tilde{R}) + \varepsilon \bar{\mathcal{L}}_p(x), \quad (\text{C.13})$$

with $\varepsilon > 0$, the real-valued function $\mathcal{L}_R(\tilde{R}) = \text{tr}((I - \tilde{R})M)$ defined in (C.1), and the real-valued function $\bar{\mathcal{L}}_p : \mathbb{R}^6 \rightarrow \mathbb{R}^+$ defined as

$$\bar{\mathcal{L}}_p(x) = x^\top P^{-1}x \quad (\text{C.14})$$

It is easy to verify that $\frac{1}{p_M} \|x\|^2 \leq \bar{\mathcal{L}}_p \leq \frac{1}{p_m} \|x\|^2$. Let $|x_2^c|_{\mathcal{A}_2} \geq 0$ denote the distance to the set \mathcal{A}_2 such that $|x_2^c|_{\mathcal{A}_2}^2 := \inf_{y=(\bar{X}, I_3, 0, \bar{t}) \in \mathcal{A}_2} (\|\bar{X} - \hat{X}\|_F^2 + |\tilde{R}|_I^2 + \|x\|^2 + \|\bar{t} - t\|^2) = |\tilde{R}|_I^2 + \|x\|^2$. Recall (C.2), one has

$$\underline{\alpha}|x_2^c|_{\mathcal{A}_2}^2 \leq \mathcal{L}(x_2^c) \leq \bar{\alpha}|x_2^c|_{\mathcal{A}_2}^2, \quad (\text{C.15})$$

where $\underline{\alpha} := \min\{4\lambda_m^{\bar{M}}, \frac{\varepsilon}{p_M}\}$, $\bar{\alpha} := \max\{4\lambda_M^{\bar{M}}, \frac{\varepsilon}{p_m}\}$. Using the fact that $\dot{P}^{-1} = -P^{-1}\dot{P}P^{-1}$, the time-derivative of $\bar{\mathcal{L}}_p$ in the flows is given by

$$\begin{aligned} \dot{\bar{\mathcal{L}}}_p &= x^\top (P^{-1}A + A^\top P^{-1} - 2C^\top Q(t)C + \dot{P}^{-1})x + 2x^\top P^{-1}\nu \\ &\leq -x^\top P^{-1}V(t)P^{-1}x - x^\top C^\top Q(t)Cx + 2x^\top P^{-1}\nu \\ &\leq -\frac{v_m}{p_M^2}x^\top x + \frac{4\sqrt{2}\|g\|}{p_m}\|x\||\tilde{R}|_I \end{aligned} \quad (\text{C.16})$$

where we made use of the facts $-\mathbf{x}^\top C^\top Q(t)C\mathbf{x} \leq 0$, $p_m I_6 \leq P \leq p_M I_6$ and $\|\nu\| \leq \|I - \tilde{R}\|_F \|\mathbf{g}\| = 2\sqrt{2}\|\mathbf{g}\|\|\tilde{R}\|_I$. In view of (C.3) and (C.16), one has

$$\begin{aligned}\dot{\mathcal{L}}(x_2^c) &\leq -\lambda_R |\tilde{R}|_I^2 - \frac{\varepsilon v_m}{p_M^2} \mathbf{x}^\top \mathbf{x} + \frac{4\sqrt{2}\varepsilon \mathbf{g}}{p_m} \|\mathbf{x}\| |\tilde{R}|_I \\ &= - \begin{bmatrix} |\tilde{R}|_I & \|\mathbf{x}\| \end{bmatrix} \underbrace{\begin{bmatrix} \lambda_R & -\frac{2\sqrt{2}\varepsilon \mathbf{g}}{p_m} \\ -\frac{2\sqrt{2}\varepsilon \mathbf{g}}{p_m} & \frac{\varepsilon v_m}{p_M^2} \end{bmatrix}}_{P_4} \begin{bmatrix} |\tilde{R}|_I \\ \|\mathbf{x}\| \end{bmatrix} \\ &\leq -\lambda_F \mathcal{L}(x_2^c), \quad x_2^c \in \mathcal{F}_2^c,\end{aligned}\tag{C.17}$$

where P_4 is positive definite by choosing $\varepsilon < \lambda_R v_m P_m^2 / (8\mathbf{g}^2 p_M^2)$, and $\lambda_F := \lambda_m^{P_4} / \bar{\alpha}$ with $\bar{\alpha}$ given in (C.15). Using the facts $\mathbf{x}^+ = \mathbf{x}$ and $\bar{\mathcal{L}}_p(\mathbf{x}^+) = \bar{\mathcal{L}}_p(\mathbf{x})$, one can also show that

$$\begin{aligned}\mathcal{L}(x_2^{c+}) - \mathcal{L}(x_2^c) &= \mathcal{L}_R(\tilde{R}^+) - \mathcal{L}_R(\tilde{R}) + \varepsilon \bar{\mathcal{L}}_p(\mathbf{x}^+) - \varepsilon \bar{\mathcal{L}}_p(\mathbf{x}) \\ &\leq -\delta, \quad x_2^c \in \mathcal{J}_2^c.\end{aligned}\tag{C.18}$$

Therefore, in view of (C.15), (C.17) and (C.18), the rest proof is completed using similar steps as in the proof of Theorem 4.1.

C.5 Proof of Theorem 4.3

In view of (2.86), (4.10), (4.19), (4.22), (4.32)-(4.33), one has the following hybrid closed-loop system:

$$\mathcal{H}_3^c : \begin{cases} \dot{x}_3^c = F_3(x_3^c) & x_3^c \in \mathcal{F}_3^c \\ x_3^{c+} = G_3(x_3^c) & x_3^c \in \mathcal{J}_3^c \end{cases}\tag{C.19}$$

where the flow and jump sets are defined as $\mathcal{F}_3^c := \{(x_1^c, \hat{b}_\omega, \tilde{b}_\omega) \in \mathcal{S}_3^c : x_1^c \in \mathcal{F}_1^c\}$ and $\mathcal{J}_3^c := \{(x_1^c, \hat{b}_\omega, \tilde{b}_\omega) \in \mathcal{S}_3^c : x_1^c \in \mathcal{J}_1^c\}$, and the flow and jump maps are given by

$$F_3(x_3^c) = \begin{pmatrix} f(\hat{X}, \omega_y - \hat{b}_\omega, a) - \Delta \hat{X} \\ \tilde{R}((\hat{R}\tilde{b}_\omega)^\times - k_R \mathbb{P}_{\mathfrak{so}(3)}(M\tilde{R})) \\ -k_p k_c \tilde{p}_e + \tilde{v} - (\tilde{R}\hat{R}\tilde{b}_\omega)^\times(p - p_c - \tilde{p}_e) \\ -k_v k_c \tilde{p}_e - (\tilde{R}\hat{R}\tilde{b}_\omega)^\times(v - \tilde{v}) + (I_3 - \tilde{R})\mathbf{g} \\ 1 \\ -k_\omega \hat{R}^\top \psi_{\mathfrak{so}(3)}(M\tilde{R}) \\ -k_\omega \hat{R}^\top \psi_{\mathfrak{so}(3)}(M\tilde{R}) \end{pmatrix}, \quad G_3(x_3^c) = \begin{pmatrix} X_g^{-1} \hat{X} \\ \tilde{R}R_q \\ \tilde{v} \\ \tilde{p}_e \\ t \\ \hat{b}_\omega \\ \tilde{b}_\omega \end{pmatrix},$$

where the following facts have been used: $\tilde{p}_e = (p - p_c) - \tilde{R}(\hat{p} - p_c)$, $\tilde{R}(\hat{R}\tilde{b}_\omega)^\times(\hat{p} - p_c) = (\hat{R}\tilde{b}_\omega)^\times \tilde{R}(\hat{p} - p_c) = (\hat{R}\tilde{b}_\omega)^\times(p - p_c - \tilde{p}_e)$, $\tilde{R}(\hat{R}\tilde{b}_\omega)^\times \hat{v} = (\hat{R}\tilde{b}_\omega)^\times \tilde{R}\hat{v} = (\hat{R}\tilde{b}_\omega)^\times(v - \tilde{v})$. Note that the sets $\mathcal{F}_3^c, \mathcal{J}_3^c$ are closed, and $\mathcal{F}_3^c \cup \mathcal{J}_3^c = \mathcal{S}_3^c$. Note also that the closed-loop system (C.19) satisfies the hybrid basic conditions given in Section 2.5.1 and is autonomous by taking ω_y, a, p, v as functions of time.

Consider the real-valued function $\mathcal{V}_R = \text{tr}((I_3 - \tilde{R})M) + \frac{1}{k_\omega} \tilde{b}_\omega^\top \tilde{b}_\omega$, whose time-derivative in the flows is given by

$$\begin{aligned}\dot{\mathcal{V}}_R &= \text{tr}(-\tilde{R}((\hat{R}\tilde{b}_\omega)^\times - k_R \mathbb{P}_{\mathfrak{so}(3)}(M\tilde{R}))M) - 2\tilde{b}_\omega^\top \hat{R}^\top \psi_{\mathfrak{so}(3)}(M\tilde{R}) \\ &= -k_R \|\mathbb{P}_{\mathfrak{so}(3)}(M\tilde{R})\|_F^2 \leq 0\end{aligned}\quad (\text{C.20})$$

where we made use of the facts $\text{tr}(-M\tilde{R}(\hat{R}\tilde{b}_\omega)^\times) = \langle (\hat{R}\tilde{b}_\omega)^\times, M\tilde{R} \rangle = 2\psi_{\mathfrak{so}(3)}(M\tilde{R})^\top \hat{R}\tilde{b}_\omega$ and $\text{tr}(M\tilde{R}\mathbb{P}_{\mathfrak{so}(3)}(M\tilde{R})) = -\langle \mathbb{P}_{\mathfrak{so}(3)}(M\tilde{R}), M\tilde{R} \rangle = -\langle \langle \mathbb{P}_{\mathfrak{so}(3)}(M\tilde{R}), \mathbb{P}_{\mathfrak{so}(3)}(M\tilde{R}) \rangle \rangle$. Then, one concludes that \mathcal{V}_R is non-increasing in the flows. By virtue of Proposition 4.2, for each jump one has

$$\mathcal{V}_R^+ - \mathcal{V}_R \leq -\delta. \quad (\text{C.21})$$

Therefore, for any $x_3^c(0, 0) \in \mathcal{S}_3^c$, there exists $c_{b_\omega} > 0$ such that $c_{b_\omega} := \sup_{(t,j) \succeq (0,0)} \|\tilde{b}_\omega(t, j)\|$ for all $(t, j) \in \text{dom}x_3^c$. Note that $\|\tilde{b}_\omega(t, j)\|^2 \leq \mathcal{V}_R(t, j) \leq \mathcal{V}_R(0, 0)$, which implies that c_{b_ω} is bounded by the initial conditions.

Let us modify the real-valued function $\bar{\mathcal{L}}_R : \text{SO}(3) \times \mathbb{R}^3 \rightarrow \mathbb{R}^+$ as follows:

$$\bar{\mathcal{L}}_R(\tilde{R}, \tilde{b}_\omega) = \mathcal{L}_R(\tilde{R}) + \frac{1}{k_\omega} \tilde{b}_\omega^\top \tilde{b}_\omega - \bar{\mu} \psi_{\mathfrak{so}(3)}(\tilde{R})^\top \hat{R}\tilde{b}_\omega, \quad (\text{C.22})$$

where $\bar{\mu} > 0$. Let $e_1 = [\|\tilde{R}\|_I, \|\tilde{b}_\omega\|]^\top$. Following similar steps as in the proof of [Berkane et al., 2017b, Theorem 1] and Theorem 3.3 in Chapter 3, there exists a constant $\bar{\mu}^*$ such that for all $\bar{\mu} \leq \bar{\mu}^*$ one has

$$\underline{c}_R \|e_1\|^2 \leq \bar{\mathcal{L}}_R \leq \bar{c}_R \|e_1\|^2, \quad (\text{C.23})$$

$$\dot{\bar{\mathcal{L}}}_R \leq -\bar{\lambda}_R \|e_1\|^2 \quad x_3^c \in \mathcal{F}_3^c \quad (\text{C.24})$$

for some positive constants $\underline{c}_R, \bar{c}_R$ and $\bar{\lambda}_R$. From [Berkane et al., 2017b, Theorem 1] and Theorem 3.3 in Chapter 3, the constant $\bar{\lambda}_R$ depends on c_{b_ω} , which is associated to the initial conditions.

On the other hand, we consider the real-valued functions \mathcal{L}_p defined in (C.4). Defining $e_2 := [\|\tilde{p}_e\|, \|\tilde{v}\|]^\top$, one verifies that $e_2^\top P_1 e_2 \leq \mathcal{L}_p \leq e_2^\top P_2 e_2$ as shown in (C.5). From Assumption 4.2, there exist two constants c_p, c_v such that $c_p := \sup_{t \geq 0} \|p - p_c\|$, $c_v := \sup_{t \geq 0} \|v\|$. Then, in the flows of (C.19) one has

$$\begin{aligned}\frac{d}{dt} \|\tilde{p}_e\|^2 &= 2\tilde{p}_e^\top (-k_c k_p \tilde{p}_e + \tilde{v} - (R\tilde{b}_\omega)^\times(p - p_c - \tilde{p}_e)) \\ &\leq -2k_c k_p \|\tilde{p}_e\|^2 + 2c_p \|\tilde{p}_e\| \|\tilde{b}_\omega\| + 2\tilde{p}_e^\top \tilde{v} \\ \frac{d}{dt} \|\tilde{v}\|^2 &= 2\tilde{v}^\top (-k_c k_v \tilde{p}_e - (R\tilde{b}_\omega)^\times(v - \tilde{v}) + (I - \tilde{R})g) \\ &\leq 2(c_v \|\tilde{b}_\omega\| + 2\sqrt{2}g|R\tilde{b}_\omega|) \|\tilde{v}\| - 2k_c k_v \tilde{v}^\top \tilde{p}_e \\ -\frac{d}{dt} \tilde{p}_e^\top \tilde{v} &= (k_c k_p \tilde{p}_e - \tilde{v} + (R\tilde{b}_\omega)^\times(p - p_c - \tilde{p}_e))^\top \tilde{v} \\ &\quad + \tilde{p}_e^\top (k_c k_v \tilde{p}_e + (R\tilde{b}_\omega)^\times(v - \tilde{v}) - (I_3 - \tilde{R})g)\end{aligned}$$

$$\begin{aligned} &\leq -\|\tilde{v}\|^2 + k_c k_p \|\tilde{p}_e\| \|\tilde{v}\| + c_p \|\tilde{v}\| \|\tilde{b}_\omega\| \\ &\quad + k_c k_v \|\tilde{p}_e\|^2 + c_v \|\tilde{b}_\omega\| \|\tilde{p}_e\| + 2\sqrt{2}g |\tilde{R}|_I \|\tilde{p}_e\| \end{aligned}$$

where we made use of the facts: $\|I_3 - \tilde{R}\|_F = 2\sqrt{2}|\tilde{R}|_I$, $((R\tilde{b}_\omega)^\times)^\top = -(R\tilde{b}_\omega)^\times$, $x^\top (R\tilde{b}_\omega)^\times x = 0$, $\forall x \in \mathbb{R}^3$. Let $c_2 := \max\{c_p + \mu c_v, \frac{c_v}{k_c k_v} + \mu c_p\}$, $c_3 := 2\sqrt{2}g \max\{\frac{1}{k_c k_v}, \mu\}$ and $c_4 := \max\{c_2, c_3\}$. Then, the time-derivative of \mathcal{L}_p in the flows of (C.19) satisfies

$$\begin{aligned} \dot{\mathcal{L}}_p &\leq -(k_p - \mu k_v) k_c \|\tilde{p}_e\|^2 - \mu \|\tilde{v}\|^2 + \mu k_c k_p \|\tilde{p}_e\| \|\tilde{v}\| \\ &\quad + c_2 (\|\tilde{p}_e\| + \|\tilde{v}\|) \|\tilde{b}_\omega\| + c_3 (\|\tilde{v}\| + \|\tilde{p}_e\|) |\tilde{R}|_I \\ &\leq -e_2^\top P_3 e_2 + 2c_4 \|e_1\| \|e_2\|, \end{aligned} \quad (\text{C.25})$$

where P_3 is given in (C.6), and the following facts have been used: $|\tilde{R}|_I + \|\tilde{b}_\omega\| \leq \sqrt{2}\|e_1\|$ and $\|\tilde{v}\| + \|\tilde{p}_e\| \leq \sqrt{2}\|e_2\|$. Pick

$$0 < \mu < \min \left\{ \frac{1}{\sqrt{k_c k_v}}, \frac{4k_p}{4k_v + k_c k_p^2} \right\}$$

such that the matrices P_1 , P_2 and P_3 are positive definite.

Consider the following Lyapunov function candidate:

$$\mathcal{L}(x_3^c) := \bar{\mathcal{L}}_R(\tilde{R}, \tilde{b}_\omega) + \varepsilon \mathcal{L}_p(\tilde{p}_e, \tilde{v}), \quad (\text{C.26})$$

where $\varepsilon > 0$. From (C.23) and (C.4), one has

$$\underline{\alpha} \|x_3^c\|_{\mathcal{A}_3}^2 \leq \mathcal{L}(x_3^c) \leq \bar{\alpha} \|x_3^c\|_{\mathcal{A}_3}^2, \quad (\text{C.27})$$

where $\underline{\alpha} := \min\{\underline{c}_R, \varepsilon \lambda_m^{P_1}\}$, $\bar{\alpha} := \max\{\bar{c}_R, \varepsilon \lambda_M^{P_2}\}$. From (C.24) and (C.25), for any $x_3^c \in \mathcal{F}_3^c$ one has

$$\begin{aligned} \dot{\mathcal{L}}(x_3^c) &\leq -\bar{\lambda}_R \|e_1\|^2 - \varepsilon \lambda_m^{P_3} \|e_2\|^2 + 2\varepsilon c_4 \|e_1\| \|e_2\| \\ &= -[\|e_1\| \quad \|e_2\|] \underbrace{\begin{bmatrix} \bar{\lambda}_R & -\varepsilon c_4 \\ -\varepsilon c_4 & \varepsilon \lambda_m^{P_3} \end{bmatrix}}_{P_4} \begin{bmatrix} \|e_1\| \\ \|e_2\| \end{bmatrix} \\ &\leq -\lambda_F \mathcal{L}(x_3^c), \end{aligned} \quad (\text{C.28})$$

where P_4 is positive definite by choosing $\varepsilon < \bar{\lambda}_R \lambda_m^{P_3}/c_4^2$, and $\lambda_F := \lambda_m^{P_4}/\bar{\alpha}$. In view of (4.16)-(4.18), (C.4), (C.19) and (C.22), for any $x_3^c \in \mathcal{J}_3^c$ one has

$$\begin{aligned} &\mathcal{L}(x_3^{c+}) - \mathcal{L}(x_3^c) \\ &= \bar{\mathcal{L}}_R(\tilde{R}^+, \tilde{b}_\omega^+) - \bar{\mathcal{L}}_R(\tilde{R}, \tilde{b}_\omega) + \varepsilon \mathcal{L}_p(\tilde{p}_e^+, \tilde{v}^+) - \varepsilon \mathcal{L}_p(\tilde{p}_e, \tilde{v}) \\ &= -\delta - \bar{\mu} \psi_{\mathfrak{so}(3)}(\tilde{R})^\top \hat{R} \tilde{b}_\omega + \bar{\mu} \psi_{\mathfrak{so}(3)}(\tilde{R} R_q)^\top R_q^\top \hat{R} \tilde{b}_\omega \\ &\leq -\delta + 4\bar{\mu} c_{b_\omega} \end{aligned}$$

where we made use of the results from (C.10), and the fact $\|\psi_{\mathfrak{so}(3)}(\tilde{R})\| \leq 1$ from $\|\psi_{\mathfrak{so}(3)}(\tilde{R})\|^2 = 4|\tilde{R}|_I^2(1 - |\tilde{R}|_I^2) \leq 1$, $\forall |\tilde{R}|_I^2 \in [0, 1]$. Choosing $\bar{\mu} < \min\{\bar{u}^*, \delta/2c_{b_\omega}\}$, one has

$$\mathcal{L}(x_3^{c+}) - \mathcal{L}(x_3^c) \leq -\delta^*, \quad x_3^c \in \mathcal{J}_3^c, \quad (\text{C.29})$$

where $\delta^* := -\delta + 2\bar{\mu}c_{b_\omega} > 0$. In view of (C.28) and (C.29), one has $0 \leq \mathcal{L}(x_3^c(t, j)) \leq \mathcal{L}(x_3^c(0, 0)) - j\delta^*$, which leads to $j \leq J := \lceil \mathcal{L}(x_3^c(0, 0))/\delta^* \rceil$. This implies that the number of jumps is finite. Moreover, one has $\mathcal{L}(x_3^c(t, j)) \leq \exp(-\lambda_F t)\mathcal{L}(x_3^c(0, 0)) \leq \exp(\lambda_F J)\exp(-\lambda_F(t+j))\mathcal{L}(x_3^c(0, 0))$. Substituting (C.27), one concludes that for each $(t, j) \in \text{dom}x_3^c$,

$$|x_3^c(t, j)|_{\mathcal{A}_3}^2 \leq \kappa \exp(-\lambda_F(t+j)) |x_3^c(0, 0)|_{\mathcal{A}_3}^2,$$

where $\kappa := \exp(\lambda_F J)\bar{\alpha}/\underline{\alpha}$. This completes the proof.

C.6 Proof of Theorem 4.4

The proof of Theorem 4.4 is similar to the proof of Theorem 4.2 and Theorem 4.3. In view of (4.19), (4.22), (4.35)–(4.38) and (2.116), one obtains the following hybrid closed-loop system:

$$\mathcal{H}_4^c : \begin{cases} \dot{x}_4^c = F_4(x_4^c) & x_4^c \in \mathcal{F}_4^c \\ x_4^{c+} = G_4(x_4^c) & x_4^c \in \mathcal{J}_4^c \end{cases} \quad (\text{C.30})$$

where the flow and jump sets are defined as $\mathcal{F}_4^c := \{(x_2^c, \hat{b}_\omega, \tilde{b}_\omega) \in \mathcal{S}_4^c : x_2^c \in \mathcal{F}_2^c\}$ and $\mathcal{J}_4^c := \{(x_2^c, \hat{b}_\omega, \tilde{b}_\omega) \in \mathcal{S}_4^c : x_2^c \in \mathcal{J}_2^c\}$ with $\mathcal{F}_2^c, \mathcal{J}_2^c$ given in (4.31), and the flow and jump maps are given by

$$F_4(x_4^c) = \begin{pmatrix} f(\hat{X}, \omega_y - \hat{b}_\omega, a) - \Delta\hat{X} \\ \tilde{R}(-k_R \mathbb{P}_{\mathfrak{so}(3)}(M\tilde{R})) \\ A\mathbf{x} - KC\mathbf{x} + \nu \\ 1 \\ -k_\omega \hat{R}^\top \psi_{\mathfrak{so}(3)}(M\tilde{R}) \\ -k_\omega \hat{R}^\top \psi_{\mathfrak{so}(3)}(M\tilde{R}) \end{pmatrix}, \quad G_4(x_4^c) = \begin{pmatrix} X_g^{-1}\hat{X} \\ RR_q \\ \mathbf{x} \\ t \\ \hat{b}_\omega \\ \tilde{b}_\omega \end{pmatrix}.$$

Note that the sets $\mathcal{F}_4^c, \mathcal{J}_4^c$ are closed, and $\mathcal{F}_4^c \cup \mathcal{J}_4^c = \mathcal{S}_4^c$. Note also that the closed-loop system (4.31) satisfies the hybrid basic conditions given in Section 2.5.1 and is autonomous by taking ω_y, a, A and K as functions of t . Consider the following Lyapunov function candidate:

$$\mathcal{L}(x_4^c) := \bar{\mathcal{L}}_R(\tilde{R}, \tilde{b}_\omega) + \varepsilon \bar{\mathcal{L}}_p(\mathbf{x}), \quad (\text{C.31})$$

where $\varepsilon > 0$, the real-valued function $\bar{\mathcal{L}}_R$ is defined in (C.22) and the real-valued function $\bar{\mathcal{L}}_p$ is defined in (C.14). It is easy to verify that $\frac{1}{p_M} \|\mathbf{x}\|^2 \leq \bar{\mathcal{L}}_p \leq \frac{1}{p_m} \|\mathbf{x}\|^2$. Using the fact $\frac{1}{p_M} \|\mathbf{x}\|^2 \leq \bar{\mathcal{L}}_p \leq \frac{1}{p_m} \|\mathbf{x}\|^2$ and property (C.23), one has

$$\underline{\alpha}|x_4^c|_{\mathcal{A}_4}^2 \leq \mathcal{L}(x_4^c) \leq \bar{\alpha}|x_4^c|_{\mathcal{A}_4}^2, \quad (\text{C.32})$$

where $\underline{\alpha} := \min\{\underline{\mathcal{L}}_R, \frac{\varepsilon}{p_M}\}$, $\bar{\alpha} := \max\{\bar{\mathcal{L}}_R, \frac{\varepsilon}{p_m}\}$. Using the facts $c_p := \sup_{t \geq 0} \|p - p_c\|$, $c_v := \sup_{t \geq 0} \|v\|$ and $\|e_1\|^2 = |\tilde{R}|_I^2 + \|\tilde{b}_\omega\|^2$, one can show that $\|\nu\|^2 \leq (c_p + c_v)\|\tilde{b}_\omega\|^2 + 8\|\mathbf{g}\|^2|\tilde{R}|_I^2 \leq c_5^2\|e_1\|^2$ with $c_5 := \max\{\sqrt{c_p + c_v}, 2\sqrt{2}\|\mathbf{g}\|\}$. Then, the time-derivative of $\bar{\mathcal{L}}_p$ in the flows is given by

$$\dot{\bar{\mathcal{L}}}_p = \mathbf{x}^\top (P^{-1}A + A^\top P^{-1} - 2C^\top Q(t)C + \dot{P}^{-1})\mathbf{x} + 2\mathbf{x}^\top P^{-1}\nu$$

$$\begin{aligned}
&\leq -\mathbf{x}^\top P^{-1}V(t)P^{-1}\mathbf{x} - \mathbf{x}^\top C^\top Q(t)C\mathbf{x} + 2\mathbf{x}^\top P^{-1}\nu \\
&\leq -\frac{v_m}{p_M^2}\mathbf{x}^\top \mathbf{x} + \frac{2c_5}{p_m}\|\mathbf{x}\|\|e_1\|
\end{aligned} \tag{C.33}$$

where we made use of the facts $-\mathbf{x}^\top C^\top Q(t)C\mathbf{x} \leq 0$ and $\|\nu\| \leq c_5\|e_1\|$. From (C.24) and (C.33), one obtains

$$\begin{aligned}
\dot{\mathcal{L}}(x_4^c) &\leq -\bar{\lambda}_R\|e_1\|^2 - \frac{\varepsilon v_m}{p_M^2}\mathbf{x}^\top \mathbf{x} + \frac{2\varepsilon c_5}{p_m}\|e_1\|\|\mathbf{x}\| \\
&= -[\|e_1\| \quad \|\mathbf{x}\|] \underbrace{\begin{bmatrix} \bar{\lambda}_R & -\frac{\varepsilon c_5}{p_m} \\ -\frac{\varepsilon c_5}{p_m} & \frac{\varepsilon v_m}{p_M^2} \end{bmatrix}}_{P_4} \begin{bmatrix} \|e_1\| \\ \|\mathbf{x}\| \end{bmatrix} \\
&\leq -\lambda_F \mathcal{L}(x_4^c), \quad x_4^c \in \mathcal{F}_4^c,
\end{aligned} \tag{C.34}$$

where P_4 is positive definite by choosing $\varepsilon < \bar{\lambda}_R v_m p_m^2 / (c_5^2 p_M^2)$, and $\lambda_F := \lambda_m^{P_4} / \bar{\alpha}$ with $\bar{\alpha}$ given in (C.32). In view of (4.16)-(4.18), (C.14), (C.22) and (C.30), for any $x_4^c \in \mathcal{J}_4^c$ one has

$$\begin{aligned}
&\mathcal{L}(x_4^{c+}) - \mathcal{L}(x_4^c) \\
&= \bar{\mathcal{L}}_R(\tilde{R}^+, \tilde{b}_\omega^+) - \bar{\mathcal{L}}_R(\tilde{R}, \tilde{b}_\omega) + \varepsilon \bar{\mathcal{L}}_p(\mathbf{x}^+) - \varepsilon \bar{\mathcal{L}}_p(\mathbf{x}) \\
&= -\delta - \bar{\mu} \psi_{\mathfrak{so}(3)}(\tilde{R})^\top \hat{R} \tilde{b}_\omega + \bar{\mu} \psi_{\mathfrak{so}(3)}(\tilde{R} R_q)^\top R_q^\top \hat{R} \tilde{b}_\omega \\
&\leq -\delta + 2\bar{\mu} c_{b_\omega}
\end{aligned}$$

where we made use of the results from (C.10), and the fact $\|\psi_{\mathfrak{so}(3)}(\tilde{R})\| \leq 1$. Choosing $\bar{\mu} < \min\{\bar{u}^*, \delta/2c_{b_\omega}\}$, one has

$$\mathcal{L}(x_4^{c+}) - \mathcal{L}(x_4^c) \leq -\delta^*, \quad x_4^c \in \mathcal{J}_4^c, \tag{C.35}$$

where $\delta^* := -\delta + 2\bar{\mu} c_{b_\omega} > 0$. In view of (C.32), (C.34) and (C.35), the rest of the proof can be completed by using similar steps as in the proof of Theorem 4.3.

C.7 Proof of Lemma 4.3

For the sake of simplicity, let $\varpi := \omega_y - \hat{b}_\omega = \omega - \tilde{b}_\omega$. From (4.43) and (C.20)-(C.21), one shows that \tilde{b}_ω and $\dot{\tilde{b}}_\omega$ are bounded. Moreover, from Assumption 4.2 and Assumption 4.3, one obtains that ω and $\dot{\omega}$ are uniformly bounded. Hence, one can show that the time-derivatives of ϖ and A are well-defined and bounded for all $t \geq 0$. Define $N_0 = C$, $N_1 = N_0 A$ and $N_2 = N_1 A + \dot{N}_1$. From Lemma (2.8), condition (2.111) is satisfied if there exist a (strictly) positive constant $\bar{\mu}$ such that

$$\mathcal{O}(\tau)^\top \mathcal{O}(\tau) \geq \bar{\mu} I_9, \quad \forall t \geq 0 \tag{C.36}$$

where

$$\mathcal{O} = \begin{bmatrix} N_0 \\ N_1 \\ N_2 \end{bmatrix} = \begin{bmatrix} I_3 & 0_{3 \times 3} & 0_{3 \times 3} \\ -\varpi^\times & I_3 & 0_{3 \times 3} \\ (\varpi^\times)^2 - \dot{\varpi}^\times & -2\varpi^\times & I_3 \end{bmatrix}$$

It is easy to verify that matrix \mathcal{O} is well-defined and has full rank (*i.e.*, $\det(\mathcal{O}) = 1$) for all $t \geq 0$. This implies that there exists a constant $\bar{\mu} > 0$ such that $\mathcal{O}(t)^\top \mathcal{O}(t) \geq \bar{\mu} I_9, \forall t \geq 0$. Therefore, applying Lemma (2.8) one can conclude that condition (2.111) is satisfied. It follows that the pair $(A(t), C)$ is uniformly observable. This completes the proof.

Appendix D

Proofs of Chapter 5

D.1 Solving the infinite-dimensional problem

In this subsection, we provide a procedure motivated by [Sferlazza et al., 2019] to solve the infinite-dimensional problem $\Xi_P(\tau) < 0$, for all $\tau \in [T_m, T_M]$. First, let $(\lambda_i(\tau), v_i(\tau)) \in \mathbb{R} \times \mathbb{S}^{n-1}$ be the i -th pair of eigenvalue and eigenvector of the matrix $\Xi_P(\tau)$ such that $\lambda_i(\tau)v_i(\tau) = \Xi_P(\tau)v_i(\tau)$. This implies that $\lambda_i(\tau) = v_i^\top(\tau)\Xi_P(\tau)v_i(\tau)$ is a continuous function of τ . Taking partial derivative with respect to τ on both sides of $\lambda_i(\tau) = v_i^\top(\tau)\Xi_P(\tau)v_i(\tau)$, one has

$$\begin{aligned}\frac{\partial \lambda_i(\tau)}{\partial \tau} &= v_i^\top(\tau) \frac{\partial \Xi_P(\tau)}{\partial \tau} v_i(\tau) + 2v_i^\top(\tau)\Xi_P(\tau) \frac{\partial v_i(\tau)}{\partial \tau} \\ &= v_i^\top(\tau) \frac{\partial \Xi_P(\tau)}{\partial \tau} v_i(\tau) + 2\lambda_i(\tau)v_i^\top(\tau) \frac{\partial v_i(\tau)}{\partial \tau} \\ &= v_i^\top(\tau) \frac{\partial \Xi_P(\tau)}{\partial \tau} v_i(\tau)\end{aligned}$$

where we made use of the facts $\|v_i(\tau)\| = 1$, $v_i^\top(\tau) \frac{\partial v_i(\tau)}{\partial \tau} = 0$ and $\lambda_i(\tau)v_i(\tau) = \Xi_P(\tau)v_i(\tau)$ for all τ . Using the definition of Ξ_P in (5.8) and the fact that $\partial \hat{\Phi}(\tau)/\partial \tau = e^{A\tau}A = Ae^{A\tau}$, the first-order derivatives of $\lambda_i(\tau)$ with respect to τ is given as

$$\begin{aligned}\left| \frac{\partial \lambda_i(\tau)}{\partial \tau} \right| &= \left| v_i^\top(\tau) \frac{\partial \Xi_P(\tau)}{\partial \tau} v_i(\tau) \right| \\ &= v_i^\top(\tau)(I - KC)^\top e^{A^\top \tau}(A^\top P + PA)e^{A\tau}(I - KC)v_i(\tau) \\ &\leq 2\|P\|\|A\|\|e^{A\tau}\|^2\|I - KC\|^2 := \delta_P^*.\end{aligned}$$

Then, according to [Sferlazza et al., 2019, Lemma 4], there exist a constant $\mu > 0$ and a value $\bar{\tau} \in [T_m, T_M]$ such that $\Xi_P(\bar{\tau}) < -2\mu I$, then the maximum eigenvalue of $\Xi_P(\tau)$ cannot be greater than $-\mu$ as long as $\tau \in [\bar{\tau} - \frac{\mu}{\delta_P^*}, \bar{\tau} + \frac{\mu}{\delta_P^*}]$.

The following procedure adapted from [Sferlazza et al., 2019, Algorithm 1] is presented to solve the infinite-dimensional problem in a finite number of steps:

Step 1: Obtain an exponential bound on $e^{A\tau}, \forall \tau \in [T_m, T_M]$ by finding a solution $\Pi = \Pi^\top > 0$ and $\beta > 0$ satisfying

$$(-A + \beta I)^\top \Pi + \Pi(-A + \beta I) > 0 \tag{D.1}$$

From [Sferlazza et al., 2019, Lemma 3], one can show that $\|e^{A\tau}\| \leq \gamma e^{\beta\tau} \leq \gamma e^{\beta T_M} := c_A$, $\forall \tau \in [T_m, T_M]$ with $\gamma := \sqrt{\lambda_M(\Pi)/\lambda_m(\Pi)}$.

Step 2: Solve the finite-dimensional optimization problem with a constant $\mu > 0$ and a discrete set $\mathcal{T} \subset [T_m, T_M]$ (initially $\mathcal{T} = \{T_m, T_M\}$)

$$\begin{aligned} (P^*, \bar{p}^*) &= \arg \min_{P=P^\top, \bar{p}} \bar{p}, \text{ subject to} \\ \Xi_P(\tau) &< -2\mu I, \tau \in \mathcal{T} \\ I &\leq P \leq \bar{p}I \end{aligned} \quad (\text{D.2})$$

Step 3: Let $\delta_{\mathcal{T}}^* := \mu(2\bar{p}^*c_A^2\|A\|\|I - CK\|^2)^{-1}$, and define a finite discrete set $\mathcal{T}_d = [T_m : 2\delta_{\mathcal{T}}^* : T_M]$. Check the eigenvalue conditions

$$\Xi_{P^*}(\tau) < -\mu I, \quad \forall \tau \in \mathcal{T}_d \quad (\text{D.3})$$

If these steps are successful, the solution P^* from Step 2 is a solution of the infinite-dimensional problem $\Xi_P(\tau) < 0$ for all $\tau \in [T_m, T_M]$ and the algorithm stops. Otherwise, add a worst-case value $\tau = \arg \max_{\tau \in \mathcal{T}_d} (\lambda_M(\Xi_{P^*}(\tau)))$ to the discrete set \mathcal{T} and restarts from Step 2 again.

Note that if the infinite-dimensional problem $\Xi_P(\tau) < 0, \forall \tau \in [T_m, T_M]$ is not feasible, one has to redesign the gain matrix K such that this optimization problem is feasible. The finite-dimensional optimization problem (D.2) and (D.1) can be solved by a convex optimization solver like CVX [Grant et al., 2009].

D.2 Proof of Lemma 5.1

From the definition of y_i given in (5.4), one has

$$\begin{aligned} \sum_{i=1}^N k_i(p_i - \bar{p} - \bar{R}y_i) &= \sum_{i=1}^N k_i(p_i - \bar{p} - \bar{R}R^\top(p_i - p)) \\ &= k_c(p_c - \bar{p} - \bar{R}R^\top(p_c - p)), \end{aligned} \quad (\text{D.4})$$

where we made use of $k_c = \sum_{i=1}^N k_i$ and $k_c p_c = \sum_{i=1}^N k_i p_i$. This implies (5.7).

On the other hand, one can show that

$$\begin{aligned} \sum_{i=1}^N k_i(p_i - p_c)^\times (p_i - \bar{p} - \bar{R}y_i) &= \sum_{i=1}^N k_i(p_i - p_c)^\times (p_i - \bar{p} - \bar{R}R^\top(p_i - p)) \\ &= \sum_{i=1}^N k_i(p_i - p_c)^\times (I - \bar{R}R^\top)p_i \\ &= \sum_{i=1}^N k_i(p_i - p_c)^\times (I - \bar{R}R^\top)(p_i - p_c), \end{aligned} \quad (\text{D.5})$$

where we made use of $\sum_{i=1}^N k_i p_i = \sum_{i=1}^N k_i p_c$, (i.e., $\sum_{i=1}^N k_i(p_i - p_c) = 0$). From the facts $(p_i - p_c)^\times (p_i - p_c) = 0$ and $-(p_i - p_c)^\times \bar{R} R^\top (p_i - p_c) = (\bar{R} R^\top (p_i - p_c))^\times (p_i - p_c)$, one can further show that

$$\sum_{i=1}^N k_i(p_i - p_c)^\times (p_i - \bar{p} - \bar{R} y_i) = \sum_{i=1}^N k_i(\bar{R} R^\top (p_i - p_c))^\times (p_i - p_c). \quad (\text{D.6})$$

Applying the property (2.46) in Lemma 2.2 and the definition of M , one obtains that

$$\sum_{i=1}^N k_i(p_i - p_c)^\times (p_i - \bar{p} - \bar{R} y_i) = 2\psi_{\mathfrak{so}(3)}(M R \bar{R}^\top), \quad (\text{D.7})$$

which gives (5.6). This completes the proof.

D.3 Proof of Theorem 5.1

First, we are going to show that $|\tilde{R}(t)|_I < 1, \forall t \geq 0$ for any $|\tilde{R}(0)|_I < \sqrt{\varsigma_M}$ and some $k_R > 0$. This step guarantees that the innovation term $\sigma_R = k_R \psi_{\mathfrak{so}(3)}(M \tilde{R})$ vanishes only at $\tilde{R} = I_3$ excluding the undesired critical points $\tilde{R} = \mathcal{R}_a(\pi, v \in \mathcal{E}(M))$. It is clear that for any $|\tilde{R}(0)|_I < \sqrt{\varsigma_M}$, there exists a constant $0 \leq \epsilon^* < 1$ such that $|\tilde{R}(0)|_I^2 = \epsilon^* \varsigma_M$.

Consider the following real-valued function on $\mathfrak{U} \times [0, T_M]$:

$$\mathcal{W} = \frac{1}{2} \text{tr}((I - \tilde{R})M) - \tau \eta^\top \psi_{\mathfrak{so}(3)}(M \tilde{R}) + \mu e^\tau \eta^\top \eta \quad (\text{D.8})$$

with some $\mu > 0$. Let $\zeta := [|\tilde{R}|_I, \|\eta\|]^\top$ such that $\|\zeta\|^2 = |\tilde{R}|_I^2 + \|\eta\|^2$. Using the properties (2.37) and (2.38), one has $\|\psi_{\mathfrak{so}(3)}(M \tilde{R})\|^2 \leq \text{tr}((I - \tilde{R})W) \leq 4\lambda_M^{\bar{W}} |\tilde{R}|_I^2$ with $\bar{W} = \frac{1}{2}(\text{tr}(W)I - W)$. For all $\tau \geq 0$, one obtains the following inequalities:

$$\lambda_m^{P_1} \|\zeta\|^2 \leq \mathcal{W} \leq \lambda_M^{P_2} \|\zeta\|^2, \quad (\text{D.9})$$

where the matrices P_1 and P_2 are given by

$$P_1 = \begin{bmatrix} 2\lambda_m^{\bar{M}} & -\sqrt{\lambda_M^{\bar{W}}} T_M \\ -\sqrt{\lambda_M^{\bar{W}}} T_M & \mu \end{bmatrix}, \quad P_2 = \begin{bmatrix} 2\lambda_M^{\bar{M}} & \sqrt{\lambda_M^{\bar{W}}} T_M \\ \sqrt{\lambda_M^{\bar{W}}} T_M & \mu e^{T_M} \end{bmatrix}.$$

To guarantee that matrices P_1 and P_2 are positive definite, it is sufficient to choose $\mu > \frac{1}{2}\lambda_M^{\bar{W}} T_M^2 / \lambda_m^{\bar{M}}$. The minimum eigenvalue of P_1 is explicitly given by

$$\begin{aligned} \lambda_m^{P_1} &= \lambda_m^{\bar{M}} + \frac{\mu}{2} - \frac{1}{2} \sqrt{(2\lambda_m^{\bar{M}} + \mu)^2 - 4(2\lambda_m^{\bar{M}}\mu - \lambda_M^{\bar{W}} T_M^2)} \\ &= \lambda_m^{\bar{M}} + \frac{\mu}{2} - \frac{1}{2} \sqrt{(2\lambda_m^{\bar{M}} - \mu)^2 + 4\lambda_M^{\bar{W}} T_M^2} \end{aligned}$$

It is easy to verify that $\lambda_m^{P_1} < \min\{2\lambda_m^{\bar{M}}, \mu\} \leq 2\lambda_m^{\bar{M}}$, $\partial \lambda_m^{P_1} / \partial \mu > 0$ for all $\mu > 0$, and $\lambda_m^{P_1} \rightarrow 2\lambda_m^{\bar{M}}$ as $\mu \rightarrow +\infty$. Hence, given a constant $0 \leq \epsilon^* < 1$, it is always possible to

find a constant $\mu_{\epsilon^*} > \frac{1}{2}\lambda_M^{\bar{W}}T_M^2/\lambda_m^{\bar{M}}$ (depending on ϵ^*) such that, for any $\mu \geq \mu_{\epsilon^*}$, one has $\lambda_m^{P_1} \geq 2\epsilon^*\lambda_m^{\bar{M}} = 2\epsilon^*\varsigma_M\lambda_M^{\bar{M}}$. Then, the time-derivative of \mathcal{W} along the flows of (5.16) is given by

$$\begin{aligned}\dot{\mathcal{W}} &= \frac{1}{2}\text{tr}(M\tilde{R}\eta^\times) + \eta^\top\psi_{\mathfrak{so}(3)}(M\tilde{R}) + \tau\eta^\top E(M\tilde{R})\eta^\top - \mu e^\tau\eta^\top\eta \\ &\leq T_M\|M\|_F\eta^\top\eta^\top - \mu\eta^\top\eta,\end{aligned}$$

where we made use of the properties (2.44) and (2.42), and the facts: $e^\tau \geq 1$ for all $\tau \geq 0$ and $\text{tr}(M\tilde{R}\eta^\times) = -\langle\langle M\tilde{R}, \eta^\times \rangle\rangle = -2\eta^\top\psi_{\mathfrak{so}(3)}(M\tilde{R})$. Choosing $\mu > \max\{\mu_{\epsilon^*}, T_M\|M\|_F\}$, one obtains

$$\dot{\mathcal{W}} \leq (T_M\|M\|_F - \mu)\eta^\top\eta \leq 0, \quad (\text{D.10})$$

which implies that $\dot{\mathcal{W}}$ is negative semidefinite and \mathcal{W} is non-increasing in the flows.

Let \mathcal{W}^+ be the value of \mathcal{W} after each jump at $\tau = 0$. Then, one can show that

$$\begin{aligned}\mathcal{W}^+ - \mathcal{W} &= \frac{1}{2}\text{tr}((I - \tilde{R}^+)M) - \frac{1}{2}\text{tr}((I - \tilde{R})M) \\ &\quad - \nu(\eta^+)^{\top}\psi_{\mathfrak{so}(3)}(M\tilde{R}^+) + \tau\eta^{\top}\psi_{\mathfrak{so}(3)}(M\tilde{R}) + \mu e^\nu\|\eta^+\|^2 - \mu e^\tau\|\eta\|^2 \\ &\leq -k_R(T_m - \mu e^{T_M}k_R)\|\psi_{\mathfrak{so}(3)}(M\tilde{R})\|^2 - \mu\|\eta\|^2\end{aligned}$$

where $\nu := \tau^+ \in [T_m, T_M]$, and we made use of the facts $\tilde{R}^+ = \tilde{R}$ and $\eta^+ = k_R\psi_{\mathfrak{so}(3)}(M\tilde{R})$. Let $k_R^* := \frac{1}{\mu}T_m e^{-T_M}$, which is dependent on ϵ^* and then $|\tilde{R}(0)|_I$. Choosing $k_R < k_R^*$, one has $\varrho^* := T_m - \mu e^{T_M}k_R > 0$. Therefore, one can further show that

$$\mathcal{W}^+ - \mathcal{W} \leq -k_R\varrho^*\|\psi_{\mathfrak{so}(3)}(M\tilde{R})\|^2 - \mu\|\eta\|^2, \quad (\text{D.11})$$

which implies that \mathcal{W} is non-increasing after each jump. From (D.9) and (D.11), one can show that $\mathcal{W}(t) \leq \mathcal{W}(0)$ for all $t \geq 0$. From the initial conditions $\|\eta(0)\| = 0$ and $|\tilde{R}(0)|_I^2 < \epsilon^*\varsigma_M$, one can show that

$$|\tilde{R}|_I^2 \leq \frac{1}{\lambda_m^{P_1}}\mathcal{W}(0) \leq \frac{1}{\epsilon^*\varsigma_M}|\tilde{R}(0)|_I^2 < 1, \quad \forall t \geq 0, \quad (\text{D.12})$$

where we made use of the facts $\|\eta(0)\| = 0$, $\mathcal{W} \geq \lambda_m^{P_1}(|\tilde{R}|_I^2 + \|\eta\|^2) \geq \lambda_m^{P_1}|\tilde{R}|_I^2$, $\mathcal{W}(0) \leq 2\lambda_M^{\bar{M}}|\tilde{R}(0)|_I^2$, and $\lambda_m^{P_1} \geq 2\epsilon^*\varsigma_M\lambda_M^{\bar{M}}$.

Now, we are going to show exponential stability of the set \mathcal{A} . Since $|\tilde{R}|_I < 1, \forall t \geq 0$, there exists a constant $0 < \varepsilon < 1$ such that $|\tilde{R}|_I^2 \leq 1 - \varepsilon$ for all $t \geq 0$. Then, it follows that $\|\psi_{\mathfrak{so}(3)}(M\tilde{R})\|^2 \geq 2(1 - |\tilde{R}|_I^2)\lambda_m^{\bar{W}}|\tilde{R}|_I^2 \geq \varepsilon\lambda_m^{\bar{W}}|\tilde{R}|_I^2$. From (D.9) and (D.11), it follows that

$$\begin{aligned}\mathcal{W}^+ &\leq \mathcal{W} - k_R\varrho^*\lambda_m^{\bar{W}}\varepsilon|\tilde{R}|_I^2 - \mu\|\eta\|^2 \\ &\leq \left(1 - \frac{c_1}{\lambda_M^{P_2}}\right)\mathcal{W} = e^{-c_2}\mathcal{W}\end{aligned} \quad (\text{D.13})$$

with $c_1 := \min\{k_R \varrho^* \lambda_m^{\bar{W}} \varepsilon, \mu\}$ and $c_2 := -\ln(1 - c_1/\lambda_M^{P_2})$. Since $\mathcal{W}^+ \geq 0$, one can show that $0 < 1 - c_1/\lambda_M^{P_2} < 1$ and then $c_2 > 0$. Consider the following real-valued function on $\text{SO}(3) \times \mathbb{R}^3 \times [0, T_M]$:

$$\mathcal{V}_1(\tilde{R}, \eta, \tau) = e^{\lambda_1^F \tau} \mathcal{W} \quad (\text{D.14})$$

with $0 < \lambda_1^F < c_2/T_M$. In view of (D.9), (D.10) and (D.13), one can show that

$$\underline{\alpha}_1 \|\zeta\|^2 \leq \mathcal{V}_1 \leq \bar{\alpha}_1 \|\zeta\|^2 \quad (\text{D.15})$$

$$\dot{\mathcal{V}}_1 \leq -\lambda_1^F \mathcal{V}_1 \quad (\text{D.16})$$

$$\mathcal{V}_1^+ \leq e^{-\lambda_1^J} \mathcal{V}_1 \quad (\text{D.17})$$

where $\underline{\alpha}_1 := \lambda_m^{P_1}$, $\bar{\alpha}_1 := e^{(\lambda_1^F T_M)} \lambda_M^{P_2}$, $\lambda_1^J := c_2 - \lambda_1^F T_M > 0$, and we made use of the facts: $\mathcal{V}_1^+ = e^{\lambda_1^F \tau^+} \mathcal{W}^+ \leq e^{(\lambda_1^F T_M - c_2)} \mathcal{W}$ and $\mathcal{W} \leq \mathcal{V}_1$.

Next, let us consider the following real-valued function:

$$\mathcal{V}_2(\mathbf{x}) = e^{\lambda_2^F \tau} \mathbf{x}^\top \hat{\Phi}^\top(\tau) P \hat{\Phi}(\tau) \mathbf{x}. \quad (\text{D.18})$$

One can easily verify that there exist two positive constants $\underline{\alpha}_2, \bar{\alpha}_2$ such that

$$\underline{\alpha}_2 \|\mathbf{x}\|^2 \leq \mathcal{V}_2(\mathbf{x}, \tau) \leq \bar{\alpha}_2 \|\mathbf{x}\|^2 \quad (\text{D.19})$$

with

$$\underline{\alpha}_2 := \min_{\tau \in [0, T_M]} e^{\lambda_2^F \tau} \lambda_m^{(\hat{\Phi}^\top(\tau) P \hat{\Phi}(\tau))}, \quad \bar{\alpha}_2 := \max_{\tau \in [0, T_M]} e^{\lambda_2^F \tau} \lambda_M^{(\hat{\Phi}^\top(\tau) P \hat{\Phi}(\tau))}.$$

The time-derivative of \mathcal{V}_2 along the flows of (5.16) is given by

$$\begin{aligned} \dot{\mathcal{V}}_2 &= -\lambda_2^F \mathcal{V}_2 + e^{\lambda_2^F \tau} \mathbf{x}^\top \hat{\Phi}^\top(\tau) (A^\top P + PA) \hat{\Phi}(\tau) \mathbf{x} \\ &\quad + e^{\lambda_2^F \tau} \mathbf{x}^\top (\dot{\hat{\Phi}}^\top(\tau) P \hat{\Phi}(\tau) + \hat{\Phi}^\top(\tau) P \dot{\hat{\Phi}}(\tau)) \mathbf{x} \\ &\leq -\lambda_2^F \mathcal{V}_2 \end{aligned} \quad (\text{D.20})$$

where we made use of the facts $A \hat{\Phi}(\tau) = \hat{\Phi}(\tau) A$ and $\dot{\hat{\Phi}}(\tau) = -A \hat{\Phi}(\tau)$. Since $\Xi_P(\nu) < 0, \forall \nu \in [T_m, T_M]$, there exists a positive small enough scalar $c_q < p_M := \lambda_M^P$ such that $\Xi_P(\nu) \leq -c_q I, \forall \nu \in [T_m, T_M]$. Then, after each jump one has

$$\begin{aligned} \mathcal{V}_2(\mathbf{x}^+) &= \mathbf{x}^\top (e^{\lambda_2^F \nu} (I - KC)^\top \hat{\Phi}(\nu)^\top P \hat{\Phi}(\nu) (I - KC)) \mathbf{x} \\ &= e^{\lambda_2^F \nu} \mathbf{x}^\top \Xi_P(\nu) \mathbf{x} + e^{\lambda_2^F \nu} \mathbf{x}^\top P \mathbf{x} \\ &\leq -e^{\lambda_2^F \nu} c_q \mathbf{x}^\top \mathbf{x} + e^{\lambda_2^F \nu} p_M \mathbf{x}^\top \mathbf{x} \\ &= (p_M - c_q) e^{\lambda_2^F \nu} \|\mathbf{x}\|^2 \\ &\leq \frac{p_M - c_q}{\bar{\alpha}_2} e^{\lambda_2^F T_M} \mathcal{V}_2 \end{aligned}$$

where $\nu := \tau^+ \in [T_m, T_M]$. Pick $\lambda_2^F < \frac{1}{T_M} \ln(\frac{\bar{\alpha}_2}{p_M - c_q})$ such that $\frac{p_M - c_q}{\bar{\alpha}_2} e^{\lambda_2^F T_M} < 1$ holds. Letting $\lambda_2^J := -\ln(\frac{p_M - c_q}{\bar{\alpha}_2} e^{\lambda_2^F T_M})$, one has

$$\mathcal{V}_2(\mathbf{x}^+) \leq e^{-\lambda_2^J} \mathcal{V}_2(\mathbf{x}). \quad (\text{D.21})$$

Let $|x_1|_{\mathcal{A}} \geq 0$ be the distance of x_1 with respect to the set \mathcal{A} such that $|x_1|_{\mathcal{A}}^2 := \inf_{(\tilde{R}, \bar{\eta}, \bar{x}_1, \bar{\tau}) \in \mathcal{A}} (|\tilde{R}\tilde{R}^\top|_I^2 + \|\eta - \bar{\eta}\|^2 + \|\mathbf{x} - \bar{x}_1\|^2 + \|\tau - \bar{\tau}\|^2) = |\tilde{R}|_I^2 + \|\eta\|^2 + \|\mathbf{x}\|^2 = \|\zeta\|^2 + \|\mathbf{x}\|^2$. Consider the Lyapunov function candidate $\mathcal{V}(x_1) = \mathcal{V}_1 + \mathcal{V}_2$. From (D.15)-(D.17) and (D.19)-(D.21), one can show that

$$\underline{\alpha}|x_1|_{\mathcal{A}}^2 \leq \mathcal{V}(x_1) \leq \bar{\alpha}|x_1|_{\mathcal{A}}^2 \quad (\text{D.22})$$

$$\dot{\mathcal{V}} \leq -\lambda_F \mathcal{V}, \quad x_1 \in \mathcal{F}_1 \quad (\text{D.23})$$

$$\mathcal{V}^+ \leq e^{-\lambda_J} \mathcal{V}, \quad x_1 \in \mathcal{J}_1 \quad (\text{D.24})$$

where $\underline{\alpha} := \min\{\underline{\alpha}_1, \underline{\alpha}_2\}$, $\bar{\alpha} := \max\{\bar{\alpha}_1, \bar{\alpha}_2\}$, $\lambda_F := \min\{\lambda_1^F, \lambda_2^F\}$ and $\lambda_J := \min\{\lambda_1^J, \lambda_2^J\}$. Let $\lambda_c := \min\{\lambda_F, \lambda_J\}$. In view of (D.23) and (D.24), one has $\mathcal{V}(x_1(t, j)) \leq e^{-\lambda_c(t+j)} \mathcal{V}(x_{0,0})$. Then, from (D.22) one can conclude that, for all $(t, j) \in \text{dom}x_1$,

$$|x_1(t, j)|_{\mathcal{A}} \leq \sqrt{\frac{\bar{\alpha}}{\underline{\alpha}}} e^{-\frac{1}{2}\lambda_c(t+j)} |x_1(0, 0)|_{\mathcal{A}}, \quad (\text{D.25})$$

which shows that the set \mathcal{A} is exponentially stable. This completes the proof.

D.4 Proof of Theorem 5.2

Following the same steps as the first part of the proof of Theorem 5.1, one can guarantee that $|\tilde{R}|_I < 1, \forall t \geq 0$ with the initial conditions $|\tilde{R}(0)|_I < \sqrt{\varsigma_M}$ and $\|\eta(0)\| = 0$. Moreover, considering the real-valued function \mathcal{V}_1 defined in (D.14), inequalities (D.15)-(D.17) hold.

On the other hand, let us consider the following real-valued function:

$$\mathcal{V}_2 = e^{-\gamma\tau} \mathbf{x}^\top P^{-1} \mathbf{x} \quad (\text{D.26})$$

with some $\gamma > 0$. From Lemma 2.12, one has

$$\underline{\alpha}'_2 \|\mathbf{x}\|^2 \leq \mathcal{V}_2 \leq \bar{\alpha}'_2 \|\mathbf{x}\|^2 \quad (\text{D.27})$$

where $\underline{\alpha}'_2 := \frac{1}{p_M} e^{-\gamma T_M}$ and $\bar{\alpha}'_2 := \frac{1}{p_m}$. The time-derivative of \mathcal{V}_2 along the flows of (5.25) is given by

$$\begin{aligned} \dot{\mathcal{V}}_2 &= \gamma \mathcal{V}_2 + e^{-\gamma\tau} \mathbf{x}^\top (A_t^\top P^{-1} + P^{-1} A + \dot{P}^{-1}) \mathbf{x} \\ &= \gamma \mathcal{V}_2 - e^{-\gamma\tau} \mathbf{x}^\top P^{-1} V P^{-1} \mathbf{x} \\ &\leq \left(\gamma - e^{-\gamma T_M} \frac{v_m p_m}{p_M^2} \right) \mathcal{V}_2 \\ &= -\lambda_2^F \mathcal{V}_2 \end{aligned} \quad (\text{D.28})$$

where $\lambda_2^F := -\gamma + e^{-\gamma T_M} \frac{v_m p_m}{p_M^2}$ and $v_m := \inf_{t \geq 0} \lambda_m^V$. Let $\varpi(\gamma) = -\gamma + e^{-\gamma T_M} \frac{v_m p_m}{p_M^2}$. In view of the facts $\varpi(0) > 0$, $\varpi(\frac{v_m p_m}{p_M^2}) < 0$, and $\partial\varpi/\partial\gamma = -1 - e^{-\gamma T_M} \frac{v_m p_m T_M}{p_M^2} < 0$ for all $\gamma > 0$, there exists a constant $\gamma^* \in (0, \frac{v_m}{p_M})$ such that $\varpi(\gamma^*) = 0$. Therefore, one can always pick

a small enough positive constant γ , *i.e.*, $\gamma < \gamma^*$ such that $\lambda_2^F > 0$. Since the solution of P is well defined for all $(t, j) \in \text{dom}x_2$ and $(P^+)^{-1} = P^{-1} + C^\top QC$, one verifies that $I - K_t C$ has full rank and $(P^+)^{-1}$ can be rewritten as $(P^+)^{-1} = P^{-1}(I - KC)^{-1}$. Therefore, for each jump at $\tau = 0$, one has

$$\begin{aligned}\mathcal{V}_2^+ &= e^{-\gamma\nu}(\mathbf{x}^+)^{\top}(P^+)^{-1}\mathbf{x}^+ \\ &= e^{-\gamma\nu}\mathbf{x}^{\top}(I - KC)^{\top}(P^+)^{-1}(I - K_t C)\mathbf{x} \\ &= e^{-\gamma\nu}\mathbf{x}^{\top}(I - KC)^{\top}P^{-1}\mathbf{x} \\ &= e^{-\gamma\nu}\mathbf{x}^{\top}P^{-1}\mathbf{x} - e^{-\gamma\nu}\mathbf{x}^{\top}C^{\top}(CPC^{\top} + Q)^{-1}CPP^{-1}\mathbf{x} \\ &\leq e^{-\lambda_2^J}\mathcal{V}_2\end{aligned}\tag{D.29}$$

where $\lambda_2^J := \gamma T_m$, $\nu = \tau^+ \in [T_m, T_M]$, and we made use of the fact that $C^{\top}(CPC^{\top} + Q)^{-1}C$ is positive semidefinite.

Let $|x_2|_{\mathcal{A}} \geq 0$ be the distance of x_1 with respect to set \mathcal{A} such that $|x_2|_{\mathcal{A}}^2 := \inf_{(\bar{R}, \bar{\eta}, \bar{\mathbf{x}}_2, \bar{\tau}) \in \mathcal{A}}(|\bar{R}\bar{R}^{\top}|_I^2 + \|\eta - \bar{\eta}\|^2 + \|\mathbf{x} - \bar{\mathbf{x}}_2\|^2 + \|\tau - \bar{\tau}\|^2) = \|\zeta\|^2 + \|\mathbf{x}\|^2$. Consider the Lyapunov function candidate $\mathcal{V}(x_2) = \mathcal{V}_1 + \mathcal{V}_2$. From (D.15)-(D.17) and (D.27)-(D.29), one can show that

$$\underline{\alpha}|x_2|_{\mathcal{A}}^2 \leq \mathcal{V}(x_2) \leq \bar{\alpha}|x_2|_{\mathcal{A}}^2\tag{D.30}$$

$$\dot{\mathcal{V}} \leq -\lambda_F \mathcal{V}, \quad x_2 \in \mathcal{F}_2\tag{D.31}$$

$$\mathcal{V}^+ \leq e^{-\lambda_J} \mathcal{V}, \quad x_2 \in \mathcal{J}_2\tag{D.32}$$

where $\underline{\alpha} := \min\{\underline{\alpha}_1, \underline{\alpha}_2\}$, $\bar{\alpha} := \max\{\bar{\alpha}_1, \bar{\alpha}_2\}$, $\lambda_F := \min\{\lambda_1^F, \lambda_2^F\}$ and $\lambda_J := \min\{\lambda_1^J, \lambda_2^J\}$. Let $\lambda_c := \min\{\lambda_F, \lambda_J\}$. In view of (D.31) and (D.32), one has

$$\mathcal{V}(x_2(t, j)) \leq e^{-\lambda_c(t+j)} \mathcal{V}(x_2(0, 0)).$$

Then, from (D.30) one can conclude that, for all $(t, j) \in \text{dom}x_2$,

$$|x_2(t, j)|_{\mathcal{A}} \leq \sqrt{\frac{\bar{\alpha}}{\underline{\alpha}}} e^{-\frac{1}{2}\lambda_c(t+j)} |x_2(0, 0)|_{\mathcal{A}},\tag{D.33}$$

which shows that the set \mathcal{A} is exponentially stable. This completes the proof.

D.5 Proof of Lemma 5.2

In view of (5.31) and (5.33), one obtains

$$\begin{aligned}\varepsilon \dot{\mathcal{V}}_1 + \dot{\mathcal{V}}_2 &= -\varepsilon \lambda_1 \mathcal{V}_1 - \lambda_2 \mathcal{V}_2 + \beta \|\zeta\| \|\mathbf{x}\| \\ &\leq -\varepsilon \lambda_1 \mathcal{V}_1 - \lambda_2 \mathcal{V}_2 + \frac{\varepsilon \lambda_1 \underline{\alpha}_1}{2} \|\zeta\|^2 + \frac{\beta^2}{2\varepsilon \lambda_1 \underline{\alpha}_1} \|\mathbf{x}\|^2\end{aligned}$$

where we made use of the inequality $\beta \|\zeta\| \|\mathbf{x}\| \leq \frac{\varepsilon \lambda_1 \underline{\alpha}_1}{2} \|\zeta\|^2 + \frac{\beta^2}{2\varepsilon \lambda_1 \underline{\alpha}_1} \|\mathbf{x}\|^2$. From (5.30) and (5.32), one can further show that

$$\varepsilon \dot{\mathcal{V}}_1 + \dot{\mathcal{V}}_2 \leq -\varepsilon \lambda_1 \mathcal{V}_1 - \lambda_2 \mathcal{V}_2 + \frac{\varepsilon \lambda_1}{2} \mathcal{V}_1 + \frac{\beta^2}{2\varepsilon \lambda_1 \underline{\alpha}_1 \underline{\alpha}_2} \mathcal{V}_2$$

$$= -\frac{\varepsilon \lambda_1}{2} \mathcal{V}_1 - \left(\lambda_2 - \frac{\beta^2}{2\varepsilon \lambda_1 \underline{\alpha}_1 \underline{\alpha}_2} \right) \mathcal{V}_2$$

From the fact $\varepsilon > \frac{\beta^2}{2\lambda_1 \lambda_2 \underline{\alpha}_1 \underline{\alpha}_2}$, one has $\lambda_2 - \frac{\beta^2}{2\varepsilon \lambda_1 \underline{\alpha}_1 \underline{\alpha}_2} > 0$, and applying the definition of λ , one obtains (5.34).

D.6 Proof of Theorem 5.3

Following the same steps as the first part of the proof of Theorem 5.1, one can guarantee that $|\tilde{R}|_I < 1, \forall t \geq 0$ with the initial conditions $|\tilde{R}(0)|_I < \sqrt{\zeta_M}$ and $\|\eta(0)\| = 0$. Moreover, considering the real-valued function \mathcal{V}_1 defined in (D.14), inequalities (D.15)-(D.17) hold.

On the other hand, consider the real-valued function $\mathcal{V}_2 = e^{\lambda_2^F \tau} \mathbf{x}^\top \hat{\Phi}^\top(\tau) P \hat{\Phi}(\tau) \mathbf{x}$ as (D.18), whose upper and lower bounds are given by (D.19). The time-derivative of \mathcal{V}_2 along the flows of (5.39) is given as

$$\begin{aligned} \dot{\mathcal{V}}_2 &= -\lambda_2^F \mathcal{V}_2 + e^{\lambda_2^F \tau} \mathbf{x}^\top \hat{\Phi}^\top(\tau) (A^\top P + PA) \hat{\Phi}(\tau) \mathbf{x} + 2e^{\lambda_2^F \tau} \mathbf{x}^\top \hat{\Phi}^\top(\tau) P \hat{\Phi}(\tau) \delta_g \\ &\quad + e^{\lambda_2^F \tau} \mathbf{x}^\top (\dot{\hat{\Phi}}^\top(\tau) P \hat{\Phi}(\tau) + \hat{\Phi}^\top(\tau) P \dot{\hat{\Phi}}(\tau)) \mathbf{x} \\ &\leq -\lambda_2^F \mathcal{V}_2 + 2\bar{\alpha}_2 \|\mathbf{x}\| \|\delta_g\| \\ &\leq -\lambda_2^F \mathcal{V}_2 + \beta \|\mathbf{x}\| \|\zeta\| \end{aligned} \quad (\text{D.34})$$

where $\beta := 4\sqrt{2}c_g \bar{\alpha}_2$, and we made use of the facts $\|\delta_g\| \leq c_g \|I - \tilde{R}\|_F = 2\sqrt{2}c_g \|\tilde{R}\|_I \leq 2\sqrt{2}c_g \|\zeta\|$, $A\hat{\Phi}(\tau) = \hat{\Phi}(\tau)A$, and $\dot{\hat{\Phi}}(\tau) = -A\hat{\Phi}(\tau)$. Similar to the \mathcal{V}_2 defined in (D.18), one can verify that \mathcal{V}_2 satisfies (D.21) after each jump.

Let $|x_3|_{\bar{\mathcal{A}}} \geq 0$ be the distance of x_3 with respect to the set $\bar{\mathcal{A}}$ such that $|x_3|_{\bar{\mathcal{A}}}^2 := \inf_{(\tilde{R}, \bar{\eta}, \bar{x}_3, \bar{\tau}) \in \bar{\mathcal{A}}} (|\tilde{R}\bar{R}^\top|_I^2 + \|\eta - \bar{\eta}\|^2 + \|\mathbf{x} - \bar{x}_3\|^2 + \|\tau - \bar{\tau}\|^2) = \|\zeta\|^2 + \|\mathbf{x}\|^2$. Consider the Lyapunov function candidate $\mathcal{V} = \varepsilon \mathcal{V}_1 + \mathcal{V}_2$, with some $\varepsilon > 0$. From (D.15) and (D.19), one can show that

$$\underline{\alpha} |x_3|_{\bar{\mathcal{A}}}^2 \leq \mathcal{V}(x_3) \leq \bar{\alpha} |x_3|_{\bar{\mathcal{A}}}^2 \quad (\text{D.35})$$

where $\underline{\alpha} := \min\{\underline{\alpha}_1, \underline{\alpha}_2\}$ and $\bar{\alpha} := \max\{\bar{\alpha}_1, \bar{\alpha}_2\}$. In view of (D.14)-(D.16), (D.18)-(D.19) and (D.34), applying Lemma 5.2, one has

$$\dot{\mathcal{V}} = -\lambda_F \mathcal{V}, \quad x_3 \in \mathcal{F}_3 \quad (\text{D.36})$$

with $\varepsilon > \frac{\beta^2}{2\lambda_1^F \lambda_2^F \underline{\alpha}_1 \underline{\alpha}_2}$ and $\lambda_F = \min\{\frac{\lambda_1^F}{2}, (\lambda_2^F - \frac{\beta^2}{2\varepsilon \lambda_1^F \underline{\alpha}_1 \underline{\alpha}_2})\}$. From (D.17) and (D.21), one obtains

$$\mathcal{V}^+ \leq \varepsilon e^{-\lambda_1^J} \mathcal{V}_1 + e^{-\lambda_2^J} \mathcal{V}_2 \leq e^{-\lambda_J} \mathcal{V}, \quad x_3 \in \mathcal{J}_3 \quad (\text{D.37})$$

where $\lambda_J := \min\{\lambda_1^J, \lambda_2^J\}$. Let $\lambda_c := \min\{\lambda_F, \lambda_J\}$. In view of (D.36) and (D.37), one has $\mathcal{V}(x_3(t, j)) \leq e^{-\lambda_c(t+j)} \mathcal{V}(x_3(0, 0))$. Then, from (D.35) one can conclude that, for all $(t, j) \in \text{dom}x_3$,

$$|x_3(t, j)|_{\bar{\mathcal{A}}} \leq \sqrt{\frac{\bar{\alpha}}{\underline{\alpha}}} e^{-\frac{1}{2}\lambda_c(t+j)} |x_3(0, 0)|_{\bar{\mathcal{A}}}, \quad (\text{D.38})$$

which shows that the set $\bar{\mathcal{A}}$ is exponentially stable. This completes the proof.

D.7 Proof of Theorem 5.4

Following the same steps as the first part of the proof of Theorem 5.1, one can guarantee that $|\tilde{R}|_I < 1$, $\forall t \geq 0$ with the initial conditions $|\tilde{R}(0)|_I < \sqrt{\varsigma_M}$ and $\|\eta(0)\| = 0$. Moreover, considering the real-valued function \mathcal{V}_1 defined in (D.14), inequalities (D.15)-(D.17) hold.

Consider the real-valued function $\mathcal{V}_2 = e^{-\gamma\tau} \mathbf{x}^\top P^{-1} \mathbf{x}$ as (D.26), whose upper and lower bounds are given by (D.27). The time-derivative of \mathcal{V}_2 along the flows of (5.47) is given as

$$\begin{aligned}\dot{\mathcal{V}}_2 &= \gamma \mathcal{V}_2 + e^{-\gamma\tau} \mathbf{x}^\top (A^\top P^{-1} + P^{-1} A + \dot{P}^{-1}) \mathbf{x} + 2e^{-\gamma\tau} \mathbf{x}^\top P^{-1} \bar{\delta}_{\mathbf{g}} \\ &\leq \left(\gamma - e^{-\gamma T_M} \frac{v_m}{p_M} \right) \mathcal{V}_2 + \frac{2}{p_m} \|\mathbf{x}\| \|\bar{\delta}_{\mathbf{g}}\| \\ &= -\lambda_2^F \mathcal{V}_2 + \beta \|\mathbf{x}\| \|\zeta\|\end{aligned}\tag{D.39}$$

where $\lambda_2^F := -\gamma + e^{-\gamma T_M} \frac{v_m p_m}{p_M^2} > 0$ with γ small enough, $v_m := \inf_{t \geq 0} \lambda_m^V$, $\beta := 4\sqrt{2}c_{\mathbf{g}}/p_m$, and we made use of the facts $\|\bar{\delta}_{\mathbf{g}}\| \leq c_{\mathbf{g}} \|I - \tilde{R}\|_F \leq 2\sqrt{2}c_{\mathbf{g}} \|\zeta\|$. Similar to the \mathcal{V}_2 defined in (D.26), one can verify that \mathcal{V}_2 satisfies (D.29) after each jump.

Let $|x_4|_{\bar{\mathcal{A}}} \geq 0$ be the distance of x_4 with respect to the set $\bar{\mathcal{A}}$ such that $|x_4|_{\bar{\mathcal{A}}}^2 := \inf_{(\bar{R}, \bar{\eta}, \bar{x}_4, \bar{\tau}) \in \bar{\mathcal{A}}} (|\tilde{R}\bar{R}^\top|_I^2 + \|\eta - \bar{\eta}\|^2 + \|\mathbf{x} - \bar{x}_4\|^2 + \|\tau - \bar{\tau}\|^2) = \|\zeta\|^2 + \|\mathbf{x}\|^2$. Consider the Lyapunov function candidate $\mathcal{V} = \varepsilon \mathcal{V}_1 + \mathcal{V}_2$, with some $\varepsilon > 0$. In view of (D.15) and (D.27), one has

$$\underline{\alpha} |x_4|_{\bar{\mathcal{A}}}^2 \leq \mathcal{V}(x_4) \leq \bar{\alpha} |x_4|_{\bar{\mathcal{A}}}^2\tag{D.40}$$

where $\underline{\alpha} := \min\{\underline{\alpha}_1, \underline{\alpha}'_2\}$ and $\bar{\alpha} := \max\{\bar{\alpha}_1, \bar{\alpha}'_2\}$. In view of (D.14)-(D.16), (D.26)-(D.27) and (D.39), applying Lemma 5.2, one has

$$\dot{\mathcal{V}} = -\lambda_F \mathcal{V}, \quad x_4 \in \mathcal{F}_4\tag{D.41}$$

with $\varepsilon > \frac{\beta^2 p_M}{2\lambda_1^F \lambda_2^F \lambda_m^{P_1} e^{-\gamma T_M}}$ and $\lambda_F = \min\{\frac{\lambda_1^F}{2}, (\lambda_2^F - \frac{\beta^2 p_M}{2\varepsilon \lambda_1^F \lambda_m^{P_1}})\}$. From (D.17) and (D.29), one obtains

$$\mathcal{V}^+ \leq \varepsilon e^{-\lambda_1^J} \mathcal{V}_1 + e^{-\lambda_2^J} \mathcal{V}_2 \leq e^{-2\lambda_J} \mathcal{V}, \quad x_4 \in \mathcal{J}_4\tag{D.42}$$

where $\lambda_J := \frac{1}{2} \min\{\lambda_1^J, \lambda_2^J\}$. Let $\lambda_c := \min\{\lambda_F, \lambda_J\}$. In view of (D.41) and (D.42), one has $\mathcal{V}(x_4(t, j)) \leq e^{-\lambda_c(t+j)} \mathcal{V}(x_4(0, 0))$. Then, from (D.40) one can conclude that, for all $(t, j) \in \text{dom}x_4$,

$$|x_4(t, j)|_{\bar{\mathcal{A}}} \leq \sqrt{\frac{\bar{\alpha}}{\underline{\alpha}}} e^{-\frac{1}{2}\lambda_c(t+j)} |x_4(0, 0)|_{\bar{\mathcal{A}}},\tag{D.43}$$

which shows that the set $\bar{\mathcal{A}}$ is exponentially stable. This completes the proof.

Appendix E

Proofs of Chapter 6

E.1 Proof of Theorem 6.1

From the assumption that the pair (A, C) in (6.3) is uniformly observable, as per Lemma 2.10, there exist positive constants $0 < p_m \leq p_M < \infty$ such that the solution of the CRE (2.116) satisfies $p_m I_n \leq P(t) \leq p_M I_n$. Consider the following real-valued function:

$$\mathcal{L}_P(x) = x^\top P^{-1}x. \quad (\text{E.1})$$

One can show that $\frac{1}{p_M} \|x\|^2 \leq \mathcal{L}_P(x) \leq \frac{1}{p_m} \|x\|^2$. In view of (6.3) and (2.116), the time-derivative of \mathcal{L}_P is given by

$$\begin{aligned} \dot{\mathcal{L}}_P &= x^\top (P^{-1}A + A^\top P^{-1} - 2C^\top QC + \dot{P}^{-1})x \\ &= -x^\top C^\top QCx - x^\top P^{-1}V P^{-1}x \\ &\leq -\frac{v_m}{p_M^2} \|x\|^2 \leq -\lambda \mathcal{L}_P, \end{aligned} \quad (\text{E.2})$$

where $\lambda = v_m p_m / p_M^2$, $v_m := \inf_{t \geq 0} \lambda_{\min}^{V(t)}$, and we made use of the facts $-C^\top QC \leq 0$, $\dot{P}^{-1} = -P^{-1}PP^{-1} = -P^{-1}A - A^\top P^{-1} + 2C^\top QC - P^{-1}VP^{-1}$. Hence, one has $\|x(t)\| \leq \sqrt{p_M/p_m} e^{-\frac{\lambda}{2}t} \|x(0)\|$, which implies that x, \dot{x} are bounded, and x converges to zero exponentially. Note that the convergence of x is independent from the dynamics of the rotation. Then, from (6.3)-(6.4) and Assumption 6.2, one can easily show that the set of equilibria of the system is given by $\Psi = \{(\tilde{R}, x) \in \text{SO}(3) \times \mathbb{R}^n : \psi_{\mathfrak{so}(3)}(M\tilde{R}) = 0, x = 0\}$. From $\psi_{\mathfrak{so}(3)}(M\tilde{R}) = 0$ and using the facts $\psi_{\mathfrak{so}(3)}(M\tilde{R}) = \text{vec} \circ \mathbb{P}_{\mathfrak{so}(3)}(M\tilde{R})$ and $\mathbb{P}_{\mathfrak{so}(3)}(M\tilde{R}) = (M\tilde{R} - \tilde{R}^\top M)/2$, one has $M\tilde{R} = \tilde{R}^\top M$. From Lemma 2.3, it follows that $\tilde{R} \in \{\tilde{R} \in \text{SO}(3) : \tilde{R} = \mathcal{R}_\alpha(\pi, v), v \in \mathcal{E}(M)\}$, which proves item (i).

On the other hand, consider the following real-valued function

$$\mathcal{L}_M = \text{tr}((I - \tilde{R})M), \quad (\text{E.3})$$

whose time-derivative is given by

$$\begin{aligned} \dot{\mathcal{L}}_M &= k_R \text{tr}(-M\tilde{R}(-\psi_{\mathfrak{so}(3)}(M\tilde{R}) + \phi(x, t))^\times) \\ &\leq -2k_R \|\psi_R\|^2 + 2k_R c_\phi \|x\| \|\psi_R\|, \end{aligned} \quad (\text{E.4})$$

where $\psi_R := \psi_{\mathfrak{so}(3)}(M\tilde{R})$, and we made use of the Assumption 6.2 and the facts $\text{tr}(-Ax^\times) = \langle\langle A, x^\times \rangle\rangle = 2x^\top \psi_{\mathfrak{so}(3)}(A)$ for all $A \in \mathbb{R}^{3 \times 3}$. Consider the following Lyapunov function candidate:

$$\mathcal{L}(\tilde{R}, x) = \mathcal{L}_M(\tilde{R}) + \kappa \mathcal{L}_P(x), \quad (\text{E.5})$$

From (E.2) and (E.4), the time-derivative of \mathcal{L} is given by

$$\begin{aligned} \dot{\mathcal{L}}(\tilde{R}, x) &\leq -2k_R \|\psi_R\|^2 + 2k_R c_\phi \|x\| \|\psi_R\| - \kappa \frac{v_m}{p_M^2} \|x\|^2 \\ &= -\zeta^\top H \zeta, \quad H := \begin{bmatrix} 2k_R & -k_R c_\phi \\ -k_R c_\phi & \kappa \frac{v_m}{p_M^2} \end{bmatrix} \end{aligned} \quad (\text{E.6})$$

where $\zeta := [\|\psi_R\|, \|x\|]^\top$. Choosing $\kappa > \frac{k_R c_\phi^2 p_M^2}{2v_m}$, one can show that the matrix H is positive definite and $\dot{\mathcal{L}} \leq 0$. From (2.37) and (2.38) given in Lemma 2.1, one has $\|\psi_R\|^2 \leq \text{tr}(\underline{M}(I - R)) \leq 4\lambda_{\max}^W |\tilde{R}|_I^2 \leq 4\lambda_{\max}^W$ with $W := \frac{1}{2}(\text{tr}(M)I_3 - \underline{M})$, which implies that ψ_R is bounded. From (6.3), (6.4) and (2.44), one has $\dot{\psi}_R = E(M\tilde{R})(-k_R \psi_R + k_R \phi(x, t))$ with $E(M\tilde{R}) := \frac{1}{2}(\text{tr}(M\tilde{R})I_3 - \tilde{R}^\top M)$. Using the fact that x is bounded, $\|E(M\tilde{R})\| \leq \|\bar{M}\|_F$ in (2.42), and $\|\phi(x, t)\| \leq c_\phi \|x\|$, one can verify that $\dot{\psi}_R$ is bounded. Thus, from the fact that x, \dot{x} and $\psi_R, \dot{\psi}_R$ are bounded, it follows that $\dot{\mathcal{L}}$ is bounded. Therefore, from Barbalat's lemma, one has $\dot{\mathcal{L}} \rightarrow 0$ as $t \rightarrow \infty$, and in turn, $\zeta \rightarrow 0$ as $t \rightarrow \infty$, i.e., $(\|\psi_R\|, \|x\|) \rightarrow (0, 0)$ as $t \rightarrow \infty$. This implies that the solution (\tilde{R}, x) to (6.3)-(6.4) converges to the set Ψ .

Next, we need to show that the undesired equilibria $\Psi/(I_3, 0)$ are unstable. For each $v \in \mathcal{E}(M)$, let us define $R_v^* = \mathcal{R}_\alpha(\pi, v)$ and the open set $U_v^\delta := \{(\tilde{R}, x) \in \text{SO}(3) \times \mathbb{R}^n : \tilde{R} = R_v^* \exp(\delta u^\times), u \in \mathbb{S}^2, x = 0\}$ with δ sufficiently small. For any $(\tilde{R}, x) \in U_v^\delta$, pick a sufficiently small ϵ such that $(R_v^*)^\top \tilde{R} := \exp(\epsilon^\times) \approx I_3 + \epsilon^\times$. Consequently, from the first equation of (6.3) one obtains the dynamics of ϵ as follows:

$$\dot{\epsilon} = -\psi_{\mathfrak{so}(3)}(k_R M R_v^*(I_3 + \epsilon^\times)) = -k_R W_v \epsilon \quad (\text{E.7})$$

where $W_v = \text{tr}(M R_v^*) I_3 - (M R_v^*)^\top = (2v^\top M v - \text{tr}(M)) I_3 - (2vv^\top M - M)$, and we made use of the facts $\psi_{\mathfrak{so}(3)}(M R_v^*) = 0$, $\psi_{\mathfrak{so}(3)}(M R_v^* \epsilon^\times) = \text{vec} \circ \mathbb{P}_a(M R_v^* \epsilon^\times)$ and $M R_v^* \epsilon^\times + \epsilon^\times (M R_v^*)^\top = (W_v \epsilon)^\times$. Using the fact that M is positive semi-definite with three distinct eigenvalues, one verifies that $-v^\top W_v v = -v^\top M v + \text{tr}(M) > 0$, which implies that for each $v \in \mathcal{E}(M)$, the matrix $-W_v$ has at least one positive eigenvalue. It follows that the undesired equilibrium $(R_v^*, 0) \in \Psi/(I_3, 0)$ is unstable, and hence, the desired equilibrium $(I_3, 0)$ is almost globally asymptotically stable. This completes the proof of item (ii).

Now, let us prove the local exponential stability result in item (iii). From (E.6) with $\kappa > \frac{k_R c_\phi^2 p_M^2}{2v_m}$, one has $\mathcal{L}_M(\tilde{R}(t)) \leq \mathcal{L}(\tilde{R}(t), x(t)) \leq \mathcal{L}(\tilde{R}(0), x(0)) \leq \varepsilon_R$, for all $t \geq 0$. Hence, one verifies that $|\tilde{R}(t)|_I < 1$ for all $t \geq 0$. Moreover, one has $\varrho |\tilde{R}|_I^2 \leq \|\psi_R\|^2 \leq 4\lambda_{\max}^W |\tilde{R}|_I^2$ with $\varrho := \min_{\mathcal{L}_M(\tilde{R}) \leq \varepsilon_R} (1 - |\tilde{R}|_I^2 \cos \langle u, \bar{M}u \rangle) 4\lambda_{\min}^W > 0$ and $\tilde{R} = \mathcal{R}_a(\theta, u)$. Let $\bar{\zeta} := [|\tilde{R}|_I, \|x\|]^\top$. In view of (2.37), (E.1) and (E.3), one obtains

$$\alpha \|\bar{\zeta}\|^2 \leq \mathcal{L} \leq \bar{\alpha} \|\bar{\zeta}\|^2, \quad (\text{E.8})$$

where $\underline{\alpha} := \min\{4\lambda_{\min}^{\bar{M}}, \frac{\kappa}{p_M}\}$ and $\bar{\alpha} := \max\{4\lambda_{\max}^{\bar{M}}, \frac{\kappa}{p_m}\}$. Substituting $\varrho|\tilde{R}|_I^2 \leq \|\psi_R\|^2 \leq 4\lambda_{\max}^W|\tilde{R}|_I^2$ into (E.6), one has

$$\begin{aligned}\dot{\mathcal{L}} &\leq -2k_R\varrho|\tilde{R}|_I^2 + 4k_Rc_Wc_\phi\|x\||\tilde{R}|_I - \kappa\frac{v_m}{p_M^2}\|x\|^2 \\ &\leq -\bar{\zeta}^\top \bar{H} \bar{\zeta}, \quad \bar{H} := \begin{bmatrix} 2k_R\varrho & -2k_Rc_Wc_\phi \\ -2k_Rc_Wc_\phi & \kappa v_m/p_M^2 \end{bmatrix}.\end{aligned}\quad (\text{E.9})$$

where $c_W := \sqrt{\lambda_{\max}^W}$. Choosing $\kappa^* := \frac{2k_R\lambda_{\max}^W c_\phi^2 p_M^2}{\varrho v_m}$, for any $\kappa \geq \kappa^*$ both matrices H and \bar{H} are positive definite since $\varrho \leq 4\lambda_{\max}^W$. In view of (E.8) and (E.9), one concludes

$$\|\bar{\zeta}(t)\| \leq \sqrt{\bar{\alpha}/\underline{\alpha}} e^{-\frac{1}{2}\lambda_{\min}^{\bar{H}} t} \|\bar{\zeta}(0)\|, \quad (\text{E.10})$$

for all $t \geq 0$, which implies that (\tilde{R}, x) converges to $(I_3, 0)$ exponentially. This completes the proof.

E.2 Proof of Lemma 6.2

Let us define a $3N$ -by- $3N$ block diagonal matrix $\Theta(t) := \text{blkdiag}(\Pi_1, \Pi_2, \dots, \Pi_N) \in \mathbb{R}^{(3N \times 3N)}$. Then, one verifies that $C(t) = \Theta \bar{C}$ with constant matrix \bar{C} given as

$$\bar{C} = \begin{bmatrix} I_3 & 0_{3 \times 3} & \cdots & 0_{3 \times 3} & 0_{3 \times 3} & 0_{3 \times 3} \\ I_3 & -I_3 & \cdots & 0_{3 \times 3} & 0_{3 \times 3} & 0_{3 \times 3} \\ \vdots & \vdots & \ddots & \vdots & \vdots & \vdots \\ I_3 & 0_{3 \times 3} & \cdots & -I_3 & 0_{3 \times 3} & 0_{3 \times 3} \end{bmatrix}. \quad (\text{E.11})$$

Let $\Sigma(t) := \Theta^\top(t)\Theta(t) \in \mathbb{R}^{(3N \times 3N)}$. Since Π_i is positive definite for all $i = 1, 2, \dots, N$, there exists a positive constant ϵ_i for each $i = 1, 2, \dots, N$ such that $\Pi_i(t) \geq \epsilon_i I_3$ for all $t \geq 0$. It follows that $\Sigma(t) \geq \bar{\epsilon}^2 I_{3N}$ with $\bar{\epsilon} := \min\{\epsilon_1, \dots, \epsilon_N\}$. From Definition 2.11, the Observability Gramian $W_O(t, t + \delta)$ defined in (2.111) is given by

$$\begin{aligned}W_O(t, t + \delta) &= \frac{1}{\delta} \int_t^{t+\delta} \Phi(\tau, t)^\top \bar{C}^\top \Theta^\top(\tau) \Theta(\tau) \bar{C} \Phi(\tau, t) d\tau \\ &= \frac{1}{\delta} \int_t^{t+\delta} \Phi^\top(\tau, t) \bar{C}^\top \Sigma(\tau) \bar{C} \Phi(\tau, t) d\tau \\ &\geq \frac{\bar{\epsilon}^2}{\delta} \int_t^{t+\delta} \Phi^\top(\tau, t) \bar{C}^\top \bar{C} \Phi(\tau, t) d\tau\end{aligned}\quad (\text{E.12})$$

Suppose that there exist constants $\delta', \mu' > 0$ such that

$$W'_O(t, t + \delta') := \frac{1}{\delta'} \int_t^{t+\delta'} \Phi^\top(\tau, t) \bar{C}^\top \bar{C} \Phi(\tau, t) d\tau > \mu' I$$

for all $t \geq 0$. Choosing $\delta \geq \delta'$, one can show that $W_O(t, t + \delta) \geq \frac{\bar{\epsilon}^2 \delta'}{\delta} W'_O(t, t + \delta') \geq \frac{\bar{\epsilon}^2 \delta'}{\delta} \mu' I := \mu I$. From Definition 2.11, one concludes that the pair $(A(t), C(t))$ is uniformly observable.

Next, we are going to show that there exist constant δ', μ' such that $W'_O(t, t + \delta') > \mu'I$ for all $t \geq 0$. Consider a time-varying rotation matrix $\bar{R}(t)$ with $\dot{\bar{R}}(t) = (-\omega^\times)\bar{R}$ and $\bar{R}(0) \in \text{SO}(3)$. It is clear that $\bar{R}(t) \in \text{SO}(3)$ for all $t \geq 0$. Let us introduce two block diagonal matrices $T(t) = \text{blkdiag}(\bar{R}, \bar{R}, \dots, \bar{R}) \in \mathbb{R}^{(9+3N) \times (9+3N)}$ and $S(t) = \text{blkdiag}(-\omega^\times, -\omega^\times, \dots, -\omega^\times) \in \mathbb{R}^{(9+3N) \times (9+3N)}$ and a constant matrix $\bar{A} = A(t) - S(t)$. One can verify that $\dot{T}(t) = S(t)T(t)$, $T^{-1}(t) = T^\top(t)$ and $T(t)\bar{A} = \bar{A}T(t)$. From Lemma 2.7, the state transition matrix $\Phi(t, \tau)$ associated to $A(t)$ can be expressed as

$$\Phi(t, \tau) = T(t)\bar{\Phi}(t, \tau)T^{-1}(\tau). \quad (\text{E.13})$$

with $\bar{\Phi}(t, \tau) = \exp(\bar{A}(t - \tau))$ denoting the state transition matrix associated to \bar{A} .

Define the block matrix $\bar{T}(\tau) := \text{blkdiag}(\bar{R}, \bar{R}, \dots, \bar{R}) \in \mathbb{R}^{(3N \times 3N)}$ such that $\bar{T}^\top(\tau)\bar{T}(\tau) = I_{3N}$ and $\bar{C}T(\tau) = \bar{T}(\tau)\bar{C}$. Therefore, making use the fact $\Phi(\tau, t) = T(\tau)\bar{\Phi}(\tau, t)T^\top(t)$, one can show that $W'_O(t, t + \delta') = T(t)(\frac{1}{\delta'} \int_t^{t+\delta'} \bar{\Phi}^\top(\tau, t)\bar{C}^\top\bar{C}\bar{\Phi}(\tau, t)d\tau)T^\top(t)$. One can easily verify that the pair (\bar{A}, \bar{C}) is uniformly observable, and there exist constants $\delta'', \mu'' > 0$ such that $\frac{1}{\delta''} \int_t^{t+\delta''} \bar{\Phi}^\top(\tau, t)\bar{C}^\top\bar{C}\bar{\Phi}(\tau, t)d\tau \geq \mu''I$ for all $t \geq 0$. Choosing $\delta' \geq \delta''$, one shows that

$$\begin{aligned} & \frac{1}{\delta'} \int_t^{t+\delta'} \bar{\Phi}^\top(\tau, t)\bar{C}^\top\bar{C}\bar{\Phi}(\tau, t)d\tau \\ & \geq \frac{\delta''}{\delta'} \left(\frac{1}{\delta''} \int_t^{t+\delta''} \bar{\Phi}^\top(\tau, t)\bar{C}^\top\bar{C}\bar{\Phi}(\tau, t)d\tau \right) \geq \frac{\delta''\mu''}{\delta'} I. \end{aligned}$$

Applying the fact that $T(t)T^\top(t) = I$, one obtains $W'_O(t, t + \delta') \geq \frac{\delta''\mu''}{\delta'} I := \mu'I$. This completes the proof.

E.3 Proof of Lemma 6.3

Let us define a $3N$ -by- $3N$ block diagonal matrix $\Theta(t) := \text{blkdiag}(\Pi_1, \Pi_2, \dots, \Pi_N) \in \mathbb{R}^{(3N \times 3N)}$. Then, one verifies that $C(t) = \Theta\bar{C}$ with constant matrix \bar{C} given as

$$\bar{C} = \begin{bmatrix} I_3 & -p_{11}I_3 & -p_{12}I_3 & -p_{13}I_3 & 0_{3 \times 3} & 0_{3 \times 3} \\ I_3 & -p_{21}I_3 & -p_{22}I_3 & -p_{23}I_3 & 0_{3 \times 3} & 0_{3 \times 3} \\ \vdots & \vdots & \vdots & \vdots & \vdots & \vdots \\ I_3 & -p_{N1}I_3 & -p_{N2}I_3 & -p_{N3}I_3 & 0_{3 \times 3} & 0_{3 \times 3} \end{bmatrix}. \quad (\text{E.14})$$

Since $\Sigma(t) = \Theta^\top(t)\Theta(t) > \bar{\epsilon}I$ with some constant $\bar{\epsilon} > 0$, one can obtain (E.12) as in the proof of Lemma 6.2. Similar to the proof of Lemma 6.2, define a time-varying rotation matrix $\bar{R}(t)$ with $\dot{\bar{R}} = (-\omega^\times)\bar{R}$ and $\bar{R}(0) \in \text{SO}(3)$. Let us introduce two block diagonal matrices $T(t) = \text{blkdiag}(\bar{R}, \bar{R}, \dots, \bar{R}) \in \mathbb{R}^{18 \times 18}$ and $S(t) = \text{blkdiag}(-\omega^\times, -\omega^\times, \dots, -\omega^\times) \in \mathbb{R}^{18 \times 18}$ and a constant matrix $\bar{A} = A(t) - S(t)$. Then, one has $T(t)\bar{A} = \bar{A}T(t)$ and $\dot{T}(t) = S(t)T(t)$. From Lemma 2.7, the state transition matrix $\Phi(t, \tau)$ associated to $A(t)$ can be expressed as

$$\Phi(t, \tau) = T(t)\bar{\Phi}(t, \tau)T^{-1}(\tau). \quad (\text{E.15})$$

with $\bar{\Phi}(t, \tau) = \exp(\bar{A}(t - \tau))$ denoting the state transition matrix associated to \bar{A} .

Define $\bar{T}(\tau) := \text{blkdiag}(\bar{R}, \bar{R}, \dots, \bar{R}) \in \mathbb{R}^{(3N \times 3N)}$ such that $\bar{T}^\top(\tau)\bar{T}(\tau) = I_{3N}$ and $\bar{C}\bar{T}(\tau) = \bar{T}(\tau)\bar{C}$. From (E.12) and (E.15), one shows

$$\begin{aligned} W_O(t, t + \delta) &\geq \frac{\bar{\epsilon}^2}{\delta} \int_t^{t+\delta} \Phi^\top(\tau, t) \bar{C}^\top \bar{C} \Phi(\tau, t) d\tau \\ &\geq \frac{\bar{\epsilon}^2}{\delta} T(t) \left(\int_t^{t+\delta} \bar{\Phi}^\top(\tau, t) \bar{C}^\top \bar{C} \bar{\Phi}(\tau, t) d\tau \right) T^\top(t) \end{aligned}$$

Suppose that there exist constants $\delta'', \mu'' > 0$ such that

$$W_o''(t, t + \delta'') := \frac{1}{\delta''} \int_t^{t+\delta''} \bar{\Phi}^\top(\tau, t) \bar{C}^\top \bar{C} \bar{\Phi}(\tau, t) d\tau \geq \mu'' I$$

for all $t \geq 0$. Choosing $\delta \geq \delta''$, one can show that $W_O(t, t + \delta) \geq \frac{\bar{\epsilon}^2 \delta''}{\delta} T(t) W_o''(t, t + \delta'') T^\top(t) \geq \frac{\bar{\epsilon}^2 \delta'}{\delta} \mu'' I := \mu I$, which implies that the pair $(A(t), C(t))$ is uniformly observable.

Next, we are going to show that there exist constants $\delta'', \mu'' > 0$ such that $W_o''(t, t + \delta') \geq \mu'' I$ for all $t \geq 0$. For the sake of simplicity, we assume that the landmarks $i = 1, 2, 3, 4$ are not coplanar. Define

$$\Xi := \begin{bmatrix} 1 & -p_{11} & -p_{12} & -p_{13} \\ 1 & -p_{21} & -p_{22} & -p_{23} \\ 1 & -p_{31} & -p_{32} & -p_{33} \\ 1 & -p_{41} & -p_{42} & -p_{43} \end{bmatrix}, \quad (\text{E.16})$$

from which, one can verify that $\det(\Xi) \neq 0$. Define $N_0 = \bar{C}$, $N_1 = N_0 A$, $N_2 = N_1 A$, and \bar{N}_1, \bar{N}_2 as the first row of N_1, N_2 , respectively. Let \bar{N}_0 be the first four rows of N_0 . The matrix $\bar{\mathcal{O}} = [\bar{N}_0^\top, \bar{N}_1^\top, \bar{N}_2^\top]^\top$ is given by

$$\bar{\mathcal{O}} = \begin{bmatrix} I_3 & -p_{11}I_3 & -p_{12}I_3 & -p_{13}I_3 & 0_{3 \times 3} & 0_{3 \times 3} \\ I_3 & -p_{21}I_3 & -p_{22}I_3 & -p_{23}I_3 & 0_{3 \times 3} & 0_{3 \times 3} \\ I_3 & -p_{31}I_3 & -p_{32}I_3 & -p_{33}I_3 & 0_{3 \times 3} & 0_{3 \times 3} \\ I_3 & -p_{41}I_3 & -p_{42}I_3 & -p_{43}I_3 & 0_{3 \times 3} & 0_{3 \times 3} \\ 0_{3 \times 3} & 0_{3 \times 3} & 0_{3 \times 3} & 0_{3 \times 3} & I_3 & 0_{3 \times 3} \\ 0_{3 \times 3} & I_3 \end{bmatrix} \quad (\text{E.17})$$

The determinate of matrix $\bar{\mathcal{O}}$ is given by

$$\begin{aligned} \det(\bar{\mathcal{O}}) &= \det \left(\begin{bmatrix} I_3 & -p_{11}I_3 & -p_{12}I_3 & -p_{13}I_3 \\ I_3 & -p_{21}I_3 & -p_{22}I_3 & -p_{23}I_3 \\ I_3 & -p_{31}I_3 & -p_{32}I_3 & -p_{33}I_3 \\ I_3 & -p_{41}I_3 & -p_{42}I_3 & -p_{43}I_3 \end{bmatrix} \right) \\ &= \det(I_3)^4 \det(\Xi)^3 \neq 0, \end{aligned} \quad (\text{E.18})$$

where we made use of the fact that $\det(A \otimes B) = \det(A)^m \det(B)^n$ for any $A \in \mathbb{R}^{n \times n}$ and $B \in \mathbb{R}^{m \times m}$ with \otimes being the Kronecker product. Then, one can conclude that the pair (\bar{A}, \bar{C}) is uniformly observable, and there exist constants $\delta'', \mu'' > 0$ such that $W_o''(t, t + \delta') \geq \mu'' I$ for all $t \geq 0$. This completes the proof.

E.4 Proof of Lemma 6.4

Similar to the proof of Lemma 6.2, one can show that $C(t) = \Theta\bar{C}$ with constant matrix \bar{C} given as

$$\bar{C} = \begin{bmatrix} I_3 & 0_{3 \times 3} & \cdots & 0_{3 \times 3} & 0_{3 \times 3} & 0_{3 \times 3} & 0_{3 \times 3} \\ I_3 & -I_3 & \cdots & 0_{3 \times 3} & 0_{3 \times 3} & 0_{3 \times 3} & 0_{3 \times 3} \\ \vdots & \vdots & \ddots & \vdots & \vdots & \vdots & \vdots \\ I_3 & 0_{3 \times 3} & 0_{3 \times 3} & -I_3 & 0_{3 \times 3} & 0_{3 \times 3} & 0_{3 \times 3} \end{bmatrix}. \quad (\text{E.19})$$

Since $\Sigma(t) = \Theta^\top(t)\Theta(t) > \bar{\epsilon}I$ with some constant $\bar{\epsilon} > 0$, one can obtain (E.12) as in the proof of Lemma 6.2.

Next, we are going to show that there exist constants $\delta', \mu' > 0$ such that

$$W'_O(t, t + \delta') := \frac{1}{\delta'} \int_t^{t+\delta'} \Phi^\top(\tau, t) \bar{C}^\top \bar{C} \Phi(\tau, t) d\tau > \mu' I$$

for all $t \geq 0$. Define $N_0 = \bar{C}, N_1 = N_0 A + \dot{N}_0, \dots, N_4 = N_3 A + \dot{N}_3$, and $\bar{N}_1, \dots, \bar{N}_4$ as the first row of N_1, \dots, N_4 , respectively. We introduce the following matrix:

$$\bar{\mathcal{O}} := [N_0^\top, \bar{N}_1^\top, \bar{N}_2^\top, \bar{N}_3^\top]^\top = \begin{bmatrix} \bar{\mathcal{O}}_1 & \mathbf{0} \\ \bar{\mathcal{O}}_2 & \bar{\mathcal{O}}_3 \end{bmatrix} \quad (\text{E.20})$$

where

$$\begin{aligned} \bar{\mathcal{O}}_1 &= \begin{bmatrix} I_3 & 0_{3 \times 3} & \cdots & 0_{3 \times 3} \\ I_3 & -I_3 & \cdots & 0_{3 \times 3} \\ \vdots & \vdots & \ddots & \vdots \\ I_3 & 0_{3 \times 3} & \cdots & -I_3 \end{bmatrix} \in \mathbb{R}^{3N \times 3N} \\ \bar{\mathcal{O}}_2 &= \begin{bmatrix} -\omega^\times & 0_{3 \times 3} & \cdots & 0_{3 \times 3} \\ \varpi_1 & 0_{3 \times 3} & \cdots & 0_{3 \times 3} \\ \varpi_2 & 0_{3 \times 3} & \cdots & 0_{3 \times 3} \end{bmatrix}, \bar{\mathcal{O}}_3 = \begin{bmatrix} I_3 & 0_{3 \times 3} & 0_{3 \times 3} \\ -2\omega^\times & I_3 & I_3 \\ \varpi_3 & 6\varpi_1 & \varpi_4 \end{bmatrix} \end{aligned}$$

with $\varpi_1 = (\omega^\times)^2 - \dot{\omega}^\times, \varpi_2 = (\omega^\times)^4 - 6(\omega^\times)^2\dot{\omega}^\times + 4(\omega^\times)\ddot{\omega}^\times + 3(\dot{\omega}^\times)^2 - \dddot{\omega}^\times, \varpi_3 = 12\omega^\times\dot{\omega}^\times - 4(\omega^\times)^3 - 4\ddot{\omega}^\times$ and $\varpi_4 = 3(\omega^\times)^2 - 5\dot{\omega}^\times$. The determinate of matrix $\bar{\mathcal{O}}$ is given by

$$\begin{aligned} \det(\bar{\mathcal{O}}) &= (-1)^{N-1} \det(\bar{\mathcal{O}}_3) \\ &= (-1)^{N-1} \det \left(\begin{bmatrix} I_3 & I_3 \\ 6\varpi_1 & 3(\omega^\times)^2 - 5\dot{\omega}^\times \end{bmatrix} \right) \\ &= (-1)^N \det(3(\omega^\times)^2 - \dot{\omega}^\times), \end{aligned} \quad (\text{E.21})$$

where we made use of the same property of the Kronecker product as in (E.18). Using [Scandaroli, 2013, Eqn. A.15], one has $\det(3(\omega^\times)^2 - \dot{\omega}^\times) = -3\|\omega \times \dot{\omega}\|^2$. It follows that $\det(\bar{\mathcal{O}}) = (-1)^{N+1}3\|\omega \times \dot{\omega}\|^2$. From assumption (6.26) and the fact $\det(\bar{\mathcal{O}}^\top \bar{\mathcal{O}}) = \det(\bar{\mathcal{O}})^2 = 9\|\omega \times \dot{\omega}\|^4$, one verifies condition (2.115) in Lemma 2.9, which implies that there exist constants $\delta', \mu' > 0$ such that $W'_O(t, t + \delta) > \mu' I$. From (E.12), one has $W_O(t, t + \delta) \geq \frac{\bar{\epsilon}^2 \delta'}{\delta} W'_O(t, t + \delta) \geq \frac{\bar{\epsilon}^2 \delta'}{\delta} \mu' I := \mu I$, which implies that the pair $(A(t), C(t))$ is uniformly observable. This completes the proof.

E.5 Proof of Lemma 6.5

Let us define a $3N$ -by- $3N$ block diagonal matrix $\Theta(t) := \text{blkdiag}(\Pi_1, \Pi_2, \dots, \Pi_N)$. Then, one verifies that $C(t) = \Theta(t)\bar{C}$ with constant matrix \bar{C} given as

$$\bar{C} = \begin{bmatrix} I_3 & -p_{11}I_3 & -p_{12}I_3 & -p_{13}I_3 & 0_{3 \times 3} & 0_{3 \times 3} & 0_{3 \times 3} \\ I_3 & -p_{21}I_3 & -p_{22}I_3 & -p_{23}I_3 & 0_{3 \times 3} & 0_{3 \times 3} & 0_{3 \times 3} \\ \vdots & \vdots & \vdots & \vdots & \vdots & \vdots & \vdots \\ I_3 & -p_{N1}I_3 & -p_{N2}I_3 & -p_{N3}I_3 & 0_{3 \times 3} & 0_{3 \times 3} & 0_{3 \times 3} \end{bmatrix}. \quad (\text{E.22})$$

Similar to the proof of Lemma 6.2, one obtains (E.12) and we are going to show that there exist constants $\delta', \mu' > 0$ such that

$$W'_O(t, t + \delta') := \frac{1}{\delta'} \int_t^{t+\delta'} \Phi^\top(\tau, t) \bar{C}^\top \bar{C} \Phi(\tau, t) d\tau > \mu' I$$

for all $t \geq 0$. For the sake of simplicity, we assume that the landmarks $i = 1, 2, 3, 4$ are not coplanar. Define $N_0 = \bar{C}$, $N_1 = N_0 A + \dot{N}_0, \dots, N_4 = N_3 A + \dot{N}_3$, and $\bar{N}_1, \dots, \bar{N}_4$ as the first row of N_1, \dots, N_4 , respectively. Let \bar{N}_0 be the first four rows of N_0 . The matrix $\bar{\mathcal{O}}$ is given by

$$\bar{\mathcal{O}} := [\bar{N}_0^\top, \bar{N}_1^\top, \bar{N}_2^\top, \bar{N}_3^\top]^\top = \begin{bmatrix} \Xi \otimes I_3 & \mathbf{0} \\ \bar{\mathcal{O}}_2 & \bar{\mathcal{O}}_3 \end{bmatrix} \quad (\text{E.23})$$

with $\varpi_1, \varpi_2, \dots, \varpi_4$ and $\bar{\mathcal{O}}_3$ defined in (E.20) and

$$\bar{\mathcal{O}}_2 = \begin{bmatrix} -\omega^\times & p_{11}\omega^\times & p_{12}\omega^\times & p_{13}\omega^\times \\ \varpi_1 & -p_{11}\varpi_1 & -p_{12}\varpi_1 & -p_{13}\varpi_1 \\ \varpi_2 & -p_{11}\varpi_2 & -p_{12}\varpi_2 & -p_{13}\varpi_2 \end{bmatrix}$$

The determinate of matrix $\bar{\mathcal{O}}$ is given by

$$\begin{aligned} \det(\bar{\mathcal{O}}) &= \det(I_3)^4 \det(\Xi)^3 \det(\bar{\mathcal{O}}_3) \\ &= \det(\Xi)^3 \det(3(\omega^\times)^2 - \dot{\omega}^\times) \\ &= -3\det(\Xi)^3 \|\omega \times \dot{\omega}\|^2, \end{aligned} \quad (\text{E.24})$$

where we made use of the same property of the Kronecker product as in (E.18). The rest of proof is obtained using similar steps as in the proof of Lemma 6.3.

E.6 Proof of Theorem 6.2

Consider the following real-valued function:

$$\mathcal{L}_P(x) = x^\top P^{-1} x. \quad (\text{E.25})$$

One can show that $\frac{1}{p_M} \|x\|^2 \leq \mathcal{L}_P(x) \leq \frac{1}{p_m} \|x\|^2$. Define $c_g := \|g\|$ and $c_p, c_v > 0$ such that $\|p(t)\| \leq c_p, \|v(t)\| \leq c_v$ for all $t \geq 0$. In view of (6.32) and (2.116), the time-derivative of \mathcal{L}_P is given by

$$\dot{\mathcal{L}}_P = x^\top (P^{-1}A + A^\top P^{-1} - 2C^\top QC + \dot{P}^{-1})x$$

$$\begin{aligned}
& + 2x^\top P^{-1} \varphi(\tilde{R}, \tilde{b}_\omega, t) \\
& = -x^\top P^{-1} V P^{-1} x - x^\top C^\top Q C x + 2x^\top P^{-1} \varphi(\tilde{R}, \tilde{b}_\omega, t) \\
& \leq -\frac{v_m}{p_M^2} \|x\|^2 + \frac{2\|\varphi(\tilde{R}, \tilde{b}_\omega, t)\|}{p_m} \|x\|,
\end{aligned} \tag{E.26}$$

where $v_m = \inf_{t \geq 0} \lambda_{\min}^{V(t)}$. Making use of the fact $\|\varphi(\tilde{R}, \tilde{b}_\omega, t)\| \leq (\|p\| + \|v\| + \sum_{i=1}^3 1) \|\tilde{b}_\omega\| + \|I - \tilde{R}\|_F \|g\| \leq (c_p + c_v + 3)(2c_b + \delta) + 2\sqrt{2} \|g\| := c_\varphi$, one has

$$\begin{aligned}
\dot{\mathcal{L}}_P & \leq -\frac{v_m}{2p_M^2} \|x\|^2 + \frac{2p_M^2}{v_m} \left(\frac{4c_\varphi p_M^2}{p_m v_m} - \|x\| \right) \|x\| \\
& \leq -\frac{v_m p_m}{2p_M^2} \mathcal{L}_P(x), \quad \forall \|x\| \geq \frac{4c_\varphi p_M^2}{p_m v_m}.
\end{aligned} \tag{E.27}$$

For each $c_x > 0$, let $v_m \geq \frac{4c_\varphi p_M^2}{p_m c_x}$ such that

$$\|x(t)\|^2 \leq p_m \mathcal{L}_P(x(t)) \leq p_m \exp\left(-\frac{v_m p_m}{2p_M^2} t\right) \mathcal{L}_P(x(0))$$

as long as $\|x(t)\| \geq c_x \geq \frac{4c_\varphi p_M^2}{p_m v_m}$. This implies that, for any $x(0)$, there exists a finite time

$$T = \frac{2p_M^2}{v_m p_m} \ln\left(\frac{p_m \mathcal{L}_P(x(0))}{c_x^2}\right) \tag{E.28}$$

such that $\|x(t)\| \leq c_x$ for all $t \geq T$.

On the other hand, in view of the first equation of (6.32), the time-derivative of $|\tilde{R}|_I^2 = \frac{1}{4} \text{tr}(I_3 - \tilde{R})$ is given by

$$\frac{d}{dt} |\tilde{R}|_I^2 = \frac{1}{2} \psi_{\mathfrak{so}(3)}(\tilde{R})^\top \left(\hat{R} \tilde{b}_\omega + \sigma_R \right) \leq \frac{\bar{c}_b + c_{\sigma_R}}{2} \tag{E.29}$$

where $c_{\sigma_R} := \rho_0 \|m_I\|^2 + \sum_{i=1}^3 \rho_i c_e$, $\|\tilde{b}_\omega\| \leq \delta + 2c_b := \bar{c}_b$, and we made use of the fact $\|\psi_{\mathfrak{so}(3)}(\tilde{R})\|^2 = 4(1 - |\tilde{R}|_I^2) |\tilde{R}|_I^2 \leq 1$. For any $\tilde{R}(0) \in \mathcal{U}(\varepsilon_R)$, the minimum necessary time for the state to leave the set $\mathcal{U}(\varepsilon_R)$ satisfies $T_{\varepsilon_R} := 2(\varepsilon_R^2 - |\tilde{R}(0)|_I^2) / (\bar{c}_b + c_{\sigma_R})$. Let $c_x := \min\{2\lambda_{\min}^{\bar{M}} \varepsilon_R (1 - \varepsilon_R) / c_\phi, c_e - 1\}$, and then choose $V(t)$ and $Q(t)$ for (2.116) such that

$$v_m \geq \max \left\{ \frac{4c_\varphi p_M^2}{p_m c_x}, \frac{2p_M^2}{T_{\varepsilon_R} p_m} \ln\left(\frac{p_m \mathcal{L}_P(x(0))}{c_x^2}\right) \right\} := \bar{v}_m.$$

Then, one can verify that $T \leq T_{\varepsilon_R}$ and $\|x\| \leq c_x = \min\{2\lambda_{\min}^{\bar{M}} \varepsilon_R (1 - \varepsilon_R) / c_\phi, c_e - 1\}$ for all $t \geq T$. It follows that $\sigma_R = -\psi_{\mathfrak{so}(3)}(M\tilde{R}) + \phi(x, t)$ since $\|\tilde{e}_i\| \leq \|\tilde{e}_i\| + 1 \leq c_x + 1 \leq c_e$, and $c_\phi \|x\| \leq \lambda_{\min}^{\bar{M}} \varepsilon_R (1 - \varepsilon_R)$ for all $t \geq T$. Then, the time-derivative of $|\tilde{R}|_I^2$ for all $t \geq T$ can be rewritten as

$$\begin{aligned}
\frac{d}{dt} |\tilde{R}|_I^2 & = \frac{1}{2} \psi_{\mathfrak{so}(3)}(\tilde{R})^\top (\hat{R} \tilde{b}_\omega - k_R \psi_{\mathfrak{so}(3)}(M\tilde{R}) + k_R \phi(x, t)) \\
& \leq -\frac{k_R}{2} \psi_{\mathfrak{so}(3)}(\tilde{R})^\top \bar{M} \psi_{\mathfrak{so}(3)}(\tilde{R}) + \frac{1}{2} (\bar{c}_b + k_R \|\phi(x, t)\|)
\end{aligned}$$

$$\leq -2k_R\lambda_{\min}^{\bar{M}}\|\psi_{\mathfrak{so}(3)}(\tilde{R})\|^2 + \frac{1}{2}(\bar{c}_b + k_R c_\phi \|x\|)$$

Choosing $k_R > \bar{c}_b/(2\lambda_{\min}^{\bar{M}}\varepsilon_R(1-\varepsilon_R)) := \bar{k}_R$, one shows that $\frac{d}{dt}|\tilde{R}|_I^2 \leq -k_R\lambda_{\min}^{\bar{M}}\varepsilon_R(1-\varepsilon_R) + \frac{\bar{c}_b}{2} < 0$ at $|\tilde{R}|_I^2 = \varepsilon_R$. This implies, due to the continuity of the solution, that \tilde{R} will never leave the set $\mathcal{U}(\varepsilon_R)$ for all $t \geq T$ as long as $\tilde{R}(T) \in \mathcal{U}(\varepsilon_R)$. Therefore, one can conclude that the set $\mathcal{U}(\varepsilon_R)$ is forward invariant for all $t \geq 0$.

Now, we are going to show the exponential convergence of the estimation errors for all $t \geq T$. Consider the following real-valued function

$$\mathcal{L}(\tilde{R}, \tilde{b}_\omega, x) = \text{tr}(I - \tilde{R}) + \frac{k_R\mu}{2k_\omega}\tilde{b}_\omega^\top\tilde{b}_\omega - \mu\mathfrak{X} + \mathcal{L}_P(x), \quad (\text{E.30})$$

with some scalar $\mu > 0$ and $\mathfrak{X} := -\tilde{b}_\omega^\top\hat{R}^\top\psi_{\mathfrak{so}(3)}(\tilde{R})$. Using the fact $\|\psi_{\mathfrak{so}(3)}(\tilde{R})\| \leq 2|\tilde{R}|_I$, one can show that \mathcal{L} satisfies the quadratic inequality $\varsigma^\top H_1 \varsigma \leq \mathcal{L} \leq \varsigma^\top H_2 \varsigma$, where the matrices H_1 and H_2 are given by

$$H_1 = \begin{bmatrix} 4 & -\mu & 0 \\ -\mu & \frac{k_R\mu}{2k_\omega} & 0 \\ 0 & 0 & \frac{1}{p_M} \end{bmatrix}, \quad H_2 = \begin{bmatrix} 4 & \mu & 0 \\ \mu & \frac{k_R\mu}{2k_\omega} & 0 \\ 0 & 0 & \frac{1}{p_m} \end{bmatrix}.$$

Moreover, the time-derivative of \mathfrak{X} is given by

$$\begin{aligned} \dot{\mathfrak{X}} &= -\tilde{b}_\omega^\top\hat{R}^\top E(\tilde{R})(\hat{R}\tilde{b}_\omega + k_R\sigma_R) + \tilde{b}_\omega^\top(\omega - \tilde{b}_\omega - k_R\hat{R}^\top\sigma_R)^\times\hat{R}^\top\psi_{\mathfrak{so}(3)}(\tilde{R}) \\ &\quad - \psi_{\mathfrak{so}(3)}(\tilde{R})^\top\hat{R}\mathbf{P}_\delta^\epsilon(\hat{b}_\omega, k_\omega\hat{R}^\top\sigma_R) \\ &\leq -\|\tilde{b}_\omega\|^2 + \tilde{b}_\omega^\top\hat{R}^\top(I_3 - E(\tilde{R}))\hat{R}\tilde{b}_\omega - k_R\tilde{b}_\omega^\top\hat{R}^\top\sigma_R \\ &\quad + k_R\tilde{b}_\omega^\top\hat{R}^\top(I_3 - E(\tilde{R}))\sigma_R + 2c_\omega\|\tilde{b}_\omega\||\tilde{R}|_I + 2(k_R\bar{c}_b + k_\omega)\|\sigma_R\||\tilde{R}|_I \\ &\leq -\|\tilde{b}_\omega\|^2 + 2c_1|\tilde{R}|_I\|\tilde{b}_\omega\| - \mu k_R\tilde{b}_\omega^\top\hat{R}^\top\sigma_R \\ &\quad + 2(c_2k_R + c_3)|\tilde{R}|_I^2 + 2(c_4k_R + c_5)|\tilde{R}|_I\|x\| \end{aligned} \quad (\text{E.31})$$

where $c_1 := \bar{c}_b + c_\omega$, $c_2 := (4 + \sqrt{2})\bar{c}_b\sqrt{\lambda_{\max}^W}$, $c_3 := 2k_\omega\sqrt{\lambda_{\max}^W}$, $c_4 := (2 + \sqrt{2}/2)\bar{c}_b c_\phi$, $c_5 := k_\omega c_\phi$, and we have made use of the facts $\|\psi_{\mathfrak{so}(3)}(M\tilde{R})\|^2 \leq 4\lambda_{\max}^W|\tilde{R}|_I^2$, $\tilde{b}_\omega^\top\hat{R}^\top(I_3 - E(\tilde{R}))\hat{R}\tilde{b}_\omega \leq 2|\tilde{R}|_I^2\|\tilde{b}_\omega\|^2 \leq 2\bar{c}_b|\tilde{R}|_I\|\tilde{b}_\omega\|$ in (2.40), $\tilde{b}_\omega^\top\hat{R}^\top(I_3 - E(\tilde{R}))\sigma_R \leq \frac{1}{2}\text{tr}(I - \tilde{R})\tilde{b}_\omega^\top\sigma_R + \frac{1}{2}\|I - \tilde{R}\|_F\|\tilde{b}_\omega\|\|\sigma_R\| \leq (2 + \sqrt{2})\bar{c}_b|\tilde{R}|_I\|\sigma_R\|$ in (2.41) and $\|\sigma_R\| \leq 2\sqrt{\lambda_{\max}^W}|\tilde{R}|_I + c_\phi\|x\|$. In view of (E.26) and (E.31), the time-derivative of \mathcal{L} for all $t \geq T$ is given by

$$\begin{aligned} \dot{\mathcal{L}} &= \text{tr}(-\tilde{R}(\hat{R}\tilde{b}_\omega - k_R\psi_{\mathfrak{so}(3)}(M\tilde{R}) + k_R\phi(x, t))^\times) + \frac{\mu k_R}{k_\omega}\tilde{b}_\omega^\top\mathbf{P}_\delta^\epsilon(\hat{b}_\omega, k_\omega\hat{R}^\top\sigma_R) + \mu\dot{\mathfrak{X}} + \dot{\mathcal{L}}_P \\ &\leq -2k_R\psi_{\mathfrak{so}(3)}(\tilde{R})^\top\psi_{\mathfrak{so}(3)}(M\tilde{R}) + 2\|\psi_{\mathfrak{so}(3)}(\tilde{R})\|\|\tilde{b}_\omega\| \\ &\quad + 2k_Rc_\phi\|\psi_{\mathfrak{so}(3)}(\tilde{R})\|\|x\| + \mu k_R\tilde{b}_\omega^\top\hat{R}^\top\sigma_R + \mu\dot{\mathfrak{X}} + \dot{\mathcal{L}}_P \\ &\leq -2k_R\varrho|\tilde{R}|_I^2 + 4|\tilde{R}|_I\|\tilde{b}_\omega\| + 4k_Rc_\phi|\tilde{R}|_I\|x\| - \mu\|\tilde{b}_\omega\|^2 + 2\mu c_1|\tilde{R}|_I\|\tilde{b}_\omega\| \\ &\quad + 2\mu(c_2k_R + c_3)|\tilde{R}|_I^2 + 2\mu(c_4k_R + c_5)|\tilde{R}|_I\|x\| - \frac{v_m}{p_M^2}\|x\|^2 \end{aligned}$$

$$\begin{aligned}
& + \frac{2}{p_m} ((c_p + c_v + 3) \|\tilde{b}_\omega\| + 2\sqrt{2}\|\mathbf{g}\| |\tilde{R}|_I) \|x\| \\
& \leq -2(k_R \varrho - \mu(c_2 k_R + c_3)) |\tilde{R}|_I^2 + 2(2 + \mu c_1) |\tilde{R}|_I \|\tilde{b}_\omega\| \\
& \quad - \mu \|\tilde{b}_\omega\|^2 + 2(\mu(c_4 k_R + \mu c_5) + c_6) |\tilde{R}|_I \|x\| - v_m p_M^{-2} \|x\|^2 + 2c_7 \|\tilde{b}_\omega\| \|x\|
\end{aligned}$$

where $c_6 := 2k_R c_\phi + 2\sqrt{2}\|\mathbf{g}\|/p_m$, $c_7 := (c_p + c_v + 3)/p_m$, and we have made use of the facts $\psi_{\mathfrak{so}(3)}(\tilde{R})^\top \psi_{\mathfrak{so}(3)}(M\tilde{R}) = \psi_{\mathfrak{so}(3)}(\tilde{R})^\top M \psi_{\mathfrak{so}(3)}(\tilde{R}) \geq \varrho |\tilde{R}|_I^2$ with $\varrho := 2(1 - \varepsilon_R) \lambda_{\min}^{\tilde{M}} > 0$ and $\text{tr}(-Ax^\times) = 2x^\top \psi_{\mathfrak{so}(3)}(A)$ for all $A \in \mathbb{R}^{3 \times 3}$. Moreover, the time-derivative of \mathcal{L} can be rewritten as

$$\dot{\mathcal{L}} = -\varsigma_{12}^\top H_{12} \varsigma_{12} - \varsigma_{13}^\top H_{13} \varsigma_{13} - \varsigma_{23}^\top H_{23} \varsigma_{23} \quad (\text{E.32})$$

where $\varsigma_{ij} = [\varsigma_i, \varsigma_j]^\top$ and the matrices H_{ij} are given by

$$\begin{aligned}
H_{12} &= \begin{bmatrix} k_R(\varrho - 2\mu c_2) - 2\mu c_3 & -(2 + \mu c_1) \\ -(2 + \mu c_1) & \frac{\mu}{2} \end{bmatrix} \\
H_{13} &= \begin{bmatrix} k_R \varrho & -(\mu(c_4 k_R + \mu c_5) + c_6) \\ -(\mu(c_4 k_R + \mu c_5) + c_6) & \frac{v_m}{2p_M^2} \end{bmatrix} \\
H_{23} &= \begin{bmatrix} \frac{\mu}{2} & -c_7 \\ -c_7 & \frac{v_m}{2p_M^2} \end{bmatrix}
\end{aligned}$$

To guarantee that matrices H_1, H_2, H_{12}, H_{13} and H_{23} are positive definite, let us choose

$$\begin{aligned}
\mu &< \frac{\rho}{2c_2} \\
k_R &> \max \left\{ \bar{k}_R, \frac{\mu k_\omega}{2}, \frac{2\mu^2 c_3 + 2(2 + \mu c_1)^2}{\mu(\varrho - 2\mu c_2)} \right\} \\
v_m &> \max \left\{ \bar{v}_m, \frac{4c_7^2 p_M^2}{\mu}, \frac{2(\mu(c_4 k_R + \mu c_5) + c_6)^2 p_M^2}{k_R \rho} \right\}
\end{aligned}$$

Then, one obtains

$$\dot{\mathcal{L}}(\tilde{R}, \tilde{b}_\omega, x) \leq -2\lambda \mathcal{L}(\tilde{R}, \tilde{b}_\omega, x), \quad \forall t \geq T,$$

with $\lambda := \frac{1}{2} \min\{\lambda_{\min}^{H_{12}}, \lambda_{\min}^{H_{23}}, \lambda_{\min}^{H_{14}}\}/\lambda_{\max}^{H_2}$. Therefore, one can conclude (6.35) with $\kappa := (\lambda_{\max}^{H_2}/\lambda_{\min}^{H_1})^{\frac{1}{2}}$. This completes the proof.

Curriculum Vitae

Name: Miaomiao WANG

Post-Secondary Education and Degrees: Huazhong University of Science and Technology
Wuhan, Hubei, China
Automation
2009-2013 B.Eng.

Lakehead University
Thunder Bay, ON, Canada
Control Engineering
2014 - 2015 M.Sc.

Western University
London, ON, Canada
Robotic and Control
2016 - 2019 Ph.D.

Honours and Awards: ECE Graduate Student Research Award
Western University
London ON, Canada, 2019

Ontario Graduate Scholarship
Western University
London ON, Canada, 2018-2019

Related Work Experience: Teaching Assistant
Western University
London ON, 2016 - 2019

Teaching Assistant
Lakehead University
Thunder Bay, ON, 2014 - 2015

Selected Publications:

- M. Wang and A. Tayebi, ‘Nonlinear State Estimation for Inertial Navigation Systems With Intermittent Measurements’. *Automatica*, 2019, submitted.
- M. Wang and A. Tayebi, ‘Hybrid Nonlinear Observers for Inertial Navigation Using Landmark Measurements’. *IEEE Transactions on Automatic Control*, 2020, accepted.
- M. Wang and A. Tayebi, ‘Hybrid Pose and Velocity-bias Estimation on $\text{SE}(3)$ Using Inertial and Landmark Measurements’. *IEEE Transactions on Automatic Control*, 64(8), pp. 3399-3406, 2019.
- S. Qiu, M. Wang and M. Kermani, ‘A new formulation for Hand-eye Calibration as Point set Matching’, *IEEE Transactions on Instrumentation and Measurement*, 2020, accepted.
- M. Wang and A. Tayebi, ‘A New Hybrid Control Strategy for the Global Attitude Tracking Problem’. In *Proc. of the 58th IEEE Conference on Decision and Control (CDC)*, Nice, France, pp. 7222-7227, 2019.
- M. Wang and A. Tayebi, ‘Nonlinear Observers for Stereo-Vision-Aided Inertial Navigation’. In *Proc. of 58th IEEE Conference on Decision and Control (CDC)*, Nice, France, pp. 2516-2521, 2019.
- M. Wang and A. Tayebi, ‘A Globally Exponentially Stable Nonlinear Hybrid Observer for 3D Inertial Navigation’. In *Proc. of the 57th IEEE Conference on Decision and Control (CDC)*, Miami Beach, FL, USA, pp. 1367- 1372, 2018.
- M. Wang and A. Tayebi, ‘Geometric Nonlinear Observer Design for SLAM on a Matrix Lie Group’. In *Proc. of the 57th IEEE Conference on Decision and Control (CDC)*, Miami Beach, FL, USA, pp. 1488-1493, 2018.
- M. Wang and A. Tayebi, ‘Globally Asymptotically Stable Hybrid Observers Design on $\text{SE}(3)$ ’. In *Proc. of the 56th IEEE Conference on Decision and Control (CDC)*, Melbourne, Australia, pp. 3033-3038, 2017.
- M. Wang, H. Su, M. Zhao, M.Z. Chen and H. Wang, ‘Flocking of Multiple Autonomous Agents with Preserved Network Connectivity and Heterogenous Nonlinear Dynamics’, *Neurocomputing*, 32(6), pp. 2867-2881, 2013.